

ENVIRONMENTAL MANAGEMENT
J. Phyllis Fox, Ph.D., REA II, QEP, PE, DEE
745 White Pine Ave
Rockledge, FL 32955
321-626-6885

Dominion Virginia City Hybrid Energy Center
c/o Cindy M. Berndt
Department of Environmental Quality
P.O. Box 1105
Richmond, VA 23218

Dear Air Pollution Control Board of the Virginia Department of Environmental Quality:

I am an environmental engineer with over 30 years of experience in Clean Air Act permitting, including BACT and MACT analyses for over 75,000 MW of coal, gas, wood, oil and other power plants. I submit these comments on my own behalf. I address two MACT issues raised by Mr. Buckheit in his April 14, 2008 memorandum to Board Members ("Buckheit Memo").

MACT

PM As A Surrogate For Metal HAPs

Mr. Buckheit notes that VDEP's MACT analysis assumed high control efficiencies for metal HAPs based on the use of particulate matter as a surrogate, but provided nothing to support the assumed 99.7% to 99.9% control efficiencies into a PM MACT limit. Buckheit Memo at 15. I agree. These assumptions are not likely to be met in practice unless the baghouse is designed to meet them and they are required as permit limits, or are converted into HAP-specific permit emission limits.

First, most metallic HAPs are volatilized in the boiler and condense as very fine particulate matter or nanoparticles (<2.5 microns) in the pollution control train. Ex. 1.¹ The highest concentrations are consistently found in the

¹ R.C. Flagan and S.K. Friedlander, Particle Formation in Pulverized Coal Combustion – A Review, In: *Recent Developments in Aerosol Science*. D.T. Shaw (Ed.), 1978, Chapter 2 (Ex. 1A); A.S. Damale, D.S. Ensor, and M.B. Ranade, Coal Combustion Aerosol Formation Mechanisms: A Review, *Aerosol Science & Technology*, v. 1, no. 1, 1982, pp. 119-133. See also: S.K. Friedlander, *Smoke, Dust, and Haze. Fundamentals of Aerosol Dynamics*, 2nd Ed., Oxford University Press, 2000.

smallest particles. Exs. 2,² 3.³ The particulate collection efficiency for conventional baghouses designed to collect PM and PM10 is generally lower for these nanoparticles that contain most of the metallic HAPs than for larger particles.⁴ Ex. 3, p. 1538; Ex. 4,⁵ p. 1582. Thus, a fabric filter system designed to meet BACT for PM and PM10, as is the case here, does not necessarily meet MACT for metallic HAPS as these are present in particles smaller than 10 microns which are not as effectively controlled. These smaller particles also cause proportionately more of the adverse health impacts because they can penetrate deep into the lung. Ex. 4.

Second, not all HAPs condense and are present as fine particles that can be captured by a baghouse. Selenium is the most problematic as 50% to 100% of the selenium in coal is present as a vapor in exhaust gases. Further, depending upon the fuel and control train, some of the otherwise nonvolatile trace metals, including chromium and nickel, may be present in the vapor phase. Finally, mercury controls, including powdered activated carbon and sorbent enhancements, have been demonstrated to increase the amount of chromium and nickel in stack gases, compared to no mercury control.⁶

Thus, it is premature to conclude that particulate matter is a reasonable surrogate for HAPs, especially based only on conventional baghouse control. Other technology may be required to control volatile metallic HAPs. Further, much higher control efficiencies can be achieved for particulate HAPs using advanced filtration media and wet electrostatic precipitators, among others. Permit limits should be established for each individual HAP to assure that MACT is required.

² Richard L. Davidson and others. Trace Elements in Fly Ash. *Environmental Science & Technology*, v. 8, no. 13, December 1974, pp. 1107-1113 (Ex. 2A); E.S. Gladney and others. Composition and Size Distribution of In-State Particulate Material at a Coal-Fired Power Plant. *Atmospheric Environment*, v. 10, 1976, pp. 1071-1077 (Ex. 2B); John M. Ondov, Richard C. Ragaini, and Arthur H. Biermann. Emissions and Particle-size Distributions of Minor and Trace Elements at Two Western Coal-fired Power Plants Equipped with Cold-side Electrostatic Precipitators, *Environmental Science & Technology*, v. 13, 1979, pp. 946-953 (Ex. 2C).

³ W.P. Linak and others. Comparison of Particle Size Distributions and Elemental Partitioning from Combustion of Pulverized Coal and Residual Fuel Oil. *J. Air & Waste Manage. Assoc.*, v. 50, 2000, pp. 1532-1544.

⁴ AP-42, Table 1.1-5.

⁵ JoAnn S. Lighty, John M. Veranth, and Adel F. Sarofim. Combustion Aerosols: Factors Governing their Size and Composition and Implications to Human Health, *J. Air & Waste Manage. Assoc.*, v. 50, 2000, pp. 1565-1618.

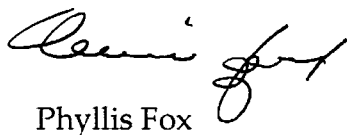
⁶ McIlvaine Hot Topic Hour. Hazardous Air Pollutants. May 15, 2008, Presentation of John Pavlish, EERC. Voice recording available online to subscribers of McIlvaine Power Plant Knowledge System and available for purchase.

Baghouse Design

Mr. Buckheit states that the best baghouses have an air to cloth ("A/C") ratio of less than 2:1 (presumably 2 ft/min). Buckheit Memo at 16. However, fabric filter design to achieve the high filtration efficiencies assumed for HAPs is a bit more complex, requiring specification of grain loading, control efficiency, type of bag cleaning, filtration media, etc. The stated A/C of less than 2 ft/min is typical for reverse air fabric filters. However, pulse jet fabric filters, proposed here, typically operate at 3.0 to 4.0 ft/min. Steam⁷ at 33-10.

Fabric filter baghouses are only as efficient as the bags they use. The filtration media determines the control efficiency of a baghouse for very small particles. There is a wide range of media that can be used, most of which are more efficient for larger particles. The design basis filtration media (Ryton is a type of material, not the design basis media) for the proposed baghouse is unknown and should be determined. The exhaust gas conditions should allow wide latitude in selection of filtration media to achieve high removal of the smallest particles where metallic HAPs are concentrated.

Media have been developed over the last decade that remove over 99.99%+ of the 2.5 micron particles. These include Daikin's AMIREX™, PTFE membrane filters⁸ and W.L. Gore's L3650.⁹ See summary of U.S. EPA's ETV test results in Exhibit 5. The BACT and MACT analyses do not identify the type of filtration media that are assumed nor the removal efficiency as a function of particle size, which are required to determine if MACT for metallic HAPs has been required.



Phyllis Fox

⁷ Babcock & Wilcox CO., *Steam. It's Generation and Use*, 41st Ed., 2005.

⁸ McIlvaine Hot Topic Hour, Filter Media Selection for Coal-Fired Boilers. September 13, 2007, Presentation by Todd Brown, Daikin America, Inc. Voice recording available online to subscribers of McIlvaine Power Plant Knowledge System and available for purchase.

⁹ USEPA, ETV Joint Verification Statement, Baghouse Filtration Products, W.L. Gore & Associates, L3650 .at <http://epa.gov/etv/pubs/600etv06042s.pdf>.

EX 1A

RECENT DEVELOPMENTS IN AEROSOL SCIENCE

Edited by

DAVID T. SHAW

State University of New York at Buffalo

A WILEY-INTERSCIENCE PUBLICATION

JOHN WILEY & SONS New York • Chichester • Brisbane • Toronto

Copyright © 1978 by John Wiley & Sons, Inc.

All rights reserved. Published simultaneously in Canada.

Reproduction or translation of any part of this work beyond that permitted by Sections 107 or 108 of the 1976 United States Copyright Act without the permission of the copyright owner is unlawful. Requests for permission or further information should be addressed to the Permissions Department, John Wiley & Sons, Inc.

Library of Congress Cataloging in Publication Data

Symposium on Aerosol Science and Technology,
Atlantic City, N.J., 1976.

Recent developments in aerosol science.

"A Wiley-Interscience publication."

Includes bibliographies and index.

1. Aerosols—Congresses. 2. Air—Pollution—
Congresses. I. Shaw, David T. II. Title.

TD884.5.S97 1976 660.2'94515 78-17487
ISBN 0-471-02950-5

Printed in the United States of America

10 9 8 7 6 5 4 3 2 1

CONTRIBUTORS

- R. P. Andres, Beam Kinetics Laboratory, Department of Chemical Engineering, Princeton University, Princeton, New Jersey
- K. A. Bell, Environmental Health Laboratories, Ranchos Los Amigos Hospital, Downey, California
- D. Boulaud, Nuclear Research Center of Fontenay Aux Roses and the University of Paris, Paris, France
- J. Bricard, Nuclear Research Center of Fontenay Aux Roses and the University of Paris, Paris, France
- H. Chew, Clarkson College of Technology, Potsdam, New York
- B. Dahneke, Department of Radiation Biology and Biophysics, University of Rochester, Rochester, New York
- R. C. Flagan, Department of Environmental Engineering Science, California Institute of Technology, Pasadena, California
- S. K. Friedlander, Department of Chemical Engineering, California Institute of Technology, Pasadena, California
- E. Hederer, Department of Radiation Biology and Biophysics, School of Medicine and Dentistry, University of Rochester, Rochester, New York
- S. L. Heisler, Environmental Research & Technology, Inc., Westlake Village, California
- G. M. Hidy, Environmental Research & Technology, Inc., Westlake Village, California
- M. Kerker, Clarkson College of Technology, Potsdam, New York
- G. Madelaine, Nuclear Research Center of Fontenay Aux Roses and the University of Paris, Paris, France
- T. B. Martonen, Department of Radiation Biology and Biophysics, School of Medicine and Dentistry, University of Rochester, Rochester, New York
- P. J. McNulty, Clarkson College of Technology, Potsdam, New York

2. D. Grosjean and S. K. Friedlander, *JAPCA*, **25**, 1038 (1975).
3. R. C. Flagan and S. K. Friedlander, "Particle Formation in Pulverized Coal Combustion—A Review," Chap. 2 this volume.
4. S. K. Friedlander, *Smoke, Dust and Haze: Fundamentals of Aerosol Behavior*, Wiley-Interscience, New York, 1977.
5. C. T. R. Wilson, "On the Cloud Method of Making Visible Ions and the Tracks on Ionizing Particles," in *Nobel Lectures in Physics 1922-1941*, 1927.
6. J. Frenkel, *Kinetic Theory of Liquids*, Dover, 1955.
7. B. J. Mason, *The Physics of Clouds*, Clarendon, Oxford, 1971.
8. P. P. Wegener and A. A. Pouring, *Phys. Fluids*, **7**, 352 (1964).
9. R. H. Heist and H. Reiss, *J. Chem. Phys.*, **59**, 665 (1971).
10. P. T. Roberts and S. K. Friedlander, *Environ. Health Perspect.*, **10**, 103 (1975).
11. S. P. Sander and J. H. Seinfeld, *Environ. Sci. Technol.*, **10**, 1114 (1976).
12. J. G. Calvert, "Interactions of Air Pollutants," in *Proceedings of the Conference on Health Effects of Air Pollutants*, U.S. Government Printing Office No. 93-15, 1973.
13. H. Reiss, *J. Chem. Phys.*, **18**, 840 (1950).
14. D. Grosjean, personal communication, 1975.
15. C. S. Kiang and D. Stauffer, *Faraday Symp. Chem. Soc.*, No. 7, 29 (1973).
16. P. Mirabel and J. L. Katz, *J. Chem. Phys.*, **60**, 1138 (1974).
17. N. A. Fuchs and A. G. Sutugin, "High-Dispersed Aerosols," in G. M. Hidy and J. R. Brocks, Eds., *Topics in Current Aerosol Research*, Pergamon, New York, 1971.
18. P. H. McMurry, "On the Relationship between Aerosol Dynamics and the Rate of Gas-to-Particle Conversion," Ph.D Thesis in Environmental Engineering Science, California Institute of Technology, Pasadena, Calif., May 2, 1975.
19. W. D. Scott and P. V. Hobbs, *J. Atmos. Sci.*, **24**, 54 (1967).
20. C. E. Junge and T. G. Ryan, *Q. J. R. Meteorol. Soc.*, **84**, 46 (1958).
21. J. Freiberg, *Environ. Sci. Technol.*, **8**, 731 (1974).
22. K. G. Denbigh, *The Principles of Chemical Equilibrium*, 2nd ed., Cambridge University Press, New York, 1966.
23. J. R. Brock, *Atmos. Environ.*, New York, **5**, 833 (1971).
24. J. L. Katz, C. J. Scoppa, N. G. Kumar, and P. Mirabel, *J. Chem. Phys.*, **62**, 448 (1975).
25. S. L. Heisler and S. K. Friedlander, *Atmos. Environ.* **11**, 185 (1977).

CHAPTER 2 PARTICLE FORMATION IN PULVERIZED COAL COMBUSTION—A REVIEW

R. C. FLAGAN AND S. K. FRIEDLANDER

California Institute of Technology, Pasadena, California 91125

- | | |
|---|--|
| <ol style="list-style-type: none"> 1. Nomenclature, 25 2. Introduction, 26 3. Pulverized Coal Combustion, 28 4. Mineral Matter in Coal, 30 5. A Fly Ash Particle Formation, 34 6. Fine Particle Formation, 40 | <ol style="list-style-type: none"> 7. Fine Particle Enrichment by Volatile Species, 47 8. Sulfate Formation, 52 9. Concluding Comment, 55 <p style="text-align: center;">References, 56</p> |
|---|--|

1. NOMENCLATURE

		$n(d_p)$	particle size distribution function, particles $\text{cm}^{-3}\text{cm}^{-3}$
C_i	concentration, molecules cm^{-3}	$\bar{n}(v, t)$	particle size distribution function, particles $\text{cm}^{-3}\text{cm}^{-3}$
\bar{C}	concentration in fly ash	P	pressure
C_0, C_r	coefficients	p	number of ash particles produced per coal particle
d, d_p	particle diameter	R	gas constant
D	diffusivity	T	temperature
F	diffusion flux to particle surface	t	time
I_1, I_2, I_3	moments of free molecule regime self-preserving size distribution	u	gas velocity
I_D	integral for diffusion to surfaces of large particles	\bar{V}	total aerosol volume, cm^3g^{-1}
K	coefficient, defined by Eq. 12	v	particle volume
Kn	Knudsen number	α	mass fraction ash in coal
k	Boltzmann constant	α_c	accommodation coefficient
M	total mass per unit volume	α_v	volume fraction ash in coal
m	mass of gas molecule	$\beta(v, v')$	collision parameter
$\bar{N}(t)$	total number of particles per unit mass at time t	η	dimensionless particle volume
$n(v, t)$	particle size distribution function, particles $\text{cm}^{-3}\text{cm}^{-3}$	λ	mean free path
		τ	time parameter, defined by Eq. 12
		$\Psi(\eta)$	dimensionless distribution function

Subscripts

<i>r</i>	particle
<i>s</i>	small particles produced by homogeneous nucleation
<i>a</i>	ash
<i>c</i>	coal
<i>l</i>	large particles produced by breakup

2. INTRODUCTION

Particulate emissions from coal combustion sources were among the first forms of air pollution to be controlled. The opacity of stack plumes and the total mass of particulate matter emitted have been significantly reduced through improvements in combustor operation and the use of gas cleaning devices such as electrical precipitators. In spite of these improvements, coal combustion is still a major source of particulate emissions. Moreover, electrical precipitators may show a minimum in collection efficiency for particles in the 0.1–1.0 μm size range [1]. Such particles have longer atmospheric residence times and greater effects on health and visibility than would an equal mass of larger particles.

Coal combustion is an important source of heavy metals in the environment [2–9]. Many species, including cadmium, arsenic, selenium, lead, nitrogen, zinc, and antimony, are present in the fly ash particles emitted by coal fired power plants and in ambient urban aerosols in concentrations much larger than their natural crustal abundance [10] as shown in Fig. 1. Recent studies have shown that the concentrations of several trace species in fly ash increase with decreasing particle size [11–17]. Few measurements of ash size distributions have been made using techniques suitable for particles smaller than about 5 μm diameter [18]. Studies of the fractional efficiency of particle collection equipment have recently provided some more complete size distribution data [1, 19, 20]. Data on the composition-size distribution have been obtained for few sources and have not been extended far into the submicron size range.

The composition-size distributions of particles emitted by coal combustion sources are influenced by furnace design and operating conditions. A wide variety of coal combustion equipment is currently in use. New designs are being developed because of recent constraints on emissions of gaseous and particulate pollutants and on fuel availability. Electrostatic precipitator performance may be seriously impaired when a low sulfur coal is substituted for a coal with a higher sulfur content and correspondingly lower resistivity ash. Fabric filters may replace electrical precipitators for particle collection where low sulfur coal is burned. Some combustion modifications may change the quantities of fine particles in the flue gases. To anticipate the future requirements for particulate emission control and

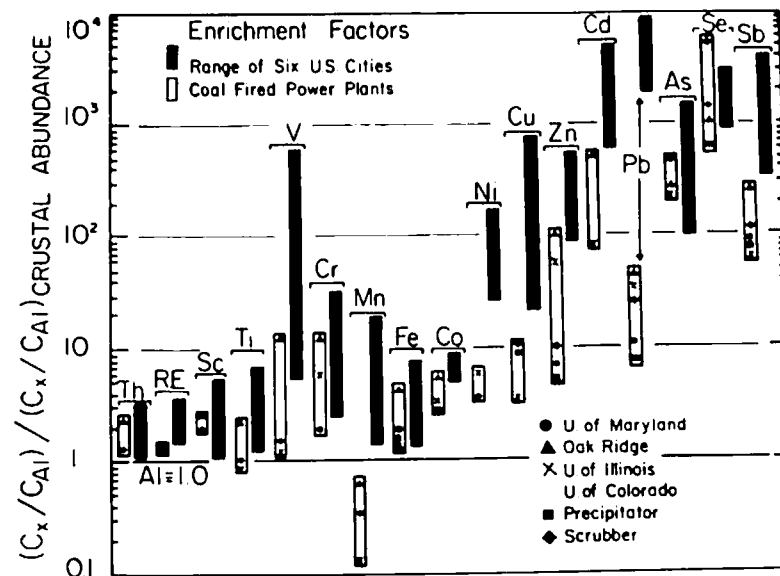


Fig. 1. Enrichment factors for several elements on ambient particles collected in several U.S. cities and on particles collected downstream of gas cleaning devices on coal fired power plants. Enrichment is calculated relative to the natural crustal abundance of the elements. (Data from Ref. 10.)

to evaluate the environmental impact of increased coal use, it is necessary to know the characteristics of the aerosol entering the gas cleaning devices. An examination of the mechanism of particle formation during coal combustion may provide much of the necessary information.

Emissions from coal combustion may include several types of materials, such as char, soot, fly ash, and droplets containing sulfuric acid. Improvements in combustion conditions have, in recent years, reduced the amount of partially burned coal char emitted from utility boilers. The combustible content of the particulate emissions from large sources generally accounts for only a small fraction of the total mass of emissions [11, 21]. Soot is formed by the condensation and subsequent pyrolysis of high molecular weight hydrocarbons [22, 23]. Fly ash is formed from the mineral matter in the coal. During combustion the mineral matter undergoes chemical transformations to form ash and, if temperatures are sufficiently high, the ash fuses to form spherical particles [24–34]. Some ash may be vaporized in the high temperature flame region and later condense homogeneously to

form large numbers of very small fly ash particles [35–37]. Submicron fly ash particles may also be produced by the bursting of bubbles as gases are evolved within molten ash particles [28, 29].

The presence of sulfur trioxide (SO_3) in the flue gases of coal fired boilers results in the formation of alkali metal sulfates or sulfuric acid when it condenses [37]. The homogeneous oxidation of sulfur to form SO_2 is fairly well understood [38]. Less is known about the mechanism of SO_3 formation. Generally about 1% of the sulfur is present in the flue gases as SO_3 [38]. As the flue gases cool, this SO_3 may condense with water vapor to form sulfuric acid droplets. Stack temperatures are usually maintained above the dew point of the SO_3 – H_2O mixture to prevent acid condensation within the stack.

Studies of the occurrence of deposits in boilers [37] and microscopic examinations of fly ash particles [24–34] provide the basis for a preliminary analysis of fly ash formation and identify some of the important processes that occur. The present study is restricted to the examination of particle formation in pulverized coal fired systems. This is the predominant method of coal combustion for electric power generation. Moreover, most of the available data on particle formation and emissions have been obtained on pulverized fuel equipment.

3. PULVERIZED COAL COMBUSTION

Pulverized coal fired boilers burn coal that has been crushed and ground to a fine powder [39, 40]. The mass mean diameter of the coal particles is typically in the range of 30 to 70 μm . The distribution of coal sizes is broad. A coal powder with a 50 μm mass mean diameter may have 10% of the mass smaller than 10 μm and 10% larger than 100 μm . The few reported measurements of coal size distributions indicate that the distribution varies significantly from one power plant to another [41]. Coal burned in a suspension at 1800–2500°K must remain at high temperature long enough for the largest particles to burn completely. About 1 sec is required to burn a 200 μm diameter coal particle. Smaller particles burn much more rapidly.

Pulverized coal fired boilers are generally large; units producing 500 MW electrical output are common. Many furnaces larger than about 600 MW are divided into two combustor chambers. Pulverized coal is injected into the furnace with about one-fifth of the total air flow, the primary air, through a number of burners [39]. A 500 MW boiler, illustrated in Fig. 2, may have 30 or more burners arranged in one of a number of possible patterns in the furnace walls. Preheated air is introduced into the furnace through air registers coaxial with the burners. In the furnace the coal is heated by thermal radiation and by mixing with hot combustion products,

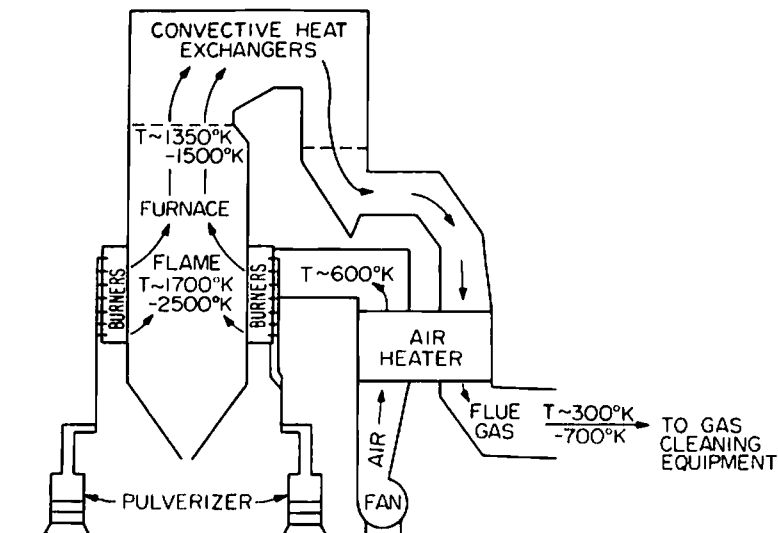


Fig. 2. Pulverized coal fired boiler.

igniting the coal particles. The temperatures of the burning coal particles and the gas surrounding them rise rapidly. Mixing in the furnace is relatively slow. As a result, the temperature and composition of the combustion gases are far from uniform. Although peak temperatures may be as high as 2500°K, some coal particles may be subjected to much lower combustion temperatures. The variability in time–temperature history of the coal particles may be responsible for much of the diversity of ash characteristics observed in the emissions from a combustion system. A complete representation of the kinetic processes occurring in a furnace would require a statistical description of the composition and temperature fluctuations and the residence time distribution in the boiler [42, 43].

In the furnace the temperature of the combustion products is reduced by the combined effects of radiation and convective heat transfer. About one-half of the heat released during combustion is transferred to the water tube walls of the furnace before the combustion products enter the convective heat exchangers. The temperature at the furnace outlet is limited to about 1350–1500°K in order to prevent damage to the superheater tubes. A long residence time of the combustion gases in the boiler, about 1 to 2 sec. is necessary to assure both complete combustion and adequate heat transfer upstream of the superheaters.

A typical 500 MW pulverized coal fired electric power plant has a furnace about 30 m high with a cross-sectional area of about 260 m^2 [44].

Operating at about 35% thermal efficiency, this unit requires about 1430 MW of thermal input, for instance, approximately 48 Kg sec^{-1} (170 T hr^{-1}) of a bituminous coal with a lower heating value of $3 \times 10^7 \text{ J kg}^{-1}$ ($12900 \text{ Btu lb}^{-1}$). Burning a coal containing 10% ash, this unit produces about 4.8 kg sec^{-1} (17 T hr^{-1}) of ash. If all the ash were carried out of the furnace in the flue gases, the aerosol mass loading would be about 9 g m^{-3} at standard conditions.

Pulverized coal is burned in a variety of types of combustors. The peak temperatures and the amount of ash impacting on the boiler walls are strongly influenced by the furnace design. Some units, designed to achieve rapid mixing of fuel and air, result in high combustion intensities and thus high flame temperatures. Boilers in which fuel and air mix relatively slowly have lower flame temperatures. Because nitric oxide emissions increase at high temperature, the latter designs are being favored for new installations. Cyclone burners were designed to remove most of the ash from the flue gases before they enter the superheaters where deposits cause reliability problems. As much as 80–90% of the ash is impacted on the burner of a cyclone fired furnace [45]. A large fraction of the ash, 60–100%, leaves the combustion chambers of most other types of boilers with the flue gases.

After the combustion products leave the combustion chamber, they enter a series of heat exchangers where heat is transferred from the hot gases to the heat transfer surfaces primarily by convection. In this region the combustion products are cooled from the boiler outlet temperature to the inlet temperature of the emission control equipment, $300\text{--}700^\circ\text{K}$, in a residence time of several seconds. The formation of deposits in this region and the corrosion that accompanies the deposits are major causes of boiler failure. The fraction of the ash deposited in this region is probably small.

4. MINERAL MATTER IN COAL

The ash forming constituents of coal occur in two main classes. Inherent mineral matter, which seldom exceeds 2% of the coal mass, is derived from the original plant substance. Extraneous mineral matter is inorganic material that was mixed with the plant substance as the coal was formed or during mining operations [37].

The extraneous mineral matter may be present as very fine inclusions dispersed throughout the coal volume, or it may be made up of large, distinct structures. The mineral inclusions are generally small compared to the mean coal particle size. Padia [33] has reported Rosin–Rammmler distributions fit to mineral size distributions measured after the carbon matrix of coal was oxidized in a low temperature ($T \approx 425^\circ\text{K}$) oxygen plasma. The measured volume mean diameters were 1.7 and $2 \mu\text{m}$ for a

lignite and a bituminous coal, respectively. From the size distribution parameters reported, the number mean diameter of the lignite inclusions is about $1 \mu\text{m}$. It is not possible to determine the number mean diameter using the parameters given for the inclusions in the bituminous coal.

The mineral matter in coal consists primarily of kaolinite ($\text{Al}_2\text{O}_3 \cdot 2\text{SiO}_2 \cdot 2\text{H}_2\text{O}$), pyrites (FeS_2), and calcite (CaCO_3) [37, 46]. The major elements in the coal minerals are those found in silicate rocks, silicon, aluminum, calcium, magnesium, iron, sulfur, sodium, potassium, chlorine, and titanium [47]. The mean concentrations of these major elements and a number of minor and trace species in coal are presented in Table 1.

Table 1. MEAN COMPOSITION FOR 101 COALS*

Constituent ^b	Mean		Standard		
			Deviation	Min	Max
As	14.02	PPM	17.70	0.50	93.00
B	102.21	PPM	54.65	5.00	224.00
Be	1.61	PPM	0.82	0.20	4.00
Br	15.42	PPM	5.92	4.00	52.00
Cd	2.52	PPM	7.60	0.10	65.00
Co	9.57	PPM	7.26	1.00	43.00
Cr	13.75	PPM	7.26	4.00	54.00
Cu	15.16	PPM	8.12	5.00	61.00
F	60.94	PPM	20.99	25.00	143.00
Ga	3.12	PPM	1.06	1.10	7.50
Ge	6.59	PPM	6.71	1.00	43.00
Hg	0.20	PPM	0.20	0.02	1.60
Mn	49.40	PPM	40.15	6.00	181.00
Mo	7.54	PPM	5.96	1.00	30.00
Ni	21.07	PPM	12.35	3.00	80.00
P	71.10	PPM	72.81	5.00	400.00
Pb	34.78	PPM	43.69	4.00	218.00
Sb	1.26	PPM	1.32	0.20	8.90
Se	2.08	PPM	1.10	0.45	7.70
Sn	4.79	PPM	6.15	1.00	51.00
V	32.71	PPM	12.03	11.00	78.00
Zn	272.29	PPM	694.23	6.00	5350.00
Zr	72.46	PPM	57.78	8.00	133.00
Al	1.29	%	0.45	0.43	3.04
Ca	0.77	%	0.55	0.05	2.67
Cl	0.14	%	0.14	0.01	0.54
Fe	1.92	%	0.79	0.34	4.32
K	0.16	%	0.06	0.02	0.43
Mg	0.05	%	0.04	0.01	0.25

Table 1. (Continued)

Constituent ^b	Mean	Standard Deviation	Min	Max
Na	0.05	%	0.04	0.20
Si	2.49	%	0.80	6.09
Ti	0.07	%	0.02	0.15
ORS	1.41	%	0.65	3.09
PYS	1.76	%	0.86	3.78
SUS	0.10	%	0.19	1.06
TOX ^c	3.27	%	1.35	6.47
SXRF	2.91	%	1.24	5.40
ADL	7.70	%	3.47	16.70
MOIS	9.05	%	5.05	20.70
VOL	39.70	%	4.27	52.70
FIXC	48.82	%	4.95	65.40
ASH	11.44	%	2.89	25.80
BTU/LB	12748.91		464.50	14362.00
C	70.28	%	3.87	80.14
H	4.95	%	0.31	5.79
N	1.30	%	0.22	1.84
O	8.68	%	2.44	16.03
HTA	11.41	%	2.95	25.85
LTA	15.28	%	4.04	31.70

^aFrom Ref. 47, reprinted with permission.

^bAbbreviations other than standard chemical symbols: organic sulfur (ORS), pyritic sulfur (PYS), sulfate sulfur (SUS), total sulfur (TOS), sulfur by X-ray fluorescence (SXRF), air-dry loss (ADL), moisture (MOIS), volatile matter (VOL), fixed carbon (FIXC), high temperature ash (HTA), low temperature ash (LTA).

When coal is heated, the mineral matter undergoes a number of transitions [48]. At temperatures below about 500°K dehydration and changes in mineral forms occur. Pyrite is oxidized at temperatures below about 800°K. Carbonates and sulfates decompose at temperatures in the range 500–1100°K, evolving CO₂, SO₂, and SO₃. Alkali salts, such as chlorides, are volatilized at an appreciable rate when the temperature exceeds about 1350°K. Silica may volatilize at temperatures higher than about 1900°K [33, 35, 36, 49–54], largely because of the reduction of SiO₂ by reaction with carbon to form SiO, which is much more volatile than SiO₂. At temperatures higher than about 2500°K, a condition that is not achieved in conventional pulverized coal combustion but may occur in magnetohydrodynamic generators, appreciable quantities of alumina may also be volatilized. Measurements of the distribution of ash composition as a function of

particle size suggest that many minor ash constituents are also vaporized during coal combustion.

The tests that determine the ash content of coals involve the slow combustion of coal at a relatively low temperature, about 1000°K, and determination of the quantity of the residual ash. Since combustion in boilers occurs at much higher temperatures, transitions that do not occur in the standard tests may take place. Some of these changes result in the evolution of considerable quantities of CO₂, SO₂, and SO₃. This decomposition may account for a major fraction of the weight loss of the ash, as is shown in Fig. 3. Nonetheless, a substantial fraction of the ash may be lost through vaporization. As much as 4–8% of the ash was vaporized in Padia's experiments [33].

The tendency of ash to melt when heated has posed problems for engineers since the earliest days of steam generation [37]. When coal is

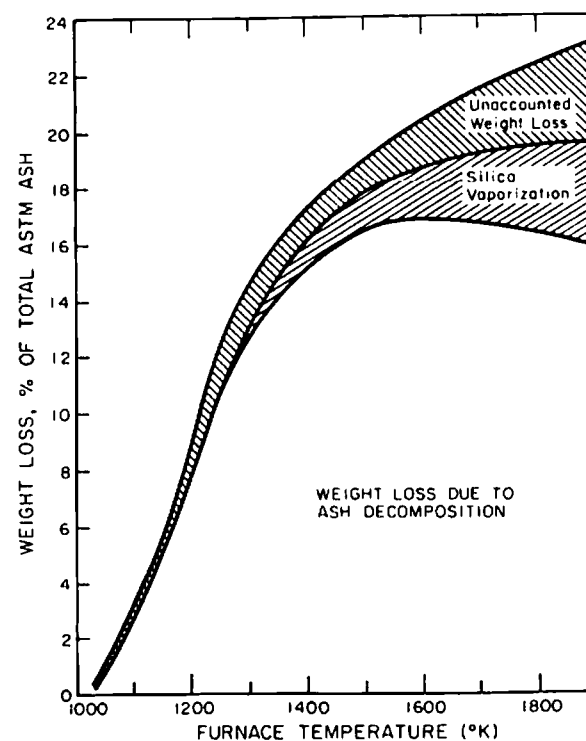


Fig. 3. Loss of ash during fuel lean combustion of 38–45 μm lignite particles in a laminar flow furnace. (From Ref. 33.)

burned in a fuel bed, the ash softens and then may fuse to form clinkers. To determine the relative tendencies of different coals to form clinkers, tests were devised to measure the fusibility of ash. Empirical tests have been developed to determine the initial deformation temperature, the softening temperature, and the fluid temperature [37]. More quantitative information is obtained for some ashes by measuring the viscosity of the ash as a function of temperature. The viscosity of the ash decreases rapidly with increasing temperature and also depends strongly on the composition of the ash. The presence of iron as Fe_2O_3 in the ash results in the ash behaving as a fluid at much lower temperatures than the same ash would behave if the iron were present only in its reduced state, FeO [37]. Other species have similar strong effects on the characteristics.

Examination of fly ash particles reveals that most particles were molten during their formation process. The particles tend to be spherical except where considerable agglomeration has occurred. Since the temperature at which the ash becomes fluid may vary over several hundred degrees, depending on the coal characteristics and whether the combustion environment is oxidizing or reducing, and since the peak temperatures are determined by the combustion conditions, it is expected that combustion conditions may strongly influence the character of the ash emissions.

5. FLY ASH PARTICLE FORMATION

The processes that influence the ash particle formation occur primarily in the final stages of coal particle burnout. Initially, as a coal particle is heated, volatile hydrocarbons originally present in the coal or produced by pyrolysis are vaporized. Some of the mineral matter inherent in the organic structure of the coal may be vaporized during this process. Mercury and other extremely volatile ash constituents may also be vaporized during this early phase of combustion. After the volatile hydrocarbons are vaporized, the residual char burns by heterogeneous oxidation, both on the external surface of the coal particle and internally. Under some conditions a coal particle may burn with very little change in diameter, the particle density decreasing because of internal burning. The rate at which coal particles smaller than about $100\ \mu\text{m}$ burn is, at temperatures below about $2000\text{--}2500^\circ\text{K}$, controlled by chemical kinetic processes. Diffusion of oxygen to the particle surface limits the rate of combustion of larger particles.

On heating, coal swells and becomes hollow or porous [28, 32, 55–59]. The degree of swelling depends on both the coal type and the combustion conditions. Hollow char particles, known as cenospheres, may be formed, particularly if the heating takes place in a reducing atmosphere [55].

Porous vesicular particles are more likely to form if the heating occurs in an oxidizing environment. Coal particles burn on both external and internal surfaces, so as a particle burns, fragile, lacy char structures are formed that eventually disintegrate [28, 56–59].

Ramsden [28] has postulated that mineral inclusions in coal particles melt within the carbon lattice as the combustion front approaches. Water vapor, carbon dioxide, and other gases are evolved because of the temperature rise. If the heating occurs sufficiently rapidly, the sudden increase in pressure within an inclusion and the decrease in the ash viscosity may shatter the inclusion, dispersing the ash into minute droplets. This dispersal may be accompanied by the disintegration of the carbon framework, releasing submicron particles into the gas stream, or the droplets may remain within the carbon framework and coalesce into a liquid layer. The ash has very high surface tension and does not wet the carbon surface. Therefore as the receding carbon surface brings molten inclusions into contact, the ash may coalesce to form spherical droplets larger than the original mineral inclusions. If the temperature of the particle is below the fusion point, the ash inclusions will not coalesce but may agglomerate and, if the temperature is not too low, sinter to form irregularly shaped ash particles. Hollow spherical fly ash particles, known as cenospheres, may form if gas evolution occurs within the particles at temperatures sufficiently high ($T \gtrsim 1200^\circ\text{K}$) for the ash to be fluid but low enough ($T \lesssim 1500^\circ\text{K}$) that the viscosity prevents the particles from expanding so rapidly that they burst [26, 33, 34]. Cenospheres are usually large ($d_p \gtrsim 50\ \mu\text{m}$) and, in large furnaces, account for no more than a few percent of the fly ash mass [26]. Fly ash particles containing bubbles have also been observed [24]. These particles may be formed at temperatures too low to result in cenosphere formation. Cenospheres that contain fly ash or char particles, called plerospheres [34], are probably formed from these particles.

Only a few of these processes need be considered to describe the formation of the dense fly ash particles that account for most of the mass of the particulate matter produced. These processes are summarized in Fig. 4. As a coal particle burns, the mineral inclusions melt and, when the receding carbon surface brings them into contact with one another, coalesce. Because of internal burning, the char particle may break up into a number of fragments. Thus more than one ash particle may be produced from each coal particle, but the total number of ash particles produced may be much less than the total number of mineral inclusions in the coal particle.

Laboratory experiments in which size segregated coal samples were burned in a laminar flow furnace have demonstrated the relationship

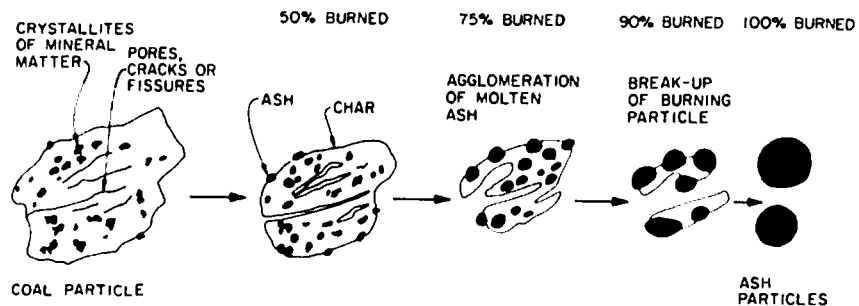


Fig. 4. Breakup mechanism for the formation of large fly ash particles.

between the coal particle size distribution and the size of large, dense ash particles produced during combustion [33]. Two size cuts, 38–45 μm and 75–90 μm , of two coals, a Pennsylvania bituminous coal and a Montana lignite, were burned under nearly constant temperature conditions. The swelling bituminous coal formed more cenospheres than did the relatively nonswelling lignite. Cenospheres were removed from the ash samples by density segregation in water. The ash particles denser than water were then sized by electron microscopy. Because of the sampling system, which used water to cool the ash, the density segregation system, and the large numbers of particles collected on the electron microscope grids, only particles larger than a few microns in diameter could be counted reliably. The measured size distribution of the ash particles could be correlated with the coal particle size by assuming that three ash particles per lignite particle and about five ash particles per bituminous coal particle were produced during combustion. These numbers are consistent with the expectation that the highly porous char particles formed by the highly swelling bituminous coal would break up into a larger number of fragments than the relatively nonswelling lignite. The number of ash particles produced per coal particle did not vary significantly over a factor of 2 change in the coal particle size.

Application of this breakup model to the formation of large fly ash particles in coal fired combustors requires knowledge of the coal particle size distribution, the ash forming characteristics of the coal being burned, and the combustion conditions. These data are not available for any studies in which the ash particle size distributions were also measured. Most measurements of coal particle size distributions have been made by mechanical sieving of the coal and provide little information about particles smaller than 50 μm . Measurements made using aerodynamic sizing and microscopy provide some data on the quantities of particles as small as a few microns in diameter, but the data are limited. Littlejohn [41]

measured the size distribution of pulverized coal as supplied to the burners in a number of boilers. The coal particle size distribution varied considerably from one installation to another. The ash content was also found to vary with coal particle size as a result of the design of pulverizers. The pulverized coal is removed from the mills aerodynamically. Since the mineral density, 2–6 g cm^{-3} , is higher than the coal density, about 1.3 g cm^{-3} , particles that contain significant quantities of mineral matter tend to remain in the pulverizers longer than do particles with a lower mineral content. The finest particles measured by Littlejohn, of about 14 μm diameter, included many consisting entirely of mineral matter and had a mean ash content as much as two times higher than the bulk of the coal.

In spite of these complications, we use these data to test the breakup model for ash formation. For the present purposes we assume that the mineral matter is uniformly distributed through all the coal particles and that p equal mass ash particles are produced from each coal particle. We further assume that the number of ash particles produced is independent of the coal particle size and the density of the ash particles is constant. If the mass fraction of ash in the coal is α (typically 5–20%), a coal particle of mass m produces p particles of mass $m = \alpha m' / p$. Noting that the ash density ρ_a is greater than the coal density ρ_c , the volume of the ash particles produced is

$$v = \frac{\alpha_c v'}{p} \quad (1)$$

where

$$\alpha_v = \alpha \left(\frac{\rho_c}{\rho_a} \right) \quad (2)$$

If the coal particle size distribution is $n_c(d_c)$, the ash particle size distribution is

$$n(d_p) = p \left(\frac{p}{\alpha_v} \right)^{1/3} n_c \left(d_p \left(\frac{p}{\alpha_v} \right)^{1/3} \right) \quad (3)$$

It is unlikely that the burnout of coal particles will result in the formation of ash particles smaller than the original mineral inclusions. For this reason the predicted ash size distribution has been truncated at the particle size where the ash particles predicted by the breakup model are the same size as the mass mean inclusion size. Below this size the coal particles are not expected to contain enough separate mineral grains to produce more than one ash particle per coal particle. These fine ash particles are assumed

to have the same size distribution as the mineral inclusions in the coal and to be unaffected by the coal particle size.

These calculations are compared in Fig. 5 with the mass size distribution data of McCain et al. [1], normalized with respect to the total mass of aerosol expected from a coal containing 10% ash burned at a fuel-air equivalence ratio of 0.85, that is, 15% excess air, with no loss of ash to the boiler walls. The data (solid points) are the averages of the measurements obtained at the electrostatic precipitator inlets of six pulverized coal fired power plants. The curve is the prediction of the breakup model assuming that the coal contains 10% ash and that the coal and ash densities are 1.3 and 2.3 g cm⁻³, respectively, and using a Rosin-Rammler mass distribution, which Field [40] suggests is typical for pulverized coal:

$$dM/d(d_p) = \left(\frac{1.2M}{d_p} \right) \left(\frac{d_p}{53\mu\text{m}} \right)^{1.2} \exp \left(- \left(\frac{d_p}{53\mu\text{m}} \right)^{1.2} \right) \quad (4)$$

where M is the total mass of coal per unit volume. It is assumed in this calculation that $p=4$. The coal size data of Littlejohn [41] are used to illustrate the sensitivity of the ash particle size distribution to the value of p

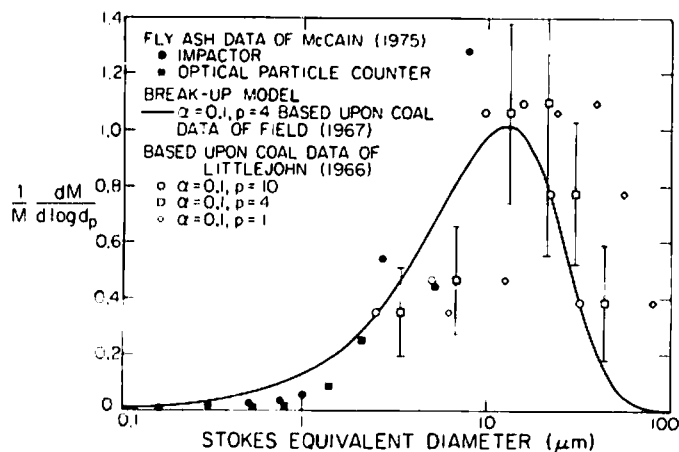


Fig. 5. Comparison of the mass distribution calculated using the breakup model with the fly ash size distribution measured upstream of electrical precipitators on coal fired power plants. The error bars on the $p=4$ points indicate the standard deviation in the calculated size distribution that results from the highly variable coal particle size distribution data of Littlejohn [41].

points. Values of $p=1$ (diamonds), $p=4$ (squares), and $p=10$ (circles) are illustrated. In spite of the large uncertainty in the coal size data and the use of coal size data and breakup model parameters derived in systems different from those in which the measurements were made, the calculations are in qualitative agreement with the data. Part of the discrepancy may be due to the arbitrary parameters used to estimate the total mass loading used in normalizing the fly ash data. The available coal size data permit predictions of ash size distributions only for particles larger than a few microns in diameter.

The fly ash number size distribution provides more information about the submicron particles. McCain et al. [1] have measured the distribution of submicron fly ash particles by using a combination of particle sizing

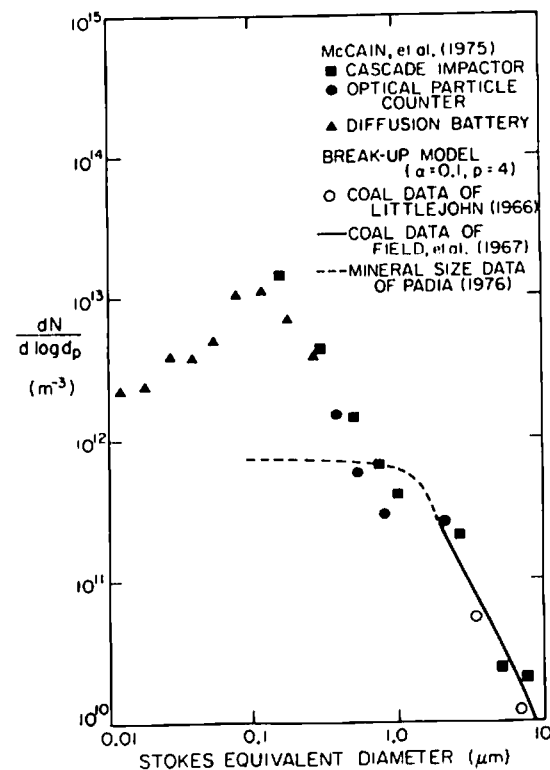


Fig. 6. Comparison of the number distribution predicted using the breakup model with the data of McCain et al. [1].

techniques, including a cascade impactor, an optical particle counter, and a diffusion battery. These data are presented in Fig. 6. The predictions of the breakup model for fly ash particle formation were made assuming $p=4$ and using the assumptions described earlier for ash constant and combustion conditions. The solid line is the prediction made using the coal size distribution of Field [40] and the open points are based on the data of Littlejohn [41]. The broken line shows the effect of truncating the size distribution with mineral size data obtained by Padia [33] for bituminous coal. The total number of particles predicted by this model is much less than the number measured by McCain et al. [1]. It does, however, show very close agreement with the measured numbers of particles larger than about $1 \mu\text{m}$ diameter. The discrepancy between the theory and the data below $1 \mu\text{m}$ is sufficiently large that minor changes in the parameters used in the calculations do not account for the difference.

6. FINE PARTICLE FORMATION

The simple breakup model predicts the size distribution of fly ash particles larger than the mineral inclusions. The calculated size distribution is in reasonable agreement with the measured volume distribution of fly ash, but does not agree with the measured number distribution for particles smaller than about $1 \mu\text{m}$ diameter. A mechanism that can produce several fly ash particles from a single mineral inclusion is required to explain the formation of large numbers of fine particles.

Two mechanisms of fine particle production have been identified. Gas evolution inside molten ash particles forms bubbles that may burst, breaking a single molten ash particle into a number of fine droplets [28]. The size of particles produced by this mechanism is not known, but will certainly depend on the ash composition and temperature, both of which strongly influence the viscosity of the ash [37]. Measurements of the contribution of this mechanism to fine particle formation are required before the breakup model can be extended to include this process. Some ash constituents vaporize in the flame. As the combustion products cool or when the chemical form of the volatilized ash changes (e.g., oxidation of SiO to form the less volatile species, SiO_2), the ash may condense. In spite of the high number densities produced by the breakup mechanism, some of the vapor may condense homogeneously to form very fine particles. Soot particles that are about $0.03\text{--}0.1 \mu\text{m}$ in diameter are formed in this manner [22, 23, 28], and there have been observations of production of a very fine silica aerosol, $0.01\text{--}0.15 \mu\text{m}$ in diameter, during coal combustion [35, 36]. The quantity of ash formed by homogeneous nucleation is not known. Homogeneous nucleation can produce finer particles than would be expected by any mechanical breakup process. With the limited data available

the relative importance of the two mechanisms for fine particle formation cannot be evaluated.

The quantity of ash in the submicron size range is only a small fraction, $0.5\text{--}4\%$ [1], of the total mass produced during combustion. Condensation of volatilized ash could, based on available data, form this mass of submicron sized particles. Silica accounting for as much as 4% of the ash was vaporized in laminar flow furnace experiments [33]. Another 4% ash loss that was not explained by ash decomposition may be the result of ash vaporization (see Fig. 3). Although these data were not obtained in large pulverized coal combustors, they do suggest that ash vaporization could result in the formation of a quantity of fine fly ash comparable to the measured mass of submicron particles. In the following analysis the contribution of homogeneous nucleation to fine particle production is explored qualitatively by assuming that a small fraction of the ash vaporizes during combustion.

Vaporization of 1% of the ash produces about 0.1 g of condensible material per standard cubic meter. Homogeneous nucleation of this ash would yield a very large number of extremely small particles, probably much smaller than $0.01 \mu\text{m}$ in diameter. These particles may coagulate with other particles produced by homogeneous nucleation, or they may diffuse to the surfaces of the much larger particles produced by the breakup process. In addition, heterogeneous condensation may occur after homogeneous nucleation. These processes reduce the number of particles produced by condensation and increase their average size.

As long as the particles are much smaller than the mean free path of the gas molecules, the evolution of the aerosol produced by homogeneous nucleation may be described by the theory of self-preserving size distributions for the free molecule regime [60, 61]. Previous applications of this theory have dealt with aerosol evolution in constant density systems. Since the temperature in combustion systems may change over nearly an order of magnitude, the analysis of Lai et al. [60] must be modified to treat variable density flows. For a fluid with uniform composition, the kinetic equation for aerosol evolution is [62]

$$\begin{aligned} \frac{\partial n(v, t)}{\partial t} + \nabla \cdot n(v, t) \mathbf{u} \\ = \frac{1}{2} \int_0^v \beta(\bar{v}, v - \bar{v}) n(\bar{v}, t) n(v - \bar{v}, t) d\bar{v} \\ - \int_0^\infty \beta(v, \bar{v}) n(v, t) n(\bar{v}, t) d\bar{v} \end{aligned} \quad (5)$$

where v is the particle volume, \mathbf{u} the gas velocity, and β the collision

frequency function. It is convenient to write the aerosol size distribution in terms of unit mass of carrier fluid instead of volume, that is,

$$\tilde{n}(v, t) = \frac{n(v, t)}{\rho} \quad (6)$$

Substituting Eq. 6 into Eq. 5 and using conservation of mass, the result is

$$\begin{aligned} \rho \frac{\partial \tilde{n}(v, t)}{\partial t} + \rho \mathbf{u} \cdot \nabla \tilde{n}(v, t) \\ = \frac{\rho^2}{2} \int_0^v \beta(\tilde{v}, v - \tilde{v}) \tilde{n}(\tilde{v}, t) \tilde{n}(v - \tilde{v}, t) d\tilde{v} \\ - \rho^2 \int_0^\infty \beta(v, \tilde{v}) \tilde{n}(v, t) \tilde{n}(\tilde{v}, t) d\tilde{v} \end{aligned} \quad (7)$$

The left-hand side represents the substantial derivative

$$\rho \frac{d\tilde{n}}{dt} = \rho \frac{\partial \tilde{n}}{\partial t} + \rho \mathbf{u} \cdot \nabla \tilde{n}$$

The right-hand side represents the usual coagulation terms written in terms of number per unit mass. The total number and volume of particles may also be calculated on a mass basis, namely,

$$\begin{aligned} \tilde{N}_s &= \int_0^\infty \tilde{n}(v, t) dv \\ \tilde{V}_s &= \int_0^\infty v \tilde{n}(v, t) dv \end{aligned} \quad (8)$$

Following the analysis of Lai et al. [60], we find that the total number of fine particles decays according to

$$\frac{d\tilde{N}_s}{dt} = -\frac{1}{2} \left[\frac{3}{4\pi} \right]^{1/6} \left(\frac{6kT}{\rho_p} \right)^{1/2} \left(\frac{P}{RT} \right) I_1 \tilde{V}_s^{1/6} \tilde{N}_s^{11/6} \quad (9)$$

where $I_1 = 6.67$ [60] is the dimensionless collision integral. From this result we see that the rate of loss of particles due to coagulation varies inversely with the $1/2$ power of the temperature.

The number and size of the fine particles also change by diffusion of fine particles to larger particles and heterogeneous condensation. The self-preserving theory is a reasonable approximation for the evolution of

the fine aerosol if the rate of loss of fine particles to the surfaces of larger particles is slow compared to the rate of coagulation and the rate of particle growth by condensation is small compared to the growth by coagulation. The number of particles of size d_s to $d_s + d(d_s)$ diffusing to the surface of a large particle of size d_L per unit time is

$$F = \frac{2\pi D(1 + \text{Kn}_L) \tilde{n}_s(d_s) d(d_s)}{(1 + 1.71 \text{Kn}_L + 1.333 \text{Kn}_L^2)} \quad (10)$$

where $\text{Kn}_L = 2\lambda/d_L$ is the Knudsen number and the Fuchs and Sutugin interpolation formula [63] has been used to describe the diffusion of particles in the transition regime. The total rate of loss of small particles to all large particles is

$$\left(\frac{d\tilde{N}_s}{dt} \right)_D = \frac{-I_D I_2 (2\pi mkT)^{1/2} \tilde{N}_s^{5/3} \tilde{V}_s^{-2/3}}{\left(\frac{2}{3} \right) (1 + \pi\alpha_c/8) (6/\pi)^{2/3}} \quad (11)$$

The diffusion integral is defined as

$$I_D = \int_{d_L} \frac{(1 + \text{Kn}_L) d_L \tilde{n}_L(d_L) d(d_L)}{d_L (1 + 1.71 \text{Kn}_L + 1.333 \text{Kn}_L^2)} \quad (12)$$

and is a function of temperature since $\lambda \propto T$. The integral

$$I_2 = \int_0^\infty \psi(\eta) \eta^{-2/3} d\eta \quad (13)$$

has a value of 1.87. Thus total rate of decay of the number of particles is the sum of Eqs. 9 and 11, that is,

$$\begin{aligned} \frac{d\tilde{N}_s}{dt} = & - \left(\frac{I_1}{2} \right) \left[\frac{3}{4\pi} \right]^{1/6} \left(\frac{6kT}{\rho_p} \right)^{1/2} \left(\frac{P}{RT} \right) \tilde{V}_s^{1/6} \tilde{N}_s^{11/6} \\ & - \frac{I_D I_2 (2\pi mkT)^{1/2} \tilde{N}_s^{5/3} \tilde{V}_s^{-2/3}}{\left[\left(\frac{2}{3} \right) (1 + \pi\alpha_c/8) (6/\pi)^{2/3} \right]} \end{aligned} \quad (14)$$

It is important to note that this equation is valid only if the magnitude of the second term is much smaller than that of the first term.

The volume of small particles also decreases as a result of diffusion to the surface of large particles. The rate of decay of the volume of fine

particles is

$$\frac{d\bar{V}_s}{dt} = \frac{-I_D I_3 \left(\frac{3}{2}\right) (2\pi mkT)^{1/2} (\pi/6)^{2/3} \bar{N}_s^{2/3} \bar{V}_s^{1/3}}{(1 + \pi\alpha_c/8)} \quad (15)$$

where

$$I_3 = \int_0^\infty \eta^{1/3} \psi(\eta) d\eta = 0.885 \quad (16)$$

This model for the evolution of the size distribution has been used to examine the contribution of homogeneous nucleation to the formation of submicron ash particles. Several important assumptions were made. The large particle size distribution given by the breakup model was assumed to be unaffected by coagulation or by diffusion of fine particles to the surfaces of the large particles. This assumption is reasonable for particles larger than $1 \mu\text{m}$ but may not be appropriate for smaller particles. The furnace, illustrated in Fig. 2, is modeled as a plug flow reactor with uniform composition and temperature at any point. The temperature is assumed to remain constant at a flame temperature of 1800°K for 0.5 sec. The temperature of the combustion products then decreases at a constant rate to the furnace outlet temperature, 1400°K , in 1 sec. Once the combustion products enter the convective heat exchangers, heat transfer is more rapid; the temperature decreases to 425°K in 2 sec. It was further assumed that 1% of the fly ash was vaporized during combustion and immediately condensed by homogeneous nucleation.

The fly ash size distribution calculated using this model is shown in Fig. 7. The total number of particles predicted is an order of magnitude greater than the measured value, and the calculated size distribution has a narrow peak at a particle diameter of about one-fifth that of the broader peak of the measured distribution. Although the predicted small particle number concentration is too large, we estimate that only one-fourth of the fine particle volume is lost by diffusion to the surfaces of the larger particles. We can, therefore, neglect the second term of Eq. 14 in the examination of the causes of this large discrepancy.

The total number of particles is obtained by integrating Eq. 9 with the assumption that the number initially is infinite:

$$\bar{N}_s = \left(\frac{5}{6} K \bar{V}_s^{1/6} \tau\right)^{-6/5} \quad (17)$$

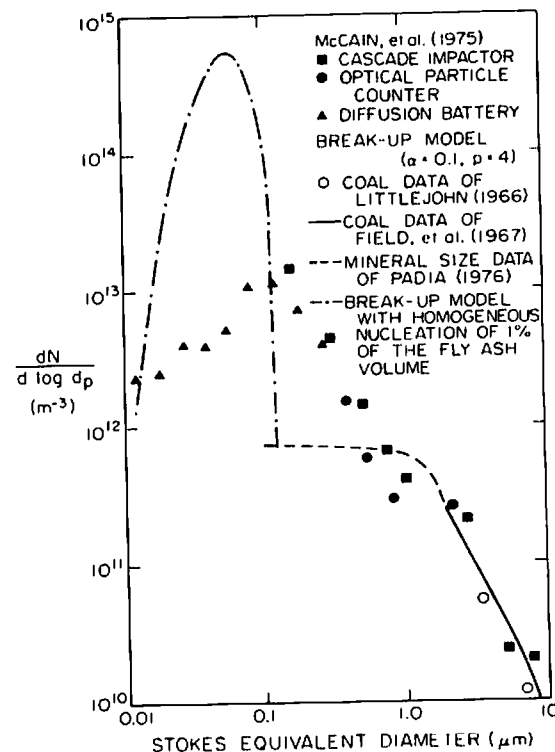


Fig. 7. Comparison of the number distribution calculated using the breakup model with homogeneous nucleation of 1% of the ash with the measured size distribution.

where

$$K = \left(\frac{I_1}{2}\right) \left[\frac{3}{(4\pi)}\right]^{1/6} \left(\frac{6kT_0}{\rho_p}\right)^{1/2} \left(\frac{P}{RT_0}\right)$$

$$\tau = \int_0^t \sqrt{T_0/T} dt \quad (18)$$

and T_0 is an arbitrary reference temperature. The total number of particles is proportional to $\tau^{-6/5}$. Even with this strong dependence on the residence time, increase in the residence time alone cannot account for all the discrepancy. The residence time would have to be increased by about a factor of 30 to bring the calculations into reasonable agreement with the

measurements. Such a factor would not be reasonable for the usual combustion conditions.

Interparticle dispersion forces increase the rate of coagulation of aerosols in the free molecule regime by a factor that depends on the sizes of the colliding particles and the ratio $A/(kT)$ [61]. The Hamaker constant A depends on the nature of the two interacting materials. Graham and Homer [61] have estimated the effect of dispersion aerosols on the coagulation of a free molecular aerosol of lead with a self-preserving size distribution. The coagulation rate increased by a factor of 2 for a value of $A/(kT)=15$ and a factor of 2.5 for $A/(kT)=39$. The Hamaker constant of silica is $6-12 \times 10^{-13}$ erg [64, 65]. The ratio A/kT is in the range 1.7-30 for a silica aerosol in a combustion system. Based on the calculation of Graham and Homer [61], we estimate that the coagulation rate increases by less than a factor of 2.5. Thus dispersion forces may reduce the total number of particles by as much as a factor of 3, but cannot account for the full difference between the measured and calculated number of particles.

The number of ash particles depends only weakly on the volume of ash in the fine particle mode,

$$\tilde{N}_s \propto \tilde{V}_s^{-1/5} \quad (19)$$

however, the size of the particles produced is a somewhat stronger function

$$d_s = \left(\frac{6}{\pi} \cdot \frac{\tilde{V}_s}{\tilde{N}_s} \right)^{1/3} \propto \tilde{V}_s^{2/5} \quad (20)$$

Thus an increase in the concentration of the condensing species would reduce the number and increase the size of the particles produced by homogeneous nucleation. A large change in concentration is required to produce a significant change in the aerosol characteristics.

The composition of the gas in a flame is highly nonuniform. Although a furnace is supplied with excess air, regions of the combustion zone have greater than the stoichiometric fuel-air ratio. Spatial variations in composition occur in the regions of fuel and air injection, and some spatial inhomogeneity may persist throughout the flow. Localized fluctuations in composition that are dissipated by turbulence are also important to aerosol evolution. Corrsin [66] has shown that second order kinetic processes, such as aerosol coagulation, are accelerated by these small scale fluctuations in composition.

Several processes not considered in the model may have major influence on the particle size distribution. Heterogeneous condensation may increase the size of the fine particles. Highly volatile ash constituents may condense

after large numbers of particles have been produced by the homogeneous nucleation of less volatile species. Because of the very large surface area of the fine particles, the more volatile compounds may condense on existing particles. Species other than ash may also condense on the fine particles. Sulfur trioxide and water vapor are both present in the combustion products. As the combustion products cool, these two species may react to form sulfuric acid and condense.

Some of the fine particles are soot rather than fly ash. The quantity of soot produced during coal combustion is not known. Soot is formed by the condensation and subsequent pyrolysis of high molecular weight hydrocarbons [22]. These soot precursors are formed only in very fuel-rich regions of flames. The soot particles burn readily in the presence of oxygen at combustion temperatures but burn very slowly at lower temperatures [67]. Relatively minor changes in combustion conditions may result in substantial changes in the quantity of soot produced. In a recent study, combustion modifications designed to reduce emissions of oxides of nitrogen resulted in a factor of 5 increase in the number of particles in the range 0.01-0.1 μm diameter [20], the typical size range for soot particles.

Until the chemical composition of the submicron particles is known, we can only speculate about the relative importance of ash, sulfates, and soot. The contributions of these components may vary significantly from one combustor to another. The formation of fine ash and soot particles is dependent on combustion conditions. Sulfates may be present as either gases or particles, depending on the flue gas temperature at the point where the sample is taken.

Finally, the discrepancy between the model calculations and the measured number of submicron particles may be attributed in part to uncertainties in the experimental measurements. Even diluting the sample by a ratio of 1000:1, the number concentration of particles measured is sufficiently high (initially 10^{13} m^{-3} measured and $2 \times 10^{14} \text{ m}^{-3}$ calculated) that either the diffusion battery-condensation nuclei counter system [1] or the electrical aerosol analyzer [20] might not be able to count all the particles. Moreover, neither of the two instruments has perfect size resolution, so it is expected that the measured peak in the number distribution would be somewhat broader than the actual distribution.

7. FINE PARTICLE ENRICHMENT BY VOLATILE SPECIES

A number of ash species vaporize during combustion and later condense either homogeneously or heterogeneously. Homogeneous nucleation produces very fine particles containing the volatile ash species. Heterogeneous condensation may also concentrate volatile species in fine particles. The

number of molecules of condensing species condensing per unit time on the surface of a particle of size d_p (number per second) in the free molecule regime ($Kn > 1$) is

$$F_i = \alpha_c \pi d_p^2 \left(\frac{kT}{2\pi m_i} \right)^{1/2} (C_i - C_{i,s}) \quad (21)$$

where C_i is the concentration in molecules per unit volume and $C_{i,s}$ is the saturation concentration. The number of molecules condensing on particles of size d_p per unit mass of particles is

$$\frac{F_i}{[\rho_p (\pi/6) d_p^3]} \propto d_p^{-1} \quad (22)$$

Thus the concentration of a condensing species on particles in the free molecule regime is expected to be inversely proportional to the particle diameter.

In the continuum regime, $Kn < 1$, the number of particles and the number of molecules condensing per unit time on a particle is

$$F_i = 2\pi d_p D (C_i - C_{i,s}) \quad (23)$$

Thus the number of molecules of the condensed species per unit mass of particles is inversely proportional to the square of the particle diameter, for example,

$$\frac{F_i}{[\rho_p (\pi/6) d_p^3]} \propto d_p^{-2} \quad (24)$$

Composition-size distribution data are available for a number of fly ash species in particles larger than about $1 \mu\text{m}$ diameter, that is, the continuum size range even at the highest temperatures in a furnace [11–17]. Davison et al. [11] have shown that the concentrations of several volatile ash constituents were well correlated with the particle size by the expression,

$$\bar{C} = C_0 + \frac{6C_s}{\rho_p d_p} \quad (25)$$

which is consistent with adsorption on the particle surface. The data are also well correlated by Eq. 24 as is shown in Fig. 8. The correlations of the concentrations of the species that exhibited the most pronounced increase

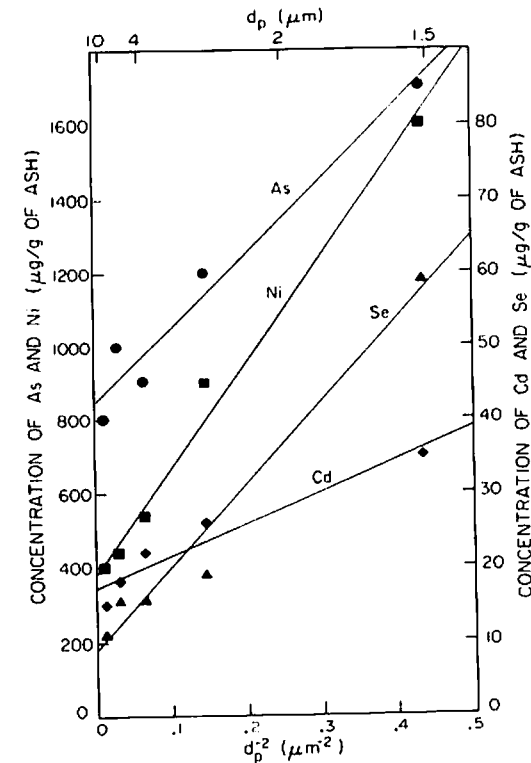


Fig. 8. Dependence of element concentration on particle size fly ash emitted from a coal fired power plant [11].

in concentration with decreasing particle size are summarized in Table 2. The linear correlation coefficients calculated using both models are comparable for all species considered. These data are not sufficient to differentiate between condensation and adsorption. Sulfur is present in fine fly ash particles in concentrations too large to be explained by adsorption alone, so it appears that some species do condense [11]. The existence of a surface layer containing high concentrations of volatile ash species has recently been confirmed by ion microprobe studies on large fly ash particles [68].

There are few data on the composition-size distribution for submicron fly ash particles. Ragaini and Ondov [16] observed two peaks in the number distribution, a sharp peak occurring at about $0.1 \mu\text{m}$ diameter and a second peak at about $1 \mu\text{m}$. A number of species were found in the

Table 2. PARAMETERS DERIVED FROM SURFACE DEPOSITION MODELS

Element	Present Work				Davidson et al. [11]		
	a (μgg^{-1})	$c = a + b/d_p^2$ b ($\mu\text{g}\cdot\mu\text{m}^2\cdot\text{g}^{-1}$)	Linear Correlation Coefficient	C_0 (μgcm^{-2})	$c = C_0 + 6C_i/(\rho_p d_p)$ C_i (μgg^{-1})	Linear Correlation Coefficient	
Pb	1400	530	0.58	0.04	1000	0.73	
Tl	55	53	0.71	0.003	40	0.80	
Sb	30	54	0.97	0.007	20	0.93	
Cd	17	43	0.96	0.002	10	0.99	
Se	9	110	0.98	0.004	0.7	0.92	
As	850	2000	0.98	0.009	600	0.97	
Zn	7400	16000	0.59	0.6	6000	0.60	
Ni	770	2900	0.99	0.1	100	0.98	
Cr	220	7200	0.99	0.3	300	0.94	

smaller peak in much higher concentrations than in the larger peak. The data are only qualitative, however, since neither the total mass loading of the collected aerosol nor the quantities of particles larger than about 3 μm were reported.

The condensation of a volatile species onto the submicron ash can be explored by a simple calculation. The rate of condensation onto particles over the entire range of particle sizes can be described by using the Fuchs and Sutugin interpolation formula [63], for example,

$$F_i = \frac{2d_p D_i (1 + K_n)}{(1 + 1.71K_n + 1.333K_n^2)(C_i - C_{i,s})} \quad (26)$$

The total deposition rate (molecules $\text{sec}^{-1} \text{g}^{-1}$) of a species condensing at a temperature T on an aerosol with a size distribution $\bar{n}(d_p, t)$ is

$$f_i(d_p, T) = \int_0^\infty F_i(d_p, T) \bar{n}(d_p, t) d(d_p) \quad (27)$$

The calculated condensation rate distribution of a species condensing on particles with the size distribution measured by McCain et al. [1] is shown in Fig. 9.

This result suggests that the majority of a species condensing at this temperature would be concentrated in the submicron particles. If the

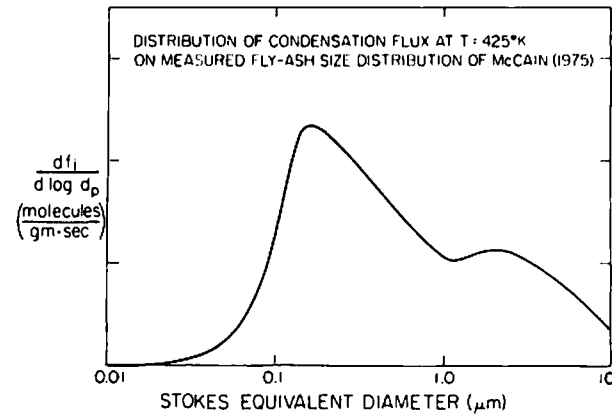


Fig. 9. Calculated distribution of condensation flux to the size distribution measured by McCain et al. [1].

condensation took place earlier in the evolution of the aerosol, the enrichment of submicron particles would be increased because of the larger surface area per unit mass of the smaller particles.

A volatile species that condenses by homogeneous nucleation would probably be uniformly distributed over submicron sized particles since the fine particles undergo considerable growth by coagulation. These fine particles diffuse to the surfaces of larger particles, that is, $F_i \alpha d_p$. Thus we again find that the concentration of the condensing species on particles in the continuum regime would be proportional to d_p^{-2} .

8. SULFATE FORMATION

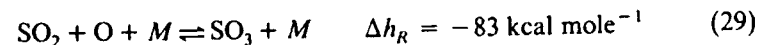
The particulate matter produced during coal combustion contains high concentrations of sulfur [11]. As has been observed with other volatile species, the sulfur concentration is greater in fine particles than in larger particles. This may be due to the condensation of sulfur trioxide and water to form a sulfuric acid mist. Although only a small fraction of the sulfur in coal is oxidized to form SO_3 , the sulfur trioxide has a major impact on boiler operation and aerosol characteristics. Most boiler corrosion appears to be related to the formation of sulfates from SO_3 [37]. The sulfate concentration of fly ash has a strong effect on its electrical resistivity and thus on the collection efficiency of electrical precipitators. The fly ash produced by combustion of low sulfur coals is difficult to remove because of its high electrical resistivity. At some power plants that burn low sulfur coal, SO_3 is added to the flue gases to improve precipitator efficiency.

Cullis and Mulcahy [38] have provided a comprehensive review of the literature on sulfur chemistry and the formation of SO_3 and sulfates in combustion systems, so we only briefly discuss some of the important points influencing the formation of sulfate aerosols within a coal fired boiler. Sulfur contained in fossil fuels is rapidly oxidized to form SO_2 in the high temperature combustion region. Generally less than a few percent of the SO_2 is oxidized to form SO_3 even in the presence of excess oxygen. The thermodynamic equilibrium



favors SO_3 formation at ambient temperatures. In the presence of the stoichiometric proportion of oxygen at atmospheric pressure, the equilibrium fractions of the sulfur present as SO_3 rather than SO_2 at 575, 775, and 1275°K are about 1, 0.5, and 0.0, respectively. Increasing the oxygen concentration two orders of magnitude changes these figures to about 1, 0.95, and 0.02.

The primary reaction leading to SO_3 production appears to be



Since the concentration of oxygen atoms is much higher than its equilibrium value within the flame front, SO_3 is formed in much greater than equilibrium concentrations in the flame front [38]. This super-equilibrium SO_3 concentration decreases toward the equilibrium value as the combustion products cool.

The equilibrium SO_3 concentration increases with decreasing temperature, but the low equilibrium oxygen atom concentration prevents the formation of SO_3 via the reaction in Eq. 29 at temperatures lower than about 1375°K. Thus the homogeneous gas phase formation of SO_3 occurs primarily in the furnace when temperatures are higher than this value (Fig. 2). Catalysis by heat transfer surfaces of particles may facilitate SO_3 formation at lower temperatures in the convective passes of the boiler.

The total SO_3 formed by homogeneous chemistry in a flame generally accounts for about 1% of the sulfur. Under normal combustion conditions, 10–30% excess air, the conversion of SO_2 to SO_3 is insensitive to the amount of oxygen present in the combustion products as is shown in Fig. 10 [69]. The SO_3 concentration decreases rapidly, however, as the quantity of excess air is reduced.

Catalytic oxidation of SO_2 may occur on the surfaces of fly ash particles in boilers. Ferric oxide and vanadium pentoxide are both efficient catalysts for SO_3 formation. Other species present in the fly ash may reduce the effectiveness of these materials as catalysts. The relative importance of homogeneous chemistry and catalysis to the formation of SO_3 has been a source of controversy. The strong dependence of the SO_3 concentration on the oxygen concentration in the range 0–3% O_2 and the much weaker dependence at high oxygen concentrations is the strongest evidence that most of the SO_3 is formed in the flame. A catalytic mechanism would be expected to produce more SO_3 with increasing oxygen concentration beyond the 3% level. Moreover, the levels of SO_3 produced in coal fired boilers are comparable to those produced in the absence of catalysts.

Sulfur dioxide may also react with ash constituents and metal surfaces. Sodium accounts for about 0.02–0.15% of the coal mass; potassium is about 0.08–0.3% of the coal [47]. These two species readily form sulfates, which are the source of many of the corrosion problems in coal fired boilers. Sodium salts are completely converted to atomic sodium in the high temperature regions of a flame. Sodium intermediates may react with SO_2 or SO_3 to form Na_2SO_4 in the flame, or it may be formed on surfaces. Sodium sulfite is formed under reducing conditions. The chemistry of

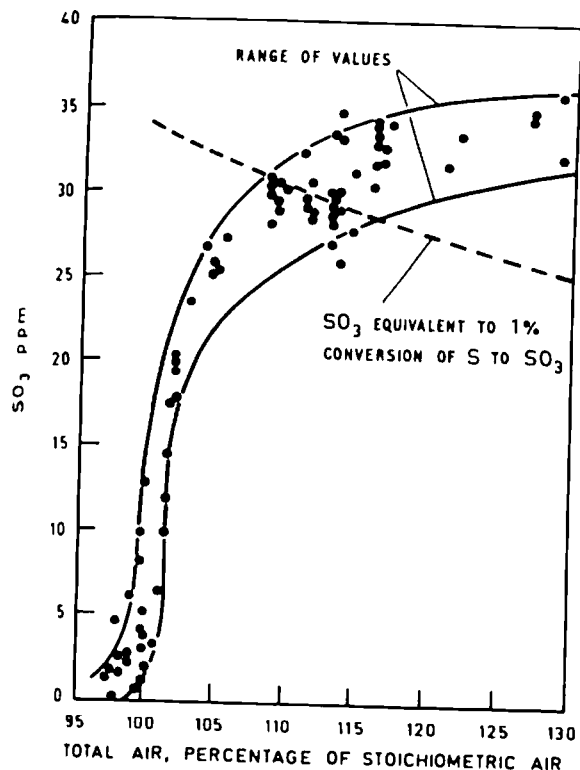


Fig. 10. Effect of excess air on the formation of SO_3 in premixed combustion of natural gas with 5.5 weight percent S as H_2S . (After Ref. 68.)

formation of alkali sulfates and sulfites in flames is poorly understood. Sulfur oxides may also react with other metal oxides, such as Fe_3O_4 [70], to form sulfates.

Sulfur trioxide in the flue gases increases the dew point to as high as 430°K . When the combustion products are cooled below this temperature, SO_3 may condense with water to form sulfuric acid droplets. This condensation may account for a significant fraction of the fine particle mass and cause severe corrosion when it occurs in the boiler or stack. Stack temperatures are usually maintained at higher levels than the dew point to prevent condensation within the plant.

9. CONCLUDING COMMENT

This chapter has reviewed the current understanding of the processes involved in particle formation during the combustion of pulverized coal. Ash derived from the mineral matter in coal accounts for the major portion of the particulate matter produced. It is also the source of many potentially toxic constituents of the particulate emissions. A number of processes that contribute to fly ash formation are summarized in Fig. 11. We have seen that the particle size distribution of ash particles larger than about $1\ \mu\text{m}$ diameter can be related to the coal particle size distribution. This model was based on observations of ash particle formation under conditions similar to those occurring in conventional pulverized coal combustion. New combustion systems may have much different emission characteristics. If coal is burned at temperatures below the ash fusion temperature, the mineral inclusions in a burning coal particle may not agglomerate. The size of the ash particles produced in such a system (e.g., a fluidized bed combustor) may more closely resemble the size distribution of the mineral grains than the coal size distribution. Very high temperature combustion, such as in magnetohydrodynamic power generation, would certainly increase the quantity of ash vaporized.

The formation of submicron sized particles probably occurs by homogeneous nucleation of volatilized ash, soot, and sulfates as well as by the breakup of burning coal particles. The relative contributions of these components can only be determined by further experimental work. Chemical analysis of the submicron aerosol can provide valuable information on the sources of fine particles.

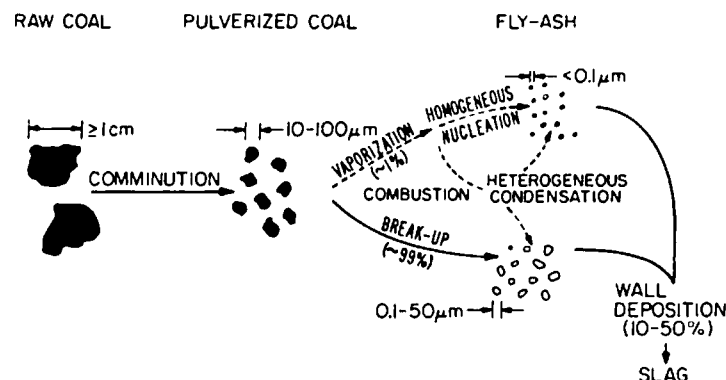


Fig. 11. Processes that contribute to fly ash particle formation.

Simple calculations have shown that condensation can result in substantial enrichment of submicron particles with volatile species. The fraction of a vapor that condenses on fine particles is a strong function of the particle size distribution. The calculations were for heterogeneous condensation on the aerosol present at the inlet to the electrostatic precipitator on a coal fired power plant. This aerosol may contain sulfuric acid and water, which condense at low temperatures. If these components contribute significantly to the submicron aerosol, the surface area of submicron particles available for condensation at higher temperatures is smaller than was assumed in our calculations. The quantity of an ash component that condenses on submicron particles may therefore be less than our calculations suggest. The quantities of sulfuric acid and water contained in the fine particles is not known. Measurements of the composition-size distribution of the fine particles present upstream of gas cleaning equipment will be required to determine the degree to which fine particles are enriched with volatile species.

ACKNOWLEDGMENT

This work was conducted under grants from the Caltech Energy Research Program, which is supported by the Ford Motor Company and the Exxon Corporation, and from the National Science Foundation, Project RANN.

REFERENCES

1. J. D. McCain, J. P. Gooch, and W. B. Smith, *J. Air Poll. Control Assoc.*, **25**, 117-121 (1975).
2. O. I. Joensuu, *Science*, **172**, 1027-1028 (1971).
3. K. K. Bertine and E. D. Goldberg, *Science*, **173**, 233-235 (1971).
4. C. E. Billings and W. R. Matson, *Science*, **174**, 1232-1233 (1972).
5. D. H. Klein and P. Russell, *Environ. Sci. Technol.*, **7**, 357-358 (1973).
6. A. W. Andren, D. H. Klein, and Y. Talmi, *Environ. Sci. Technol.*, **9**, 856-858 (1975).
7. C. Block and R. Dams, *Environ. Sci. Technol.*, **9**, 146-150 (1975).
8. C. Block and R. Dams, *Water, Air, Soil Pollut.*, **5**, 207-211 (1975).
9. D. F. Gatz, *Atmos. Environ.*, **9**, 1-16 (1975).
10. G. E. Gordon, D. D. Davis, G. W. Israel, H. E. Landsberg, T. C. O'Haree, S. W. Staley, and W. H. Zoller, "Atmospheric Impact of Major Sources and Consumers of Energy," Progrec Report-75, 1 October 1974 to 31 August 1975, University of Maryland, College Park.
11. R. L. Davison, D. F. S. Natusch, J. R. Wallace, and C. A. Evans, Jr., *Environ. Sci. Technol.*, **8**, 1107-1113 (1974).

12. R. E. Lee, Jr., and D. J. von Lehmden, *J. Air Pollut. Control Assoc.*, **23**, 853-857 (1973).
13. R. E. Lee, Jr., H. L. Crist, A. E. Riley, and K. E. MacLeod, *Environ. Sci. Technol.*, **9**, 643-647 (1975).
14. J. W. Kaakinen, R. M. Jorden, M. H. Lawasani, and R. E. West, *Environ. Sci. Technol.*, **9**, 862-869 (1975).
15. D. H. Klein, A. W. Andren, J. A. Carter, J. F. Emergy, C. Feldman, W. Fulkerson, W. S. Lyon, J. C. Ogle, Y. Talmi, R. I. Van Hook, and M. Bolton, *Environ. Sci. Technol.*, **9**, 973-979 (1975).
16. R. C. Ragaini and J. M. Ondow, "Trace Contaminants from Coal-Fired Power Plants," presented at the International Conference on Environmental Sensing and Assessment, Las Vegas, September 1975.
17. C. Block and R. Davis, *Environ. Sci. Technol.*, **10**, 1011-1017 (1976).
18. L. J. Shannon, P. G. Gorman, and M. Reichel, "Particulate Pollutant Emission Study: Vol. II. Fine Particle Emissions," EPA Report No. APTD 0744, August 1971.
19. E. J. Schulz, R. B. Engdahl, and T. T. Frankenberg, *Atmos. Environ.*, **9**, 111-119 (1975).
20. E. W. Schmidt, J. A. Gieseke, and J. M. Allen, "Size Distribution of Fine Particulate Emissions from a Coal-Fired Power Plant," *Atmos. Environ.*, **10**, 1065-1069 (1976).
21. *Steam, Its Generation and Use*, Babcock and Wilcox, New York, 1972.
22. J. Lahaye, G. Prado, and J. B. Donnet, *Carbon*, **12**, 27-35 (1974).
23. G. P. Prado, M. L. Lee, R. A. Hites, P. P. Hoalt, and J. B. Howard, "Soot and Hydrocarbon Formation in a Turbulent Diffusion Flame," 649-661, The Combustion Institute, 1976.
24. J. D. Watt and D. J. Thorne, *J. Appl. Chem.*, **15**, 585-594 (1965).
25. E. Raask, *J. Eng. Power*, **88**, 40-44 (1966).
26. E. Raask, *J. Institute Fuel*, **41**, 339-344 (1968).
27. A. R. Ramsden, *J. Institute Fuel*, **41**, 451-454 (1968).
28. A. R. Ramsden, *Fuel (Lond.)*, **48**, 121-237 (1969).
29. E. Raask, *Fuel (Lond.)*, **48**, 366-374 (1969).
30. I. Fells and D. Richardson, *J. Institute Fuel*, **42**, 245-248 (1969).
31. C. A. J. Paulson and A. R. Ramsden, *Atmos. Environ.*, **4**, 175-185 (1970).
32. J. Yerushalani, M. Kolodney, R. A. Graff, and A. M. Squares, *Science*, **187**, 646-648 (1975).
33. A. S. Padia, "The Behavior of Ash in Pulverized Coal under Simulated Combustion Conditions." D.Sc. thesis, Massachusetts Institute of Technology, Cambridge, Mass., January 1976.
34. G. L. Fisher, D. P. Y. Chang, and M. Brummer, *Science*, **192**, 553-555 (1976).
35. P. Murphy, Jr., J. D. Piper, and C. R. Schmansky, *Trans. ASME*, **73**, 821-843 (1957).

36. E. Raask and D. M. Wilkins, *J. Institute Fuel*, **38**, 255-261 (1965).
37. W. T. Reid, *External Corrosion and Deposits: Boilers and Gas Turbines*, American Elsevier, New York, 1971.
38. C. F. Cullis and M. F. R. Mulcahy, *Combust. Flame*, **18**, 225-292 (1972).
39. B. P. Breen, "Combustion in Large Boilers: Design and Operating Effects on Efficiency and Emissions," presented at the Sixteenth Symposium (International) on Combustion, Cambridge, Mass., August 1976.
40. M. A. Field, D. W. Gill, B. B. Morgan, and P. G. W. Hanksley, *Combustion of Pulverized Coal*, British Coal Utilization Research Association, Leatherhead, England, 1967.
41. R. F. Littlejohn, *J. Institute Fuel*, **38**, 59-67 (1965).
42. R. C. Flagan and J. P. Appleton, *Combust. Flame*, **23**, 249-267 (1974).
43. D. Pratt, *Prog. Energy Combust. Sci.*, **1**, 73-86 (1976).
44. L. Lamb, *J. Institute Fuel (Lond.)*, **45**, 443-448 (1972).
45. S. T. Cuffe and R. W. Gerstle, "Emissions from Coal-Fired Power Plants. A Comprehensive Summary," U.S. Public Health Service Report No. AP-35, 1967.
46. J. V. O'Gorman and P. L. Walker, Jr., *Fuel (Lond.)*, **51**, 135-151 (1971).
47. R. R. Ruch, H. J. Gluskoter, and N. F. Shimp, "Occurrence and Distribution of Potentially Volatile Trace Elements in Coal," EPA Report No. EPA-650/2-74-054, July 1974.
48. R. J. Mitchell and H. J. Gluskoter, *Fuel (Lond.)*, **55**, 90-96 (1976).
49. C. A. Zappfe, *J. Am. Ceram. Soc.*, **27**, 293-298 (1944).
50. L. Brewer, *Chem. Rev.*, **52**, 1-75 (1953).
51. H. L. Schick, *Chem. Rev.*, **60**, 331-362 (1960).
52. R. J. Ackerman and R. J. Thorn, *Prog. Ceram. Sci.*, **1**, 39-88 (1961).
53. H. Beecher and R. E. Rosenweig, *Amer. Rocket Soc. J.*, **31**, 532-539 (1961).
54. M. Ladadacki, *AIAA J.*, **4**, 1445-1447 (1966).
55. F. S. Sinnat, *J. Soc. Chem. Ind., Lond.*, **47**, 151-155 (1928).
56. P. J. Street, R. P. Weight, and P. Lightman, *Fuel (Lond.)*, **48**, 343-365 (1969).
57. M. A. Field, *Combust. Flame*, **13**, 237-252 (1969).
58. M. D. Gray, G. M. Kimber, and D. E. Granger, *Fuel (Lond.)*, **46**, 399-400 (1967).
59. A. R. Ramsden and I. W. Smith, *Fuel (Lond.)*, **47**, 253-256 (1968).
60. F. S. Lai, S. K. Friedlander, J. Pich, and G. M. Hidy, *J. Colloid Interface Sci.*, **39**, 395-405 (1972).
61. S. C. Graham and J. B. Homer, *Faraday Symp. Chem. Soc.*, **7**, 85-96 (1973).
62. S. K. Friedlander, *Smoke, Dust and Haze: Fundamentals of Aerosol Behavior*, Wiley-Interscience, New York, 1977.
63. N. A. Fuchs and A. G. Sutugin, in *Topics in Current Aerosol Research*, G. M. Hidy and J. R. Brock, Eds., Pergamon, New York, 1971.
64. J. Gregory, *Adv. Colloid Interface Sci.*, **2**, 396-417 (1969).
65. J. Visser, *Adv. Colloid Interface Sci.*, **3**, 331-363 (1972).
66. S. Corrsin, *Phys. Fluids*, **1**, 42-47 (1958).
67. C. Park and J. P. Appleton, *Combust. Flame*, **20**, 369-379 (1973).
68. R. W. Linton, A. Loh, D. F. S. Natusch, C. A. Evans, Jr., and P. Williams, *Science*, **191**, 852-854 (1976).
69. R. E. Barrett, J. D. Hummell, and W. T. Reid, *Trans ASME, J. Eng. Power*, **88**, 165-172 (1966).
70. H. H. Krause, A. Levy, and W. T. Reid, *Trans. ASME, J. Eng. Power*, **91**, 216-222 (1969).

EX 1B

Coal Combustion Aerosol Formation Mechanisms: A Review

A. S. Damle, D. S. Ensor, and M. B. Ranade

Research Triangle Institute, Post Office Box 12194, Research Triangle Park, NC 27709

The composition and size distribution of particles emitted by coal combustion sources depend upon various mechanisms leading to their formation. A review of current ideas about possible mechanisms for formation of combustion aerosols is presented. Available

data regarding fly ash size distribution and elemental concentrations in various size fractions were analyzed. These data were qualitatively compared with theoretical model predictions to indicate the relative contributions of various mechanisms in the formation of aerosols.

INTRODUCTION

With the anticipated increase in use of coal for electric power generation, there is continued concern about the atmospheric emissions associated with coal. Coal combustion is a major source of particulate emissions into the atmosphere. Emission of fine particles in size range 0.1–5 μm in diameter have relatively long atmospheric residence times and may affect health and visibility. These particles are the most difficult to collect by conventional collection equipment (Burchard, 1974; Shannon, 1974).

There is evidence of enrichment or preferential concentration of certain toxic trace elements (e.g., As, Se, Sb, Zn) in the finer fractions of combustion aerosols (Davison et al., 1974; Kaakinen et al., 1975; Ondov et al., 1979a, b; Smith et al., 1979a, b). This raises the question of the respirable emissions from coal combustion as a potential health hazard. The concentration of these trace species increases with decreasing particle size. Thus, it is important to characterize these emissions to assess adequately their health hazards and to facilitate their control.

Combustion aerosols may be characterized by their size as well as their elemental com-

position. Their characteristics depend on a number of factors, such as the type and properties of the parent coal and the size distribution of the parent coal particles being burned. The composition–size distributions of particles emitted by coal combustion sources are also influenced by furnace design and operating conditions such as temperature. The combustion aerosols contain primarily inorganic matter associated with coal but may also contain unburnt carbon particles—soot, condensed aromatic hydrocarbons, and sulfuric acid droplets. The size and composition of these aerosols depend upon the mechanisms leading to their formation.

Limited data are available regarding detailed size distribution and chemical composition of coal combustion emissions. Careful analysis of these data is necessary to understand the underlying mechanisms involved in their formation. An extensive review of particle formation in coal combustion was made by Flagan and Friedlander (1978). It is the purpose of this paper to analyze and qualitatively compare the data published since this review.

A brief account of coal properties and overall combustion processes is presented first, followed

by a survey of proposed particle formation mechanisms. Available data are considered first from a particle size distribution point of view. Elemental size distributions are reviewed next. Qualitative comparison of the data is then made with the predictions from various mechanisms.

PROPERTIES OF COAL

Coal structure and composition have definite influence on resulting emissions. The properties vary greatly with coal origin. Even two samples of coal from the same mine may be significantly different.

Distribution and Variability

Coal is distributed widely throughout the United States in the Appalachian, Illinois, and Western basins. Its chemical and physical properties vary greatly from one region to another, as shown in Table 1. The Eastern coals (Appalachian and Illinois) are generally higher in sulfur and iron, producing a more acidic ash than Western coal. Western coal is generally

rich in the lighter elements and low in sulfur with a more alkaline ash. Since an extensive study of coal composition has been compiled by Gluskoter et al. (1977), only a limited review will be presented here.

Coal can also be classified by age, as shown in Table 2. Generally, most of the coal consumed for power generation is either bituminous or subbituminous.

Coal Structure

Coal is a complex, heterogeneous, and variable material. Incorporated within the fossilized carbonaceous material are minerals from the original plant tissue and silt deposited during the formation of the coal. In addition, when the coal seam is mined, overburden may be mixed with the coal. Finkelman (1970), in a microscopic analysis of coal, reported that the minerals are dispersed in the coal with diameters ranging down to the submicron region. Sarofim et al. (1977) reported that the inorganic minerals are widely distributed in size with a mean diameter of 1 μm . In addition, clays composed of sub-

TABLE 1. Selected Coal Analysis for the Major Basins in the United States

	Western (28 samples)		Illinois (144 samples)		Appalachian (23 samples)	
	Arithmetic mean	Min:max	Arithmetic mean	Min:max	Arithmetic mean	Min:max
aluminum (%)	1.0	0.3 : 2.2	1.2	0.42: 3.0	1.7	1.1 : 3.1
calcium (%)	1.7	0.44: 3.8	0.67	0.01: 2.7	0.47	0.09: 2.6
chlorine (%)	0.03	0.01: 0.13	0.14	0.01: 0.54	0.17	0.01: 0.80
iron (%)	0.53	0.03: 1.2	2.0	0.45: 4.1	1.5	0.50: 2.6
potassium (%)	0.05	0.01: 0.32	0.17	0.04: 0.56	0.25	0.06: 0.06
magnesium (%)	0.14	0.03: 0.39	0.05	0.01: 0.17	0.06	0.02: 0.15
sodium (%)	0.14	0.01: 1.60	0.05	— : 0.2	0.04	0.01: 0.08
silicon (%)	1.7	0.38: 4.7	2.4	0.58: 4.7	2.8	1.0 : 6.3
titanium (%)	0.05	0.02: 0.13	0.06	0.02: 0.15	0.09	0.05: 0.15
moisture (%)	18	4.1 :13.7	9.4	0.5 :18	2.7	1.0 : 6.8
volatiles (%)	44	33 :53	40	27 :46	33	17 :42
fixed carbon (%)	46	35 :55	49	41 :61	55	45 :72
ash (%)	9.6	4.1 :20	11	4.6 :20	12	6.1 :25
sulfur (%)	0.76	0.34: 1.9	3.6	0.56: 6.4	2.3	0.55: 5.0
heat value (Btu/lb)	11,409	10,084:12,901	12,712	11,562:14,362	13,111	11,374:13,816

From Gluskoter et al. (1977).

TABLE 2. Composition as a Function of Coal Type

Component	Anthracite	Bituminous	Subbituminous	Lignite
moisture (%)	1.4	4.8	18.4	41.5
vol. matter (%)	6.5	32.3	33.8	23.0
fixed carbon (%)	79.5	51.2	39.0	20.9
ash (%)	12.5	11.7	8.8	14.6
hydrogen (%)	2.4	5.0	5.9	6.8
carbon (%)	80.1	69.1	54.3	29.9
nitrogen (%)	0.8	1.3	1.0	0.5
oxygen (%)	3.2	10.3	29.3	46.5
sulfur (%)	0.8	2.7	0.7	1.7
heat value (Btu/lb)	12,780	12,260	9140	5000
sulfate sulfur (%)	0.02	0.16	0.04	0.24
pyritic sulfur (%)	0.35	1.70	0.35	0.68
organic sulfur (%)	0.48	0.88	0.32	0.75

From Swanson et al. (1976).

micron particles may be incorporated in the coal. It appears from the rather limited studies on coal that the mineral inclusions are sub-micron and vary over a wide range of sizes. However, very few quantitative data on coal-mineral size distribution exist. Major forms of the minerals appear to be aluminosilicates with pyrites, calcites, and magnesites in various proportions (Gluskoter et al., 1981).

COMBUSTION PROCESS

Qualitative Description

Pulverized firing systems are most commonly used for large modern power plants using coal (Babcock and Wilcox, 1978). The crushed coal from the mine is pulverized into a fine powder, usually 100–200 mesh. The mean mass diameter of coal particles may vary from plant to plant, and the size distribution is usually very broad. The pulverized coal is blown into the furnace with carrier air. Coal particles are heated by radiation and mixing with hot gases. Combustion temperature depends upon percent excess air, quality of coal, and effectiveness of mixing. Temperatures up to 2000°C are usual. Different coal particles may be subjected to varying temperatures due to differences in size and nonuniformity in mixing.

A number of processes may occur during

coal-particle burnout. As a coal particle is being heated, it may mechanically break up into fragments because of thermal stresses induced by internal fissures, cracks, and structural imperfections initially present (Flagan and Friedlander, 1978). Volatile fractions originally present in the coal or formed by pyrolysis are vaporized. Chemical decomposition may take place evolving gaseous CO₂, SO₂, and SO₃. A particle may burst open from pressure generated internally by evolution of such gases (Smith et al., 1979b). A heated coal particle swells and may become porous. The degree of swelling depends both on the coal type and combustion conditions.

The general range of behavior of solid particles during gas–solid reactions was discussed by Levenspiel (1962). In extreme cases a coal particle may either retain the ash layer as burning proceeds inward or continuously shed the ash layer as the particle burns and thus shrink in size (Figure 1). The physical state of the ash layer would depend upon ash temperature and mineral composition. The shedding of ash layer may be caused by the evolution of off gases or by cracking or breakup of the particle.

Three temperature ranges that have varying influence on the behavior of mineral inclusions may be indicated. At low enough temperatures the mineral ash inclusions may remain solid. These inclusions may undergo chemical trans-

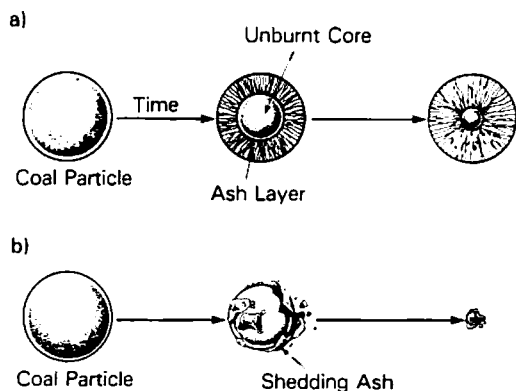


FIGURE 1. Two extreme types of coal particle combustion: coal particle burning (a) at constant size and (b) with shrinking size.

formations such as decomposition as well as physical transformations such as sintering. A medium temperature range may be designated as the one at which mineral inclusions may fuse, thereby producing highly viscous molten ash. At higher temperatures the viscosity of molten ash is considerably reduced with increased fluidity. The actual temperature values for these ranges would depend upon the mineral ash compositions involved.

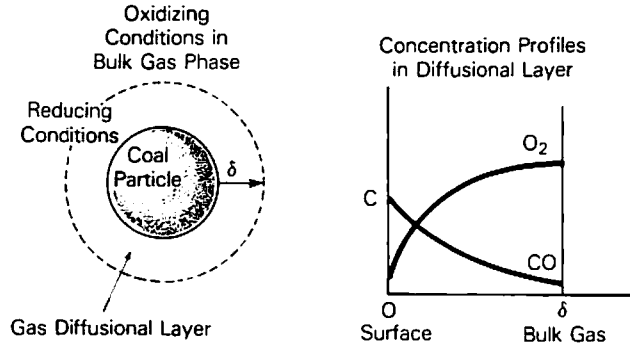
The individual mineral inclusions, whether solid or liquid, eventually form the resulting fly ash particles. These inclusions may undergo several physical transformations modifying their size distribution.

Coalescence of Individual Mineral Inclusions. Molten mineral ash inclusions present on a burning coal particle may coalesce and form larger ash droplets. For low combustion temperatures, where the ash remains solid, obviously there would be no coalescences, although some sintering may take place joining adjacent solid small particles. The higher the temperature, the greater the extent of coalescence that may be expected, because of the higher mobility of molten ash. The extent of coalescence may be expected to be greatly reduced with significant shedding of ash. Uncoalesced mineral inclusions and shedded ash may eventually form fine particles.

Bubble Formation. Molten mineral inclusions may come together to form a liquid layer. Gases may evolve within this layer so as to form bubbles. At medium temperatures, because of high viscosity these bubbles may remain stable and form large hollow spheres or cenospheres (Sarofim et al., 1977). At high temperatures, however, these bubbles may burst open owing to lower ash viscosity releasing fine molten ash droplets (Smith et al., 1979b). Bubble-bursting phenomena are not yet well understood, and any conclusive evidence in support of this mechanism has not yet been provided. Based upon aqueous bubble-bursting studies reported in the literature (Tomaides and Whitby, 1975), a broad bimodal droplet size distribution may be expected from such ash bubble bursting. Again in this case, shedding of ash may be expected to reduce the extent of bubble formation.

Evaporation and Condensation of Relatively Volatile Species. An ash species may vaporize depending upon the ash temperature, composition, and relative volatility of the species concerned. The volatility of an element depends on its chemical form in the ash. Thus observed elemental volatilities may be expected to be different from pure element-relative volatilities. Because of the reactive atmosphere near a particle surface, several chemical reactions are possible modifying the volatility of a species. A reducing or oxidizing atmosphere may prevail in the vicinity of a coal particle, depending on the mixing of gases, percent excess air, kinetics of combustion reactions, and presence of an ash layer surrounding the "burning front" that may introduce diffusional effects. Close to a particle surface reducing conditions may be expected whereas slightly away from the coal particle oxidizing conditions may be present in the gas phase. This model was proposed by Levenspiel (1962) to explain solid-gas reaction kinetics and is diagrammed in Figure 2. The reducing conditions near the particle surface may produce more volatile, reduced species that would vaporize, oxidize in the bulk gas phase away from the particle surface, and subsequently condense owing to the lower volatilities of oxidized species, e.g., SiO (Sarofim et al., 1977).

FIGURE 2. Reducing boundary layer at the particle surface.



The vaporized species may condense downstream upon gas cooling, either homogeneously forming new very fine, rapidly coagulating particles or heterogeneously condensing on existing particles. The fine particles and particle surfaces in general would then be preferentially enriched with volatile species. The degree of enrichment would depend upon the volatility of the species in question.

Homogeneous condensation would result in bulk enrichment of volatilized species in the fine size fractions. Heterogeneous condensation, on the other hand, would result in surface enrichment of the volatilized species. The enrichment would be most prominent in the finer size fractions because of their greater available surface area for condensation per unit volume.

In addition to these three major processes, several other mechanisms are also possible. Some fine mineral inclusions may remain separate without coalescing with others owing to surface tension effects or simply adequate spatial separation from other molten inclusions. These fine inclusions may eventually detach to form fine particles. Extraneous clay particles that adhere to the coal during mining and processing may easily disintegrate, separate out, and pass through the combustion process unchanged. Some fraction of carbon may remain unburnt and appear in the aerosols. Aromatic hydrocarbons may vaporize and burn and partially release fine carbon particles, or soot (Green and Lane, 1964).

The minerals may form solid solutions and may exhibit different properties as compared to

individual species in the solution. This apparently affects relative volatilities of some species. Thus, elements structurally incorporated into aluminosilicate matrix tend to show reduced volatility, e.g., Na. A physical rearrangement within the solid solutions similar to dissolution and precipitation may also be possible in varying temperature conditions.

Figure 3 presents a qualitative picture of what might be happening during the combustion and shows the multitude of processes that may be occurring simultaneously.

Particle Formation Mechanisms

Although a number of mechanisms of qualitative nature have been proposed, a semiempirical quantitative treatment has been developed for two mechanisms.

Breakup Model. A detailed account of this model is presented by Flagan and Friedlander (1978). The model considers melting of mineral inclusions followed by coalescence as the combustion front recedes. Each coal particle is then assumed to yield a number P of particles of equal size. Knowing the coal particle size distribution, the mass fraction of mineral ash, and the densities of coal and ash fractions, an ash particle size distribution may be predicted for a given value of P .

The mean mass diameter of ash may be given as adapted from Flagan and Friedlander (1978),

$$\bar{D}_{ash} = \sqrt{\frac{f}{P} \frac{\rho_c}{\rho_a}} \bar{D}_{coal} \quad (1)$$

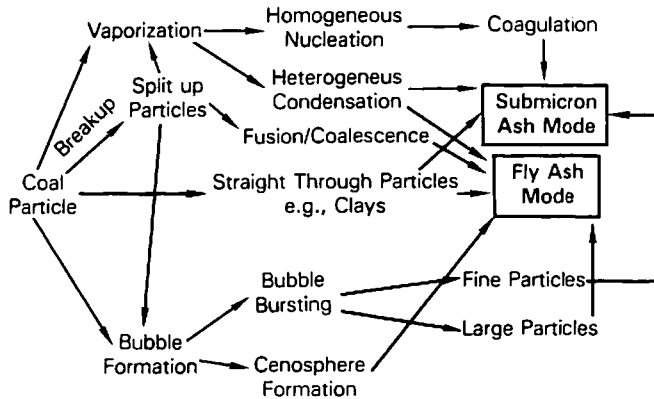


FIGURE 3. Schematic of coal combustion aerosol formation.

where

\bar{D}_{coal} is the mass mean diameter of coal (μm),

\bar{D}_{ash} the mass mean diameter of ash (μm),

ρ_c the density of coal (g/cm^3),

ρ_a the density of ash (g/cm^3),

P the number of coal fragments produced per particle, and

f the mass fraction of ash in coal.

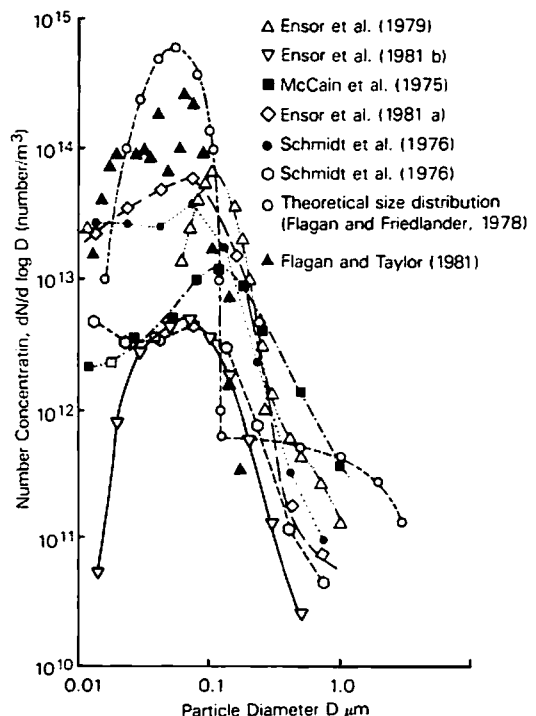
Equation (1) is a simplified view of the ash formation process. The value of P is usually considered to be between 3 and 5. Laboratory studies by Sarofim et al. (1977) are consistent with this model.

Since Eq. (1) implies that the ash forming process from each coal particle is similar in the breakup model, all resulting ash particles are predicted to be similar in their physical, morphological, and chemical nature. No explanation of cenospheres or fine submicron particles is contained in this model.

Vaporization-Condensation Model. This model suggests a mechanism for submicron particle formation. Basically a fraction of ash ($\sim 1\%$) is assumed to be vaporized and homogeneously condensed to form primary particles of the order of 10^3 \AA in size, followed by coagulation to yield self-preserving particle-size distribution within a few seconds (Flagan and Friedlander, 1978). Such a process predicts a submicron mode in particle size distribution around $0.1 \mu\text{m}$.

The resulting size distribution, when compared with the fine particle data of McCain et al. (1975), was found to predict an order of magnitude larger number of particles with a smaller mean diameter (Figure 4). Flagan (1979) later included accelerated coagulation due to inter-particle dispersion and nonhomogeneous

FIGURE 4. Aerosol size distribution in the submicron range.



mixing, which reduced the discrepancy but still predicted larger than observed fine particle densities. Additional recent data (Ensor et al., 1979, 1981a) also showed similar discrepancies between theory and experimental observations.

The model has some flexibility through the empirical parameter — the fraction of ash vaporized. This fraction would actually depend upon ash mineral composition and temperature. The model predicts a sharp submicron mode in mass or number size distribution at about $0.1 \mu\text{m}$. Vaporization of species depends upon their relative volatilities. Hence, such a submicron ash mode formed by vaporized material may be expected to be composed primarily of volatile materials, and its composition may be expected to differ significantly from larger particles formed in breakup. This model has also been strongly supported by laboratory combustion studies (Sarofim et al., 1977; Mims et al., 1979; Flagan and Taylor, 1980; Neville et al., 1980).

Other mechanisms that have not been quantified but have been justified by experimental observations are as follows:

1. Bubble formation due to evolution of gases in the coal particles. This mechanism has been supported by the presence of large cenospheres observed microscopically by various investigators. Laboratory studies by Sarofim et al. (1977) indicated the mass fraction of cenospheres to be dependent upon temperature and to peak at 6% at 1500 K .
2. Condensation of volatile species on existing particles to produce surface layers enriched in volatile species. Numerous observations have indicated surface enrichments of volatile species, especially on fine particles. The concentration of certain volatile species has been observed to increase with decreasing particle size. Biermann and Ondov (1980) have recently analyzed their surface enrichment data to indicate a $C \propto 1/d^2$ relationship.
3. Bubble bursting at high temperatures as a source of fine particles with compositions similar to the large-particle parents (Ramsden, 1969; Smith et al., 1979b). No quantification of particle size distribution

resulting from bubble bursting has been made. Conclusive evidence for this mechanism is yet to be provided.

These mechanisms may now be compared with some of the available data regarding mass-size distribution and elemental-size distribution.

PARTICLE SIZE DISTRIBUTION

Measurement Techniques

The measurement of aerosol size distributions should be reviewed before examining the data and comparing them to theories. The study of experimental techniques is still a research activity. Major problems with measurements and data analysis include these:

- a. In situ cascade impactors have limited resolution of particle populations greater than $10 \mu\text{m}$ because of wall and inlet nozzle losses (Cushing et al., 1976; Knapp, 1980). Lower cutpoint is usually limited to about $0.2 \mu\text{m}$. Impactors may have problem with particle bounce and reentrainment, which is especially serious for lower range of cut sizes.
- b. Extractive sampling to condition stack gas for measurement by electrical aerosol analyzers (EAA) and optical particle counters introduces a bias in the particles larger than $1 \mu\text{m}$. Also, a large dilution of stack gas sample is necessary to use these instruments. The EAA data for combustion aerosol should be corrected for cross sensitivities of neighboring channels (Markowski et al., 1980). The sharpness of the submicron mode may also be affected by coagulation within the sampling probe.

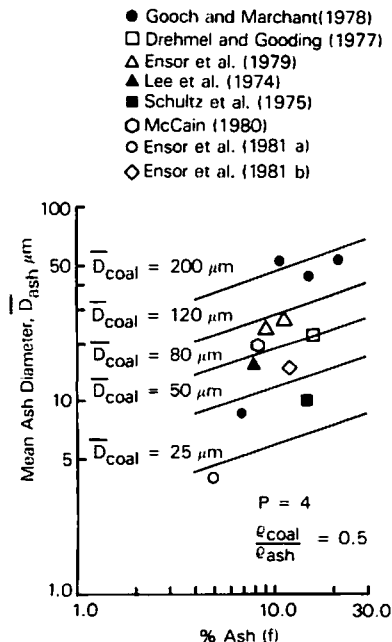
In general, conventional impactors are best suited for the size range of $0.5\text{--}10 \mu\text{m}$, whereas EAA has better resolution in the submicron range. Diffusion batteries have also been used (McCain et al., 1975) for submicron ash analysis, but this instrument does not have cutpoints that are as sharp as those of EAA. The smallest cutpoint diameter of an impactor may be lowered further by operating the impactor under subatmospheric pressures. Particles as small as

0.02 μm can be impacted under partial vacuum because resistance from air molecules is reduced (Pilat, 1978; Flagan, 1981). This technique was successfully used by Ensor et al. (1981b) for field experimental evaluations and in the laboratory by Flagan and Taylor (1980).

Coarse Ash Fraction

Available data indicate that the majority of fly ash is above 1 μm in size with a broad peak in the range of 3–50 μm diameter. The actual mass mean diameter and shape of the size distribution depend upon several factors, such as coal type and composition and coal-particle size distribution. The large diameter mode may be called a *fly ash mode* and is generally explained by the breakup model, with P being the number of fragments produced per coal particle as a variable parameter. Laboratory data by Sarofim et al. (1977) indicate that P ranges from 3 to 5. With this model the mean ash diameter is given by Eq. (1). In Figure 5 the literature data on coal ash

FIGURE 5. Mean fly ash particle diameter for uncontrolled sources as a function of coal ash mass fraction.



concentration and mean particle diameter are compared to curves predicted with Eq. (1) (Ensor, 1980). The value of P was assumed to be 4 and ρ_c/ρ_a to be ~ 0.5 . Since all the data correspond to pulverized coal-fired systems, the mean coal particle diameter is expected to be $\sim 80 \mu\text{m}$. Only fair agreement with the model is seen. Several reasons are believed to contribute to the differences.

1. The accuracy of impactor measurements in determining ash size distribution may not be sufficient. Usually data are truncated at 10 μm and extrapolated assuming a log-normal distribution. This approximation can lead to large errors in mean ash diameter.
2. The coal size distribution is usually not known accurately at the time of the impactor measurements.
3. Usually some mass fraction of the ash is composed of cenospheres (up to 5%). Since these are large particles with lower density, a bias in the ash size distribution may be introduced.
4. The parameter P is assumed to be constant for all coal particle sizes. However, it may be a function of coal size and type. For a given coal type, the mean ash diameter may be reasonably expected to depend on mean coal particle size.
5. Morphological analysis of a coal flyash sample by Fisher et al. (1978) indicated 11 major classes of fly ash particles. The breakup model, on the other hand, predicts only particles of similar physical and chemical nature.

Submicron Ash Fraction

Submicron ash usually makes up less than 2% of the total fly ash mass. The lowest cutpoint diameter of a conventional cascade impactor is about 0.2 μm . With a low pressure impactor the cutpoint diameter can be lowered up to 0.02 μm (Ensor et al., 1981b; Flagan and Taylor, 1980), but the quantity collected on submicron stages is usually too small to weigh accurately. As a result, an impactor has limited sensitivity in the submicron range. Much better sensitivity in the

submicron range is obtained by an EAA or a diffusion battery technique.

A distinct submicron mass mode was observed around $0.1 \mu\text{m}$ diameter when these instruments were used for analysis. McCain et al. (1975) found a broad submicron peak in number distribution by taking measurements with a diffusion battery. The peak reported by McCain disappears when size distribution is plotted on a mass basis. Sharper submicron peaks were observed when measurements were made by an EAA (Schmidt et al., 1976; Ensor et al., 1979; Flagan and Taylor, 1980; Markowski et al., 1980). These data retained the peaks when plotted on a mass basis. Peaks are especially sharp when the data reduction process takes into account cross sensitivities of neighboring channels of the EAA (Markowski et al., 1980). Ondov et al. (1979b) analyzed the impactor filter samples with scanning electron microscopy (SEM) and detected a mode at $0.16 \mu\text{m}$. Particles were sized and counted from SEM photographs for this purpose.

These observations tend to support qualitatively the vaporization-condensation mechanism that predicts a submicron mode at $0.1 \mu\text{m}$ due to coagulation. When the observed number concentration of submicron particles from field measurements is compared with theoretical predictions, one or two orders of magnitude discrepancies are seen (Figure 4). The agreement is much better for the laboratory data taken by Flagan and Taylor (1980). Part of the discrepancies in field measurements may be explained by coagulation in the sampling probe. The difference in the submicron distribution data by Ensor et al. (1979, 1981a, b) taken with similar equipment and procedures at various sites indicates a strong influence of coal composition on the magnitude of the submicron distribution peak. Site-dependent variability was reported by McElroy et al. (1982).

ELEMENTAL SIZE DISTRIBUTIONS

Measurement Techniques

Several analytical techniques have been developed for the elemental analysis of a sample and

have been summarized by Smith (1980). The most commonly used techniques are

1. x-ray fluorescence analysis (XRF),
2. instrumental neutron activation analysis (INAA),
3. atomic absorption analysis (AAA), and
4. x-ray photoelectron spectroscopy (ESCA).

The first three (XRF, INAA, and AAA) analyze bulk or volume samples, whereas ESCA analyzes the surface. A sputter-etching technique is normally used to remove surface layers of different depths and to expose internal material.

Sample preparation for analysis is of course an important step. Size-classified samples are required to determine elemental size distributions and concentrations. Most commonly, samples are collected on cascade impactor stages for later analysis for chemical compositions. In this scheme a filter collects all particles below the cutpoint of the last impaction stage, usually $0.2 \mu\text{m}$. With the low pressure impactor it has been possible to collect samples of particles down to $0.02 \mu\text{m}$; however, only limited data using this technique are available (Ensor et al., 1981b). Since the low pressure impactor has a larger number of stages, the possibility of contamination due to larger particles bouncing off from preceding stages is minimized. In a conventional impactor, with fewer stages and a lowest cutpoint diameter of $0.2 \mu\text{m}$, the larger particles bouncing off from earlier stages are likely to contaminate the submicron fraction collected on the filter.

Impactor sampling provides in situ samples. Some analyses have also been made on bulk fly ash samples collected by control equipments. This ash was later size classified by techniques such as elutriation to provide samples for elemental analysis (Ondov et al., 1978; Desrosiers et al., 1979; Smith et al., 1979b). This scheme has been controversial. This procedure would work well provided there are no physical or chemical changes in accumulation and re-dispersion of the fly ash samples. This is probably the case for larger particle sizes. For small particles, however, particle interactions are expected to become significant. Upon collection and accumulation, small particles are likely to

agglomerate among themselves to form larger ones; they also may adhere to larger particles. The smaller the particle is, the more energy that is required to separate it. With higher energy abrasion of large particles, the generation of "new" fine particles may become significant. Thus redispersion of collected fly ash, especially of the fine fraction, may introduce some measurement artifacts.

Data Analysis

Elemental size distribution data are only recently being investigated, and the techniques are still in experimental stages. The limited amount of data therefore understandably shows variations (e.g., Klein et al., 1975; Block and Dams, 1976).

Some broad generalizations may be made from the data obtained on coal-fired utility boilers. Most of the mass of ash is composed of so-called aluminosilicate matrix elements. These include Al, Si, Ca, Mg, and Fe. Na, K, and Ti are also usually present in significant quantities. The proportions of each of these elements depends on the coal type used. These elements are generally found in all size fractions, including submicron fractions, in similar proportions.

Most of the data show distinct enrichments of trace elements—As, Se, Sb, Zn, Mo, Pb, Ga, and Cd—in the finer size fractions. Enrichment has also been reported for W, but the data are limited. These may be called group I elements. A second group of elements may be made which show slight depletion or no change in elemental concentration with respect to particle size. These include Al, Si, Fe, Ca, Ti, Mg, K, Ce, Hf, and other rare-earth elements. A third grouping of elements includes those that show slight enrichment or intermediate undeterminable behavior. Also included in this group are those elements for whom conflicting trends have been reported. The group III elements include Ba, Sr, Ni, Cr, Co, Mn, Na, U, and V.

These groupings have been made to indicate general trends. Unusual behaviors have also been reported, e.g., slight enrichment of Ca (Ondov et al., 1979a), slight enrichment of Fe (Smith et al., 1979a), no change with Zn and Ga

(Gladney et al., 1976), enrichment of Ti (Ondov et al., 1979b), depletion of Fe and of Ce relative to Al (Gladney et al., 1976), etc. These observations and the conflicting reports for group III elements may be the effect of coal type, different operating parameters (such as combustion temperature), and inaccuracies involved in sampling and analytical procedures.

Strong evidence of surface enrichments attributable to evaporation of volatile species followed by heterogeneous condensation have been found by Linton et al. (1976), Smith et al. (1979a, b), Hansen and Fisher (1980), Neville et al. (1981), and several other investigators. Since small particles have higher surface area-to-volume ratio, the enrichment is expected to increase with decreasing particle size. From simple geometrical considerations, Davison et al. (1974) proposed that the enrichment concentration of volatile species should be proportional to $1/d$, where d is fly ash particle diameter. For the continuum regime, condensation indicates $c \propto 1/d^2$ (Flagan and Friedlander, 1978). Flagan found that both relations fit reasonably well to data by Davison et al. (1974). Biermann and Ondov (1980) found better agreement with the $1/d^2$ relationship when data are taken with a cascade impactor of high resolution in the submicron range. Data taken with a conventional cascade impactor are usually available only to 0.2 μm . Extrapolation of the above relationship to the finer size range may be potentially misleading as it would predict a rapid increase in surface concentrations for every volatile element. Such extrapolations by Biermann and Ondov (1980) show that a particle of pure condensed material would have a diameter of 0.045 μm . The data taken with a low pressure cascade impactor (with a smallest cutpoint diameter of 0.02 μm), on the other hand, indicated an absence of particles below 0.08 μm (Ensor et al., 1981b).

Contrary to findings by Biermann and Ondov (1980) and others, data by Smith et al. (1979a, b) indicate the concentration of most of the volatile species in size fractions smaller than 1 μm to be independent of size. There is definite enrichment of volatiles in these particles com-

pared with their concentration in larger particles. The concentrations have been shown to increase as the particle size decreased from 10 to 1 μm , where it levels off. These data were obtained by separating hopper ash, instead of in situ impactor sampling as used by several other researchers (Ensor et al., 1979, 1981 a, b; Biermann and Ondov, 1980). This discrepancy may be explained as measurement artifacts, as discussed earlier. Smith et al. (1979b) suggest bursting of bubbles as a possible mechanism for the formation of such fine particles.

The effect of matrix structure and surface segregation was pointed out by Stinespring and Stewart (1981). They showed that, at the elevated temperatures experienced during and after the combustion process, diffusive transport of the trace and minor elements to the surface of the ash particles (i.e., surface segregation) could contribute to the observed surface enrichment. Such processes require residence times of several hours at elevated temperatures to be significant in combustion processes. However, such processes may be possible after collection and deposition of fly ash particles or in advanced combustion processes utilizing fluid beds.

A common observation in the majority of the field data is the presence of relatively less volatile major matrix elements in the fine submicron fractions. These are seen even in the nearly monodisperse submicron modes observed by Ensor et al. (1979, 1981b). A submicron mass mode is qualitatively explained by the vaporization-condensation mechanism, as discussed earlier. However, the submicron mode may also be expected to be considerably depleted in less volatile species. To explain the presence of less volatile species like Al and Si in submicron fractions, a reduction of the refractory species Al_2O_3 , SiO_2 , and MgO to more volatile reduced species AlO , SiO , and Mg in the reducing zone near the burning particle surface has been suggested (Sarofim et al., 1977; Desrosiers et al., 1979; Mims et al., 1979; Neville et al., 1980). The vaporized reduced species may later oxidize in the oxidizing gas atmosphere away from the particle. The oxidized species would then condense out, because of their low

volatility. To predict resulting submicron ash composition, kinetic data related to the listed reactions and thermodynamic data related to all compounds involved are needed. Such predictions, made by Ulrich et al. (1977) for a cyclone coal-fired boiler ash, were compared with experimental fly ash composition. Considerable discrepancies regarding Al_2O_3 , CaO , and FeO compositions were observed and were attributed to the mixing of two sets of fine ash particles, one originating by vaporization-condensation and the other having composition similar to large particles and entrained by some other mechanism (Desrosiers et al., 1979). It may be pointed out that the presence of major matrix elements in submicron ash may also arise simply as an artifact of sampling technique, e.g., larger particles bouncing off impactor stages onto the filter.

Based on the vaporization mechanism, the relative volatilities of the species in the three groups may be expected to be in the following order:

group I > group III > group II.

Such an order, however, does not follow the expectations based on the volatility data of pure species or compounds. (Table 3 gives the boiling points of the elements and their compounds.) For example, Mg and K from group II are relatively more volatile than Ba, Sr, or Mn of group III. Also, it appears that for some species their specific chemical compounds need to be formed to justify their relative high volatility. Thus, for Ni and Mo, their carbonyls appear to be the volatilizing species. Halides seem to be the choice for U, V, Co, Cr, Sb, and Mn. The lower volatilities experienced by Na, K, and Mg may perhaps be explained if they are considered to be structurally incorporated into an aluminosilicate matrix structure.

Laboratory studies under controlled conditions by Sarofim et al. (1977) and by Flagan and Taylor (1980) show much different results compared with field studies regarding the behavior of major matrix elements. The role of evaporation and submicron ash composition were clearly shown to be a function of tempera-

TABLE 3. Boiling Points of Elements and Their Compounds

Species	Boiling point (°C)
As	613 (sublimes)
Se	685
Sb	1750
SbCl ₃	283
Zn	907
ZnO	>2500
Mo	4612
Mo(CO) ₆	156
MoO ₃	1155 (sublimes)
Cd	765
Pb	1740
Al	2467
Al ₂ O ₃	2980
Ca	1484
CaO	2850
Si	2355
SiO	1880
SiO ₂	2230
Ti	3287
TiCl ₄	136
Mg	1090
MgO	3600
K	774
Ba	1640
BaO	>2000
Sr	1384
SrO	>3000
Ni	2732
NiO	>3000
Ni(CO) ₄	43
Cr	2672
Cr ₂ O ₃	4000
CO	2870
CoO	>2000
Mn	1962
MnCl ₂	1190
Na	883
U	3818
UCl ₄	792
V	3380
VCl ₄	148

From Perry and Chilton (1973).

ture and reflect the effect of reaction kinetics and relative volatilities of the species (Mims et al., 1979; Neville et al., 1980). More volatile Mg, Fe, and Na were considerably enriched, and Al and Ca were correspondingly depleted. Results with Si analysis indicated dependence upon coal type

and structure. The nature and chemical composition of mineral species were found to effect its reactivity and volatility. The work of Flagan and Taylor indicated a large percentage of soot (unburned carbon), as well as sulfur in the submicron mode. The high concentration of Si in submicron fractions observed in these laboratory studies may be explained by formation of more volatile SiO near the particle surface because of the presence of reducing conditions. The submicron size distribution observed in Flagan and Taylor's work is in good agreement with that predicted by vaporization-homogeneous condensation mechanism. Thus the laboratory studies tend strongly to support the vaporization-condensation model for submicron particle formation.

CONCLUSIONS

(1) The formation of fly ash particles larger than 1 μm is reasonably explained by coal-particle breakup and the coalescence of molten grains of mineral matter during combustion. Cenospheres caused by inflation of the molten ash depend on the ash viscosity, but in most circumstances it is only a small fraction of the total ash on a weight basis. Laboratory data suggest the parameter P in the breakup model (indicating number of ash particles formed per coal particle) to be between 3 and 5. The data obtained from commercial coal-fired boilers show only moderate agreement with the model. This discrepancy may be primarily due to the difficulty in obtaining accurate particle size distributions above 10 μm in field tests.

(2) The physical particle size distribution in the less than 1 μm range is qualitatively explained by a vaporization-homogeneous condensation mechanism. The most likely explanation of the submicron mode observed in various field and laboratory data is vapor-to-particle conversion. Also, the concentration variability of submicron particles is indicative of a temperature and coal composition dependence. The concentration of submicron particles determined in field measurements on commercial scale boilers is, however, lower, often by two

orders of magnitude, than the laboratory measurements and theoretical predictions. Part of the explanation may be the coagulation of the submicron material in the sampling systems used in field tests. However, some of the field-size distributions (Ensor et al. 1981a) obtained with equipment designed to minimize coagulation did not appear to be significantly different than the other field data.

(3) The elemental size distribution from field measurements on commercial scale boilers indicates that the ash is mostly composed of so-called aluminosilicate major matrix elements. These are generally found in all size fractions, including submicron fractions, in similar proportions. These observations are not consistent with a simple vaporization-homogeneous nucleation model for submicron particle formation. Alternative mechanisms suggested for the formation of such fine particles containing aluminosilicate matrix elements include (a) the presence of extraneous submicron particles not associated with coal such as clays, (b) mineral inclusions released as submicron particles without coalescence (c) the bursting of molten ash bubbles releasing fine submicron particles, and (d) the reduction of matrix elements at the coal particle surface during combustion, producing more volatile species.

The laboratory studies with controlled combustion conditions indicate a greater concentration particle size dependence for major matrix elements than reported from field tests. The laboratory results are consistent with the vaporization homogeneous condensation mechanism, with the enrichment and depletion of a species depending on its relative volatility. The enrichment of silicon in fine-size fractions is considered to be due to formation of volatile SiO in the reducing atmosphere near the coal-particle surface, while aluminum is depleted in the fine-size fractions. The elemental size distributions are also found to depend on coal composition. The laboratory particle separation experiments have been conducted under conditions to minimize measurement artifacts introduced by impactors, which may have been significant in field tests.

(4) The observed particle surface enrichment by trace volatile species over the whole size range is generally explained by a vaporization-heterogeneous condensation mechanism. The enrichment is especially dominant in fine-size fractions owing to their higher surface area to volume ratio compared to coarse size fractions. The concentration of trace species increases with decreasing particle size and is found to vary as $1/(\text{particle diameter})^2$ with reasonable accuracy for limited data.

REFERENCES

- Babcock and Wilcox (1978). *Steam/Its Generation and Use*. 39th ed., New York.
- Biermann, A. H., and Ondov, J. M. (1980). Applications of surface-deposition models to size-fractionated coal fly ash, *Atmos. Env.* 14:289-295.
- Block, C., and Dams, R. (1976). Study of fly ash emission during combustion of coal, *Environ. Sci. Technol.* 10:1011-1017.
- Burchard, J. K. (1974). The significance of particulate emissions, *J. Air Poll. Control Assoc.* 24:1140-1142.
- Cushing, K. M., Lacey, G. E., McCain, J. D., and Smith, W. B. (1976). Particulate sizing techniques for control device evaluation: Cascade impactor calibration, EPA Rep. 600/2-76-280, October.
- Davison, R. L., Natusch, D. F. S., Wallace, J. R., and Evans, C. A., Jr. (1974). Trace elements in fly ash dependence of concentration on particle size, *Environ. Sci. Technol.* 8:1107-1113.
- Desrosiers, R. E., Riehl, J. W., Ulrich, G. D., and Chiu, A. S. (1979). Submicron fly ash formation in coal fired boilers, *Proc. 17th symp. Combust., Combust. Inst.*, 1395-1403.
- Drehmel, D. C., and Gooding, C. H. (1977). Field tests of a hot-side electrostatic precipitator. Proceedings: particulate collection problems using ESPs in the metallurgical industry. EPA Rep. 600/2-77-208, October.
- Ensor, D. S., Cowen, S., Hooper, R., Markowski, G., Scheck, R., Farrell, J. D., and Burnham, J. (1979). Evaluation of the george meal No. 3 electrostatic precipitator, EPRI Rep. FP-1145, August.
- Ensor, D. S. (1980). Stationary source aerosol emissions, presented Symp. Plume and Visibility: Measurements and Model Components, Grand Canyon, AZ, November.
- Ensor, D. S., Lawless, P. A., Damle, A. S., and Sparks, L. E. (1981a). Evaluation of the United McGill electrostatic precipitator, presented at the EPA 3rd Symp. Transfer and Utilization of Particulate Control Technology, Orlando, FL, March.
- Ensor, D. S., Cowen, S., Shendrikar, A., Markowski, G., Woffinden, G., Pearson, R., and Scheck, R. (1981b).

- Kramer station fabric filter evaluation. EPRI Rep. CS-1069, January.
- Finkelman, R. B. (1970). Determination of trace element sites in the Waynesburg by SEM analysis of accessory minerals, *Scanning Electron Microscopy* 1:60.
- Fisher, L. L., Prentice, B. A., Iberman, D. S., Ondov, J. M., Bierman, A. H., Ragaini, R. C., and McFarland, A. R. (1978). *Environ. Sci. Technol.* 12:447-451.
- Flagan, R. C. (1979). Submicron particles from coal combustion, *Proc. 17th Symp. Combustion, Combustion Inst.*, 97-104.
- Flagan, R. C. (1981). Temperature and pressure effects in low pressure cascade impactors, presented at ACS-81 Winter Symp. Aerosol Sci. Tucson, AZ, January.
- Flagan, R. C., and Friedlander, S. K. (1978). Particle formation in pulverized coal combustion—a review, in *Recent Developments in Aerosol Science* (D. T. Shaw, ed.), Wiley, New York, Ch. 2.
- Flagan, R. C., and Taylor, D. D. (1980). Laboratory studies of submicron particles from coal combustion, *Proc. 18th Symp. Combustion, Combustion Inst.*, 1227-1237.
- Gladney, E. S., Small, J. A., Gordon, G. E., and Zoller, W. H. (1976). Composition and size distribution of in-stack particulate material at a coal-fired power plant, *Atmos. Environ.* 10:1071-1077.
- Gluskoter, H. J., Ruch, R. R., Miller, W. H., Cahill, R. W., Dreher, G. B., and Kuhn, J. K. (1977). Trace elements in coal: Occurrence and distribution, EPA Rep. 600/7-77-064, June.
- Gluskoter, H. J., Shimp, N. F., and Ruch, R. R. (1981). Coal analyses, trace elements, and mineral matter, in *Chemistry of Coal Utilization* (M. A. Elliott, ed.), Wiley, New York, Ch. 7.
- Gooch, J. P., and Marchant, G. H. (1978). Electrostatic precipitator rapping reentrainment and computer model studies, EPRI Rep. FP-792.
- Green, H. L., and Lane, W. R. (1964). *Particulate Clouds: Dust, Smokes and Mists*, 2nd ed., Van Nostrand Reinhold, New York.
- Hansen, L. D., and Fisher, G. L. (1980). Elemental distribution in coal fly ash particles, *Environ. Sci. Technol.* 14:1111-1117.
- Kaakinen, J. W., Jorden, R. M., Lawasani, H. H., and West, R. E. (1975). Trace element behavior in coal-fired power plant, *Environ. Sci. Technol.* 9:862-869.
- Klein D. H., Andren, A. W., Carter, J. A., Emery, J. F., Feldman, C., Fulkerson, W., Lyon, W. S., Ogle, J. C., Talmi, Y., Van Hook, R. I., and Bolton, N. (1975). Pathways of thirty-seven trace elements through coal-fired power plant, *Environ. Sci. Technol.* 9:973-979.
- Knapp, K. T. (1980). The effects of nozzle losses on impactor sampling, Paper 6, Proc. Advances in Particle Sampling and Measurement, EPA Rep. 600/9-80-004, January.
- Lee, R. E., Crist, H. L., Riley, A. E., and McLeod, K. E. (1974). Concentration and size of trace metal emissions from a Power Plant, a steel plant, and a cotton gin, *Environ. Sci. Technol.* 9:643-647.
- Levenspiel, O. (1962). *Chemical Reaction Engineering*, Wiley, New York.
- Linton, R. W., Loh, A., Natusch, D. F. S., Evans, C. A., and Williams, P. (1976). Surface predominance of trace elements in airborne particles, *Science* 191:852-854.
- Markowski, G. R., Ensor, D. S., Hooper, R. G., and Carr, R. C. (1980). Submicron aerosol mode in flue gas from a pulverized coal utility boiler, *Environ. Sci. Technol.*, 14:1400-1402.
- McCain, J. D., Gooch, J. P., and Smith, W. B. (1975). Results of field measurements of industrial particulate sources and electrostatic precipitator performance, *J. Air Poll. Control Assoc.* 25:117-121.
- McElroy, M. W., Carr, R. C., Ensor, D. S., and Markowski, G. R. (1982). Size distribution of fine particles from coal combustion, *Science* 215:13-49.
- Mims, C. A., Neville, M., Quann, R. J., and Sarofim, A. F. (1979). Laboratory studies of trace element transformation during coal combustion, paper No. 78, presented 87th AIChE Meeting, August.
- Neville, M., Quann, R. J., Haynes, B. S., and Sarofim, A. F. (1980). Vaporization and condensation of mineral matter during pulverized coal combustion, presented at 18th Symp. Combust., Waterloo, Canada, August.
- Neville, M., Quann, R. J., Haynes, B. S., and Sarofim, A. F. (1981). Factors governing the surface enrichment on fly ash of volatile trace species, presented at the ACS/IEC Winter Symp., Tucson, AZ, January.
- Ondov, J. M., Ragaini, R. C., Biermann, A. H. (1978). Elemental particle-size emissions from coal-fired power plants: Use of an internal cascade impactor, *Atmos. Environ.* 12:1175-1185.
- Ondov, J. M., Ragaini, R. C., and Biermann, A. H. (1979a). Emissions and particle size distributions of minor and trace elements at two western coal-fired power plants equipped with cold-side electrostatic precipitators, *Environ. Sci. Technol.* 13:946-953.
- Ondov, J. M., Ragaini, R. C., and Biermann, A. H. (1971). Elemental emissions from a coal-fired power plant. Comparison of a Venturi wet scrubber system with a cold-side electrostatic precipitator, *Environ. Sci. Technol.* 13:598-607.
- Perry, R. H., and Chilton, C. H. (1973). *Chemical Engineers' Handbook*, 5th ed., McGraw Hill, New York.
- Pilat, M. J. (1978). Development of a cascade impactor system, EPRI Project Rep. FP-844, August.
- Ramsden, A. R. (1969). A microscopic investigation into the formation of fly ash during the combustion of a pulverized bituminous coal, *Fuel (London)* 48:121-237.
- Sarofim, A. F., Howard, J. B., and Padia, A. S. (1977). The physical transformation of the mineral matter in pulverized coal under simulated combustion conditions, *Combust. Sci. Technol.* 16:187-204.
- Schmidt, E. W., Gieseke, J. A., and Allen, J. M. (1976). Size distribution of fine-particulate emissions from a coal-fired power plant, *Atmos. Environ.* 10:1065-1069.
- Schultz, E. J., Engdahl, R. B., and Frankenberg, T. T.

- (1975). Submicron particles from a pulverized coal-fired boiler, *Atmos. Environ.* 9:111-119.
- Shannon, L. J. (1974). Control technology for fine particulate emissions, EPA Rep. 650/2-74-027, May.
- Smith, R. D. (1980). The trace element chemistry of coal during combustion and the emissions from coal-fired plants, *Progr. Energy Combust. Sci.* 6:53-119.
- Smith, R. D., Campbell, J. A., and Nielson, K. K. (1979a). Concentration dependence upon particle size of volatilized elements in fly ash, *Environ. Sci. Technol.* 13:553-558.
- Smith, R. D., Campbell, J. A., and Nielson, K. K. (1979b). Characterization and formation of submicron particles in coal-fired plants, *Atmos. Environ.* 13:607-617.
- Stinespring, C. D., and Stewart, G. W. (1981). Surface enrichment of aluminosilicate minerals and coal combustion ash particles, *Atmos. Environ.* 15:307-313.
- Swanson, V. E., Medlin, J. H., Hatch, J. R., Coleman, S. L., Wood, G. H., Woodruff, S. D., and Hildebrand, R. T. (1976). Collection, chemical analysis, and evaluation of coal samples in 1975, U.S. Geol. Survey Rep. 76-468.
- Tomaidis, M., and Whitby, K. T. (1975). Generation of aerosols by bursting of single bubbles, presented at Symp. Fine Particles, Minneapolis.
- Ulrich, G. D., Richl, J. W., French, B. R., and Desrosiers, R. E. (1977). Mechanism of submicron fly-ash formation in a cyclone, coal-fired boiler, ASME Int. Symp. Corrosion and Desposits from Combustion Gases, Henniker, NH, June.

Received 25 September 1981; accepted 5 January 1982

EX 2A

Trace Elements in Fly Ash

Dependence of Concentration on Particle Size

Richard L. Davison, David F. S. Natusch,* and John R. Wallace

School of Chemical Sciences, University of Illinois, Urbana, Ill. 61801

Charles A. Evans, Jr.

Materials Research Laboratory, University of Illinois, Urbana, Ill. 61801

144-3

■ The concentrations of 25 elements in fly ash emitted from a coal-fired power plant have been measured as a function of particle size using spark source mass spectroscopy, optical emission spectrography, atomic absorption spectroscopy, and X-ray fluorescence spectroscopy. Of these elements, the concentrations of Pb, Tl, Sb, Cd, Se, As, Zn, Ni, Cr, and S were found to increase markedly with decreasing particle size. A mechanism involving high-temperature volatilization of a species containing the trace element followed by preferential condensation or adsorption onto the smallest particles is proposed to account for the trace element concentration dependence on particle size. The environmental significance of the results is discussed.

It is now well established that many high-temperature combustion and smelting operations emit particles containing toxic elements such as Be, Cd, As, Se, Pb, Sb, Hg, Tl, and V into the atmosphere (1). Many of these elements are enriched in ambient urban aerosols by as much as 100- to 1000-fold over their natural crustal abundance (2). Furthermore, most of their mass is concentrated in the particle size range 0.5-10.0 μm , which is inhaled and deposited in the human respiratory system.

A number of workers (3-5) have shown that inhaled airborne particles are deposited in different regions of the body depending on their aerodynamic size. This behavior is illustrated for three compartments of the respiratory system (5) in Figure 1. From a toxicological standpoint, the smallest particles (<1 μm) which deposit in the pulmonary region of the respiratory tract are of greatest concern. This is because the efficiency of extraction of toxic species from particles deposited in the pulmonary region is high (60-80%) (1, 4, 6-8), whereas the extraction efficiency from the larger particles, which deposit in the nasopharyngeal and tracheobronchial regions and are removed to the pharynx by ciliary action and swallowed, is low (5-15%). Consequently, toxic species, which predominate in submicrometer-sized particles, will have their entry to the bloodstream enhanced over those which predominate in larger particles.

In fact, a number of toxic elements including Pb, Se, Sb, Cd, Ni, V, Sn, and Zn in urban aerosols have been reported to have equivalent mass median diameters of the order of 1 μm or less, which is considerably less than those reported for common matrix elements such as Fe, Al, and Si. Mass median diameters of these elements lie in the range of 2.5-7.0 μm (9-12). It is therefore meaningful to determine whether certain toxic elements predominate in the smallest particles emitted from particulate sources or whether the mass median diameter differences in urban aerosols are simply due to mixing of particles characteristic of individual source emissions.

The work reported here was designed to establish whether elements present in fly ash particles emitted from coal-fired power plants (essentially ubiquitous contribu-

tors to urban aerosols) exhibit a dependence of element concentration on particle size. A variety of analytical techniques was employed to choose the most reliable for the determination of individual elements in fly ash and to establish the data firmly.

Experimental

Sample Collection and Size Differentiation. Two types of samples are represented: (a) fly ash retained in the cyclonic precipitation system of a coal-fired power plant and (b) airborne fly ash collected in the ducting approximately 10 ft from the base of the stack. The retained material was collected in bulk and was size differentiated physically by sieving and aerodynamically in the laboratory with a Roller particle size analyzer (American Instrument Co.). Airborne fly ash samples were collected and size differentiated in situ using an Andersen stack sampler fabricated from stainless steel and designed to operate at the stack temperature. Although results are reported for samples collected in a single plant, the trace element content of fly ash collected in this plant equipped with cyclonic precipitators and using southern Indiana coal was shown to be representative of that in eight U.S. power plants utilizing a variety of coal types.

Particle size calibrations were based on the data supplied by the manufacturers of the analyzers employed. These data are established in terms of equivalence to the aerodynamic diameter of spherical particles of unit density (13, 14). Since fly ash particles are predominantly spherical, a rough check on the validity of the aerodynamic sizes can be obtained by determining the average physical size of particles in a given size fraction. For this pur-

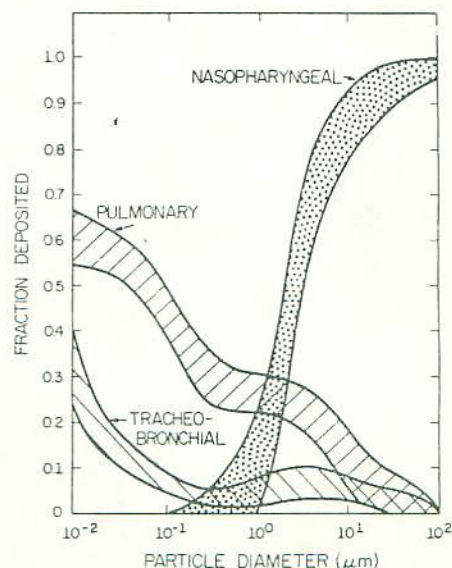


Figure 1. Efficiency of particle deposition in the three respiratory system compartments (5)

pose, particles collected on the third and fourth plates (4.6–7.1 μm and 3.0–4.6 μm equivalent aerodynamic diameter) of the Andersen stack sampler were examined using a Coulter counter (Coulter Electronics Inc., Hialeah, Fla.) in the timed analysis mode with a 100- μm aperture.

Milligram portions of the fly ash were dispersed in a 50% mixture of methanol in water and ultrasonically agitated for 5 min before adding the suspension to the counter. When we assumed a particle density of 2.5 g/cm^3 to convert volume median diameters to approximate aerodynamic diameters, values of 6.3 and 4.3 μm equivalent aerodynamic diameter were obtained. These indicate the general validity of the aerodynamic size calibration data.

In this experiment there was no evidence of particle diameter changing with time due to particle solubility in the methanol-water mixture. Indeed, none was expected since the particle matrices consist predominantly of insoluble aluminum and silicon and iron oxides, and soluble species are relatively minor constituents.

Analytical Procedures. The analytical methods employed fall into two classes, those which analyze the fly ash directly as the solid and those which analyze the sample in solution following wet digestion. The former methods retain sample integrity but involve calibration uncertainties: the latter allow easy calibration but are susceptible to possible formation of analytically intractable compounds during digestion.

Sample digestion was achieved by heating 0.5 gram of fly ash, 3.5 ml of 3:1 concentrated HCl/HNO_3 (aqua regia), 0.5 ml water, and 2.5 ml of an aqueous solution containing 48% HF for 2 hr at 110°C in a 25-ml Teflon-lined Parr pressure bomb (Parr Instrument Co., Moline, Ill.). After it cooled, 2.5 grams of boric acid were added to neutralize the HF. The small amount of black solid residue remaining was removed by centrifugation and was shown by spark sources mass spectrometry to contain mainly Ca, F, and Al in addition to carbon. At least 95% extraction of the elements of interest was achieved.

Atomic absorption analyses were performed by direct aspiration of dilutions of the original digest for Pb, Tl, Cd, As, Ni, and Be. Air-acetylene flames were employed for all elements except Be for which nitrous oxide-acetylene was used. A Jarrel Ash 8-10 dual-beam double monochromator instrument was employed. Background corrections were achieved by monitoring a nonabsorbing wavelength within 40 Å of the analytical wavelength. Se was determined by its atomic absorption after conversion to volatile H_2Se according to the method of Schmidt and Royer (15). Standard addition calibrations were performed in all cases, and a precision of $\pm 10\%$ was achieved.

The elements Pb, Be, Cr, Mn, Co, and Ni were determined by dc arc emission spectroscopy using a Baird-Atomic 3-meter spectrograph. Samples coarser than 325 mesh (Tyler series) were ground to pass through a 325-mesh sieve. One part by weight of fly ash was mixed with four parts of spectroscopic graphite for 1 min in a Wig-L-Bug mechanical shaker (Spex Industries). Spex mix A-7 pure graphite standards doped with 49 elements were used for comparative standards. Approximately 50 mg of graphite diluted sample were burned to completion in a cup electrode operating with a 4-mm gap and 10-amp current. Element concentrations were obtained with a precision of $\pm 30\%$.

The fly ash matrix elements Fe, Ti, Al, Si, Ca, K, S, and Mg were determined using a vacuum-path, single-crystal, Phillips X-ray spectrometer. All samples of nominal particle diameter $> 4 \mu\text{m}$ were ground further so as to minimize surface sampling and inhomogeneity effects.

The powders were suspended in propanol and dispersed ultrasonically before deposition by filtration onto 0.4- μm millipore membrane filters (16). Mineral standards previously calibrated against NBS mineral standards were supplied by the Illinois State Geological Survey. K_α radiation was monitored for all elements and a vacuum radiation path maintained for all elements except Fe and Ti. A lithium fluoride crystal was employed for detecting Fe and Ti, EDDT was used for Al, Si, Ca, K, and S, and ADP was used for Mg. For this method, precisions of $\pm 5\%$ were achieved.

An AEI model MS-7 spark source mass spectrometer was used for the qualitative determination of all elements of atomic number greater than 11 and for quantitative determination of Bi, Pb, Tl, Sb, Sn, As, Zn, Cu, Ni, Fe, V, Ca, K, and Si. One part of fly ash was mixed by weight with two parts of spectroscopic graphite for 5 min in a Wig-L-Bug and the mixture pressed into an electrode. Electrodes were manually positioned and sparked using a 25- μsec spark duration and a repetition rate of 300 sec^{-1} at 10^{-6} torr source pressure. Mass spectra were recorded photographically.

Internal standardization of the mass spectra was achieved by referencing line intensities both to the Pb in the sample and to 60 $\mu\text{g}/\text{g}$ of solution-doped Au. The Pb was determined independently by atomic absorption spectroscopy. The $^{197}\text{Au}^+$ ion was at least two orders of magnitude more intense than $^{181}\text{Ta}^{160+}$ from source contamination. Element concentrations were calculated from the expression by Farrar (17).

$$C_x = C_{st} \frac{I_x}{I_{st}} \left[\frac{M_x}{M_{st}} \right]^2 \frac{\phi_{st} k}{\phi_x} \quad (1)$$

where

I = peak intensity of ion beam

ϕ = isotopic abundance

M = mass

C = concentration

k = sensitivity factor for a given element relative to the standard

st and X = internal standard and analyte quantities, respectively

This expression assumes that the line width on the photographic plate is proportional to $M^{1/2}$ (18). Values of k were determined by doping increasing amounts of Pb, Tl, Sb, Sn, As, and Ni into the graphite before forming a series of electrodes with fly ash. For these elements, values of k ranged from 1.0–1.8. For the remaining elements, k was set equal to unity, an assumption usually valid within a factor of three (17). Precisions of $\pm 20\%$ were achieved.

Carbon present as SiC, FeC, and free C was determined as CO_2 after combustion with O_2 on a V_2O_5 catalyst (19).

Results

Results of the fly ash analyses are listed in Tables I–III for the technique considered most reliable for each element. Sieved fly ash fractions are listed with physical diameters, but all other fractions are represented in terms of equivalent aerodynamic diameters. Fly ash particles larger than 74 μm (200 mesh, Tyler series) exhibited no dependence of element concentration on particle size so that the concentrations listed for this fraction are averages over all larger fractions.

The 25 elements are classified into three groups. In Table I are listed those elements exhibiting concentration increases with decreasing particle diameter. These concentration increases, which were well above experimental error and confirmed by at least two analytical techniques,

were consistently observed in a range of samples and were present in the airborne fly ash collected from the ducting. Table II contains elements which showed concentration trends only in the retained or in the airborne particle size fractions or which, like V, Mn, and Be, exhibited nonuniform dependence on particle size. Table III contains elements

which showed no convincing trends within our experimental errors.

It should be noted that some of the values listed in Tables I-III show considerable deviation from the apparent trends. Repeated analyses of duplicate samples indicate that such deviations are essentially random and are thus

Table I. Elements Showing Pronounced Concentration Trends

Particle diam, μm	Pb	Tl	Sb	Cd	Se	As	Ni	Cr	Zn	S, wt %	Mass fraction %
	$\mu\text{g/g}$										
A. Fly Ash Retained in Plant											
Sieved fractions											
>74	140	7	1.5	<10	<12	180	100	100	500	...	66.30
44-74	160	9	7	<10	<20	500	140	90	411	1.3	22.89
Aerodynamically sized fractions											
>40	90	5	8	<10	<15	120	300	70	730	<0.01	2.50
30-40	300	5	9	<10	<15	160	130	140	570	0.01	3.54
20-30	430	9	8	<10	<15	200	160	150	480	...	3.25
15-20	520	12	19	<10	<30	300	200	170	720	...	0.80
10-15	430	15	12	<10	<30	400	210	170	770	4.4	0.31
5-10	820	20	25	<10	<50	800	230	160	1100	7.8	0.33
<5	980	45	31	<10	<50	370	260	130	1400	...	0.08
Analytical method											
	a	a	a	a	a	a	b	a	a	a	a
B. Airborne Fly Ash											
>11.3	1100	29	17	13	13	680	460	740	8100	8.3	
7.3-11.3	1200	40	27	15	11	800	400	290	9000	...	
4.7-7.3	1500	62	34	18	16	1000	440	460	6600	7.9	
3.3-4.7	1550	67	34	22	16	900	540	470	3800	...	
2.1-3.3	1500	65	37	26	19	1200	900	1500	15000	25.0	
1.1-2.1	1600	76	53	35	59	1700	1600	3300	13000	...	
0.65-1.1	48.8	
Analytical method											
	d	a	a	d	d	d	d	d	a	c	

a Dc arc emission spectrometry. b Atomic absorption spectrometry. c X-ray fluorescence spectrometry. d Spark source mass spectrometry.

Table II. Elements Showing Limited Concentration Trends

Particle diameter, μm	Fe, wt %	Mn, $\mu\text{g/g}$	V, $\mu\text{g/g}$	Si, wt %	Mg, wt %	C, wt %	Be, $\mu\text{g/g}$	Al, wt %
A. Fly Ash Retained in Plant								
Sieved fractions								
>74	...	700	150	12	...
44-74	18	600	260	18	0.39	11	12	9.4
Aerodynamically sized fractions								
>40	50	150	250	3.0	0.02	0.12	7.5	1.3
30-40	18	630	190	14	0.31	0.21	18	6.9
20-30	...	270	340	0.63	21	...
15-20	...	210	320	2.5	22	...
10-15	6.6	160	320	19	0.16	6.6	22	9.8
5-10	8.6	210	330	26	0.39	5.5	24	13
<5	...	180	320	24	...
Analytical method								
	a	b	c	d	d	d	d	d
B. Airborne Fly Ash								
>11.3	13	150	150	34	0.89	0.66	34	19.7
7.3-11.3	...	210	240	0.70	40	...
4.7-7.3	12	230	420	27	0.95	0.62	32	16.2
3.3-4.7	...	200	230	0.57	55	...
2.06-3.3	17	240	310	35	1.4	0.81	43	21.0
1.06-2.06	...	470	480	0.61	60	...
0.65-1.06	15	23	0.19	9.8
Analytical method								
	d	b	c	d	d	e	b	d

a Dc arc emission spectrometry. b X-ray fluorescence spectrometry. c Atomic absorption. d Spark source mass spectrometry. e Oxygen fusion.

attributed to poor sampling statistics, a result of the heterogeneous nature of fly ash. It is considered appropriate, however, to present raw data obtained for a coherent set of size fractions to illustrate this problem of sampling and to avoid possible biases in the data.

Discussion

The results presented in Tables I, II, and III demonstrate four significant points:

A coal-fired power plant produces enrichment of certain elements in the smallest emitted particles.

The highest concentrations of these trace elements are found in particles which deposit in the pulmonary region of the respiratory system.

Existing particle control devices are least effective for removing the most toxic particles.

Estimates of toxic element emissions based on analyses of undifferentiated fly ash collected from particle precipitators will be much lower than actual emissions.

In fact, only a small fraction of the total fly ash mass has particle diameters $<10 \mu\text{m}$ (Table I) and by no means all of this is emitted to the atmosphere. However, the fraction emitted undoubtedly presents a greater potential health hazard per unit weight than that retained. Furthermore, the dependences of element concentration on particle size presented in Table I may be less pronounced than actually occurs. This is a result of the substantial overlap of size fractions deposited on different plates of the Andersen stack sampler (20).

Essentially similar dependence of element concentration on fly ash particle size has been obtained by Lee and von Lehmden (21) for Cd, Pb, Mn, and Cr and by Toca (22) for Pb and Cd. Toca also found that 70% of the Cd present in flue gases was associated with particles $<5 \mu\text{m}$ in diameter. More recently, Sparks (23) reported that the elements Pb, Ba, Sr, Rb, As, and Zn in fly ash particles collected on a $0.4\text{-}\mu\text{m}$ millipore filter, following the last stage of a Brinks impactor, were enriched on a weight-for-weight basis by at least an order of magnitude over those deposited on the last impactor stage.

One explanation of the dependence of element concentration on particle size is that the ashing characteristics of pyritic inclusions that contain many of the trace elements (24, 25) predominantly give rise to small particles. However, we incline to the view that certain elements or their compounds are volatilized in the high-temperature coal combustion zone and then either condense or adsorb onto entrained particles. The mass deposited is thus greatest per unit weight for the smallest particles.

In support of this volatilization adsorption-condensation hypothesis, it is noteworthy that all the elements (except Cr and Ni) listed in Table I have boiling points comparable to or below the temperature of the coal combustion zone (1300–1600°C). This is also true of Ba, Sr, and Rb as determined by Sparks (23). This statement implies that metal compounds are reduced to the element before volatilization. However, while reduction in the combustion zone is certainly feasible, such reduction is not necessary to our basic hypothesis. Indeed, neither Ni nor Cr, both of which exhibit a marked dependence of concentration on particle size (Table I), would exist as stable vapors (Table IV). It is suggested that these elements have access to the vapor phase as sulfides or, conceivably, as carbonyls whose highly transient formation during coal combustion has been postulated (1). Mercury, of course, undoubtedly volatilizes as the element and is predicted to exhibit a dependence of concentration on particle size if the proposed mechanism is valid.

Additional support for the mechanism is provided by the work of Hulett (26). He has shown by scanning elec-

tron microscopic analyses of individual argon ion etched fly ash particles that Zn, Cr, and Ni (the most concentrated elements in Table I) predominate on particle surfaces.

A simple model can be constructed by considering a single particle in which an element, X, is uniformly deposited on the particle surface at a concentration C_s ($\mu\text{g}/\text{cm}^2$). In addition, X is assumed to be uniformly distributed throughout the particle with a concentration C_o ($\mu\text{g}/\text{g}$). The total concentration of X, C_x ($\mu\text{g}/\text{g}$), is then given by

$$C_x = C_o + \frac{C_s A}{\rho V} \quad (2)$$

Table III. Elements Showing No Concentration Trends

Particle diameter, μm	Bi, $\mu\text{g}/\text{g}$	Sn, $\mu\text{g}/\text{g}$	Cu, $\mu\text{g}/\text{g}$	Co, $\mu\text{g}/\text{g}$	Ti, wt %	Ca, wt %	K, wt %
A. Fly Ash Retained in Plant							
Sieved fractions							
>74	>2	>2	120	28
44-74	>2	>2	260	27	0.61	5.4	1.2
Aerodynamically sized							
>40	>2	>2	220	75	0.01	2.5	2.54
30-40	>2	>2	120	76	0.64	6.3	6.26
20-30	>2	>2	160	55
15-20	>2	>2	220	50	...	4.5	4.46
10-15	>2	>2	220	55	0.66	4.0	4.04
5-10	>2	>2	390	46	1.09
>5	>2	>2	490	54
B. Airborne Material							
>11.3	>1.7	7	270	60	1.12	4.9	4.9
7.3-11.3	>3.5	11	390	85
4.7-7.3	>4.0	18	380	90	0.92	4.2	4.2
3.3-4.7	>4.8	19	...	95
2.06-3.3	>4.5	16	330	90	1.59	5.0	5.0
1.06-2.06	>4.4	18	300	130
0.65-1.06	1.08	2.6	2.6
Analytical method							
	a	a	a	b	c	c	c

a Spark source mass spectrometry. b Dc arc emission spectrometry. c X-ray fluorescence spectrometry.

Table IV. Boiling Points of Possible Inorganic Species Evolved During Coal Combustion

Species boiling or subliming, $<1550^\circ\text{C}$	Species boiling or subliming, $>1550^\circ\text{C}$
As, As ₂ O ₃ , As ₂ S ₃	Al, Al ₂ O ₃
Ba	BaO
	BeO
Bi	Bi ₂ O ₃
Ca	C
Cd, CdO, CdS	CaO
Cr(CO) ₆ , CrCl ₃ , CrS (155°)	Co, CoO, CoS
K	Cr, Cr ₂ O ₃
Mg	Cu, CuO
Ni(CO) ₄	Fe, Fe ₂ O ₃ , Fe ₃ O ₄ , FeO
PbCl ₂ , PbO, PbS	MgO, MgS
Rb	Mn, MnO, MnO ₂
S	Ni, NiO
	Pb 1620-1750°C
Se, SeO ₂ , SeO ₃	Si, SiO ₂
Sb, Sb ₂ S ₃ , Sb ₂ O ₃	Sn, SnO ₂
	SrO
SnS	Ti, TiO ₂ , TiO
Sr	U, UO ₂
Ti, Ti ₂ O, Ti ₂ O ₃	
Zn, ZnS	ZnO

where

- C_o = bulk concentration of X
- C_s = surface concentration of X
- C_x = total concentration of X
- V = particle volume
- A = particle surface area
- ρ = particle density

By summing overall fly ash particles and assuming spherical particles, the average concentration of X , \bar{C}_x , is given by.

$$\bar{C}_x = \bar{C}_o + \frac{6\bar{C}_s}{\bar{\rho}} \frac{1}{\bar{D}} \quad (3)$$

where D is the particle diameter and the bars denote average values. Microscopic observation does, in fact, show that most particles are spherical.

To substitute the values in Table I into Equation 3, it is necessary either to make the assumption that $\bar{\rho}$ is not a function of particle diameter, D , or to determine $\bar{\rho}$ for each size fraction. Appropriate values of D for each size fraction can be obtained by assuming

$$\bar{D} = \frac{(ECD)_u + (ECD)_l}{2} \quad (4)$$

where $(ECD)_u$ and $(ECD)_l$ are the upper and lower 50% cutoff diameters for each stage of the Andersen stack sampler. Equation 2 thus assumes a symmetrical distribution of the mass of X over the diameter range $(ECD)_u$ to $(ECD)_l$. Incorporating these assumptions enables construction of a plot of \bar{C}_x vs. \bar{D}^{-1} as depicted in Figure 2 from which it can be seen that the results are in at least qualitative agreement with the proposed model.

The thickness, l , of the deposition layer can then be estimated from the expression

$$l = \bar{C}_s / \bar{\rho}' \quad (5)$$

where $\bar{\rho}'$ is the density of the deposition layer which was assumed equal to 3 g/cm^3 . Values of \bar{C}_s , \bar{C}_o , and l are presented in Table V. These values, with the notable exception of those for sulfur, are considered reasonable for a thin surface-deposited layer. The $0.06 \text{ }\mu\text{m}$ "layer thickness" obtained for sulfur is considered too great to be accounted for by a simple adsorption process. Indeed, the high concentrations of S obtained for the $0.65\text{--}1.1 \text{ }\mu\text{m}$ size fraction (Table I) can only be accounted for if sulfur is present as the element. This suggestion is at variance with the findings of Hulet (27) who has shown, using electron spectroscopy, that S predominates as sulfate. We, therefore, consider that the sulfur values listed in Table I are all proportionately high owing to lack of a fly ash standard having sulfur deposited on the surface of appropriately sized particles, as required for our X-ray fluorescence analysis.

If the observed dependence of element concentration on particle size is, in fact, due to volatilization followed by adsorption or condensation, as is suggested, one would expect the same phenomenon to be exhibited by particles derived from all high-temperature solid combustion operations. Data for sources other than coal-burning power plants are not currently available to substantiate this suggestion but, if correct, it means that many sources may preferentially emit small particles high in toxic elements or their compounds. The mass median diameters of such elements in the emitted particle distribution will thus be reduced as a direct result of surface deposition. The extent of reduction can be determined by combining Equation 3 with the mass distribution function appropriate

for a given particle source. In the case of a log-normal distribution, this gives the following:

$$\frac{dM_x}{d(\ln D)} = \frac{1}{\sqrt{2\pi} \ln \sigma_g} \left\{ \bar{C}_o \exp \left[-\frac{(\ln D/D_g)^2}{2(\ln \sigma_g)^2} \right] + \frac{6C_s}{\bar{\rho}} \exp \left[\frac{(\ln \sigma_g)^2}{2} \right] \exp \left[-\frac{(\ln D/D_g + \ln^2 \sigma_g)}{2 \ln^2 \sigma_g} \right] \right\} \quad (6)$$

where

- σ_g = geometric standard deviation
- M_x = mass of X
- D_g = mass median diameter of original substrate distribution

Equation 6 does not provide a simple analytical expression for the mass median diameter of the adsorbed species, $D_g(X)$, except when $C_o = 0$ —i.e., X is present only in the deposited layer. In this case, it can readily be shown (28) that

$$\ln D_g(X) = \ln D_g - \ln^2 \sigma_g \quad (7)$$

Equations 6 and 7 demonstrate that the mass median diameter of a surface-deposited species, X , is considerably less than that of the total mass.

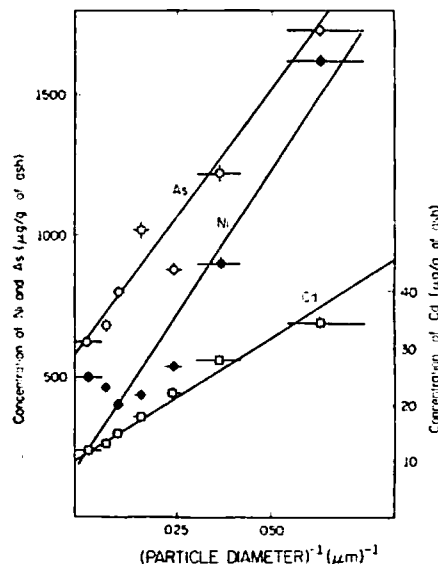


Figure 2. Dependence of element concentration on particle size for As, Ni, and Cd in fly ash emitted from a coal-fired power plant

Table V. Parameters Derived from Surface Deposition Model

Element	Sample pairs	$C_o, \mu\text{g/cm}^2$	$C_s, \mu\text{g/g}$	Linear correlation coeff.	Estimated surface thickness, \AA
Pb	6	0.04	1000	0.73	1.0
Tl	6	0.003	40	0.80	0.1
Sb	6	0.003	20	0.93	0.1
Cd	6	0.002	10	0.99	0.7
Se	6	0.004	0.7	0.92	0.1
As	6	0.009	600	0.97	0.3
Zn	6	0.6	6000	0.60	20
Ni	6	0.1	100	0.98	4.0
Cr	6	0.3	300	0.94	9.0
S	4	19.0	5×10	...	600

The validity of Equations 3 and 6 is destroyed as soon as particles from different sources become mixed into the ambient aerosol. However, if surface deposition is a widespread phenomenon as suggested earlier, one would expect volatile elements present in urban aerosols to have significantly lower mass median diameters than nonvolatile elements. In fact, data obtained by the National Air Surveillance Network (NASN) have shown the volatilizable elements Zn, Ni, Pb, Cd, and Ba to have statistically lower mass median diameters than common nonvolatilizable particle matrix elements. Also, although not substantiated statistically, Se and Sb have been shown to have small mass median diameters in ambient aerosols (12). Lead, of course, is not expected to be typical since it is derived mainly from a single source (the automobile) known to produce small particles.

The predominance of certain elements in small particles is also significant in determining the degree of enrichment of these elements in an urban aerosol, since the smallest particles have the longest atmospheric residence time. Indeed, Gladney et al. (29) have shown enrichment factors of greater than ten times over natural crustal abundance for Tl, Cr, Ni, Cu, Zn, As, Cd, Sn, Pb, Se, S, Cl, and Br in the Boston aerosol and have established substantial correlations with enrichment patterns in coal fly ash, municipal incinerator fly ash, and residual fuel oil. In the present context, it is noteworthy that the majority of these elements could be volatilized during combustion.

Although we have considered only trace elements present in particulate matter, the importance of vapor species such as SeO_2 and As_2O_3 should not be overlooked. Thermodynamic data (30) indicate that at 25°C as much as $80 \mu\text{g}/\text{m}^3$ of Se as SeO_2 and $70 \mu\text{g}/\text{m}^3$ of As as As_2O_3 can exist as vapors. These levels are much greater than normally observed for Se and As in urban aerosols ($\leq 10 \text{ ng}/\text{m}^3$). It is possible, therefore, that additional amounts of these elements may be emitted as vapors. Consistent with this suggestion, Pillay and Thomas (31) have reported that at least 50% of the Se present in urban air passes through a filter designed to collect all particles greater than $0.1 \mu\text{m}$ in diameter. Comparable data are not available for As, but future sampling operations should undoubtedly undertake gaseous sampling procedures for both elements.

By employing a variety of analytical techniques in this study it has been possible to establish which are the most reproducible, precise, and interference free for individual elements in fly ash. Spark source mass spectrometry undoubtedly affords the greatest advantage for multielemental determination in solid fly ash although the analyses are extremely time consuming. In addition, interferences prevent the analysis of Te, Cd, Se, Co, Mn, Cr, and S and permit only a semiquantitative estimate for Be. Dc arc emission spectroscopy exhibits no significant advantages over spark source mass spectroscopy other than detection of Co, Mn, Cr, and Be and wider availability. The X-ray fluorescence method employed has the advantages of high speed and precision but is somewhat limited by calibration difficulties and matrix effects. The shallow penetration depths of soft X-rays from the lighter elements such as sulfur and magnesium necessitate high matrix identity between samples and standards and a very small particle size (32).

Atomic absorption spectrometry is considered to be the most accurate technique employed in this work. However, large amounts of samples are required if more than a few elements are determined. Also, great care must be taken to achieve good background corrections due to the large number of elements present. Atomic absorption spectrometry displayed no evidence of loss of sample integrity as a

result of the fly ash digestion except, possibly, in the case of Tl where analyses were consistently 3-5 times lower than those obtained by spark source mass spectrometry and anodic stripping voltammetry after removal of the Pb interference. The reasons for this are being investigated.

Comparison of results obtained by different techniques has enabled confirmation of the size dependences represented in Tables I-III. The absolute values of concentrations obtained by different techniques are only in semi-quantitative agreement. However, this is in accord with the findings of von Lehmden et al. (33), who demonstrated, in a major interlaboratory comparison, that the absolute values obtained for trace elements in fly ash varied considerably between techniques and between laboratories. Nevertheless, the reproducibilities obtained for a given element using a single technique were within 10% except for occasional samples where the deviations are attributed to poor sampling statistics as discussed earlier. Since our findings and conclusions rely only on the relative accuracies of values obtained for different size fractions using a single technique for each element, the uncertainties in absolute accuracy are not of major consequence in this work.

Acknowledgments

The authors gratefully acknowledge valuable discussions with G. E. Gordon, University of Maryland, and W. E. Fulkerson, Oak Ridge National Laboratory, and their colleagues. The authors are also indebted to the personnel at the Environmental Research Laboratory (University of Illinois) and the Illinois State Geological Survey (Urbana) for analytical assistance.

Literature Cited

- (1) Schroeder, H. A., *Environment*, 13, 18-32 (1971).
- (2) Gordon, G. E., Zoller, W. H., "Normalizations and Interpretation of Atmospheric Trace-Element Concentration Patterns," Oak Ridge Trace Elements Conference, Oak Ridge, 1973.
- (3) Morrow, P. E., *Amer. Ind. Hyg. Assoc. J.*, 25, 213-36 (1964).
- (4) Hatch, T. F., Gross, Paul, "Pulmonary Deposition and Retention of Inhaled Aerosols," Academic Press, New York, N.Y., 1964.
- (5) United States Department of Health, Education, and Welfare, National Air Pollution Control Boards, Pub. No. AP-49, "Air Quality Criteria for Particulate Matter," Washington, D.C., January 1969.
- (6) Langham, W. W., "Radioisotope Absorption and Methods of Elimination: Relative Significance of Portals of Entry," in "Symposium on Radioisotopes in the Biosphere," R. S. Caldecott and L. A. Snyder, Eds., Minneapolis, University of Minnesota Press, 1960.
- (7) Patterson, C. C., *Sci. Cit.*, 10, 66 (1968).
- (8) Dautreband, L., "Microaerosols," Academic Press, New York, N.Y., 1962.
- (9) Rahn, K. A., Dams, R., Robbins, J. A., Winchester, J. W., *Atmos. Environ.*, 5, 413 (1971).
- (10) Lee, R. E., Jr., Goransen, S. S., Enrione, R. E., Morgan, G. B., *Environ. Sci. Technol.*, 6, 1025-30 (1972).
- (11) Colovos, G., Wilson, G. S., Moyers, J. L., to be published in *Int. J. Environ. Anal. Chem.*, in press.
- (12) Gladney, E. S., Zoller, W. H., Jones, A. G., Gordon, G. E., *Environ. Sci. Technol.*, 8, 551-7 (1974).
- (13) Ranz, W. E., Wong, J. B., *Ind. Hyg. Occupa. Med.*, 4, 464-77 (1952).
- (14) Flesch, J. P., Norris, C. H., Nugent, A. E., Jr., *Am. Ind. Hyg. Ass. J.*, 28, 507-16 (1967).
- (15) Schmidt, F. J., Royer, J. L., *Anal. Lett.*, 6 (1), 17-23 (1973).
- (16) Price, N. B., Angell, G. R., *Anal. Chem.*, 40 (3), 660-3 (1968).
- (17) Farrar, Harry, IV, in "Trace Analysis by Mass Spectrometry," Arthur J. Ahearn, Ed., Chap. 8, Academic Press, New York, N.Y., 1972.
- (18) Owens, E. B., Giardino, N. A., *Anal. Chem.*, 35, 1172 (1963).
- (19) Quayermark, Al., "Quantitative Organic Microanalysis," p 222, Academic Press, New York, N.Y., 1961.

- (20) Gordon, G. E., Director, "Study of the Emissions from Major Air Pollution Sources and Their Atmospheric Interactions, First Year Progress Report," Nov. 1, 1972-Oct. 31, 1973, University of Maryland, College Park, Md.
- (21) Lee, R. E., Jr., von Lehmden, D. J., *J. Air Pollut. Contr. Ass.*, 23 (10), 853 (1973).
- (22) Toca, F. M., "Lead and Cadmium Distribution in the Particulate Effluent from a Coal Fired Boiler," Ph.D. Dissertation, U. of Iowa, July 1972; see also *Diss. Abstr. Int.*, 33, 3156B (1973).
- (23) Sparks, C. J., Oak Ridge National Laboratory, "Analysis of Particles Collected on a Brinks Impactor," private communication, 1973.
- (24) Nicholls, G. D., in "Coal and Coal Bearing Strata," D. Merchison and P. Stanley Westoll, Eds., pp 269-307, Oliver and Boyd, London, 1968.
- (25) Gluskoter, H. J., Lindahl, P. C., *Science*, 181, 264-6 (1973).
- (26) Hulett, L. D., Oak Ridge National Laboratory, "Analysis of Individual Fly Ash Particles," personal communication, 1973.
- (27) Hulett, L. D., *ibid.*, "The Chemical State of Sulfur in Fly Ash," personal communication, 1973.
- (28) Butcher, S. S., Charlson, R. J., "An Introduction to Air Chemistry," Chap. 9, Academic Press, New York, N.Y., 1972.
- (29) Gladney, E. S., Gordon, G. E., Zoller, W. H., "Abnormally Enriched Trace Elements in the Atmosphere," Seventh Annual Conference on Trace Substances in Environmental Health, U. of Missouri, Columbia, Mo., June 1973.
- (30) Hodgeman, C. D., Ed.-in-chief, "Handbook of Chemistry and Physics," p 2429, 44th ed., The Chemical Rubber Publishing Co., Cleveland, Ohio, 1963.
- (31) Pillay, K. K. S., Thomas, C. C., Jr., *J. Radioanal. Chem.*, 7, 107-18 (1971).
- (32) Muller, R. O., "Spectrochemical Analysis of X-ray Fluorescence," pp 72-86, Plenum Press, New York, N.Y., 1972.
- (33) von Lehmden, D. J., Jungers, R. H., Lee, R. E., Jr., *Anal. Chem.*, 46 (2), 239 (1974).

Received for review November 5, 1973. Accepted August 11, 1974. Work supported by research grants NSF-GH33634 and NSF-GI-31605-IES-7. Mention of commercial products is for identification only and does not constitute endorsement by any agency of the U.S. Government.

Partition Coefficient to Measure Bioconcentration Potential of Organic Chemicals in Fish

W. Brock Neely,^{*1} Dean R. Branson,² and Gary E. Blau³
The Dow Chemical Co., Midland, Mich. 48640

■ The bioconcentration of several chemicals in trout muscle was found to follow a straight line relationship with partition coefficient. Bioconcentration in this paper is defined as the ratio of the concentration of the chemical between trout muscle and the exposure water measured at equilibrium. Partition coefficient has the usual meaning in that it is the ratio of the equilibrium concentration of the chemical between a nonpolar and polar solvent (in this case, *n*-octanol and water were the two solvents used). The relationship was established by measuring the bioconcentration in trout of a variety of chemicals over a wide range of partition coefficients. An equation of the straight line of best fit was determined and used to predict the bioconcentration of other chemicals from their partition coefficients. The predicted values agreed with the experimental values in the literature.

The ability of some chemicals to move through the food chain resulting in higher and higher concentrations at each trophic level has been termed biomagnification or bioconcentration (1). The widespread distributions of DDT (2, 3) and the polychlorinated biphenyls (PCBs) (4) have become classic examples of such movement. From an environmental point of view this phenomenon becomes important when the acute toxicity of the agent is low and the physiological effects go unnoticed until the chronic effects become evident. Due to the insidious nature of the

bioconcentration effect, by the time chronic effects are noted, corrective action such as terminating the addition of the chemical to the ecosystem, may not take hold soon enough to alleviate the situation before irreparable damage has been done. For this reason prior knowledge of the bioconcentration potential of new or existing chemicals is desired. The importance of bioconcentration is also recognized by the Environmental Protection Agency (EPA). For example, the ability of a material to build up in the environment has become one of the proposed criteria that this regulatory agency is using in establishing toxic pollutant effluent standards (5).

In spite of the complexity of the reactions involved in the biomagnification process, we felt it important to see if a simple relationship could be established between the physicochemical properties of a chemical and its ability to bioconcentrate. It was our belief that the partition coefficient would be the most logical parameter to examine in this connection. If a simple relationship could be established it would be of great benefit in planning the future direction of any development work on a new chemical and in directing research efforts to determine the ultimate fate and distribution of others.

Materials and Methods

Chemicals. The following chemicals, representing a wide range of partition coefficients, were evaluated: 1,1,2,2-tetrachloroethylene, hexachlorobenzene, 2,2',4,4'-tetrachlorobiphenyl, 2-biphenyl phenyl ether, diphenyl ether, carbon tetrachloride, and *p*-dichlorobenzene. All materials were examined for purity by means of gas chromatography and found to be >99% pure.

Bioconcentration Factor in Fish. The method described by Branson et al. (6) was used to determine the bioconcentration factor in rainbow trout (*Salmo gairdneri* Richardson). This method is based on determining the ratio of the concentration of the chemical in trout muscle

¹ Ag-Organics Product Department, The Dow Chemical Co., Midland, Mich. 48640

² Waste Control Laboratory, The Dow Chemical Co., Midland, Mich. 48640

³ Computations Research Laboratory, The Dow Chemical Co., Midland, Mich. 48640

EX 2B

COMPOSITION AND SIZE DISTRIBUTION OF IN-STACK PARTICULATE MATERIAL AT A COAL-FIRED POWER PLANT

ERNEST S. GLADNEY

Los Alamos Scientific Laboratory, P.O. Box 1663, Los Alamos, NM 87545, U.S.A.

and

JOHN A. SMALL, GLEN E. GORDON and WILLIAM H. ZOLLER

Department of Chemistry, University of Maryland, College Park, MD 20742, U.S.A.

(First received 23 April 1976 and in final form 11 June 1976)

Abstract—The particulate material in the stack effluent of a coal-fired power plant was collected and fractionated with an in-stack cascade impactor. Samples of the pulverized coal and process ashes were taken on the same days. These materials were analyzed for 34 elements by instrumental neutron and photon activation analysis. Elements on the in-stack particulates can be separated into three groups by computing enrichment factors relative to the coal for each particle size fraction. These groups are compared to proposed mechanisms for trace element fractionation during combustion.

With the increasing importance of coal as a fuel for electric power generation, there is renewed concern about the atmospheric emissions associated with coal combustion. Potentially toxic trace elements in the coal (e.g. Se, As, Hg, Pb, Sb, and Zn) may be volatilized at the temperatures encountered in the combustion zone and either redistributed onto the smaller particles entrained in the flue gas or emitted in the gas phase. The enrichment of certain trace elements on smaller particles has been discussed by Billings and Matson (1972), Billings *et al.* (1973), Gordon *et al.* (1973), Gladney *et al.* (1974), Natusch and Wallace (1974), Natusch *et al.* (1974), Kaakinen *et al.* (1975), Klein *et al.* (1975), Lee *et al.* (1975) and Ragaini and Ondov (1975). Since coal-fired generating stations are a large source of particulate material, the emission of substantial fractions of toxic trace elements on respirable particles could pose a distinct health hazard. It is important, therefore, to measure both the composition and the particle size distribution of the emitted material.

Urban particulates of dia. $\leq 1.0 \mu\text{m}$ have unusually high enrichments of some 15 trace elements (Lee *et al.*, 1972; Gordon *et al.*, 1973; Gladney *et al.*, 1974). Sources for a few of these elements have been traced to auto emissions (Moyers *et al.*, 1972) and residual-oil combustion (Zoller *et al.*, 1973); however, sources for many of these elements remain to be identified. Careful characterization of coal-fired plant emissions should establish the importance of this source in the complex of urban emissions. Size distribution measurements may also permit the differentiation of coal-fired particulates from those of continental origin, and permit the evaluation of the former's contribution to both major- and trace-element levels observed on urban air particulates.

EXPERIMENTAL

Several varieties of cascade impactors are available for in-stack particulate sampling. The University of Washington Mark III Cascade Impactor (Pilat *et al.*, 1970) was selected as the instrument best designed to minimize wall-loss and reentrainment of collected particulates as well as having the lowest 50% effective cutoff diameter (ECD) on the final stage. This instrument can be readily attached ahead of a modified EPA sampling train (Rom, 1972; Gladney, 1974) and operated under EPA-sanctioned sampling conditions.

Impactor, pulverized coal and process ash samples were taken on several different days at the Potomac Electric Power Company's (PEPCO) Chalk Point Electric Generating Station in rural south-eastern MD. At the time of sampling the plant consisted of two 355 MW(e) generators, each consuming $10^5 \text{ kg of coal h}^{-1}$ at full load (Berberich and Bayer, 1964). The coal is ground to 50 mesh and blown from pulverizer into the furnace (water wall), and ash and flue gases are blown from the furnace through the economizer, past Cottrell electrostatic precipitators, and out two 120 m stacks. A small fraction of the coal ash (approx. 9%) is retained in the furnace and removed as bottom slag. About 12% of the ash, predominately particles of 0.1–2 mm dia., is collected at the economizer and about 75% of the ash is trapped by the precipitators and deposited in the fly ash hoppers (Reese, 1974). Approximately 4% of the total ash remains entrained in the flue gas and is emitted to the atmosphere (Whang, 1974).

The temperature of the flue gas is monitored at a number of points throughout the plant. The maximum temperature achieved in the combustion zone is 1600 C. The exhaust gas cools to 450 C during passage through the economizer. The temperatures of the inlet and outlet of the precipitator and at the base of the stack where the suspended particulates were sampled are 130, 120, and 110–120 C respectively (Reese, 1974).

The first seven stages of the Mark III impactor were covered with thin polycarbonate films that had been coated on one side with a thin layer of silicone resin. This sticky surface was employed in an effort to minimize particle bounce-off. Several different filter materials were investigated for use on the final stage of the impactor (an

Table 1. Effective cut-off diameters of mark III source test cascade impactor

Stage	ECD (μm)
1	30
2	14
3	6.0
4	2.5
5	1.4
6	0.70
7	0.35

in-line filter). Nuclepore polycarbonate filters (0.45 μm pore dia.) were selected as the best compromise among filtering capacity, blank levels, and heat resistance. This impactor has 50 μm ECD's shown in Table 1 when operated at a flow rate of 19.8 min^{-1} and at 130 C (Pilat *et al.*, 1973).

Ten minute isokinetic cascade impactor samples were taken using a modified EPA sampling train (details in Martin, 1971; Rom, 1972; Gladney, 1974). A 10 cm plug was designed so that an S-type Pitot tube, a pyrometer, and the impactor could be inserted in the port at the base of the stack simultaneously. The impactor would have its opening pointing "downstream" so that it could be warmed to stack temperature before sampling to avoid condensing volatiles from the gas stream during sampling. During this preheating process, the temperature and velocity of the stack gases were measured with the pyrometer and Pitot tube. These values were monitored for about 10 min, and if conditions were stable a sample was taken.

ANALYSIS

All samples were analyzed nondestructively by instrumental neutron and photon activation analyses. The ana-

lytical techniques, described in detail by Gladney (1974), were modified versions of those reported by Zoller and Gordon (1970) and Aras *et al.* (1973) for all elements except Hg. This element was measured by a combustion procedure described by Rook *et al.* (1972) on only a single impactor run. The powdered coal and fly ash were encapsulated in precleaned polyethylene vials and each impactor stage was folded and individually packaged in clean polyethylene bags. These samples were irradiated simultaneously with National Bureau of Standards (NBS) Standard Reference Materials (SRM) No. 1632 (coal) and No. 1633 (fly ash) and a solid multi-element standard prepared by pipetting a mixed elemental solution onto Whatman No. 1 filter paper. Neutron irradiations were performed at the NBS reactor at a flux of $6 \times 10^{13} \text{ n cm}^{-2} \text{ sec}^{-1}$, and photon irradiations were carried out at the NBS electron linac.

Spectra of the γ -rays emitted by the samples were observed several times after the various irradiations with large, high resolution Ge(Li) detectors (full-width at half maximum of 1.8 at 1332 keV) coupled to 4096-channel pulse-height analyzers. The spectra were stored on magnetic tape and the data reduced off-line by computer. Quality control of these analyses was assured by analysis of the NBS SRM's (reported in Gladney, 1974). The results for all elements compared well with data reported by Ondoy *et al.* (1975) and with the NBS certified values (NBS, 1974). The uncertainties on all elemental concentration data reported in this paper are $\pm 10\%$.

RESULTS AND DISCUSSION

Elemental concentrations in the coal, precipitator fly ash, and the suspended particulates are given in Table 2 for selected elements. Runs 1-3 were similar in nature and have been averaged, while individual

Table 2. Elemental concentrations in power plant materials

Element	Run	Coal (ppm)	Precip. Fly Ash (ppm)	Impactor stage ($\mu\text{g m}^{-3}$)							Filter	TSP*
				1	2	3	4	5	6	7		
Al	1-3	17600	130000	2300	810	1500	2300	1700	450	210	380	9600
	4	18800	135000	24	79	600	1040	810	440	52	580	3600
Na	1-3	258	2090	36	12	25	33	25	7.2	3.3	6.2	148
	4	287	2370	0.43	1.4	11	18	14	7.7	0.91	10	64
Br	1-3	42.3	6.36	0.14	0.22	0.26	0.20	0.17	0.13	0.15	0.79	2.1
	4	38.2	6.21	0.041	0.058	0.054	0.049	0.039	0.034	0.040	2.3	2.6
I	1-3	48.4	96.9	8.1	2.2	1.9	1.7	1.2	0.91	0.93	10	27
	4	52.8	131	0.72	1.1	1.3	2.2	2.6	2.7	0.36	19	30
Cr	1-3	26.3	180	3.2	1.1	2.2	3.4	2.2	0.64	0.38	1.6	15
	4	28.4	192	0.032	0.21	0.80	1.9	1.6	0.79	0.20	1.8	7.3
Ni	1-3	22.3	151	4.8	1.4	2.3	3.8	2.7	0.77	0.45	1.8	18
	4	22.0	143	0.16	0.30	1.1	2.6	1.3	0.83	0.065	1.4	7.8
Zn	1-3	27.9	229	4.7	1.8	4.0	5.1	3.8	1.0	0.63	1.3	22
	4	28.4	259	0.065	0.17	1.4	1.9	1.6	1.0	0.13	2.4	8.6
Ga	1-3	11.1	92.5	0.65	0.52	1.2	1.8	1.2	0.57	0.23	0.64	6.8
	4	13.9	81.8	0.024	0.062	0.46	0.88	0.84	0.50	0.044	0.86	3.7
As	1-3	26.0	168	6.0	3.5	8.3	12	11	5.3	3.1	32	81
	4	24.3	124	0.45	1.6	3.0	5.0	5.0	3.5	1.3	28	48
Se	1-3	3.96	23.8	3.1	3.3	3.1	1.9	0.72	0.33	0.22	1.1	14
	4	6.42	26.6	0.050	0.42	2.6	0.93	0.38	0.20	0.16	1.9	6.6
Sb	1-3	0.812	5.61	0.083	0.13	0.21	0.35	0.25	0.090	0.068	0.59	1.8
	4	1.06	7.68	0.010	0.024	0.074	0.17	0.17	0.12	0.047	0.71	1.3
Pb	1-3	10.2	59.6	1.3	1.0	2.6	2.9	2.2	0.89	0.48	3.6	15
	4	6.47	66.4	0.030	0.12	0.68	1.8	2.3	1.1	0.58	3.9	10
Hg	2	0.36	0.075	0.060	0.050	0.042	0.021	0.021	0.016	0.050	2.4	2.7

* Total suspended particulates ($\mu\text{g m}^{-3}$).

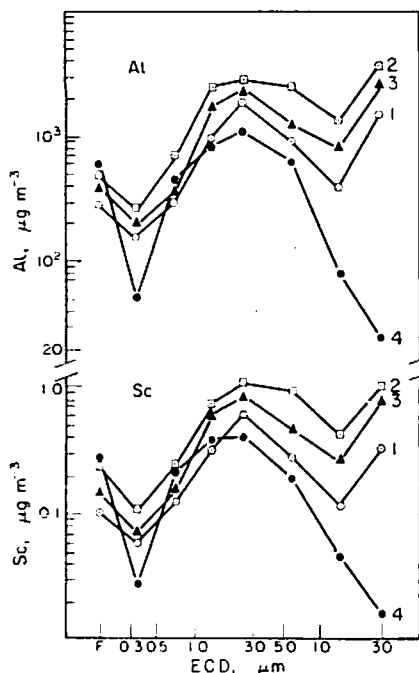


Fig. 1. In-stack size distribution of suspended particulates bearing Al and Sc at the Chalk Point Power Plant (F = backup filter)

data are presented for Run 4. Total suspended particulates are calculated by summing the concentrations across the eight impactor stages. Detailed tabular data for the 21 additional elements are reported in Gladney (1974).

Size distributions for Al, Sc, Br, and I are shown in Figs. 1 and 2. The size distributions for K, Rb, Mg, Ca, Sr, Ba, Zr, Th, Hf, Ta, V, Mn, Fe, Se, Sb, As, Ni, Cr, Co, Ti, Ga, Pb, Zn, Hg, Ce, La, Sm, Eu, Lu, and Yb were also measured, but are not shown.

The qualitative features shown by these figures are the same for all elements listed above except Hg and the halogens. Runs 1-3 usually show a higher trace element concentration on the first stage than on the second, since the particle fraction collected by the initial stage represents an integration over particle diameters greater than 30 µm. The fourth run was taken especially to get a lightly loaded sample and to avoid sampling particulates emitted as a result of "rapping" the precipitator. The rapping process removes particulates adhering to the high voltage wires in the Cottrell precipitator and results in a pulse of large diameter particulates being reentrained in the flue gas. The maximum elemental concentration occurs on particles of approx. 3 µm dia. for all four runs (except for Hg and halogens). In general, all curves, except those of Hg and the halogens, have similar shapes.

An enrichment factor, EF, for element X on each stage relative to average composition of Chalk Point Coal can be calculated using the following equation:

$$EF = \frac{[X]_s}{[X]_c} \frac{[Al]_c}{[Al]_s}$$

where $[X]_s$ and $[X]_c$ represent the concentrations of element X in the sample and the coal respectively,

and $[Al]_s$ and $[Al]_c$ represent the concentrations of aluminium in the sample and the coal respectively (Gordon and Zoller, 1973). Average EF's, relative to Chalk Point coal, for the fly ash and suspended particulates for runs 1-3, and individual values for run 4, are shown in Table 3. Mercury was measured only on Run 2 and the EF's reported have been calculated using Hg and Al data for the coal and fly ash collected on that day only.

When the EF is plotted as a function of particle size, the trace elements can be broken into at least three groups. The Na distribution depicted in Fig. 3 is typical of the first group. This distribution is almost completely featureless—the particulates have the same ratio of Na/Al as the coal across the whole size spectrum. Several elements thought to be fairly volatile (and sometimes seen at high enrichments in ambient aerosols), such as Cr, Zn, Ni, and Ga also exhibit relatively little increase in EF relative to coal. Other elements that fall into this group, and whose EF distributions have also not been shown, are K, Rb, Mg, Ca, Sr, Ba, Sc, Ti, V, Mn, Co, Zr, Th, Hf, Ta, and all rare earths except Ce.

A second group of trace elements (Pb, As, and Sb) exhibits a definite increase in EF on smaller particles. The As EF distribution shown in Fig. 4 supports the hypothesis that these elements may be condensing out of the gas phase. The Sb and Pb distributions are similar and are not shown. It is difficult to compare these observations directly with those of Natuseh *et al.* (1974) since no data on coal composition and only limited data on Al concentration as a function of particle size were reported. However, the concentration

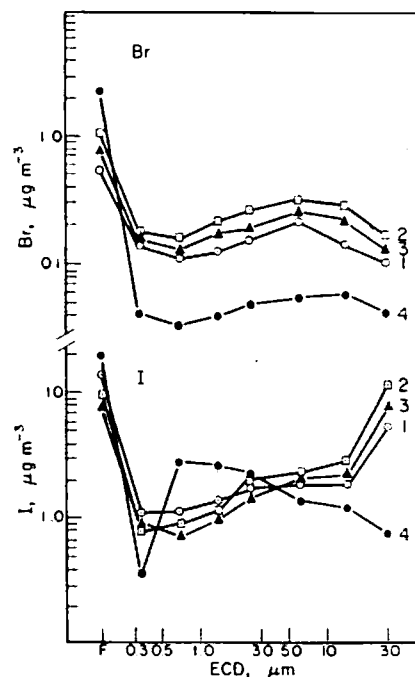


Fig. 2. In-stack size distributions of suspended particulates bearing Br and I at the Chalk Point Power Plant (F = backup filter)

Table 3. Enrichment factors of precipitator fly ash and suspended particulates relative to Chalk Point coal

Element	Run	Precip Fly Ash	Impactor stage							Filter	TSP*
			1	2	3	4	5	6	7		
Na	1-3	1.1	1.1	1.0	1.1	0.98	1.0	1.1	1.1	1.1	1.0
	4	1.2	1.2	1.2	1.1	1.1	1.1	1.1	1.1	1.1	1.2
Br	1-3	0.020	0.025	0.11	0.18	0.036	0.087	0.12	0.30	0.86	0.091
	4	0.023	0.84	0.36	0.044	0.023	0.024	0.038	0.38	2.0	0.36
I	1-3	0.26	1.7	1.3	0.62	0.36	1.3	1.0	2.2	13	1.4
	4	0.34	11	5.0	0.77	0.75	1.1	2.2	2.5	12	3.0
Cr	1-3	0.93	0.93	0.91	0.98	0.99	0.87	0.95	1.2	2.8	1.0
	4	0.94	0.88	1.8	0.88	1.2	1.3	1.2	2.5	2.0	1.3
Ni	1-3	0.92	1.6	1.4	1.2	1.3	1.2	1.4	1.7	3.7	1.5
	4	0.90	5.7	3.2	1.6	2.1	1.4	1.6	1.1	2.1	1.8
Zn	1-3	1.1	1.3	1.4	1.7	1.4	1.4	1.4	1.9	2.2	1.5
	4	1.3	1.8	1.4	1.5	1.2	1.3	1.5	1.7	2.7	1.6
Ga	1-3	1.1	0.45	1.0	1.3	1.2	1.1	2.0	1.7	2.7	1.1
	4	0.82	1.4	1.1	1.0	1.1	1.4	1.5	1.1	2.0	1.4
As	1-3	0.88	1.8	2.9	3.7	3.5	4.4	7.8	10	57	5.7
	4	0.71	14	16	3.8	3.7	4.8	6.0	19	37	10
Se	1-3	0.81	6.0	18	9.2	3.7	1.9	3.2	4.6	13	6.5
	4	0.58	6.1	16	13	2.6	1.4	1.3	9.0	9.6	5.4
Sb	1-3	0.94	0.78	3.5	3.0	3.3	3.2	4.3	7.0	34	4.1
	4	1.0	7.4	5.4	2.2	2.9	3.7	4.8	16	22	6.4
Pb	1-3	0.79	0.98	2.1	3.0	2.2	2.2	3.4	3.9	16	2.7
	4	1.4	3.6	4.4	3.3	5.0	8.2	7.3	30	19	8.1
Hg	2	0.028	0.31	0.80	0.46	0.12	0.16	0.55	3.1	80	17

* Total suspended particulates.

enhancement of these elements on the smaller particles at Chalk Point is less marked than that reported by Natusch *et al.* (1974) for Illinois power plants.

Selenium, Hg, Br, and I also fall in this second group, but they are especially interesting since their EF distributions differ in important detail from the other three elements. Since I and Br are bimodal and similar to Se (Fig. 5), except that enrichment on the smaller particles is more pronounced, individual figures for these two elements are not presented. Selenium and Hg (Figs. 5 and 6), two of the most

volatile elements studied, would be expected to epitomize the small particle preference resulting from condensation of these elements from the gas phase. As shown in Fig. 5, this is not completely true for Se. There is an enrichment of Se on smaller particles (although not to the same extent as Pb, As, and Sb), but there is also a substantial enrichment on the largest particles with a distinct minimum in the middle-sized particles ($5.0 \mu\text{m} \leq d \leq 0.7 \mu\text{m}$). Mercury also

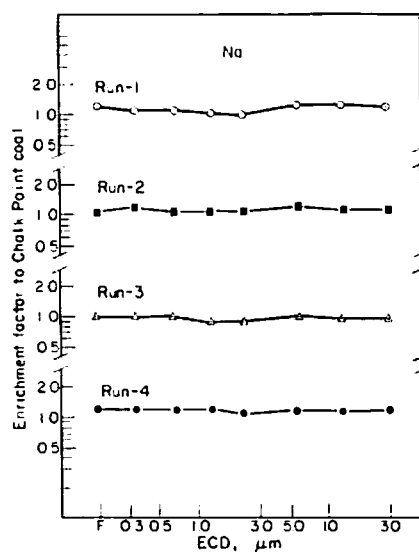


Fig. 3. Enrichment factor of Na, with respect to Chalk Point coal, as a function of in-stack particle size (F = backup filter).

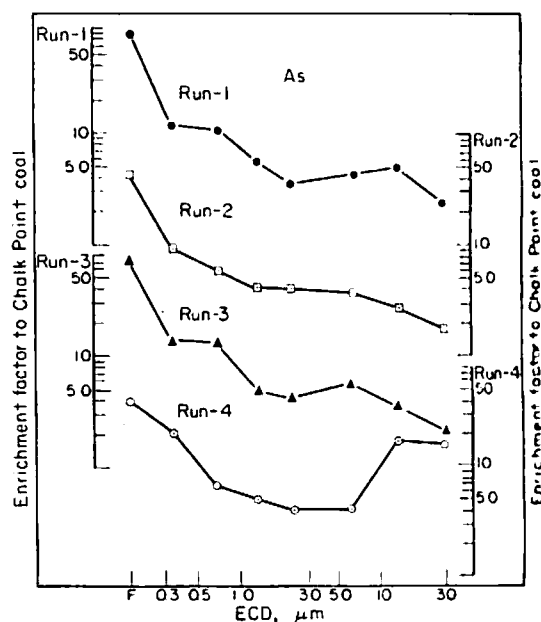


Fig. 4. Enrichment factor of As, with respect to Chalk Point coal, as a function of in-stack particle size (F = backup filter).

Fig. 5. I, Point co.

has an enrichment which is focused on the smaller particles. Billings' data on selenium, I, and I are useful to compare with the present data. The enrichment factors (Fig. 7) and the particle size distributions by noting the enrichment in a py-

Fig. 6. I, Point co.

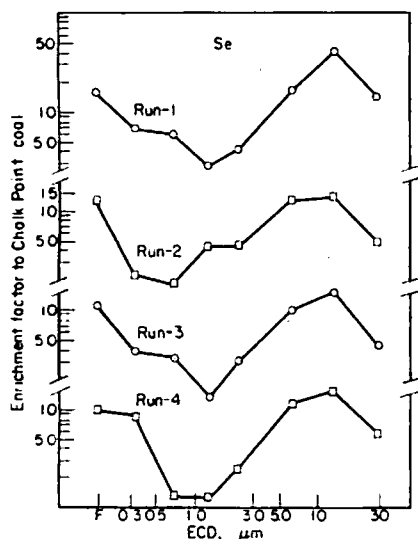


Fig. 5. Enrichment factor of Se, with respect to Chalk Point coal, as a function of in-stack particle size (F = backup filter).

has an EF minimum in the mid-size range, but the enrichment on the smallest particles is very dramatic, which agrees with other power plant studies that focused on this element (Billings and Matson, 1972; Billings *et al.*, 1973). The model for gas phase condensation proposed by Natusch *et al.* (1974) does not adequately explain this bimodal behavior for Se, Br, I, and to a lesser extent Hg. It would be extremely useful to carefully characterize the gas phase concentrations of these elements inside the stack as an approach to explaining their peculiar distributions.

The final group of elements, consisting of Fe (Fig. 7) and Ce, exhibit a strong depletion with decreasing particle size. In the case of Fe, this might be explained by noting that most of the Fe in the coal is probably in a pyrite mineral phase (Ruch *et al.*, 1973). Since

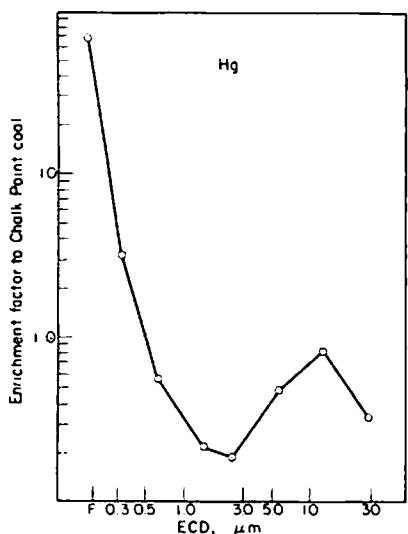


Fig. 6. Enrichment factor of Hg, with respect to Chalk Point coal, as a function of in-stack particle size (F = backup filter), Run 2 only.

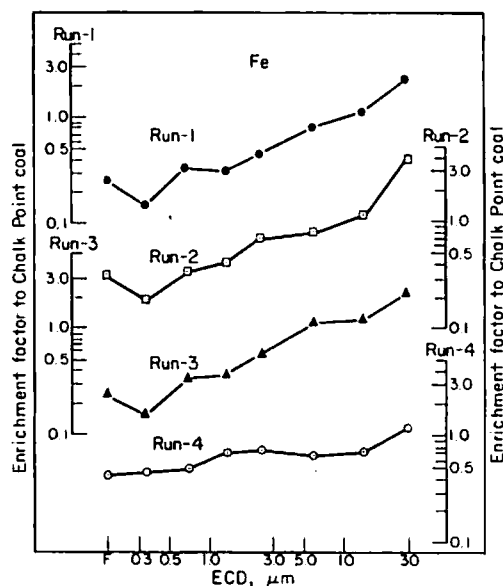


Fig. 7. Enrichment factor of Fe, with respect to Chalk Point coal, as a function of in-stack particle size (F = backup filter).

pyrites probably behave differently from aluminosilicates during combustion, Fe might be expected to yield a rather different size distribution. Other ash fractions retained inside the plant have higher EF's for Fe than the fly ash and suspended particulates, reinforcing the idea that Fe is concentrated on the larger particles (Gladney, 1974). At the present time it is not known if Fe and Ce are associated on the same particles so that the applicability of this hypothesis for Ce cannot be determined. Cerium does not follow the Fe enrichment pattern in bottom slag and economizer ash.

Two other power plant studies (Kaakinen *et al.*, 1975; Ragaini and Ondov, 1975) present sufficient data from in-stack elemental measurements to permit a comparison. Average EF's for seven elements have been calculated relative to the coal burned from these two studies and are shown in Table 4. The agreement among these three in-stack sampling efforts is reason-

Table 4. Comparison of enrichment factors for in-stack total suspended particulates*

Element	Present work†	Kaakinen <i>et al.</i> ‡	Ragaini & Ondov§
Aa	6.8	3.1	7.3 ± 3.2
Zn	1.5	3.2	6.4 ± 4.4
Sb	4.7	3.2	6.7 ± 1.6
Se	6.2	5.7	2.5 ± 1.1
Pb	4.0	5.8	—
Ga	1.2	—	3.1 ± 0.7
Cr	1.1	—	2.0 ± 0.3

* All EF's are relative to coal burned.

† Weighted average from Table 3.

‡ Precipitator outlet stream.

§ Mean ± standard deviation for unspecified number of samples.

ably good, considering differences in sampling conditions, and power plant design and operating parameters. Zinc is definitely less enriched in the Chalk Point stack emissions, although the uncertainties in Ragaini and Ondov (1975) are high. Gallium also appears to be significantly less enriched at Chalk Point. These differences may be attributable to lower combustion and in-stack temperatures at Chalk Point. The behavior of the other elements seems to be relatively similar at the three power plants.

SUMMARY AND CONCLUSIONS

The University of Washington Mark III Cascade Impactor used in this work provided good separation of particles of different sizes as shown by the contrast in size distribution curves for different elements and by comparison with trace element size distributions from other sources (Greenberg, 1974).

Three broad classes of enrichment factor distributions for particulates have been identified. Most elements show little, if any, enrichment (compared to the input coal) as a function of particle size (e.g. Fig. 3); several of the more volatile, toxic trace elements (Sb, As, Pb, Hg, Se, Br, and I) do exhibit increased enrichments on the smaller particles; and two elements, Fe and Ce, had decreasing enrichment with decreasing particle size.

The trace elemental concentration patterns and enrichment factors as functions of particle size suggest that coal-fired power plants similar to Chalk Point, despite the emission of tons of particulate matter, do not seem to account for the high enrichment factors observed for certain particulate trace elements in cities. The nature of the trace metal emissions may be strongly influenced by the temperatures within the plant and the precipitator efficiencies at different facilities. This aspect has been discussed elsewhere (Zoller *et al.*, 1974). A number of other plants should be studied to elucidate the impact of operating conditions on the particle size distribution of the toxic trace elements. Furthermore, the gas phase components of the trace elements requires investigation.

These in-stack elemental distributions do not match the ambient particle size distributions observed for many trace elements in urban areas. Elements which are highly enriched on city aerosols (e.g. V, Zn, Se and Sb) exhibit a strong increase in concentration with decreasing particle size, with typically 50% of their elemental mass found on particles of $d \leq 1.0 \mu\text{m}$ and EF's greater than 1000 (Gladney *et al.*, 1974). The in-stack concentration distributions for all elements show distinct minima in the region $0.3 \leq d \leq 1.0 \mu\text{m}$ and EF's of less than 100 on the smallest particles. If the differences between these distributions are observed at most coal-fired power stations, this suggests that the emissions from coal-fired installations do not have a major impact on the observed urban particle size distributions (Lee *et al.*, 1968; Nifong and Winchester, 1970; Lee *et al.*, 1972; Gladney *et al.*, 1974) for many toxic trace elements.

Acknowledgements—We thank the staffs of the NBS reactor and electron lineac for their cooperation during the irradiations. We thank Mr. R. Cahill, Dr. R. Greenberg, Dr. E. Mroz, Dr. T. Overcamp and Mr. S. Weber for their help with the sample collection and Ms. J. Gladney for her assistance with the manuscript. We also thank the Potomac Electric Power Co. for their excellent cooperation in providing access to their Chalk Point plant. This work comprised a portion of the first author's dissertation which was submitted to the Graduate School of the University of Maryland in partial fulfillment for the requirements of the Ph.D.

Credit This research was supported by the National Science Foundation through NSF/RANN Grant GI-36338X to the University of Maryland and by the U.S. Energy Research and Development Administration.

REFERENCES

- Aras N. K., Zoller W. H., Gordon G. E. and Lutz G. J. (1973) Instrumental photon activation analysis of atmospheric particulate material. *Analyt. Chem.* 45, 1481-1490.
- Berberich C. E. and Bayer C. B. (1964) Design features of the Chalk Point Generating Station. Presented at Southeastern Electric Exchange, Washington, D.C.
- Billings C. E. and Matson W. R. (1972) Mercury emissions from coal combustion. *Science* 176, 1232-1233.
- Billings C. E., Sacco A. M., Matson W. R., Griffin R. M., Coniglio W. R. and Harley R. A. (1973) Mercury balance on a large pulverized coal-fired furnace. *J. Air Pollut. Control Ass.* 23, 773-777.
- Gladney E. S. (1974) Trace element emissions from coal-fired power plants: A study of the Chalk Point Electric Generating Station. Ph.D. Thesis, University of Maryland.
- Gladney E. S., Zoller W. H., Jones A. G. and Gordon G. E. (1974) Composition and size distribution of atmospheric particulate matter in the Boston area. *Environ. Sci. Technol.* 8, 551-557.
- Gordon G. E., Zoller W. H. and Gladney E. S. (1973) Abnormally enriched trace elements in the atmosphere. *Trace Substances in Environmental Health VII* (Edited by Hemphill D. D.), pp. 167-174. University of Missouri, Columbia, MO.
- Gordon G. E. and Zoller W. H. (1973) Normalization and interpretation of atmospheric trace element concentration patterns. *Proc. 1st Annual NSF Trace Contaminants Conference*, Oak Ridge National Laboratory, Oak Ridge, Tenn., CONF-730802, pp. 314-325.
- Greenberg R. R. (1974) University of Maryland, private communication.
- Kaakinen J. W., Jordan R. M., Lawasani M. H. and West R. E. (1975) Trace element behavior in coal-fired power plant. *Environ. Sci. Technol.* 9, 862-869.
- Klein D. H., Andren A. W., Carter J. A., Emery J. F., Feldman C., Fulkerson W., Lyon W. S., Ogle J. C., Talmi Y., Van Hook R. I. and Boulton N. (1975) Pathways of thirty-seven elements through coal-fired power plant. *Environ. Sci. Technol.* 9, 973-979.
- Lee R. E., Patterson R. K. and Wagman J. (1968) Particle size distribution of metal components in Urban air. *Environ. Sci. Technol.* 2, 288-290.
- Lee R. E., Goranson S., Enrione R. and Morgan G. (1972) The NASN cascade impactor network. II. Size distributions of trace metal components. *Environ. Sci. Technol.* 6, 1025-1030.
- Lee R. E., Crist, H. L., Riley A. E. and MacLeod K. E. (1975) Concentration and size of trace metal emissions from a power plant, a steel plant, and a cotton gin. *Environ. Sci. Technol.* 9, 643-647.

Martin R.
source-
Office, I
APTD-
Moyers J.
L. (197
dium at
Sci. Te
National
sis, Sta
ington
National
sis, Sta
Ash) W
Natusch
Toxic
prable
Natusch
toxic
695-6
Nifong
distrib
versity
Ondov J.
G. I.
K. R.
in the
refer
Pilat M.
test
671
Pilat M.
at
Sci.
Ragaini

- Martin R. M. (1971) Construction details of isokinetic source-sampling equipment. Air Pollution Control Office, EPA, Research Triangle Park, N.C., Pub. No. APTD-0581.
- Moyers J. L., Zoller W. H., Duce R. A. and Hoffman G. L. (1972) Gaseous bromine and particulate lead, vanadium and bromine in a polluted atmosphere. *Environ. Sci. Technol.* 6, 68-71.
- National Bureau of Standards (1974) Certificate of Analysis, Standard Reference Material No. 1632 (Coal), Washington, D.C.
- National Bureau of Standards (1974) Certificate of Analysis, Standard Reference Material No. 1633 (Coal Fly Ash), Washington, D.C.
- Natusch D. F. S., Wallace J. R. and Evans C. A. (1974) Toxic trace elements: preferential concentration in respirable particles. *Science* 183, 202-204.
- Natusch D. F. S. and Wallace J. R. (1974) Urban aerosol toxicity: the influence of particle size. *Science* 186, 695-699.
- Nifong G. D. and Winchester J. W. (1970) Particle size distributions of trace elements in polluted aerosols. University of Michigan, Report C001705B.
- Ondov J. M., Zoller W. H., Olmez I., Aras N. K., Gordon G. E., Rancitelli L. A., Abel K. H., Filby R. H., Shag K. R. and Ragaini R. C. (1975) Elemental concentrations in the NBS environmental coal and fly ash standard reference materials. *Analyt. Chem.* 47, 1102-1109.
- Pilat M. J., Ensor D. S. and Bosch J. C. (1970) Source test cascade impactor. *Atmospheric Environment* 4, 671-679.
- Pilat M. J., Ensor D. S. and Shattenburg G. E. (1973) *Operation Manual for Mark III University of Washington Source Test Cascade Impactor*.
- Ragaini R. C. and Ondov J. M. (1975) Trace contaminants from coal-fired power plants. International Conference on Environmental Sensing and Assessment, Las Vegas, NV.
- Reese C. (1974) Plant Manager, Chalk Point, Potomac Electric Power Co., private communication.
- Rom J. J. (1972) Maintenance, calibration, and operation of isokinetic source-sampling equipment. Office of Air Programs, EPA, Research Triangle Park, N.C., Pub. No. APTD-0576.
- Rook H. L., Gills T. E. and LaFleur P. D. (1972) Method for determination of mercury in biological materials by neutron activation analysis. *Analyt. Chem.* 44, 1114-1117.
- Ruch R. R., Gluskoter H. J. and Shimp H. F. (1973) Occurrence and distribution of potentially volatile trace elements in coal: An interim report. Environmental Geology Notes Vol. 61. Illinois Geological Survey, Urbana, IL.
- Whang J. S. (1974) Real-time characterization of particulates emitted by a coal-fired power plant. Ph.D. Thesis, University of Maryland.
- Zoller E. H. and Gordon G. E. (1970) Instrumental neutron activation analysis of atmospheric pollutants utilizing Ge(Li) gamma-ray detectors. *Analyt. Chem.* 42, 257-265.
- Zoller W. H., Gordon G. E., Gladney E. S. and Jones A. G. (1973) The sources and distribution of vanadium in the atmosphere. In *Geochemical Cycles of Trace Elements in Our Environment* (Edited by Kothay E. L.), *Advances in Chemistry Series* pp. 31-47, No. 123. American Chemical Society, Washington, D.C.
- Zoller W. H., Gladney E. S., Gordon G. E. and Bors J. J. (1974) Emissions of trace elements from coal-fired power plants. In *Trace Substances in Environmental Health VIII* (Edited by Hemphill D. D.), Vol. 8, pp. 167-172. University of Missouri, Columbia, MO.

EX 2C

- Eng., 90, 79-107 (1964).
- (27) Adamson, A. W., "Physical Chemistry of Surfaces", 2nd ed., Interscience, New York, 1967, p 573.
- (28) Lemieux, R., Morrison, J., *Can. J. Res.*, 25B, 212 (1947).
- (29) Zechmeister, L., "Progress in Chromatography", Wiley, New York, 1950, p 189.
- (30) Weber, W. J., Jr., van Vliet, B. M., presented at the 176th National Meeting of the American Chemical Society, Miami, Fla., Sept 10-15, 1978.
- (31) Liapis, A. I., Rippin, D. W. T., *Chem. Eng. Sci.*, 32, 619 (1977).
- (32) Butler, J. A. V., Ockrent, C. J., *J. Phys. Chem.*, 34, 2841 (1930).
- (33) Jain, J. S., Snoeyink, V. L., *J. Water Pollut. Control Fed.*, 45, 2463-79 (1973).
- (34) Radke, C. J., Prausnitz, J. M., *AIChE J.*, 18, 761-8 (1972).
- (35) Jossens, L., Prausnitz, J. M., Fritz, W., Schunder, E. U., Myers, A. L., *Chem. Eng. Sci.*, 33, 1097 (1978).
- (36) Myers, A. L., Prausnitz, J. M., *AIChE J.*, 11, 121 (1965).
- (37) DiGiano, F. A., Baldauf, G., Frick, B., Sontheimer, H., *Chem. Eng. Sci.*, 33, 1667-73 (1978).
- (38) Manes, M., presented at the 176th National Meeting of the American Chemical Society, Miami, Fla., Sept 10-15, 1978.
- (39) Hofer, L. J. E., Manes, M., *Chem. Eng. Prog.*, 65, 84 (1969).
- (40) Manes, M., Hofer, L. J. E., *J. Phys. Chem.*, 73, 584 (1969).
- (41) Wohleber, D. A., Manes, M., *J. Phys. Chem.*, 75, 61 (1971).
- (42) Wohleber, D. A., Manes, M., *J. Phys. Chem.*, 75, 3720 (1971).
- (43) Rosene, M. R., Ozcan, M., Manes, M., *J. Phys. Chem.*, 80, 2586 (1976).
- (44) McGuire, M. J., Suffet, I. H., Radzail, J. V., *J. Am. Water Works Assoc.*, 70, 565 (Oct 1978).
- (45) McGuire, M. J., Ph.D. Thesis, Drexel University, Philadelphia, 1977.
- (46) Keller, R. A., Snyder, L. R., *J. Chromatog. Sci.*, 9, 346 (1971).
- (47) Sinanoglu, O., in "Molecular Associations XIN Biology", Pullman, B., Ed., Academic Press, New York, 1968, pp 427-45.
- (48) Sinanoglu, O., Abdunur, S., *Fed. Proc., Fed. Am. Soc. Exp. Biol.*, 24, No. 2, Part III, S-12 (1965).
- (49) Halicioglu, T., Sinanoglu, O., *Ann. N.Y. Acad. Sci.*, 158, 308 (1969).
- (50) Horvath, C., Melander, W., Molnar, I., *J. Chromatogr.*, 125, 129 (1976).
- (51) Aberhalden, E., Foder, A., *Fermentforschung*, 2, 74, 151 (1910).
- (52) Cheldin, V. H., Williams, R. J., *J. Am. Chem. Soc.*, 64, 1513 (1942).
- (53) Tiselius, A., Ed., The Svedberg, Almquist and Wiksells, Uppsala, 1944, p 370.
- (54) Williams, R. J. P., Hagdahl, L., Tiselius, A., *Ark. Kemi*, 7, 1 (1954).
- (55) Colin, H., Eon, C., Guiochon, G., *J. Chromatogr.*, 119, 41 (1970).
- (56) Colin, H., Eon, C., Guiochon, G., *J. Chromatogr.*, 122, 223 (1976).
- (57) Colin, H., Guiochon, G., *J. Chromatogr.*, 137, 19 (1977).
- (58) Colin, H., Ward, N., Guiochon, G., *J. Chromatogr.*, 149, 169 (1978).
- (59) Colin, H., Guiochon, G., *J. Chromatogr.*, 158, 183 (1978).
- (60) Horvath, C., Melander, W., Molnar, I., *Anal. Chem.*, 49, 142 (1977).
- (61) Horvath, C., Melander, W., *Am. Lab.*, 10, 17 (1978).
- (62) Franks, H. S., Evans, M. W., *J. Chem. Phys.*, 13(11), 507 (1945).
- (63) Kauzmann, W., *Adv. Protein Chem.*, 14, 1 (1959).
- (64) Tanford, C., *Science*, 200, 1012 (1978).
- (65) Sourirajan, S., Matsuura, T., "Reverse Osmosis and Synthetic Membranes", Sourirajan, S., Ed., National Research Council Canada, Ottawa, Canada, 1977, pp 5-43.
- (66) Barrow, G. M., *J. Phys. Chem.*, 59, 1129 (1955).
- (67) Gordy, W., *J. Chem. Phys.*, 7, 93-9 (1939).
- (68) Gordy, W., Stanford, S. C., *J. Chem. Phys.*, 8, 170-7 (1940).
- (69) Gordy, W., Stanford, S. C., *J. Chem. Phys.*, 9, 204-14 (1941).
- (70) Gordy, W., *J. Chem. Phys.*, 9, 215-23 (1941).
- (71) Kuhn, L. P., *J. Am. Chem. Soc.*, 74, 2492-9 (1952).
- (72) Kagija, T., Sumida, Y., Inoue, T., *Bull. Chem. Soc. Jpn.*, 41, 767 (1968).
- (73) Taft, R. W., Jr., in "Steric Effects in Organic Chemistry", Newman, M. S., Ed., Wiley, New York, 1956, pp 556-675.
- (74) Hammett, L. P., "Physical Organic Chemistry", 2nd ed., McGraw-Hill, New York, 1970, pp 347-90.
- (75) Pinsky, J., *Mod. Plast.*, 34(4), 145 (1957).
- (76) Diamond, J. M., Wright, E. M., *Annu. Rev. Physiol.*, 31, 581-646 (1969).

Received for review July 20, 1978. Accepted April 12, 1979.

Emissions and Particle-Size Distributions of Minor and Trace Elements at Two Western Coal-Fired Power Plants Equipped with Cold-Side Electrostatic Precipitators

John M. Ondov*, Richard C. Ragaini, and Arthur H. Biermann

Lawrence Livermore Laboratory, University of California, Livermore, Calif. 94550

Concentrations and distributions according to particle size of up to 42 elements were measured in aerosol particles collected in-stack at two western coal-fired power plants equipped with cold-side electrostatic precipitators (ESP). Elements were measured by instrumental neutron activation analysis, atomic absorption spectroscopy, and X-ray fluorescence. Particle-size distributions in filter and cascade impactor samples from both units were bimodal. Most of the particulate material from the units was emitted as large particles with mass median aerodynamic diameters of $>1.6 \mu\text{m}$. Emission rates normalized per joule of input heat strongly reflect differences in the type and efficiency of the control devices and the chemistry of the coal. However, the relative penetrations of many elements at both plants were remarkably similar despite major differences in coal composition and plant design. Our results are compared with those of three other studies of similarly equipped power plants. Relative penetrations of Zn, Pb, Ba, Cr, Co, V, Rb, and Sb differed significantly among the five plants.

The National Coal Association forecasts an increase in utility coal usage from 4.0×10^{11} kg in 1976 to approximately 7.7×10^{11} kg in 1985. The nation's expanding reliance on coal combustion in the production of electric power has increased the importance of evaluating the associated potential biomedical and environmental hazards. Coal combustion results in the release into the atmosphere of a number of potentially toxic substances, including naturally occurring radionuclides (1-5), polynuclear aromatic hydrocarbons (6-8), and various inorganic chemical species (9-16), in vapor (16, 17) and condensed phases.

Several investigators have studied the behavior of trace elements during coal combustion. Davison (18) proposed a mechanism whereby volatile species are enriched in respirable, fine particles through vaporization in the combustion zone followed by condensation on particle surfaces. Kaakinen et al. (9) and Klein et al. (11) demonstrated enrichment of elements in emitted particles resulting from the greater penetration of fine, highly enriched particles through emission control devices. Others (1, 12, 14, 15, 18) observed similar

enrichments by these mechanisms in small particles emitted from coal combustion. However, comprehensive studies of trace element emissions from the combustion of U.S. coal have been reported for only a few utility-scale generating units. These include Unit No. 5 of the Valmont Power Station (9), the T. A. Allen Steam Plant (11), and the Chalk Point Plant (12). Most of the plants studied burn Eastern and Illinois coals, and relatively few studies have been made of plants burning low-sulfur, Western coal. Thus, in general, the specific effects on emissions of coal type, differences in the chemical form and physical distribution of coal constituents, and emission-control devices have not been adequately determined.

Furthermore, insufficient attention has been given to measuring particle-distribution parameters, especially in submicrometer particles. The emission of fine particles is of special interest because these particles often contain high concentrations of potentially toxic substances in thin, surface layers (19) and can be deposited efficiently in the pulmonary alveoli (20).

In this paper, we report the results of tests on power units at two conventional, large, western, coal-fired power plants (referred to as plants A and B), one burning low-sulfur bituminous coal, the other burning low-sulfur subbituminous coal. Cold-side electrostatic precipitators (ESP) were used to control particulate emissions at both plants.

Experimental

Plant Description and Sample Collection. At plant A, we tested a 430-MW (net electrical) coal-fired steam electric generator. The unit uses tangentially fired burners and a cold-side ESP with an efficiency between 99.5 and 99.8%. The unit burns $\sim 1.45 \times 10^5$ kg of pulverized (200-mesh) western bituminous coal per hour, with ash, sulfur, and heat contents of 9.2%, 0.46%, and 28660 J/g, respectively, on a dry basis (moisture content was 6.8%). Stack gases exit through a 183-m stack.

Four filter and seven impactor samples were collected isokinetically in stack at the 91-m level during a 1-week period in January 1975. Sampling times ranged from 55 min to 3 h, the stack temperature was 117 °C, stack pressure ranged from 1.12 to 1.87 mmHg (gauge), and stack-gas velocity ranged from 23.9 to 25.9 m/s. Velocity-traverse data showed that the velocity profile was flat 91 cm beyond the inside wall. Flow rates through both impactor and filter samplers ranged from 10.8 to 16.1 L/min (wet gas volume).

At plant B, the 750-MWe ESP-equipped unit uses opposed front- and rear-fired burners. Flue gases leaving the boiler flow through two cold-side ESPs arranged in a chevron design before exiting through a 91-m stack. Each precipitator is four units wide and four mechanical sections long and has a specific collecting area of 4760 cm²/m³. When all sections are operating properly, net particle-removal efficiency of the ESP system at full load is rated at 97%.

Samples were collected in-stack at the 61-m level of the ESP-equipped unit during July 1975 (21). The gross load varied from 515 to 715 MWe, but was constant during each test. Four of the 32 separate electrical precipitator sections were inoperative during most of the test period. Precipitator efficiency in removing total suspended particles (TSP) under the test conditions was estimated at about 97% (see below). Eight filter and ten cascade impactor samples were collected. Additional samples, including simultaneous samples from the inlet, outlet, and plume (15), were collected during February 1976, but are not reported here.

Samples of coal, ESP-collected ash, and bottom ash were also taken at both plants during stack fly-ash collections. At plant A, pulverized coal samples were taken hourly, each

sample consisting of a 5-min sample from each of five feeding systems.

Sampling Procedures. Stack emissions were sampled at each plant, using a modified EPA sampling train as described previously (22). Hourly records of plant operating data, including gross generating load, coal consumption, proximate analyses, energy-conversion factors (daily at plant A, monthly at plant B), and status of ESP sections, were obtained at both plants. Velocity, temperature, and pressure of the stack gas were monitored continuously during each collection. Filter samples were collected on 47-mm, 0.4- μ m Nuclepore filters. Impactor samples were collected with 7- and 11-stage University of Washington Mark III and Mark V source test cascade impactors, using polyethylene or polycarbonate collection substrates and 47-mm, 0.4- μ m Nuclepore backup filters. Impaction substrates were coated with a vacuum grease to improve the collection efficiency.

Analyses. In addition to gravimetric analyses, up to 43 elements were analyzed in stack samples, ESP-collected ash, bottom ash, and coal by instrumental neutron activation analysis (INAA) as described previously (23, 24). Cadmium and Be were analyzed in coal and fly ash, and Pb, Cd, and Be were analyzed in filter and cascade impactor samples, all with a Perkin-Elmer Model 603 atomic absorption spectrometer equipped with a Perkin-Elmer Model 2100 heated graphite analyzer. Samples were dissolved in a mixture of perchloric, nitric, and hydrofluoric acids after ashing overnight at 450 °C. Mercury in coal was analyzed by flameless atomic absorption techniques similar to those of Murphy (25). Nickel, Pb, and Cd were measured in bulk coal and fly-ash samples with energy-dispersive X-ray fluorescence analyses (XRF). Coal samples for XRF were dry ashed at 450 °C overnight, ground to 30 to 60 μ m, and pressed into pellets with an equal amount of Avicel binding agent. γ rays from ¹⁰⁹Cd were used to excite characteristic fluorescent X-rays. The measurement and analyses of spectra are described by Bonner et al. (26). Results from each of these techniques were verified with NBS standard reference materials (SRM) 1632 (coal) and 1633 (coal fly ash), which were analyzed along with the samples, and through interlaboratory comparisons of results on SRM samples (27) and size-classified fly-ash fractions (28).

Computation of Coal Consumption and Atmospheric Discharge Rates. Rates of coal consumption were computed from data provided by plant personnel. At plant A, the coal consumption rate was measured by the plant-metering system and at plant B it was computed from the gross electrical generating load, the known heat-to-electrical conversion factor (a monthly average), and the heat content of the coal as described previously (21). Input rates of constituent elements were obtained by multiplying their concentrations in coal (listed in Table I) by the rate of coal consumption. Typical rates of coal consumption at each of the units are listed in Table II.

Rates of atmospheric discharge of minor and trace element species were computed using the measured stack concentrations and stack-gas velocities. Because the quantities of coal consumed, electric power produced, and energy-conversion factors of the units differed, comparison of the emission data is facilitated by normalizing the data to the amount of heat input into the boiler. The heat input was computed from the metered coal-flow rate and the heat content of the coal for the unit at plant A and from the gross generating load and energy-conversion factor for the unit at plant B. The energy-conversion factors are listed in Table II.

Results and Discussion

Distributions of Total Suspended Particles. Parameters used to calculate the total aerosol emitted from each of the two plants were obtained by counting particles on filter samples

Table I. Concentrations of Elements in Coal Burned at Two Western Power Plants, $\mu\text{g/g}$

	Plant A		Plant B	
	Jan 75	July 75	Jan 75	July 75
Al	7072 ± 360 (5) ^a	10300 ± 3600 (15) ^a	29500 ± 2390 (7) ^a	
Ag	0.250 ± 0.026 (1)			
As	0.583 ± 0.087 (12)	2.73 ± 0.71 (11)	2.84 ± 0.84 (5)	
Ba	78.5 ± 9.2 (12)	418 ± 88 (14)	420 ± 167 (7)	
Bcb	0.32 ± 0.11 (6)	1.6 ± 0.5 (9)	1.2 ± 0.6 (7)	
Br		0.96 ± 0.18 (2)		
Ca	6100 ± 470 (5)	5360 ± 730 (15)	5620 ± 860 (7)	
CaIb	0.14 ± 0.025 (5)	0.061 ± 0.019 (10)	0.17 ± 0.02 (7)	
Ce	8.93 ± 0.22 (12)	25.6 ± 1.7 (15)	27.0 ± 2.0 (7)	
Cl	73 ± 18 (5)	71 ± 20 (4)	48 ± 17 (1)	
Co	0.840 ± 0.040 (12)	1.98 ± 0.25 (14)	2.08 ± 0.22 (7)	
Cr	7.74 ± 0.33 (12)	5.19 ± 0.29 (15)	7.02 ± 1.28 (7)	
Cs	0.454 ± 0.012 (5)	0.70 ± 0.08 (15)	0.72 ± 0.16 (7)	
Cu	6.68 ± 0.22 (5)	13.4 ± 1.2 (6)	12.7 ± 0.6 (7)	
Dy	0.54 ± 0.02 (5)	1.63 ± 0.13 (15)	1.60 ± 0.09 (7)	
Fe	0.101 ± 0.005 (5)	0.250 ± 0.009 (14)	0.261 ± 0.018 (7)	
Fe	2860 ± 120 (11)	5720 ± 380 (15)	6470 ± 570 (7)	
Ga	2.67 ± 0.50 (12)	8.8 ± 1.4 (11)	8.48 ± 1.25 (7)	
Hf	1.14 ± 0.10 (5)	2.23 ± 0.12 (15)	2.38 ± 0.11 (7)	
Hg	0.11 ± 0.01 (5)	0.065 ± 0.015 (5)	0.10 ± 0.02 (5)	
In	0.010 ± 0.002 (3)	0.0415 ± 0.0046 (13)	0.039 ± 0.006 (5)	
K	764 ± 45 (5)	1820 ± 250 (14)	1730 ± 261 (7)	
La	5.09 ± 0.34 (5)	14.3 ± 0.8 (15)	13.4 ± 0.8 (7)	
La	0.062 ± 0.015 (5)	0.239 ± 0.009 (14)	0.23 ± 0.03 (6)	
Mg	1025 ± 109 (5)	2310 ± 470 (11)	2240 ± 753 (6)	
Mo	1.17 ± 0.03 (5)	2.60 ± 0.54 (15)	2.67 ± 0.26 (6)	
Mn	13 ± 3.4 (9)	54.1 ± 1.6 (15)	60.2 ± 20.0 (7)	
Na	2330 ± 70 (5)	2940 ± 160 (15)	2930 ± 248 (7)	
Nd	3.98 ± 0.20 (5)	9.86 ± 0.90 (15)	10.6 ± 1.1 (7)	
Ni	2.99 ± 0.45 (5)			
Pb	2.52 ± 0.13 (5)	10.2 ± 1.2 (16)	12.1 ± 0.7 (7)	
Rb	4.03 ± 0.32 (5)	9.05 ± 0.53 (15)	12.1 ± 1.8 (7)	
Sd	4600 ± 100 (5)	5200 ± 800 (2)	5800 ± 600 (12)	
Sb	0.160 ± 0.011 (5)	0.572 ± 0.049 (15)	0.614 ± 0.095 (7)	
Sc	1.46 ± 0.09 (12)	2.77 ± 0.11 (15)	2.98 ± 0.20 (7)	
Se	1.47 ± 0.09 (12)	1.55 ± 0.15 (15)	1.74 ± 0.25 (7)	
Sm	0.659 ± 0.013 (12)	1.71 ± 0.17 (15)	1.81 ± 0.16 (7)	
Sr	67.0 ± 2.7 (5)	87.2 ± 8.9 (15)	97.7 ± 8.3 (7)	
Ta	0.160 ± 0.006 (5)	0.492 ± 0.038 (15)	0.513 ± 0.056 (7)	
Th	0.0810 ± 0.003 (5)	0.165 ± 0.009 (15)	0.22 ± 0.02 (7)	
Th	1.65 ± 0.03 (5)	5.73 ± 0.32 (15)	6.21 ± 0.67 (7)	
Ti	483 ± 82 (5)	1220 ± 200 (14)	1230 ± 176 (6)	
U	0.573 ± 0.023 (5)	1.85 ± 0.19 (15)	2.12 ± 0.25 (7)	
V	9.8 ± 1.2 (12)	22.1 ± 3.2 (9)	24.9 ± 3.1 (4)	
W		0.80 ± 0.24 (5)	<0.13 (1)	
Yb	0.368 ± 0.022 (5)	0.817 ± 0.060 (15)	0.84 ± 0.06 (7)	
Zn	7.16 ± 0.29 (5)	14.7 ± 1.7 (15)	16.4 ± 3.2 (7)	
Zr	40.5 ± 6.7 (5)	52.2 ± 5.9 (15)	66.7 ± 9.8 (7)	

^a Number of replicate samples. ^b Measured by atomic absorption spectroscopy. ^c X-ray fluorescence. ^d Sulfur analyses provided by plant personnel; all others measured by instrumental neutron activation analysis.

Table II. Typical Rates of Coal Consumption and Energy-Conversion Factors

	% Full load	Coal rate (g/s)	Energy-conversion factor (Btu/AWh)
Plant A	98	3.98×10^4	9.25×10^3
Plant B	94	9.71×10^4	9.47×10^3
	82	8.57×10^4	9.38×10^3

Table III. Size-Distribution Parameters of Total Stack-Emitted Aerosols Determined from Scanning Electron Microscopy Analyses of Nuclepore Filter Samples

	Small-Particle Mode				Large-Particle Mode			
	NMD ^a	VMD ^b	MMAD ^c	σ_g^d	NMD ^a	VMD ^b	MMAD ^c	σ_g^d
Plant A	0.065	0.088	0.14	1.37	0.565	1.04	1.6	1.57
Plant B	0.055	0.082	0.13	1.42	0.74	5.2	8.1	2.2

^a Number median diameter (μm). ^b Volume median diameter (μm) determined by $\ln \text{VMD} = \ln \text{NMD} + 3 \ln^2 \sigma_g$. ^c Estimated mass median aerodynamic diameter (μm), using particle densities of 2.2 and 2.44 g/cm^3 for plants A and B, respectively. ^d Geometric standard deviation of assumed log normal distribution.

via scanning electron microscopy (SEM) techniques (see ref 22) and are given in Table III. The distributions were in each case bimodal, with distinct modes in sub- and supermicrometer size ranges. The submicrometer mode is composed of aggregates of smaller particles that may be formed in part from vapor condensation and bubble-bursting mechanisms. These particles are too small to be collected by our impactor and, ignoring wall losses and boundary effects in the impactor, are deposited totally on the backup filter. The second mode contains much larger, mostly solid, spherical particles derived

mainly from residual mineral matter in coal (29–31). Ulrich (30) observed similar particle-distribution modes and suggested that the particles in the smaller mode are largely condensed, volatile Si compounds and metal oxides.

Median diameters of the smaller particles from both units are almost identical. Median diameters of the larger particles (see Table III) strongly reflect differences in the overall collection efficiency of the control device. The smaller median diameters of the large particles emitted at plant A indicate a greater collection efficiency of the larger particles. Optimum collection efficiencies of the plant A and plant B ESP systems are 99.7 and 97.5%, respectively.

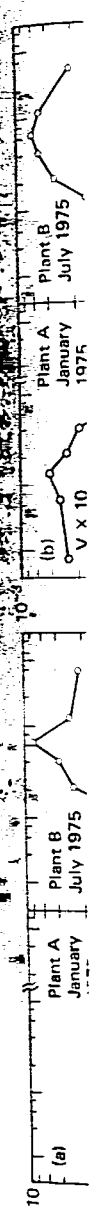
Impactor Data. In Figures 1A through E, we have plotted typical particle-size distributions of elements collected in cascade impactor samples that were placed in-stack and downstream from the ESP-equipped units at each plant. The emission factors (ng/J heat input) of several elements are plotted vs. the aerodynamic diameters of particles. Physical diameters were determined by sizing particles on impactor stages and backup filters via SEM and transformed to aerodynamic diameters using the particle density and slip-correction factor (32). We corrected the mass of each element present on backup filters by the excess mass resulting from bounce off and reentrainment of large particles as described previously (22). Thus, we can estimate more accurately the fraction of each element emitted in submicrometer particles.

Significant amounts of several elements, including V, W, Ga, Mo, Ca, Br, Ba, Se, As, Sb, U, Fe, Cr, Zn, Co, and Mn, were emitted in submicrometer particles. The fraction of other elements in submicrometer particles is generally much less, but too small to determine accurately (22).

We attempted to evaluate wall losses by comparing concentrations in impactor and filter samples; because of the variation between successively collected samples, accurate comparisons could not always be made. In general, however, concentrations of elements in the flue gas, which were determined by summing the amounts on impactor stages, were typically from 10 to 60% lower than concentrations on filters in samples from the ESP at plant A and from 12 to 40% lower in samples from the ESP at plant B. The magnitude of the discrepancy depended on the specific element, its distribution among particle sizes, and sampling time (see ref 22).

Aerosol-Distribution Parameters of Minor and Trace Elements. Elemental mass median aerodynamic diameters (EMMAD) were determined from analyses of cascade impactor samples collected at each of the units and are listed in Table IV. These data reflect only the larger particle modes. Ranges of median EMMADs of particulate emissions from the plant A and plant B ESP units were 1.8–4.9 and 4.3–12.1 μm , respectively. Thus, as in the case of the total aerosol (see Table III), the EMMADs of particles from the more efficient ESP were smaller.

Elements in emissions from each of the units show distinct behavior in their distributions according to particle size. At plant A, the distributions of Al, Ce, Cl, Fe, Hf, K, La, Na, Sc, and Th were nearly identical. The EMMADs of particles containing As, Ba, Ga, I, U, V, W, and Zn were about half those of particles with elements in the Al group. The EMMADs of Co, Cs, Cu, Mo, Mn, and Sb were slightly smaller than those containing the Al group. If an element were distributed on only the surfaces of aerosol particles, then its mass distribution would coincide with the surface-area distribution of the aerosol. The calculated surface-area median aerodynamic diameters (SMAD) of elements in the Al group (about 1.8 for particles having an EMMAD of 2.5 μm and σ_g of 2.3) are nearly equal to the EMMADs of elements in the As group, thus indicating surface occurrence of elements in the As group on particles containing elements in the Al group. This would occur if these elements were deposited from the vapor phase;



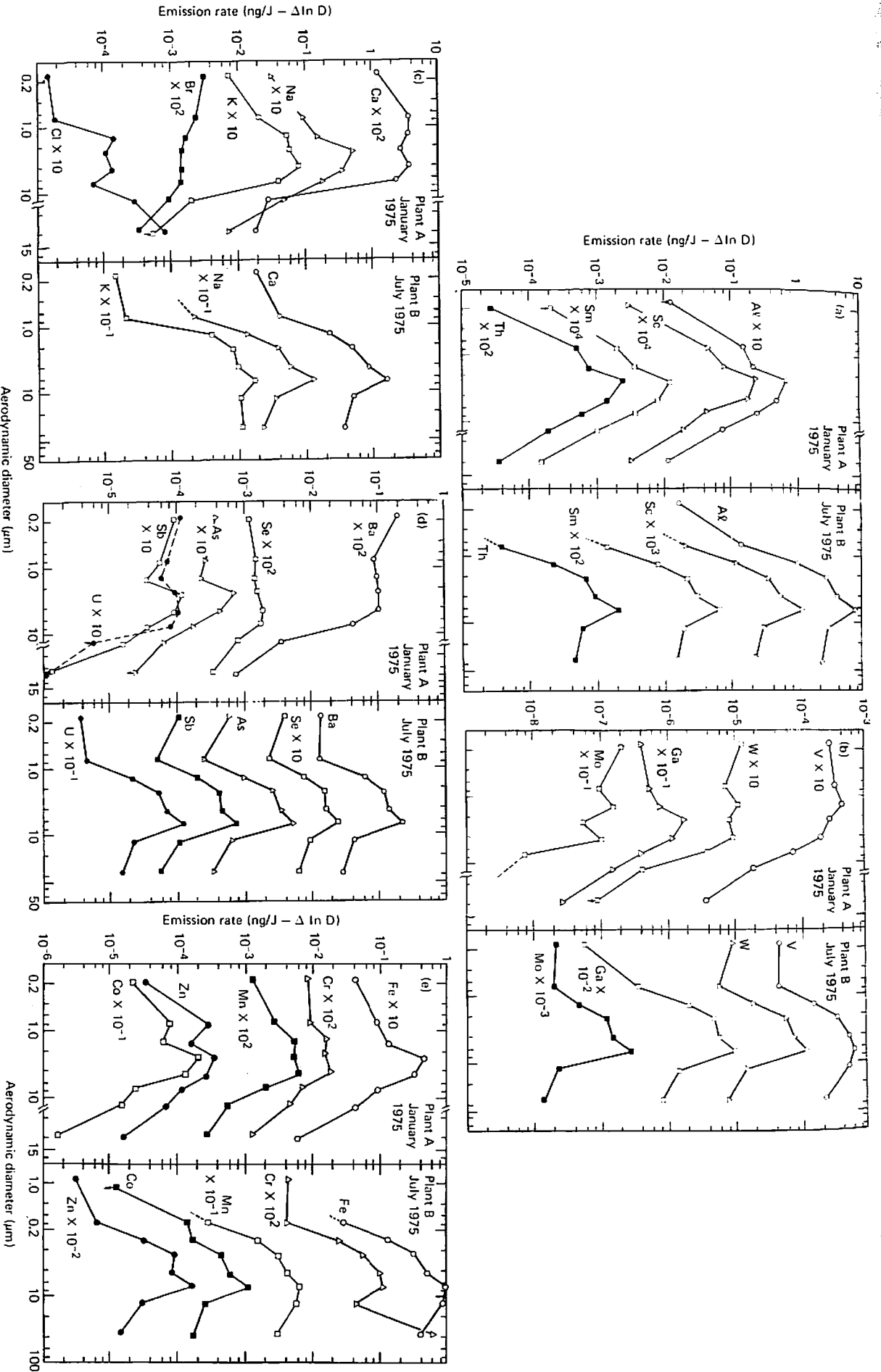


Figure 1. Typical distributions of mass vs. particle size of elements in aerosols emitted from two coal-burning steam-generating units. Masses of elements are expressed as emission rates per joule

of heat input to the boiler as discussed in the text

Table IV. Elemental Mass Median Aerodynamic Diameters of Aerosols from Two Coal-Fired Electrical Generating Units, μm

Elements	Plant A January 1975		Plant B July 1975		
	EMMAD ^a	σ_g^b	Elements	EMMAD ^c	σ_g^b
<u>La, Tb, Sc</u>	~4.5	1.4 - 2.8 ^d	Cr, Cs, Rb, Zr	~12	2.2 - 3.0
Sm, Nd, Mg, Lu, Yb, In, Eu	~3.3	1.4 - 2.4 3.0 ^d	Al, Br, Cr, Co, Dy, Eu, Fe, Hg, K, La, Lu, Mg, Nd, Se, Sm, Ta, Tb, Th, Ti	~9.5	2.2 - 3.2
Hf, K, Li, Sc, Th Al, Ce, Cl, Na	~2.5	1.6 - 2.7 ^d 1.8 - 2.3	Ca, Mn, Na, Se	~8.2	2.7 - 3.5
Ca, Mo, Sb, Cu, Mn Co, Cs, Rb, Li, Fe	~2.3	1.5 - 2.6	As, Ba, Ga, In Mo, Sb, U, V, W, Zn	4.4 - 6.3	1.9 - 3.4
Br, Cr, U, W, Zn Ga, Sr, I As, Ba, V	~1.7	1.5 - 2.0 (2.1 - 3.7) ^d 1.5 - 2.3 (2.1 - 4.2) ^d 1.6 - 2.9			

^a EMMADs estimated from up to five impactor samples. The relative standard deviation of successive determinations of the EMMADs was typically about 20%, but errors among elements are typically $\leq 10\%$. ^b Geometric standard deviation. ^c Range of median values of EMMADs of up to six impactor samples for each element. ^d Value corresponds to element underlined.

Table V. Emission Factors of Elements in Particles from Generating Units at Two Coal-Fired Power Plants (pg/J) ^a

Element	Plant A January 1975			Plant B ESP Unit July 1975		
	Median	Minimum	Maximum	625-MW Sample ^b	Minimum	Maximum
Al	320 ± 13	286	354	15,600 ± 500	3860	21,700
As	0.22 ± 0.014	0.15	0.22	15.3 ± 0.3	5.77	15.3
Ba	10.8 ± 1.6	10.3	11.1	807 ± 10	243	807
Be	-	-	-	0.72 ± 0.24	0.42	0.72 (3)
Br	0.125 ± 0.035	0.091	0.20	6.6 ± 3.5	-	(1)
Ca	216 ± 35 (2)	188	243	3400 ± 100	1590	3940
Cd	-	-	-	0.26 ± 0.04	0.097	0.26 (4)
Ce	0.48 ± 0.02	0.41	0.52	16.0 ± 0.5	8.25	21.3
Cl	0.98 ± 0.42	0.37	1.7	-	-	-
Co	0.10 ± 0.01	0.084	0.11	2.38 ± 0.04	1.12	3.05
Cr	0.81 ± 0.07	0.68	1.0	9.58 ± 0.36	3.1	30.5
Cs	0.042 ± 0.002	0.036	0.068	0.410 ± 0.031	0.209	0.615
Dy	-	-	-	1.12 ± 0.03	0.324	1.52
Eu	0.0061 ± 0.0004	0.0047	0.0070	0.164 ± 0.005	0.0047	0.218
Fe	156 ± 7	130	187	3670 ± 40	1980	5350
Ga	0.59 ± 0.18	0.49	0.63	18.7 ± 1.0	9.74	19.8
Hf	-	-	-	1.37 ± 0.03	0.717	1.85
I	3.5 ± 0.3	3.2	4.4	-	-	-
In	0.0024 ± 0.00014	0.0023	0.0031	0.108 ± 0.008	0.0339	0.108
K	43 ± 20	26	46	905 ± 200	441	1130
La	0.26 ± 0.014	0.22	0.32	8.96 ± 0.09	4.75	12.0
Lu	0.0032 ± 0.0004 (2)	0.0029	0.0036	0.164 ± 0.007	0.0701	0.231
Mg	-	-	-	1360 ± 380	1170	3240
Mo	0.079 ± 0.010	0.057	0.15	6.48 ± 0.76	2.26	8.61
Mn	0.45 ± 0.03	0.42	0.47	41.2 ± 0.5	9.07	41.2
Na	121 ± 5	77	160	2310 ± 10	1120	2810
Nd	0.21 ± 0.06	0.13	0.21	6.05 ± 0.48	3.42	8.40
Rb	0.37 ± 0.12 (1)	-	-	5.52 ± 0.57	2.52	7.52
Sb	0.052 ± 0.003	0.048	0.054	2.15 ± 0.04	0.863	2.15
Se	0.074 ± 0.0014	0.061	0.084	1.96 ± 0.02	1.03	2.72
Si	0.26 ± 0.02	0.14	0.27	5.82 ± 0.16	2.83	6.07
Sm	0.033 ± 0.002	0.029	0.036	1.14 ± 0.06	0.648	1.60
Sr	5.4 ± 0.8 (1)	-	-	85.4 ± 8.0	32.2	111
Ta	0.0077 ± 0.0014	0.0056	0.0098	0.323 ± 0.13	0.158	0.441
Tb	0.0042 ± 0.0005 (2)	0.0036	0.0047	0.112 ± 0.006	0.060	0.158
Th	0.082 ± 0.004	0.065	0.091	3.67 ± 0.06	1.96	5.09
Ti	24 ± 8 (2)	17	31	892 ± 90	338	1150
U	0.091 ± 0.014	0.084	0.10	3.29 ± 0.15	1.39	3.29
V	0.99 ± 0.04	0.65	1.8	39.7 ± 3.2	17.3	39.7 (5)
W	0.091 ± 0.009 (1)	-	-	2.78 ± 0.18	1.20	2.78
Yb	-	-	-	0.503 ± 0.019	0.271	0.789
Zn	1.6 ± 0.14	1.2	1.8	44.8 ± 2.4	16.5	44.8
Zr	1.6 ± 0.7 (1)	-	-	34.6 ± 7.1	13.1	41.1

^a All values are based on analyses of filter samples only and were calculated on a dry gas basis at standard temperature and pressure. The water vapor contents of stack gasses were 9.2 and 7.9% at plants A and B, respectively. The data reflect three and six samples for plants A and B, respectively, or the number in parentheses. Uncertainties reported are analytical uncertainties only; the total uncertainty in any given determination is typically about 20%. ^b Results of a single sample collected when the unit operated at 83% capacity and with four precipitator sections inoperative.

however, the computation is quite sensitive to the value of the σ_g .

Median EMMADs of rare earths, Al, Fe, Co, Cr, K, Mg, Ti, Zr, and Sc, emitted from the ESP unit at plant B (Table IV) ranged from about 9 to about 12 μm ; those containing As, Ba,

Table VI. Penetration of Elements Contained in Particles through the Boilers and ESPs at Two Coal-Fired Power Plants (%)

Element	Plant A		Plant B	
	Penetration ^a	Penetration ^b	Element	Penetration ^b
Br, Cl	0.029 - 0.006		Br	0.14
Al, Ti, Mn, K Ca, Hf, La, Yb	0.07 - 0.13		Al, Sc, Lanthanides Th, U, Lu, Fe, Be, Mg, Ca, Na, K, Rb	0.9 - 1.6
Sm, La, Th, Ce Fe, Sr, Na, Lu Sr, Cs	0.14 - 0.24		Mn, Co, Cr	1.6 - 2.5 1.8
V, Cr, Ba, Co	0.29 - 0.40		U, V, Ba, Ga, Mo, Pb, In	3.7 - 3.5
U, Se, Ga	0.53 - 0.56, 0.65			
Zn, In, Sb, As	0.78 - 1.1		As, Cd, Se, Sb, W, Zn	0.3 - 11.5

^a Range of median values of up to six samples. ^b Range of median values of up to eight samples. Penetration is defined as [atmospheric emission factor (ng J⁻¹/input (ng J⁻¹)) × 100 (see text)].

Ga, In, Mo, Sb, U, V, W, and Zn ranged from about 4 to 6 μm , or about half those containing elements in the Al group and near the SMADs, i.e., 5.1 μm for MMAD of 8.87 μm and σ_g of 2.87, of particles with elements in the Al group. The EMMADs of Ca, Na, Sr, and Se were generally intermediate between those containing the As and Al groups.

On comparing the EMMADs of particles emitted from ESP units at the two plants, elements in the large particle mode from plant A seem to be distributed somewhat more heterogeneously than elements in the corresponding mode from plant B. Rather high EMMADs were often observed for particles containing Br, Cl, and I (4.0, 15, and 3.7 μm , respectively) in aerosol particles from the ESP at plant A, and for Se-containing particles (5.8 μm at plant A and 9.5 μm at plant B) in aerosols from both plants. These elements are the most volatile of the elements detected, and the high EMMADs may result from the adsorption of vapors either by large porous particles or by impactor substrates. In the latter case the data may be in error. Studies to determine the importance of adsorption of vapor-phase elements on impaction substrates are in progress at our laboratory.

Partitioning and Atmospheric Emission of Elements. In Table V we list emission factors (pg/J) of elements in samples from plant A. As noted above, wall and interstage losses were severe in impactor samples collected from these ESP units. Therefore, the emission factors of elements were derived only from filter samples.

For data from plant B, instead of median values, we report values determined from a sample collected while the unit was operated at 625 MW (about 80% load). During all tests, four ESP sections were inoperative; however, the unit was operated in compliance with emission standards by reduction of the gross generating load. By far, the lowest emissions were measured consistently from plant A. Emissions from the Valmont Unit 5 (9) and Allen Steam Plant (11) (not shown) were generally in the range between those of plants A and plant B.

Further normalization of the data in Table V by dividing by the input rates of the elements in coal (expressed in ng/J) yields the penetration of each element through the boiler and ESP. Penetrations of elements are independent of their concentrations in coal and are listed in Table VI for both of the generating units.

Penetrations varied considerably, as did emissions, with the element and specific power unit. In general, the lowest pene-

frations were observed for lanthanides, Th, Zr, some alkali metals, Sc, and Al, all of which tended to be in particles with the largest MMADs (see Table IV) and are associated largely with fly ash resulting from penetration of residual mineral matter. Elements associated with smaller particles, i.e., those in the As group, typically had the largest penetrations. Penetrations of Br and Cl were quite low relative to other elements. Klein et al. (11) and others suggested that significant quantities of some highly volatile elements such as Br, Cl, Se, and Hg have significant gas-phase components. Indeed, a rough mass balance indicates that between 7 and 35% of the Se contained in coal is emitted from plant B in the vapor phase.

Median penetrations of elements in large particles were about 0.2% at plant A and about 1.4% (625-MW sample) at plant B. These values correspond to 99.8 and 98.6%, respectively, for the net removal efficiency of these elements. At both plants, about 20% of the ash is removed from the boiler as bottom ash, and the remaining 80% enters the emission-control systems. Given the efficiency of the ESPs at the two plants (99.7 and 97.5% for the total aerosol), the net efficiencies for the removal of total aerosol of the bottom-ash-ESP systems are 99.8 and 98.5% at plants A and B, respectively. The removal efficiencies of elements and total aerosol agree very closely at both plants. This indicated that only a small portion of the mass of elements is contained in fine particles that have higher penetrations.

Thus, the penetration of elements associated with the large-particle fly-ash mode that is derived from residual mineral matter and termed lithophilic by Klein et al. (11) is nearly equal to the penetration of the total aerosol. As noted by Klein et al. (11), the penetrations of what appear to be the more mobile elements (classified as calcophiles by Klein et al. (11)) that occur in small particles are much higher, their concentrations thereby becoming enriched in the total aerosol relative to the nonmobile matrix elements. The enrichment of elements in the combustion process and in systems for the removal of fly ash may be expressed by the ratio of the penetration of a given element to that of the total aerosol or to that of an element whose penetration is similar to the total aerosol. The ratios of penetrations of each of the elements to that of Se are listed in Table VII for the two plants and plotted vs. particle diameter in Figure 2. Because of this internal normalization, the penetration ratios are identical with an enrichment factor obtained via double normalization of the concentrations of elements in in-stack fly-ash and coal samples. We will refer to the penetration ratios or enrichment factors as relative penetrations (RP). Relative penetrations are affected by the distribution of the element among particle sizes, vapor-particulate fractionation of the element, and the particle-size collection-efficiency curve of the control system.

Relative Penetration vs. Particle Size. As suggested by Gladney et al. (12), the elements may be classified conveniently on the basis of the curves of the relative penetration (or enrichment factor) vs. particle size. At plant A, these curves for the lanthanides, K, Ti, Mg, Cs, Rb, Hf, Ta, Sc, and Mn were similar to that for Th (Figure 2a). These show no change in concentration throughout the size range of particles. Curves for Ce, Na, Sr, and Fe were similar to those of the Th group, but were slightly enriched in the smallest sized particles. The curves for K and Ti are similar to that for Fe, but are displaced below Sc (≈ 1) in relative penetration. The penetration of Ca (Figure 2a) was less than that of Sc, i.e., $RP < 1$, in larger particles, but greater in smaller particles.

At plant A, the curves of RP vs. particle size for V, Sb, and As were similar to that of Ba (Figure 2a). The RPs of these elements on small particles were the largest observed. Several elements, including Br, Se, Cr (Figure 2b), Mn, Ta, Co, and

Table VII. Relative Penetration of Elements ^a in Aerosols from Several Coal-Fired Power Plants

	This Work				Other Studies		
	Plant A Average ^b	Plant B		Allen ^c	Chalk Point ^d	Valmont ^e	
		625 MWC	515-530 MWd				
Sb	7.0 ± 2.0	5.3 ± 1.0	4.0 ± 0.7	6.7	4.0	-	
Cd	-	6.0 ± 2.1	-	-	-	-	
As	-	4.9 ± 3.0	3.7 ± 1.3	-	-	-	
As	6.6 ± 1.2	7.9 ± 4.1	5.7 ± 1.0	6	6.3	-	
In	5.5 ± 2.2	3.7 ± 1.0	2.6 ± 0.7	-	-	-	
Zn	4.3 ± 1.2	4.3 ± 1.1	3.0 ± 0.5	7.8	1.5	2.5	
Pb	-	3.8 ± 1.5	-	8.1	3.7	3.1	
Ga	4.3 ± 1.6	3.0 ± 1.0	2.8 ± 0.6	-	1.2	-	
U	3.3 ± 0.5	2.5 ± 0.6	1.9 ± 0.15	-	-	-	
Sc	3.0 ± 1.4	5.3 ± 1.2	4.5 ± 0.7	5.5	5.7	1.7	
Ba	2.5 ± 0.6	2.7 ± 1.1	1.8 ± 1.0	0.7	0.92	-	
Cr	2.5 ± 0.4	2.6 ± 0.4	1.75 ± 0.26	3.0	1.1	-	
Co	2.3 ± 0.2	1.7 ± 0.4	1.5 ± 0.1	1.4	1.0	-	
V	2.0 ± 1.5	2.5 ± 0.8	2.2 ± 0.7	2.5	0.75	-	
Mo	1.8 ± 1.4	3.5 ± 1.7	2.7 ± 0.9	-	-	3.0	
Rb	1.8 ± 0.7	0.89 ± 0.16	0.81 ± 0.09	0.75	-	0.94	
Cs	1.7 ± 0.4	0.82 ± 0.28	0.80 ± 0.14	1.5	-	-	
Sr	1.2 ± 0.2	1.4 ± 0.4	1.3 ± 0.3	1.0	-	-	
Eu	1.2 ± 0.15	0.92 ± 0.12	0.92 ± 0.08	0.79	0.75 ^h	-	
Mg	1.1 ± 0.2	0.8 ± 0.5	1.5 ± 0.6	0.54	-	-	
Fe	1.1 ± 0.1	0.90 ± 0.14	0.94 ± 0.02 (0.05)	0.84	0.83	≈ 1.0	
Ce	1.06 ± 0.07	0.88 ± 0.14	0.86 ± 0.02 (0.05)	0.99	0.75 ^h	-	
Na	1.0 ± 0.2	1.1 ± 0.15	1.1 ± 0.2	≈ 1.0	≈ 1.0	-	
Sc	$\approx 1.00 \pm 0.13$	$\approx 1.00 \pm 0.12$	$\approx 1.00 \pm 0.12$	≈ 1.0	≈ 1.0	-	
Lu	1.0 ± 0.4	0.97 ± 0.14	0.97 ± 0.02	0.68	0.75 ^h	-	
Ta	1.0 ± 0.1	0.88 ± 0.12	0.86 ± 0.06	-	0.75 ^h	-	
Yb	-	0.89 ± 0.16	0.94 ± 0.05	-	0.75 ^h	-	
Hf	-	0.87 ± 0.12	0.86 ± 0.04	0.76	-	-	
Mn	1.0 ± 0.15	0.96 ± 0.29	0.97 ± 0.05	0.55	0.75 ^h	-	
K	1.0 ± 0.4	0.7 ± 0.3	0.68 ± 0.10	0.95	0.83	-	
Tl	0.97 ± 0.19	0.96 ± 0.16	0.93 ± 0.11	-	0.75 ^h	-	
Ta	0.95 ± 0.27	0.89 ± 0.16	0.88 ± 0.06	1.0	-	-	
Th	0.95 ± 0.19	0.90 ± 0.13	0.90 ± 0.03	0.76	-	-	
Li	0.91 ± 0.18	1.0 ± 0.1	0.9 ± 0.3	1.2	0.75	-	
Al	0.86 ± 0.07	0.75 ± 0.16	0.73 ± 0.08	0.44	0.83	0.94	
Nd	0.84 ± 0.22	0.89 ± 0.28	0.91 ± 0.07	-	0.75 ^h	-	
Ca	0.76 ± 0.19	0.89 ± 0.28	0.81 ± 0.12	-	0.92	-	
Zr	0.7 ± 0.3	0.96 ± 0.42	0.91 ± 0.18	-	0.83	0.73	
Mn	0.68 ± 0.17	1.1 ± 0.7	0.85 ± 0.25	0.78	-	-	
Be	-	0.6 ± 0.4	-	-	0.64 ⁱ	-	
Br	0.2 ± 0.1	0.1 ± 0.1	-	-	0.17	-	

^a Penetration (Table VI) of each element to that of Sc, which is identical with the enrichment factor used by Gladney et al. (12) and Gordon et al. (33). ^b The uncertainty reported is the larger of twice the standard deviation and twice the analytical uncertainty. Rb is based on one sample. ^c The uncertainty reported is twice the individual uncertainty in the ratio that was derived from standard deviations of replicate elemental analyses of coal and aerosol samples. ^d Uncertainties reported are twice the standard deviation of the replicate determinations; twice the root mean square of the individual uncertainties is given in parentheses if larger than the 2 σ value. ^e Based on 1973 data of Klein et al. (17). ^f Unless indicated, values listed are based on data of Gladney et al. (12). ^g Derived from data of Kaakinen et al. (9) for the ESP-equipped unit. Data normalized to Fe. The value for Pb was based on ²¹⁰Pb. ^h Based on single value reported for "rare earths" in Gordon et al. (33). ⁱ Based on value of Gladney and Owens (34) renormalized to Sc.

to a lesser extent Zn, were definitely enriched in larger particles as well as in smaller particles. Gladney et al. (12) observed similar enrichments of Se and Hg in large particles. Significant quantities of Se, Hg, and Br are in the vapor phase in flue gases and may have been adsorbed onto impactor substrates, on large porous particles, or on large carbonaceous particles, which we saw on the upper stages of impactors collected at plant A.

Curves of RP vs. particle size for elements in plant B aerosols are shown in Figure 2c. Curves for the lanthanides, K, Hf, Th, Ti, Mg, Cs, Rb, Ta, Sc, and Mn were similar to those for Na and Fe. These showed little or no enrichment in any sized particle. Enrichments of W, U, Ba, Zn, V, In, Ga, Ba, As, Se, Sb, and Mo are considerable and increase with decreasing particle size. Curves for these elements tended to be somewhat bimodal (see W) with a broad maximum between 2 and 10 μ m (see W, U, and Ba in Figure 2b). The curves for Se differ somewhat from those of W, U, and Ba in that the minimum is broader. Both Cr and Co (Figure 2c) were highly enriched in the smallest sized particles, but the curves of RP vs. size were distinctly different from those of elements with curves similar to W.

Relative Penetration of Elements. In column 4 of Table VII we list RPs of elements from five samples collected at plant B when the load was 515 or 530 MW. Despite the rather large range in the absolute elemental emission rates (typically twofold or more, see Table V), the penetration ratios of the

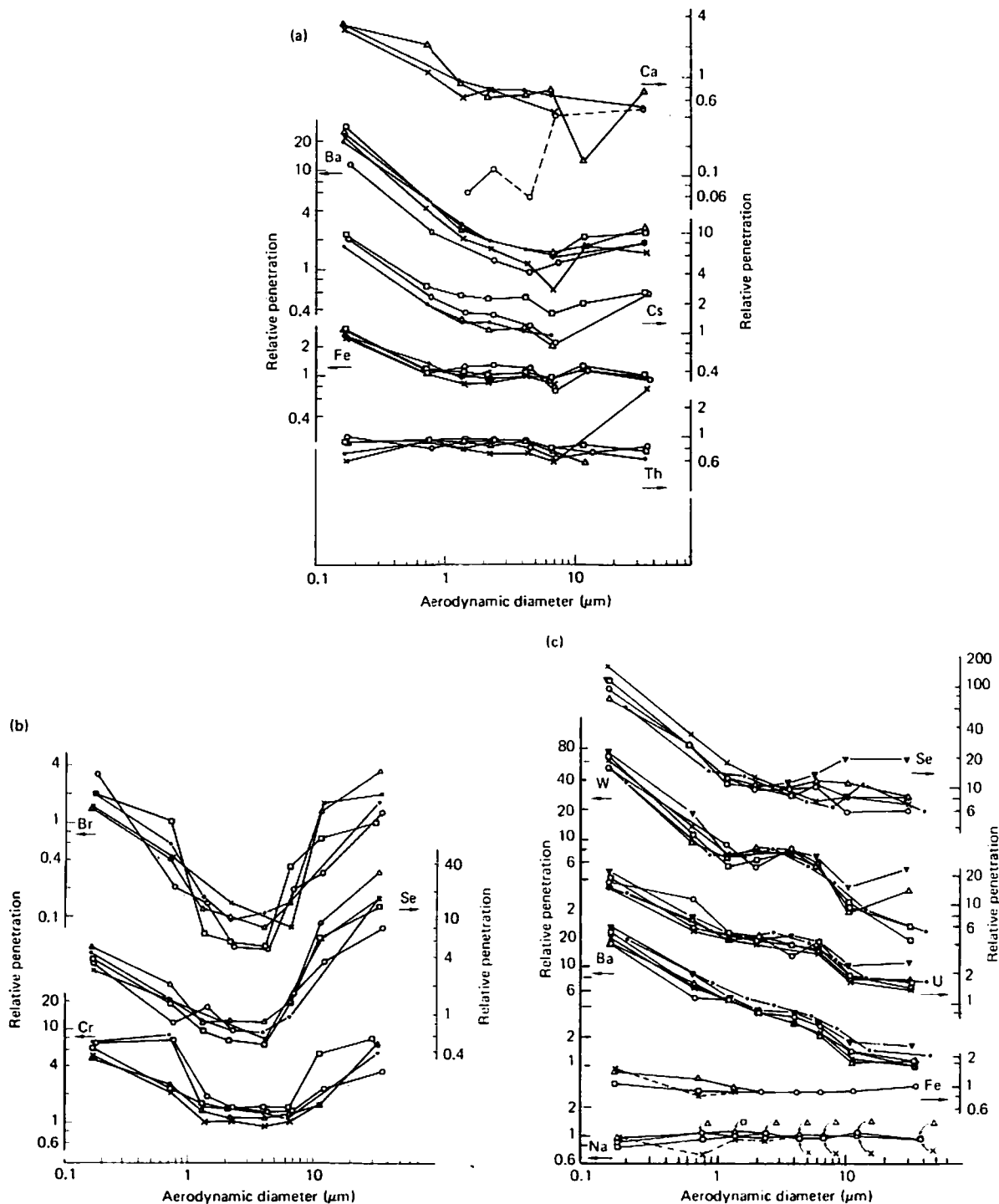


Figure 2. Relationship of relative penetration to particle size of several elements in aerosols emitted at plant A (a and b) and plant B (c). The symbols indicate different sets of data from impactors

515- and 530-MW samples varied by less than the uncertainties in the individual values (2σ typically is $<20\%$). Thus, for a given plant it appears possible to determine the RP of elements on the basis of only a few samples. Further comparison of the penetration ratios of the 625-MW and 515- to 530-MW samples shows significant, but relatively small, differences for a few elements: As, Cr, In, Mo, and Sb. Thus, the penetration ratios of the elements seem to be relatively independent of gross generating load as well as absolute emission rate.

Despite the rather large differences in the composition and origin of the coal and differences in the combustion chambers and ESPs used at the two plants, the RPs of most of the ele-

ments were equivalent to within their respective uncertainties. In fact, except for In, Se, Mo, Rb, Cs, K, Mn, and Br, the deviation between the two values (larger/smaller $\times 100$) was $\leq 35\%$. The largest differences in the two units were in values of In, Se, Mo, Rb, Cs, K, and Mn. Differences in RPs of the elements ranged from 1.4 for K to about 2 for Rb and Cs. However, only Rb, Cs, Mo, Se, and Mn are judged to be significantly different. The larger penetrations of Rb and Cs at plant A probably result from significantly greater concentrations of these elements in smaller particles as indicated in the curves of RP vs. particle size shown for Cs in Figure 2a. At plant B, the curves of relative penetration vs. particle size for Rb and Cs are similar to those shown for Fe and Na (Figure

2b).

Also listed in Table VII are the RPs of elements determined at three other conventionally designed coal-fired power units equipped with cold-side ESPs. During the work of Gladney et al. (12), the plant at Chalk Point burned high-sulfur (1.9%) coal with an ash content of about 12%. The Valmont plant burned low-sulfur (0.6%), low-ash (6%) coal. Coal at the Allen Steam Plant contained 10.4% ash and 3.1% S (1973 data of Klein et al. (11)). The removal efficiencies for fly ash at the Chalk Point, Valmont, and Allen Steam Plants were estimated at 97.96, 2. and 99.5%, respectively, including bottom-ash removal and other fly-ash-collection systems in addition to ESPs. Despite these differences, many of the values from these units are remarkably similar to those determined at plants A and B. The largest differences in the RPs at the five plants were those of Zn, Pb, Ba, Cr, Co, V, Rb, and Cs, which differed by as much as a factor of five. These include elements in each of the three geochemical classifications (i.e., chalcophilic, Zn and Pb; lithophilic, Cs and Rb; and intermediate elements, Ba, Cr, Co, and V) described by Klein et al. (11). The large range in RPs of these elements is attributed to differences in distributions of elements according to particle size (and hence coal chemistry) and the removal efficiency vs. particle size curves of the ESPs.

Summary and Conclusions

The relative penetrations of several elements from two western coal-fired power plants are nearly the same, despite variations in boiler size, electrical generating capacity, precipitator size and efficiency, and coal composition, and are quite similar to those observed at plants burning high-sulfur Eastern coal. However, significant differences exist among plants in relative penetrations of the elements Zn, Pb, Ba, Cr, Co, V, Rb, and Cs. This is attributed to differences in composition of the coal and the particle size vs. efficiency characteristics of the individual ESPs. Based on concentrations of elements reported by Gluskoter et al. (35), enrichments relative to average crustal abundances in U.S. coals are often larger and more highly variable than enrichments (RPs) that occur during coal use in the power plants discussed above. Thus, excluding fractionation of elements that can occur in power plant plumes (15), the greatest impact on the final enrichment of many elements in particles emitted from these plants is due to the original coal composition. We note, however, that enrichments of elements in particles emitted from coal-burning units equipped with other types of particulate control systems such as venturi scrubbers can be much greater than those reported above (21).

Acknowledgment

We gratefully acknowledge the assistance of D. Garvis and R. W. Wikkerink in collecting samples, R. E. Heft, W. A. Steele, and F. Bazan for elemental analyses, and B. K. Ishida and H. R. Ralston for their assistance in preparing the manuscript.

Literature Cited

- (1) Coles, D. G., Ragaini, R. C., Ondov, J. M., *Environ. Sci. Technol.*, 12, 442 (1978).
- (2) Eisenbud, M., Petrow, H. G., *Science*, 144, 228 (1964).
- (3) Martin, J. E., Harward, E. D., Oakley, D. T., Smith, J. M., Bedrosian, P. H., in "IAEA Symposium on Environmental Aspects of Nuclear Power Stations, New York, 1969", IAEA Conference 700810-24, paper IAEA-Sm-146/19, 1969, pp 325-37.
- (4) Hull, A. P., *Nucl. News*, 51-5 (April 1974).
- (5) Moore, H. E., Martell, E. A., Poet, S. E., *Environ. Sci. Technol.*, 10, 586-91 (1976).
- (6) Guerrini, R., Pennacchi, A., "La Rivista Dei Combustibili", Vol. XXIX, fasc. 7-8, Luglio-agosto, 1975.
- (7) Hangebrauck, R. P., Vonlehmden, D. J., Meeker, J. E., *J. Air Pollut. Control Assoc.*, 14, 267-78 (1964).
- (8) Jones, P. W., Giammar, R. D., Strup, P. E., Stanford, T. B., *Environ. Sci. Technol.*, 10, 806-10 (1976).
- (9) Kaakinen, J. W., Jordan, R. M., Lawasani, M. H., West, R. E., *Environ. Sci. Technol.*, 9, 862-9 (1975).
- (10) Bertine, K. K., Goldberg, E. D., *Science*, 173, 233-5 (1971).
- (11) Klein, D. H., Andren, A. W., Carter, J. A., Emery, J. F., Feldman, C., Fulkerson, W., Lyon, W. S., Ogle, J. C., Talm, Y., Van Hook, R. I., Bolton, N., *Environ. Sci. Technol.*, 9, 973-9 (1975).
- (12) Gladney, E. S., Small, J. A., Gordon, G. E., Zoller, W. H., *Atmos. Environ.*, 10, 1071-7 (1976).
- (13) Block, C., Dams, R., *Environ. Sci. Technol.*, 10, 1011-7 (1976).
- (14) Ragaini, R. C., Ondov, J. M., *J. Radioanal. Chem.*, 37, 679-91 (1977).
- (15) Ondov, J. M., Ragaini, R. C., Bierman, A. H., Choquette, C. E., Gordon, G. E., Zoller, W. H., paper presented at the 173rd National Meeting of the American Chemical Society, New Orleans, March 25, 1977, Abstract ENVT-124, Lawrence Livermore Laboratory, Preprint UCRL-78825, 1977.
- (16) Andren, A. W., Klein, D. H., *Environ. Sci. Technol.*, 9, 856-8 (1975).
- (17) Billings, C. E., Matson, W. R., *Science*, 176, 1232-3 (1972).
- (18) Davison, R. L., Natusch, D. F. S., Wallace, J. R., Evans, E. A., Jr., *Environ. Sci. Technol.*, 8, 1107-13 (1974).
- (19) Linton, R. W., Loh, A., Natusch, D. F. S., Evans, C. A., Jr., Williams, P., *Science*, 191, 852-4 (1976).
- (20) Task Group on Lung Dynamics, *Health Phys.*, 12, 173-208 (1966).
- (21) Ondov, J. M., Ragaini, R. C., Biermann, A. H., "Elemental Emissions From a Coal-Fired Power Plant: Comparison of a Venturi Wet Scrubber-System with a Cold-Side Electrostatic Precipitator," Lawrence Livermore Laboratory, Preprint UCRL-80110.
- (22) Ondov, J. M., Ragaini, R. C., Biermann, A. H., *Atmos. Environ.*, 12, 1175 (1978).
- (23) Ragaini, R. C., Heft, R. E., Garvis, D., "Neutron Activation Analysis at the Livermore Pool-Type Reactor for the Environmental Research Program", Lawrence Livermore Laboratory Report, UCRL-52092, 1976.
- (24) Heft, R. E., paper presented at the Third International Conference on Nuclear Methods in Environmental and Energy Research, Columbia, Mo., Oct 10-13, 1977.
- (25) Murphy, J., *At. Absorpt. Newsl.*, 14, 151 (1975).
- (26) Bonner, N. A., Bazan, F., Camp, D. C., *Chem. Instrum.*, 6, 1-36 (1975).
- (27) Ondov, J. M., Zoller, W. H., Olmez, K., Aras, N. K., Gordon, G. E., Ranticelli, L. A., Able, K. H., Filby, R. H., Shah, K. R., Ragaini, R. C., *Anal. Chem.*, 47, 1102-9 (1975).
- (28) Ondov, J. M., Ragaini, R. C., Heft, R. E., Fisher, G. L., Silberman, D., Prentice, B. A., in Proceedings of the 8th Materials Research Symposium, Methods and Standards for Environmental Measurement, Gaithersburg, Md., Sept 20-24, in press; Lawrence Livermore Laboratory, Preprint UCRL-78194, 1976.
- (29) Fisher, G. L., Chang, P. V., Brummer, M., *Science*, 192, 555-6 (1976).
- (30) Ulrich, G. D., "An Investigation of the Mechanism of Fly-Ash Formation in Coal-Fired Utility Boilers", Interim Report, US-ERDA FE-2205-1, May 28, 1976.
- (31) Padia, A. S., Sarafim, A. I., Howard, J. B., paper presented at the Combustion Institute's Central States Section, April 1976.
- (32) Fuch, N. A., "The Mechanics of Aerosols", MacMillan, New York, 1964, pp 21-30.
- (33) Gordon, G. E., Zoller, W. H., Gladney, E. S., Proceedings of 2nd International Conference on Nuclear Methods and Environmental Research, Columbia, Mo., 1974, pp 344-53.
- (34) Gladney, E. S., Owens, J. W., *J. Environ. Health*, A11(4&5), 297-311 (1976).
- (35) Gluskoter, H. J., Ruch, R. R., Miller, W. G., Cahill, R. A., Dreher, G. B., Kuhn, J. K., "Trace Elements in Coal: Occurrence and Distribution", Illinois State Geological Survey, Circular 499, 1977.

Received for review July 14, 1978. Accepted April 13, 1979. This work was performed under the auspices of the U.S. Department of Energy by Lawrence Livermore Laboratory under Contract No. W-7405-Eng-48. Reference to a company or product name does not imply approval or recommendation of the product by the University of California or the U.S. Department of Energy to the exclusion of others that may be suitable.

EX 3

Comparison of Particle Size Distributions and Elemental Partitioning from the Combustion of Pulverized Coal and Residual Fuel Oil

William P. Linak and C. Andrew Miller

*Air Pollution Prevention and Control Division, National Risk Management Research Laboratory,
U.S. Environmental Protection Agency, Research Triangle Park, North Carolina*

Jost O.L. Wendt

Department of Chemical and Environmental Engineering, University of Arizona, Tucson, Arizona

ABSTRACT

U.S. Environmental Protection Agency (EPA) research examining the characteristics of primary PM generated by the combustion of fossil fuels is being conducted in efforts to help determine mechanisms controlling associated adverse health effects. Transition metals are of particular interest, due to the results of studies that have shown cardiopulmonary damage associated with exposure to these elements and their presence in coal and residual fuel oils. Further, elemental speciation may influence this toxicity, as some species are significantly more water-soluble, and potentially more bio-available, than others. This paper presents results of experimental efforts in which three coals and a residual fuel oil were combusted in three different systems simulating process and utility boilers. Particle size distributions (PSDs) were determined using atmospheric and low-pressure impaction as well as electrical mobility, time-of-flight, and light-scattering techniques. Size-classified PM samples from this study are also being utilized by colleagues for animal instillation experiments.

Experimental results on the mass and compositions of particles between 0.03 and >20 μm in aerodynamic diameter show that PM from the combustion of these fuels

produces distinctive bimodal and trimodal PSDs, with a fine mode dominated by vaporization, nucleation, and growth processes. Depending on the fuel and combustion equipment, the coarse mode is composed primarily of unburned carbon char and associated inherent trace elements (fuel oil) and fragments of inorganic (largely calcium-alumino-silicate) fly ash including trace elements (coal). The three coals also produced a central mode between 0.8- and 2.0- μm aerodynamic diameter. However, the origins of these particles are less clear because vapor-to-particle growth processes are unlikely to produce particles this large.

Possible mechanisms include the liberation of micron-scale mineral inclusions during char fragmentation and burnout and indicates that refractory transition metals can contribute to PM <2.5 μm without passing through a vapor phase. When burned most efficiently, the residual fuel oil produces a PSD composed almost exclusively of an ultrafine mode (~0.1 μm). The transition metals associated with these emissions are composed of water-soluble metal sulfates. In contrast, the transition metals associated with coal combustion are not significantly enriched in PM <2.5 μm and are significantly less soluble, likely because of their association with the mineral constituents. These results may have implications regarding health effects associated with exposure to these particles.

IMPLICATIONS

Transition metals are hypothesized to play a significant role in causing adverse health effects associated with exposure to PM_{2.5}. The concentration, speciation, and solubility of transition metals in PM_{2.5} generated by the combustion of fossil fuels can depend upon the fuel type and combustor design. The results presented in this paper have implications for policymakers and researchers evaluating possible sources and control of PM_{2.5} containing transition metals.

INTRODUCTION

Fine PM has been of considerable environmental interest in recent years because of a number of research studies correlating short-term exposure of ambient levels of fine PM with acute adverse health effects.¹ These studies were summarized by the U.S. Environmental Protection Agency (EPA)^{2,3} and reviewed by EPA's Clean Air Scientific Advisory Committee, which concluded that there was evidence

linking ambient fine PM concentrations and adverse health effects.⁴ These studies were the basis for a revision of the National Ambient Air Quality Standards for PM that included a standard for PM <2.5 μm in diameter (PM_{2.5}).⁵

In the ambient atmosphere, fine PM is composed primarily of sulfates, nitrates, condensed organics, carbonaceous soot, and inorganic aerosols, formed during high-temperature processes such as the combustion of fuels containing trace quantities of metals and other impurities.^{2,6,7} Formation of these small particles is heavily influenced by vaporization, condensation, and other gas-to-particle conversion processes. In contrast, the coarse fraction of PM tends to be composed of particles formed by mechanical (e.g., fragmentation, grinding, crushing, and entrainment) processes. Because they are formed by different mechanisms, the fine and coarse fractions of PM tend to have different compositions. Particle composition has been identified as one of the possible factors driving the adverse health effects associated with exposure to ambient PM.⁸

Health effect researchers have identified at least two aspects of particle composition that appear to exacerbate health damage from particles. The first is related to water-soluble transition metals such as Cu, Fe, Ni, V, and Zn present in the particles.⁹⁻¹¹ The second is aerosol acidity in general. In addition to these composition-related properties, ultrafine particles (those particles <0.1 μm in diameter), regardless of composition, have been identified as potential factors influencing mechanisms for these health impacts.² Particles with all of these characteristics (transition metals, acidity, and ultrafine size) are contained in the PM generated from the combustion of fossil fuels such as residual fuel oils and coals. Hence, one might hypothesize fossil-fuel-fired systems to be candidate sources of toxic fine particles that play a significant role in the demonstrated association of adverse health effects with ambient concentrations of fine PM.

The research by Dreher et al.⁹⁻¹¹ has indicated that residual oil fly ash (ROFA) possesses toxic qualities. Unfortunately, the hypothesis that residual oil combustion is the prime source of fine particles causing respiratory distress is not consistent with the currently available epidemiologic data. Residual fuel oils are used in significant quantities in only selected regions of the country. Discounting sales of Bunker C oil, the majority of which is likely to be burned by ships well away from continental coastlines, significant residual oil usage occurs primarily in the northeast and southeast regions of the United States.¹² However, adverse health effects associated with exposure to fine PM are not limited to these regions,¹³ suggesting that sources of fine PM other than (or in addition to) those related to residual fuel oil combustion must also be important.

Another source of PM_{2.5} containing transition metals is pulverized coal combustion. Pulverized coal combustion is widespread throughout the United States, and emissions from coal-fired boilers and furnaces account for a much larger fraction of both PM <10 μm in aerodynamic diameter (PM₁₀) and PM_{2.5}, compared to residual fuel oil combustion. In 1997, ~165,000 tons of PM_{2.5} was emitted from utility, industrial, commercial, and institutional combustion of coal, compared to 35,000 tons of PM_{2.5} from combustion of residual oil from the same source categories.¹⁴ These values are for primary PM emitted directly from these sources and do not include secondary particles formed from gas-phase precursors such as SO₂ and NO_x. Because both coal and residual fuel oil burned in the United States contain significant levels of transition metals (see Table 1), substantial quantities of these metals are emitted into the atmosphere. In light of the potential health effects associated with inhalation exposure to transition metals, it is worthwhile to explore the formation mechanisms and partitioning of transition metals across different particle sizes for both coals and residual fuel oils.

In a previous study, Miller et al.¹⁵ explored the relationship between residual fuel oil composition, boiler operation, and the physical and chemical characteristics of the PM produced. In a subsequent study, Linak et al.¹⁶ compared the characteristics of PM produced from two types of combustion systems burning the same residual fuel oil. These systems were designed to simulate the operation of small institutional and industrial boilers and large utility boilers. In this study, we compare differences in compositions and particle size distributions (PSDs) of PM from residual fuel oil and coal. Specifically, these tests, conducted at EPA's National Risk Management Research Laboratory in Research Triangle Park, NC, examined the physical and chemical characteristics of PM generated by the combustion of residual fuel oil and coal. A single residual fuel oil was tested in two combustors with significantly different heat transfer characteristics, and three U.S. coals were tested in a single combustor under similar combustion conditions. The purpose of these tests was to examine the relationship between particle size and particle composition, specifically with respect to metal content, for different fossil fuels, and how the relationship may change as fuel or carbon burnout changes. The results of the current and previous studies are intended to form the foundation that may ultimately link measures of acute pulmonary damage to engineering variables.

EXPERIMENTAL

Residual oil experiments were performed in two types of combustion systems. These systems represent extremes of a range of practical conditions under which fuel oil is burned. Although they may not represent specific boilers

Table 1. Fuel analysis.

	Western Kentucky Bituminous	Montana Subbituminous	Utah Bituminous	High Sulfur No. 6 Oil
Proximate Analysis^a (%)				
Moisture	6.97	11.36	5.97	0.50
Volatile matter	35.86	37.18	38.58	
Fixed carbon	49.66	41.05	45.75	
Ash	7.51	10.41	9.69	0.10
HHV ^b , Btu/lb	11291	9526	11289	18270
HHV, kcal/kg	6273	5292	6272	10150
Ultimate Analysis^c (%)				
C	70.17	64.87	69.23	85.61
H	4.57	3.97	4.87	10.38
N	1.49	1.03	1.45	0.35
S	3.11	0.83	0.96	2.33
O ^d	12.59	17.56	13.18	0.92
Ash	8.07	11.74	10.31	0.10
Trace Elements^c (μg/g fuel)				
As	4.68	1	2	0.1
Be	1.6	0.4	0.8	<0.3
Cd	<0.2	<0.2	<0.2	0.60
Cl	35.5	28.7	33.9	
Cr	11	4	12	1.05
Cu	3	2.89	3.37	3.5
Fe	9210	2560	2000	21
Pb	3.06	3.42	2.87	4.5
Mg	79.4	1700	1710	
Mn	6.71	62.3	59.9	
Hg	0.15	0.08	0.07	0.10
Mo	3.25	ND	ND	
Ni	6.35	2.39	ND	30
K	81.7	ND	44.6	
Se	2	1	2	<0.1
Na	332	300	409	
V	13	4.55	4.25	220
Zn	30.8	ND	ND	74

Notes:^aAs received (wet); ^bHigher heating value; ^cDry basis, ND indicates nondetect analysis, empty cells indicate no analysis for this element was attempted; ^dBy difference.

in all respects, they were investigated here with a view to determining how this range of combustion conditions influences the characteristics of fine particles and the mechanisms that form them. The first system is a small fire-tube boiler, in which combustion occurs in tubes surrounded by water or steam. These types of small boilers have large heat transfer surfaces, small volumes, relatively short residence times, cold walls, and high gas quenching rates (~500 K/s), and often produce emissions with relatively high carbon contents due to unburned carbonaceous char. The second system is a laboratory-scale

refractory-lined combustor designed to simulate the time/temperature environments of larger utility boilers and incinerators. In large utility boilers, the water or steam, rather than the combustion gases, is contained in tubes. These systems, including the refractory-lined combustor, operate at higher temperatures with lower quenching rates (~150 K/sec). As will be discussed later, particle emissions from this system contain very little unburned carbon and better approximate emissions from large oil-fired utility boilers, as reported in the literature.^{17,18}

Fire-Tube Boiler

Residual oil experiments were performed using a commercially available, North American, three-pass, fire-tube package boiler. This unit is equipped with a 732-kW North American burner with an air-atomizing oil nozzle. Oil temperature and oil and atomizing air pressures are independently controlled to ensure proper oil atomization. PM samples were extracted at stack locations at temperatures ranging from 450 to 550 K. Additional system details are presented elsewhere.¹⁵

Refractory-Lined Combustor

Residual oil experiments were also performed using a 59-kW laboratory-scale refractory-lined combustor. This unit is equipped with an International Flame Research Foundation (IFRF) moveable-block variable-air swirl burner, which incorporates an air-atomizing oil nozzle positioned along its center axis and swirling air, which passes through the annulus around the fuel injector to promote flame stability. The burner was configured for a high swirl flame (IFRF Type 2, swirl no. = 1.48) with internal recirculation. Gas and aerosol samples were taken from stack locations at temperatures of ~670 K. All oil experiments (fire-tube boiler and refractory-lined combustor) were performed at a stoichiometric ratio (SR) of 1.2 without secondary air preheat. Additional system details are presented elsewhere.¹⁶

Pulverized Coal Combustor

Coal combustion experiments were conducted using a down-fired, refractory-lined furnace rated at 50 kW. A schematic of this furnace is presented in Figure 1. In this combustor, pulverized coal is metered from a screw feeder and carried by transport air through a fuel injector into the combustor. Additional axial and tangential airstreams are metered separately into the variable swirl burner and introduced into the combustor as an annular flow around the coal. These flows can be adjusted to create stable flames with the desired degree of swirl. The vertical 4.1 m down-fired combustor is 20-cm inside diameter (ID). At the bottom of the vertical section, the combustion gases make a 90° turn into a 3.7-m-long, 15-cm-ID horizontal sampling

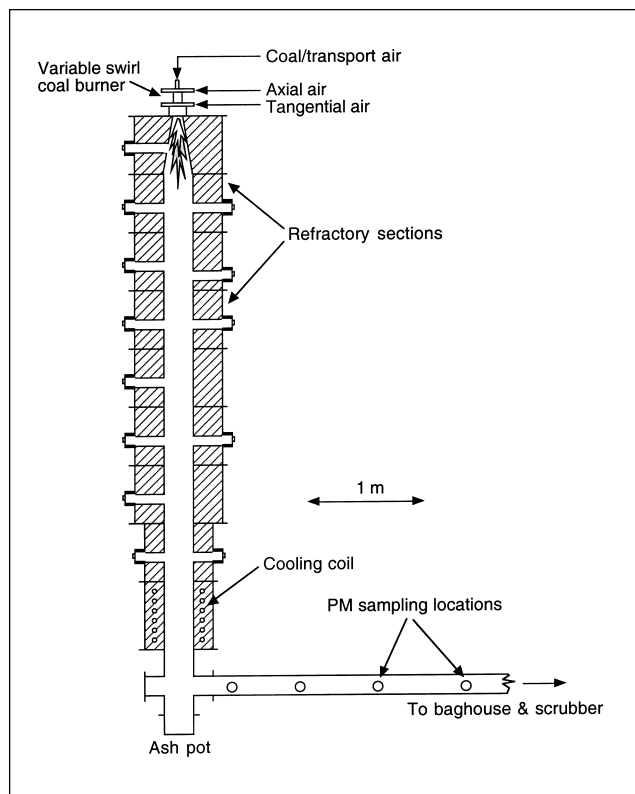


Figure 1. EPA down-fired pulverized coal combustor.

duct. Ports are available along the furnace and exhaust duct for introduction of additional staging air or for introduction of sorbents or extractive sampling. The locations of these ports are shown in Figure 1. Previous test programs burning pulverized coal have resulted in combustion conditions within the furnace similar to those found in full-scale utility units.¹⁹

Particulate Sampling and Analysis

PM measurements were performed using several methods. Standard EPA Methods 5 and 60 sampling and analytical procedures were used to determine total particulate and metal concentrations using inductively coupled argon plasma atomic emissions spectroscopy (ICP/AES).^{20–22} Other metal analyses were determined by X-ray fluorescence (XRF) spectroscopy. Additional samples were analyzed by X-ray absorption fine structure (XAFS) spectroscopy, an element-specific structural analysis that is useful for determining trace element speciation and forms of occurrence in chemically and structurally complex materials such as combustion ash.^{23–25}

PSDs were determined by a combination of four techniques used at various times. Instruments based on electrical mobility, time-of-flight, and inertial impaction measurements were used for extracted aerosols; and light-scattering measurements were used for in situ in-stack measurements. Extractive samples were taken for electrical

mobility, time-of-flight, and inertial impaction analyses using an isokinetic aerosol sampling system described elsewhere.^{26,27} These diluted samples were directed to a TSI Inc. scanning mobility particle sizer (SMPS) and a TSI Inc. aerodynamic particle sizer (APS). The SMPS and APS were configured to yield 54 and 50 channels evenly spaced (logarithmically) over 0.01- to 1.0- μm and 0.5- to 20- μm diameter ranges, respectively. Extracted samples were also directed to three cascade impactors including an Andersen Inc. eight-stage, 28 L/min atmospheric pressure impactor, an MSP Inc. ten-stage, 30 L/min micro-orifice uniform deposit impactor (MOUDI), and a custom-made eleven-stage 28 L/min Berner-type low-pressure impactor.²⁸ During the oil experiments, in situ light-scattering PSDs were obtained using an Insitac Inc. particle counter size velocimeter with a working range of ~ 0.3 –100 μm . Scanning electron microscope (SEM) samples were collected on silver membrane filters to minimize particle charging effects.

In order to collect larger quantities of size-segregated PM for parallel toxicological studies and XAFS analyses, a large dilution sampler capable of sampling 0.28 m^3/min of flue gas was used.²⁹ The extracted sample passed through a cyclone (50 and 90% collection efficiencies for 1.8- and 2.5- μm -diameter PM, respectively) and was then diluted with clean filtered ambient air (2.8 m^3/min) to approximately ambient temperature (3 sec residence time). The resulting PM was collected on 64.8-cm-diameter Teflon-coated glass fiber filters, transferred to sampling jars, and made available for subsequent chemical, physical, or biological analysis. In addition to the particle sampling and collection devices just described, continuous emission monitors were used to measure stack concentrations of CO , CO_2 , NO_x , O_2 , and SO_2 . These measurements were made in order to monitor and control the combustion environments.

Fly ash samples from the oil experiments and the three coals were subjected to a successive leaching procedure under development to examine the relative solubility of transition metals (Cu, Fe, Ni, V, and Zn) associated with different fly ash matrices. To date, only the dilution sampler filter catches ($\text{PM}_{2.5}$) for these four fuels have been examined in this manner. PM samples were placed in successive solutions (30 mL) of distilled water (pH = 7), 0.1 N (equivalent) H_3BO_3 (pH = 5.2 for 0.1 N), 0.1 N CH_3COOH (pH = 2.9), and 0.1 N HCl (pH = 1.1), and sonicated at room temperature for 2 hr. The filtrates and solid residues were separated between successive leaching steps. Finally, these leached samples (and a set of unleached samples) were subjected to a modified Method 3050B extraction procedure to determine total metal content.³⁰ Briefly, this method uses a 50/50 mixture of HNO_3 and HF, microwaved for 5 min at 340 kPa and 20 min at 550 kPa. After cooling, an additional H_3BO_3 solution is added and

microwaved for 10 min at 340 kPa. Solutes were analyzed by ICP/AES.

Experimental Conditions

The no. 6 residual oil used in both oil experimental systems contained 2.33% sulfur and 0.1% ash. Operational characteristics for both systems included similar oil temperatures (380–400 K), atomizing air pressures (200–240 kPa), and stoichiometries (SR = 1.2). The droplet PSD produced using the Delavan Airo Combustion air-atomizing oil nozzle (model 30615-84) in the fire-tube boiler was relatively narrow with a mean diameter between 30 and 40 μm . The refractory-lined combustor experiments used a similar Spraying Systems Co. (model Air Atom 1/4-JSS) air-atomizing oil nozzle and produced PSDs believed to be similar to those for the boiler studies. Therefore, any differences in carbon burnout may be attributed to differences in temperature history rather than in droplet size. Stack O_2 concentrations ranged between 3.4 and 3.6% for all experiments.

Two western U.S. coals (Montana subbituminous and Utah bituminous) and one eastern U.S. coal (western Kentucky bituminous) have been examined. The coals were burned under conditions that simulated as closely as possible those conditions typical of a full-scale utility boiler. Stack O_2 concentrations for the coal combustion tests ranged from 3.5 to 3.8%, with CO values near 60 ppm for the Montana coal and 135 ppm for the western Kentucky and Utah coals. Heat input rates averaged 22.9 kW for the Montana coal, 19.7 kW for the western Kentucky coal, and 20.2 kW for the Utah coal. Average NO_x concentrations for the three coals ranged between 440 and 480 ppm, and SO_2 concentrations averaged 430 ppm for the Montana coal, 1475 ppm for the western Kentucky coal, and 850 ppm for the Utah coal (all values uncorrected for O_2 concentration).

Table 1 presents the proximate, ultimate, and trace element analyses for the three coals and one residual fuel oil examined. Heating values are also included. In contrast to the residual oil, which contained only 0.1% ash, the coal ash contents ranged from 7.5 to 10.4% (as received). However, the residual oil sulfur concentration was almost as high as the western Kentucky coal (2.33 and 3.11%, respectively). The two western coals each had sulfur concentrations less than 1%. Also of note are the high transition metal (Fe, Ni, V, and Zn) concentrations in the residual oil and the high Fe concentrations in the coals. Although not measured and presented here, coals often contain very high concentrations of Al, Ca, and Si. Hardesty and Pohl³¹ report ranges of Al, Ca, and Si concentrations in U.S. coals of 0.3–2.3, 0.005–1.2, and 0.5–41%, respectively. Galbreath et al.²⁴ report Al and Si concentrations in a similar high sulfur no. 6 oil of 19 and

94 ppm, respectively. Walsh et al.³² report ranges of Al, Ca, and Si concentrations from three medium sulfur residual oils of 21–44, 13–23, and 23–89 ppm, respectively.

RESULTS AND DISCUSSION

PM and Trace Element Emissions

PM mass emissions, emission factors, and trace element emissions for the three coals and two fuel oil conditions are presented in Table 2. Also presented are the mass fractions of $\text{PM}_{2.5}$, as well as the weight percent of unburned carbon and loss on ignition (LOI). PM emissions for the three coals and one of the two fuel oil conditions are based on triplicate averages. Standard deviations are included. These data indicate that uncontrolled PM emissions from the three coals ranged between 3800 and 4400 mg/m^3 compared to 90 and 180 mg/m^3 for the fuel oil.

Differences seen between the two fuel oil conditions are likely the result of differences in the heat transfer, time/temperature profiles, and quenching rates characteristic of the two types of combustion equipment used, and are consistent with data published from field measurements.¹⁶ However, even though the uncontrolled PM emissions for the three coals are over 20 times greater than those for the oil experiments, Table 2 indicates that the mass fraction of $\text{PM}_{2.5}$ for the coals is very much smaller (4.3–6.7%) compared with the oil (40–100%). This is likely due to differences in the chemical and physical nature in which inorganic elements are bound within the two types of fossil fuels. Unburned carbon and LOI values for the two bituminous coals (western Kentucky and Utah) were ~10–11 and 13–14%, respectively. While somewhat high, these values are reasonable for small research coal combustors and not too unusual even for full-scale utility boilers. Lower unburned carbon (0.5%) and LOI (2.3%) are seen for the Montana subbituminous coal and are characteristic of the behavior of lower rank coals. LOI values for the two oil conditions are very different (90 and 0%), and this behavior, again, is likely the result of differences in the heat transfer characteristics between the fire-tube boiler and refractory-lined combustor. Table 2 also indicates that, in general, coal has significantly higher trace element emissions compared with oil (uncontrolled). However, notable exceptions exist, including emissions of V, Zn, and Ni, which are 8–24 times higher from residual oil combustion compared with coal combustion.

Table 3 presents size-classified trace element concentrations as well as weight percents of unburned carbon and LOI in PM less than and greater than ~2.5 μm aerodynamic diameter. These analyses were made from the cyclone and filter catches from the dilution sampling system used to collect large quantities of PM. The data indicate that the fine PM fraction tends to be enriched in many of these trace elements compared with the coarse PM fraction, and

Table 2. PM and trace element emissions and emission rates.^a

	Western Kentucky	Montana	Utah	High Sulfur No. 6 Oil Fire-Tube Boiler	High Sulfur No. 6 Oil Refractory-Lined Combustor
Total Emissions					
PM emissions ^b (mg/m ³) standard dev.	3807 (564)	4374 (246)	4323 (374)	184 (6)	93
PM mass fraction ^c <2.5 μm	0.043	0.050	0.067	0.395	~1
PM emission factor (lb/10 ⁶ Btu) (kg/10 ⁶ J)	3.00 1.44e-3	3.30 1.58e-3	3.32 1.59e-3	0.123 5.29e-5	0.052 2.50e-5
Unburned carbon ^d (wt %)	10.2	0.5	10.9		
LOI ^d (wt %)	12.9	2.3	14.5	89.9	~0
Trace Element Emissions (mg/m³)					
Sb	0.41	0.05		0.0077	
As	0.76	0.41	0.24	0.0063	
Be	0.08	0.03		0.00009	
Cd	0.04	0.01	0.003	0.0035	
Cr	0.57	0.26	0.35	0.011	
Cu	0.33	0.40	0.30	0.170	0.200
Fe	504.75	84.87	92.98	0.740	1.200
Pb	0.11	0.27	0.06	0.089	
Mg	5.83	46.52		1.200	1.700
Mn	0.46	5.23		0.016	
Hg				<0.0022	
Ni	0.48	0.17	0.21	1.200	1.400
Na					2.100
V	1.62	0.48	0.58	9.800	12.000
Zn	2.61	0.30	0.54	3.300	3.000

Notes: ^aDry basis, concentrations corrected to standard conditions (1 atm, 293 K); ^bPM emissions for four of the five experimental conditions are based on the average of three replicate measurements, standard deviation in parentheses; ^cBased on average mass loadings determined by cascade impactors; ^dTotal PM unburned carbon and LOI values are based on the sum of weighted values determined from the dilution sampler filter and cyclone catches (see Table 3).

this enrichment seems to be more pronounced for the oil combustion experiments. In fact, it is noted that essentially all the PM for the refractory-lined combustor oil experiments was <2.5 μm in aerodynamic diameter.

Table 2 presents a comparison of the trace element emissions for the fire-tube boiler and refractory-lined combustor oil experiments. As expected, these concentrations are similar because both systems fired the same high sulfur no. 6 fuel oil. However, in contrast to the PM from the boiler, which exhibited high values for LOI ranging from 60 to 85%, blank-corrected results of filter samples from the combustor tests indicate no mass lost on ignition. The sum of the concentrations of the seven analyzed elements listed in Table 2 for the refractory-lined combustor experiments (last column) account for 21.6 mg/m³ or ~23% of the total mass emissions. However, if these elements are assumed to exist as sulfates, they then account for 67.1 mg/m³ or ~72% of the total mass emissions. In fact, XAFS spectroscopy indicated that, while a large portion (40–60%) of the sulfur measured in the fire-tube boiler PM existed as unoxidized organic sulfur (predominantly thiophenic sulfur), essentially all (99%) of the particulate-

bound sulfur in the refractory-lined combustor samples was in the form of sulfates.

Emission Factors

The measured mass concentration of 93 mg/m³ determined from the refractory-lined combustor oil experiments can be converted into an emission factor of ~10.5 lb/10³ gal. This value is comparable to the emission factor of 9.2 lb/10³ gal for no. 6 residual oil-fired boilers larger than 100 × 10⁶ Btu/hr published in AP-42.³³ This comparison lends further support to the hypothesis that the refractory-lined combustor adequately simulates the combustion environment of larger industrial and utility boilers. As reported by Miller et al.,¹⁵ the range of emission factors determined for the fire-tube boiler was approximately twice that for oil-fired utility boilers. However, dilution samples for these experiments indicate that only 30–50% of the PM mass emissions had an aerodynamic diameter <2.5 μm. Hence, the fine PM emission factor for utility boilers may well be greater than that of fire-tube boilers.

Emissions results from this study can be compared to values from the literature. Goldstein and Siegmund^{34,35}

Table 3. Trace element concentrations in emitted PM size fractions.^{a,b}

Trace Element Concentration in Ash Fraction ($\mu\text{g/g}$)	Western Kentucky		Montana		Utah		High Sulfur No. 6 Oil Fire-Tube Boiler		High Sulfur No. 6 Oil Refractory-Lined Combustor	
	<2.5 μm	>2.5 μm	<2.5 μm	>2.5 μm	<2.5 μm	>2.5 μm	<2.5 μm	>2.5 μm	<2.5 μm	>2.5 μm
Sb							48.6	8.20		
As	132	68.4	62.7	45.3	89.0	59.6	35.9	8.60		
Be							0.46	0.15		
Cd	8.7	3.3	<1.0	<1.0	<1.0	<1.0	19.3	1.84		
Cr	132	108	17.5	19.6	110	78.7	60.2	41.3		
Cu	73.5	51.9	96.7	55.6	95.8	51.5	1050	222	2346	0 ^c
Fe	76500	88300	4000	3810	16000	14400	3850	2300	13993	0
Pb	34.5	16.1	93.2	48.4	40.2	<12.3	990	94.2		
Mg							6190	2220	19989	0
Mn							73.2	42.8		
Ni	110	86.2	41.5	29.3	109	39.4	8020	2270	16518	0
S (wt %)	1.12	0.46	0.74	0.01	0.68	0.27			3.2	0
V	356	330	111	84.9	186	123	58900	19900	135718	0
Zn	548	265	141	31.9	144	40.3	21000	2740	34245	0
Unburned carbon (wt %)	11.25	8.83	0.43	0.53	12.86	9.89				
LOI (wt %)	14.96	9.96	1.69	2.79	15.68	13.98	86.6	96.9	-0	0

Notes: ^aDry basis, empty cells indicate no analysis for this element was attempted; ^b<2.5- and >2.5- μm concentrations are determined from size-classified fly ash from the dilution sampler filter and cyclone catches, respectively; ^cNo material was recovered from the cyclone catch for this condition, <2.5- μm elemental concentrations were determined from M-29 samples.

examined the effect of fuel type and combustion modifications on PM emissions from a small 37-kW (50-hp) fire-tube boiler. They report similar PM emissions of ~ 180 mg/m³ with carbon contents of up to 80% while burning a similar 2.2% sulfur no. 6 fuel oil. They also noted that efforts to increase PM burnout shift the PSD toward the submicron range. Conversely, Cheng et al.¹⁷ and Bacci et al.¹⁸ examined PM emissions from 30-MW (1×10^8 Btu/hr) and 320-MW (1×10^9 Btu/hr) fuel-oil-fired power plants, respectively. PM emissions from these units were reported to be 87 mg/m³ and 40–50 mg/m³, respectively, even though the 30-MW unit was equipped with a multicyclone PM control system.

The uncontrolled measured mass concentrations for the three coals can be converted to emission factors ranging from 1.4×10^{-3} to 1.6×10^{-3} kg/10⁶ J (3.0–3.3 lb/10⁶ Btu). Like the oil experiments, these values are also comparable to emission factors determined for these coals. AP-42³³ estimates that filterable PM emission factors for these pulverized coals from dry-bottom wall-fired and dry-bottom tangentially fired utility boilers would range from 3.3 to 5.5 lb/10⁶ Btu. This agreement is remarkable considering the difference in the scales of these units. It is important to note, however, that most utility boilers are equipped with PM control systems and that actual PM emissions from these units are dependent on particle size and the control technology used.

McElroy et al.³⁶ present particle collection efficiencies for two coal-fired units equipped with a fabric filter baghouse and an electrostatic precipitator, respectively. Their measurements indicate the baghouse produced PM collection efficiencies of >99% over the entire range of particle diameters examined (0.02–10 μm). However, PM collection efficiencies for the electrostatic precipitator were >90% for most particle diameters, and between 80 and 90% for particles between 0.1 and 0.3 μm diameter. This characteristic minimum in particle collection efficiency is typical for particles between 0.1- and 1.0- μm diameter and was also seen in the baghouse data to a lesser extent. Particles in this size range contain neither the mass (momentum) to be removed by impaction nor the high diffusion velocities necessary to migrate to collection surfaces. While most large utility boilers have some kind of PM control, smaller industrial and institutional boilers (often burning residual fuel oils) are much less likely to have such controls. Additionally, these small boilers are often located within urban airsheds.

PSDs

Figure 2 presents representative particle volume distributions for the three coals and oil combustion in the fire-tube boiler (open circles) and refractory-lined combustor (shaded circles). The inset shows more detail in the ultrafine particle size range below 0.1 μm . Together, these

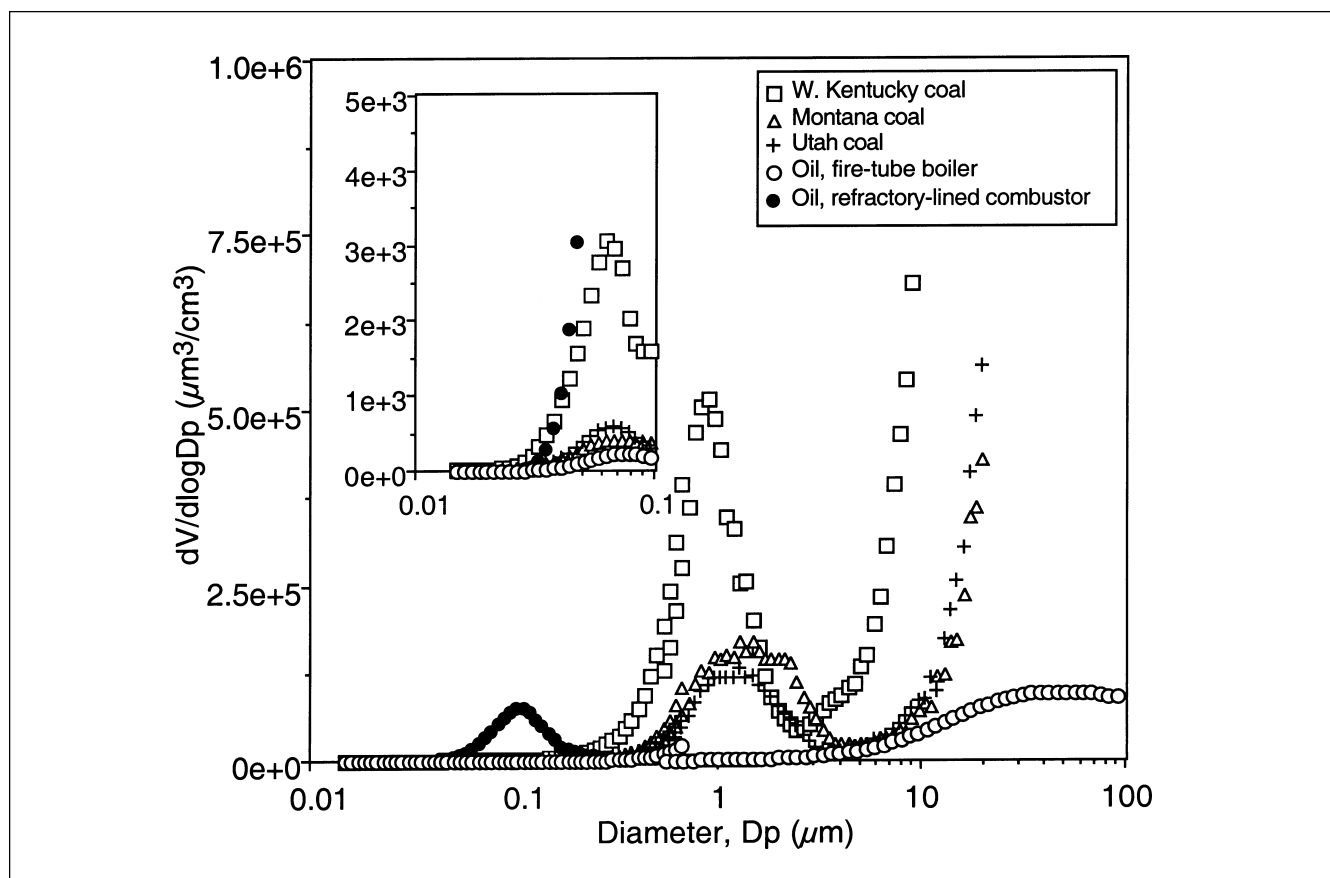


Figure 2. Measured volume PSDs. PSDs between ~ 0.01 and $1.0 \mu\text{m}$ diameter were determined by electrical mobility measurements. PSDs greater than $\sim 0.5 \mu\text{m}$ diameter were determined by light-scattering and time-of-flight measurements.

electrical mobility, time-of-flight, and light-scattering measurements span four decades of particle diameter (0.01 – $100 \mu\text{m}$). The fire-tube boiler and refractory-lined combustor oil PSDs are the same data as plotted in Miller et al.¹⁵ and Linak et al.,¹⁶ respectively. The fire-tube boiler PSDs indicate that most of the particle volume is associated with large (coarse mode) particles $>10 \mu\text{m}$ diameter. The open circle symbols in the inset show that even the fire-tube boiler produces a small accumulation mode with a mean diameter of between 0.07 and $0.08 \mu\text{m}$, but that this accumulation mode is much smaller than that for the refractory-lined furnace (shaded circles). Thus, both configurations produced an ultrafine mode, but only the fire-tube boiler produced a bimodal PSD with a very large and dominant coarse mode.

In contrast, the three coals each produce trimodal PSDs. These include small accumulation modes between 0.07 and $0.08 \mu\text{m}$, large coarse modes from 7 to $10 \mu\text{m}$, and a central mode between 0.8 and $2.0 \mu\text{m}$. Unlike the in situ light-scattering technique used during the oil tests, the APS used during the coal combustion experiments does not extend beyond $20 \mu\text{m}$. While the accumulation and coarse modes can be described by mechanisms of trace element vaporization, nucleation, and particle growth and residual ash

fragmentation, respectively, the mechanisms that produce the central mode are less clear. Model predictions^{6,7,16} indicate that coagulation of nucleated vapor cannot produce particles as large as $1\text{-}\mu\text{m}$ diameter. These particles are more likely the result of mineral inclusions that are liberated during the fragmentation and burnout of the coal char particle. This mechanism has been proposed previously to explain supermicron particle formation.³⁷

Smith et al.³⁸ proposed that the presence of cenospheres and plerospheres indicate that a bursting mechanism may be involved. They suggested that gas evolution during rapid heating causes ballooning of some large liquid ash particles. At temperatures slightly higher than that required for cenosphere formation, the viscosity of the liquid particle will be sufficiently small that the particle will burst, releasing a shower of smaller particles. Helble and Sarofim³⁹ examined the influence of fragmentation on ash PSDs. They measured a mode between 1 - and $5\text{-}\mu\text{m}$ diameter which comprised $\sim 25\%$ of the total ash mass and suggest that particles in this size range are formed by perimeter fragmentation of the char during conditions of external diffusion-controlled reaction and excess air.

Baxter⁴⁰ also developed a char fragmentation model to predict fly ash PSDs ($>0.6 \mu\text{m}$ diameter) during pulverized

coal combustion. Results indicate that the fly ash PSD is sensitive to both the extent and mechanism of fragmentation. For high rank coals, more fly ash particles of ~2- and 15- μm diameter are produced as a result of fragmentation than any other sizes, and predicted PSDs indicate modes at ~2 and 15 μm , which are qualitatively consistent with those presented in Figure 2. The model also predicts that fragmentation is much less important for lignite fuels. Previous reports of trimodal PSDs for coal fly ash are somewhat limited, and may be a consequence of limited ranges of particle diameters examined, improved resolution of current instrumentation, and field data taken downstream of PM control devices, which are very effective in controlling larger particles. McElroy et al.³⁶ present composite impactor PSDs from a small 25-MW coal-fired boiler. Their PSDs indicate modes at ~0.08-, 2-, and >10- μm diameter comparable to those presented in Figure 2. More recently, Seames and Wendt⁴¹ have also seen evidence of trimodal PSDs during combustion of an Illinois no. 6 bituminous coal in an uncontrolled laboratory-scale combustor using a low-pressure impactor.

The bimodal PSDs seen for the oil experiments are consistent with a mechanism of metal vaporization/nucleation/coagulation/condensation and incomplete burnout of residual fuel cenospheres.^{15,16} SEM images of oil char collected from the fire-tube boiler showed a sponge-like morphology that clearly suggests swelling and extensive pore formation. In general, the extent of ash (metal) vaporization is dependent on carbon burnout. For incomplete combustion, a substantial fraction of the trace metals remain trapped in the unburned char particles, and never escape into the vapor phase. However, as the combustion gases cool, those metals that have vaporized will condense on existing surfaces or, if supersaturation partial pressures are large enough, will nucleate to form new particles. The distinctive submicron peak (between 0.07- and 0.08- μm diameter) is clearly indicative of particles formed by nucleation, coagulation, and condensation of materials that have vaporized. Thus, when large portions of the metal constituents fail to vaporize (open circles), the accumulation mode will be much smaller than when they do vaporize (shaded circles).

The refractory-lined combustor volume PSD (shaded circles) consists exclusively of a narrow submicron accumulation mode with a mean diameter of ~0.1 μm , and both light-scattering measurements and the lack of any cyclone catch containing gray or black particles with measurable LOI support this. Clearly, as the oil char is consumed, the metals have vaporized almost completely and have subsequently nucleated and grown to form the distinctive accumulation mode shown in Figure 2. Comparison between the areas under the submicron volume PSD for the two types of equipment suggests that, while

only a very small fraction (<1%) of the metal trace elements are vaporized in the fire-tube boiler, well over 99% of these constituents vaporize in the refractory-lined combustor.

In contrast to residual oils whose ash is almost exclusively bound inherently within the organic molecular structure, very little coal ash is inherently bound. Rather, large fractions of ash components in coal are present as mineral inclusions within the coal particles or as excluded materials, either liberated inclusions during the grinding process or extraneous material collected during mining.⁶ As a result, the nature and behavior of coal ash is very different compared with oil. Coal refractory elements, including Al, Ca, and Si, are not easily vaporized and can act to bind otherwise volatile species. Typically, large fractions of coal ash remain in the coarse size fractions with only very small amounts (<1%) vaporizing to produce the accumulation mode. However, the central mode near 1- μm diameter (see Figure 2) indicates that fine PM (including transition metals) may be produced from coal combustion by mechanisms other than vaporization. Interactions between alkali metals and Al- and Si-containing species in coal have been studied by Gallagher et al.,⁴² who examined such processes for Na and K with implications for understanding and controlling boiler fouling processes. Additionally, several studies have purposely introduced Al-, Ca-, and Si-based compounds to adsorb toxic trace elements, including Pb and Cd, in waste incineration processes.^{26,43,44}

Figure 3 presents mass distribution data for the three coals determined by gravimetric analysis of in-stack and extractive low-pressure cascade impactors. While not as resolved or sensitive as the electronic measurements presented in Figure 2, these data indicate the same qualitative information, including a large coarse mode from 8 to 10 μm and a central mode between 1 and 5 μm . Figure 4 presents the elemental mass fraction distributions of several selected transition metals determined by XRF analysis from a set of MOUDI samples for the western Kentucky coal. These mass fraction data have been normalized by $d\log D_p$ to correct for differences in cut-off diameters that might otherwise skew the distribution. However, as a result of this normalization, the data from the first (>10 μm) and last stages (<0.056 μm) are lost. Figure 4 indicates that the trace element mass fraction distributions have the same qualitative behavior as the western Kentucky volume distribution presented in Figure 2; that is, a small accumulation mode ~0.1 μm and a central mode ~1 μm . The data also indicate that transition metals comprise a portion of the fine PM produced during coal combustion. These elemental PSDs (Figure 4) are also qualitatively similar to those presented by Kauppinen and Pakkanen⁴⁵ from a utility-scale pulverized coal boiler burning a Polish

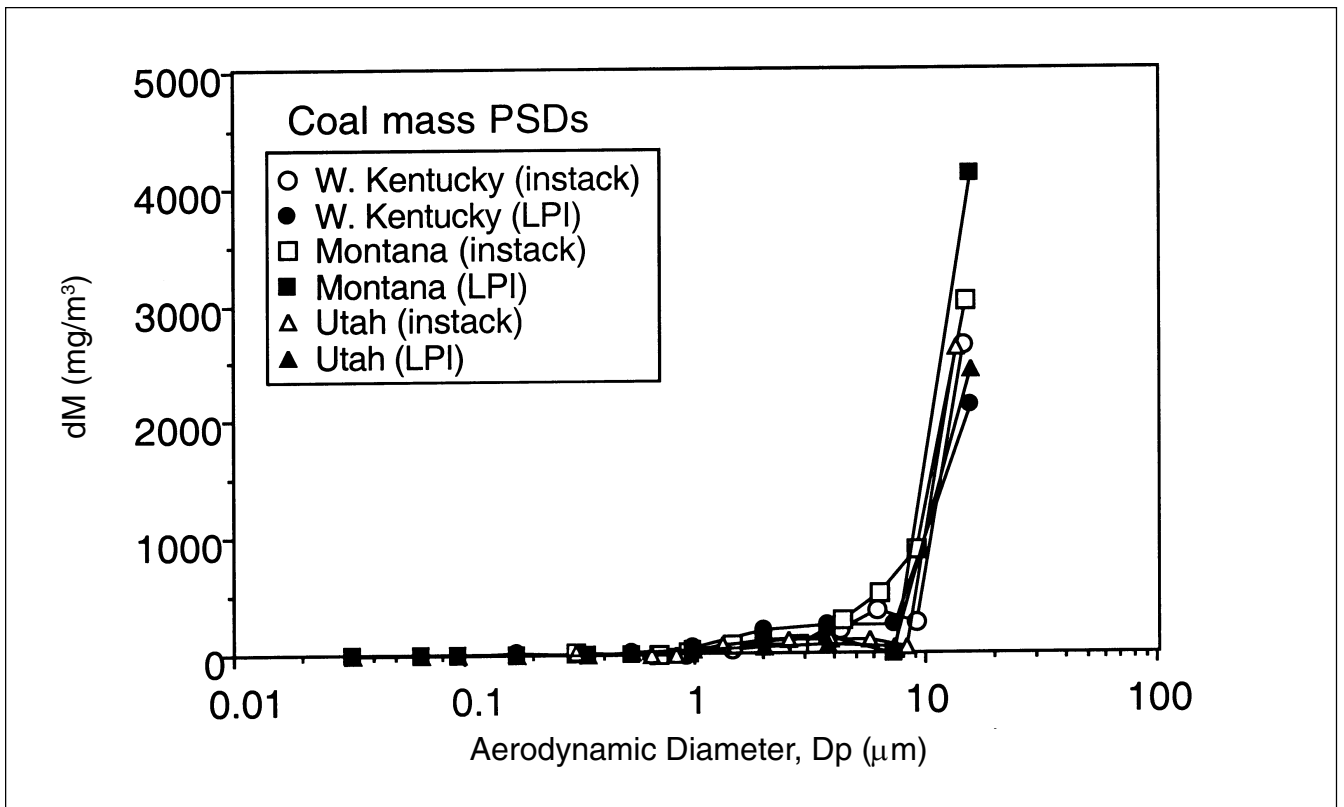


Figure 3. Measured coal mass PSDs.

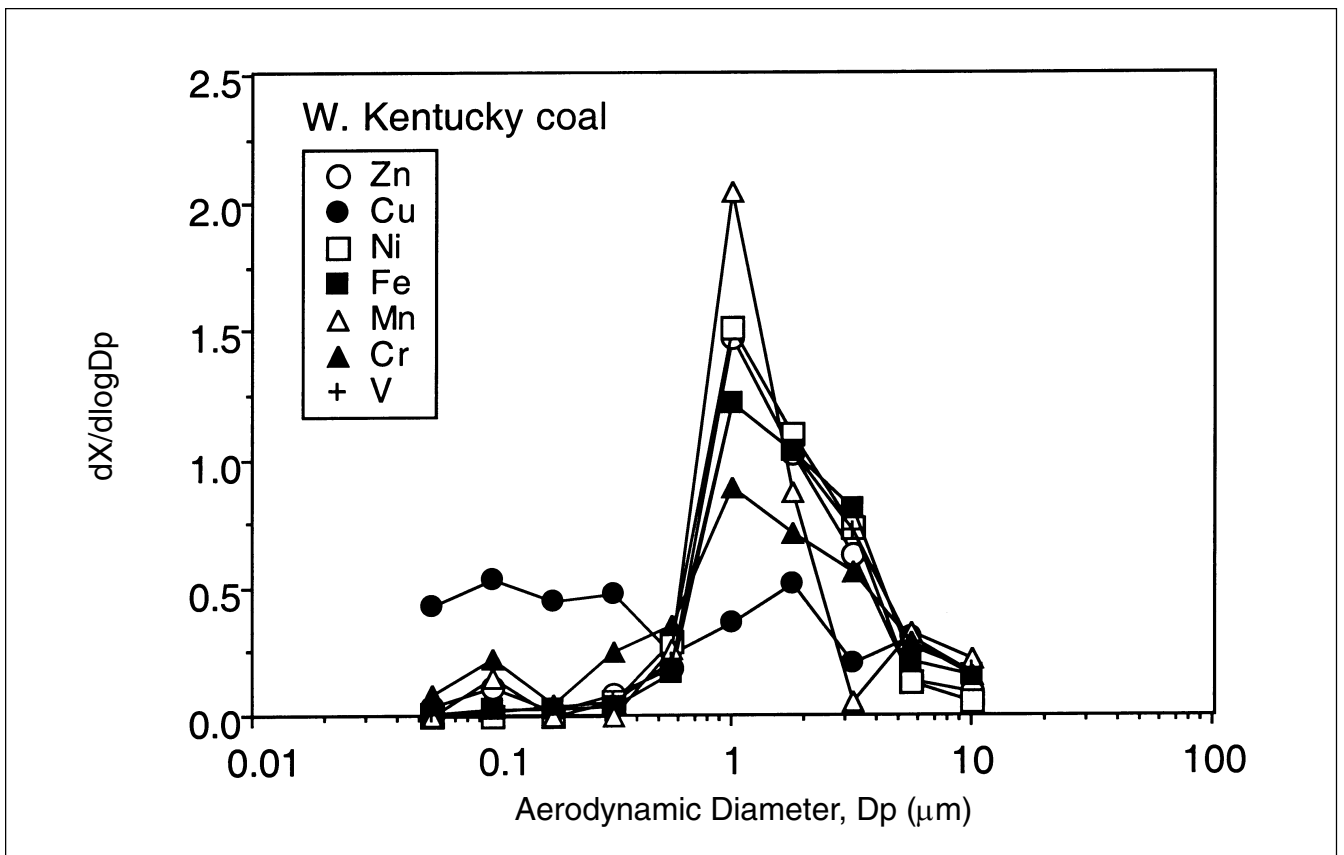


Figure 4. Elemental PSDs for the western Kentucky coal.

coal. Their measurements, taken downstream of the electrostatic precipitator, indicate total mass emissions of 24.3 mg/Nm³, of which 1.2 mg/Nm³ (~5%) was comprised of the transition metals Zn, Cu, Ni, Fe, Mn, and V (Cr was not measured).

Successive Leaching

Based on the hypothesis that soluble forms of transition metals may play important roles in the mechanisms resulting in adverse health effects, research was initiated to examine and compare the relative solubility of these elements from different fly ash matrices. This approach, based on a procedure of successively leaching fly ash samples with acids of increasing strength, was briefly described earlier and remains under development. The intent is to compare the relative solubility of these metals from different ash matrices to various health effect end points determined for the same ash samples by colleagues within EPA's National Health and Environmental Effects Research Laboratory. Figure 5 presents results comparing the relative solubility of five transition metals from the PM_{2.5} fraction of fly ash samples from the residual fuel oil and the three coals examined to date. Note, however, that the residual fuel oil fly ash used for these analyses was collected from a third in-house liquid fuel combustor designed to simulate a water-wall package boiler. These samples were collected during a test campaign to examine the combustion characteristics of an Orimulsion fuel and compare its emissions to those of a residual fuel oil.⁴⁶ Nonetheless, the package boiler simulator produced fly ash with 38% LOI. This value is higher than that for the refractory-lined combustor, but notably lower than that of the fire-tube boiler (see Table 2), and is consistent with the moderate heat transfer and quench rates associated with this boiler design.

Figure 5 indicates that several of the transition metals associated with the PM_{2.5} ROFA are readily soluble even in water, but these same metals are relatively insoluble from each of the three PM_{2.5} coal fly ash samples. The data indicate that, compared to the oil fly ash sample, strong acids are necessary to dissociate these metals from the coal fly ash. Another interesting result seen in Figure 5 is that not all of the transition metals have similar solubilities in each of the acids. The residual oil data show Ni is almost completely soluble in water, while V and Cu are partially soluble and Zn and Fe are only minimally soluble. Stronger acids are necessary to dissolve these elements. This may be related to the nature of the trace element speciation with the fly ash and may influence the potential bioavailability of the transition metal. The relative insolubility of these metals from the coal fly ashes is likely the result of the mineral nature of coal ash and large quantities of Si, Al, and Ca that are known to interact with trace metals to form relatively insoluble alumina, silica,

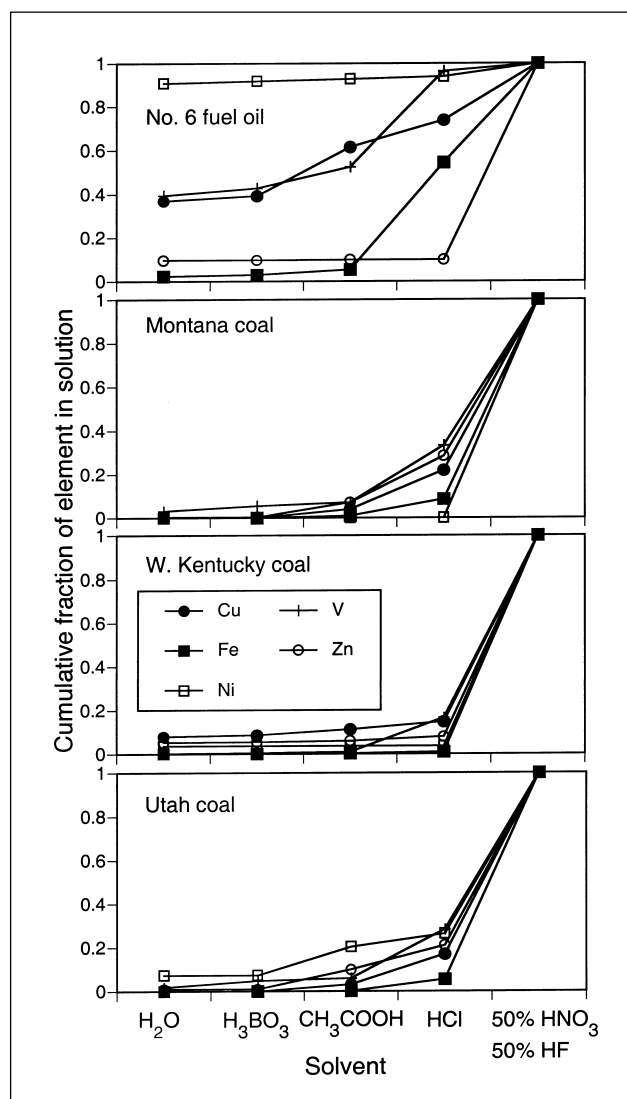


Figure 5. Elemental solubility by successive leaching of PM_{2.5} fly ash.

and calcium complexes. It should be re-emphasized that this leaching process is only intended to determine the relative solubility of different trace elements in different ash matrices. It is not intended to simulate any actual in vivo process. Other work has shown that transition metal mobility may be increased by the presence of organic chelating compounds.^{47,48}

CONCLUSIONS

Fine particle emissions from residual fuel oil and pulverized coal combustion were examined and compared. A laboratory-scale refractory-lined combustor, which was shown to simulate combustion conditions of a large utility residual oil-fired boiler (as far as particulate emission factors were concerned), produced fly ash particles with an essentially unimodal PSD with a mean diameter of ~0.1 μm. Conversely, a pilot-scale fire-tube package boiler produced particles with a weak bimodal size distribution,

which included a small fraction (~0.2%) of the mass with particle diameters below 0.1 μm and a large fraction (~99.8%) of the mass with particle diameters between 0.5 and 100 μm . Here the large particles were shown to consist of large porous carbonaceous cenospheres resulting from poor carbon burnout, a characteristic not uncommon for that class of equipment. Although the total particulate mass concentrations in the flue gas of the refractory-lined combustor were less than half those of the fire-tube boiler, ultrafine particle concentrations of the refractory-lined combustor were notably larger than those measured for the fire-tube boiler. Volume PSDs obtained from two independent particle-sizing instruments were, with only a few very reasonable assumptions, consistent with independently measured total mass emission rates for both equipment types.

Three pulverized coals burned in a laboratory-scale down-fired combustor produced trimodal PSDs. Uncontrolled mass emissions for these coals were over 20 times higher than those for the residual fuel oil. However, most of this mass contributes to a large coarse mode with only 4–7% of this mass associated with $\text{PM}_{2.5}$.

The results presented here provide insight into mechanisms of fine particle formation from residual oil and pulverized coal combustion. For the refractory-lined combustor burning residual oil, where very few large particles were formed, the PSD was nearly unimodal with a mean diameter of ~0.1 μm . These particles were composed primarily of trace species containing Cu, Fe, Ni, V, Zn, and S. Additionally, these particles contained very little carbon (based on LOI), and the particulate-bound sulfur was speciated almost exclusively as sulfates. The weak bimodal behavior of the PM generated by residual oil combustion in the fire-tube boiler produced a fine mode (composed predominantly of metals and sulfur) with a mean diameter of ~0.7–0.8 μm , and a broad coarse mode (comprised primarily of char) with a mean diameter of ~40–50 μm . Both of these types of behavior provide circumstantial evidence for a mechanism of fine particle formation from residual oil combustion. Commonly considered nonvolatile metals are likely released into the gas phase during the last stages of carbon burnout, and because of incomplete carbon burnout, the accumulation mode for particles formed from vapor nucleation was very small for the fire-tube boiler. For the refractory-lined combustor, where char burnout was nearly complete, most of the nonvolatile metals were released into the gas phase.

For the coal experiments, the unburned carbon and LOI ranged from 0.5 to 11.0% and 2.0 to 15%, respectively. While slightly high, these values are not atypical of many utility-scale boilers. The coal PSDs indicate a small accumulation mode ~0.1- μm diameter and a large coarse mode beginning ~10- μm diameter. Similar to the oil PSDs,

these modes are consistent with mechanisms involving gas-to-particle formation and growth and residual inorganic ash remaining after char burnout. However, unlike the oil PSDs, the coal data indicate a third central mode between 0.8- and 2.0- μm diameter. Particles of this size are too large to be the result of gas-to-particle growth processes, and are more likely the consequence of micron-scale mineral inclusions liberated during char fragmentation and burnout. This provides a mechanism for refractory transition metals to contribute to $\text{PM}_{2.5}$ without the necessity of passing through a vapor phase.

Successive leaching of the $\text{PM}_{2.5}$ fly ash from the different fuels may prove to be a useful technique to provide insight into mechanisms controlling elemental speciation, partitioning, and bioavailability. Preliminary results using five acidic solvents of increasing strengths indicate that five transition metals associated with coal are relatively insoluble in all but the most aggressive acids. Conversely, several of these metals associated with ROFA were readily or partially water-soluble. These results may have important implications in the determination of what particle characteristics play significant roles in causal mechanisms of pulmonary damage associated with exposure to fine PM.

ACKNOWLEDGMENTS/DISCLAIMER

Portions of this work were conducted under EPA P.O. OC-R0930NASA with J.O.L. Wendt and EPA Contract 68-C-99-201 with ARCADIS Geraghty & Miller. The authors gratefully acknowledge the contributions of C. King, D. Santoianni, D. Tabor, and J. Medlin of ARCADIS Geraghty & Miller to the experimental efforts, and of S. Wasson of the EPA Air Pollution Prevention and Control Division (APPCD) for analytical support. The research described in this article has been reviewed by the APPCD-EPA and approved for publication. The contents of this article should not be construed to represent Agency policy nor does mention of trade names or commercial products constitute endorsement or recommendation for use.

REFERENCES

1. *Particles in Our Air: Concentrations and Health Effects*; Wilson, R., Spengler, J.D., Eds.; Harvard University Press: Cambridge, MA, 1996.
2. *National Ambient Air Quality Standards for Particulate Matter: Proposed Decision*; 40 CFR, Part 50; U.S. Environmental Protection Agency; U.S. Government Printing Office: Washington, DC, 1996.
3. Bachmann, J.D.; Damberg, R.J.; Caldwell, J.C.; Edwards, C.; Koman, P.D. *Review of the National Ambient Air Quality Standards for Particulate Matter: Policy Assessment of Scientific and Technical Information*; EPA-452/R-96-013 (NTIS PB97-115406); U.S. Environmental Protection Agency; Office of Air Quality Planning and Standards: Research Triangle Park, NC, 1996.
4. Wolff, G.T. *Closure by the Clean Air Scientific Advisory Committee (CASAC) on the Staff Paper for Particulate Matter*; EPA-SAB-CASAC-LTR-96-008; Science Advisory Board: Washington, DC, June 1996.
5. *Fed. Regist.* 62 FR 38652, July 1997.
6. Linak, W.P.; Wendt, J.O.L. Toxic Metal Emissions from Incineration: Mechanisms and Control; *Prog. Energy Combust. Sci.* 1993, 19, 145-185.
7. Linak, W.P.; Wendt, J.O.L. Trace Metal Transformation Mechanisms During Coal Combustion; *Fuel Process. Technol.* 1994, 39, 173-198.
8. *Review of EPA's Particulate Matter Research Program*; National Research Council; National Academy Press: Washington, DC, 1998.

9. Dreher, K.; Costa, D.; Hoffman, A.; Bonner, J.; Osornio-Vargas, A. Pulmonary Toxicity of Urban Air Particulate Matter (PM). Presented at the A&WMA Meeting on Measurement of Toxic and Related Air Pollutants, Research Triangle Park, NC, May 1996.
10. Dreher, K.; Jaskot, R.; Richards, J.H.; Lehmann, J.R.; Winsett, D.; Hoffman, A.; Costa, D. Acute Pulmonary Toxicity of Size-Fractionated Ambient Air Particulate Matter; *Am. J. Respir. Crit. Care Med.* **1996**, *153*(4), A15.
11. Dreher, K.; Jaskot, R.; Lehmann, J.R.; Richards, J.H.; McGee, J.K.; Ghio, A.J.; Costa, D.L. Soluble Transition Metals Mediate Residual Oil Fly Ash Induced Lung Injury; *J. Toxicol. Environ. Health* **1997**, *50*, 285-305.
12. *Fuel Oil and Kerosene Sales 1997*; DOE/EIA-0535(97); Energy Information Administration; U.S. Department of Energy: Washington, DC, 1998.
13. Dockery, D.W.; Pope, C.A.; Xu, X.; Spengler, J.D.; Ware, J.H.; Fay, M.E.; Ferris, B.G.; Speizer, F.E. An Association between Air Pollution and Mortality in Six U.S. Cities; *N. Engl. J. Med.* **1993**, *329*, 1753-1759.
14. Nizich, S.V.; Pope, C.A. *National Air Pollutant Emission Trends Update: 1970-1997*; EPA-454/E-98-007; U.S. Environmental Protection Agency; Office of Air Quality Planning and Standards: Research Triangle Park, NC, December 1998.
15. Miller, C.A.; Linak, W.P.; King, C.; Wendt, J.O.L. Fine Particle Emissions from Heavy Fuel Oil Combustion in a Firetube Package Boiler; *Combust. Sci. Technol.* **1998**, *134*, 477-502.
16. Linak, W.P.; Miller, C.A.; Wendt, J.O.L. Fine Particle Emissions from Residual Fuel Oil Combustion: Characterization and Mechanisms of Formation; *Proceedings of the Combustion Institute*; in press.
17. Cheng, R.J.; Mohnen, V.A.; Shen, T.T.; Current, M.; Hudson, J.B. Characterization of Particulates from Power Plants; *J. Air Pollut. Control Assoc.* **1976**, *26*(8), 787-790.
18. Bacci, P.; Del Monte, M.; Longhetto, A.; Piano, A.; Prodi, F.; Redaelli, P.; Sabbioni, C.; Ventura, A. Characterization of the Particulate Emission by a Large Oil Fuel Fired Power Plant; *J. Aerosol Sci.* **1983**, *14*(4), 557-572.
19. Snow, G.C.; Lorrain, J.M. *Evaluation of Innovative Combustion Technology for Simultaneous Control of SO_x and NO_x*; EPA-600/2-87-032 (NTIS PB 87-188926); U.S. Environmental Protection Agency; Air and Energy Engineering Research Laboratory: Research Triangle Park, NC, 1987.
20. Garg, S. EPA Method 0060-Methodology for the Determination of Metals Emissions in Exhaust Gases from Hazardous Waste Incineration and Similar Combustion Processes. In *Methods Manual for Compliance with the BIF Regulations: Burning Hazardous Waste in Boilers and Industrial Furnaces*; EPA/530-SW-91-010 (NTIS PB91-120006); U.S. Environmental Protection Agency; Office of Solid Waste and Emergency Response: Washington, DC, 1990; pp 3-1 to 3-48.
21. *U.S. EPA Test Method 1A-Sample and Velocity Traverses for Stationary Sources with Small Stacks or Ducts*; 40 CFR Part 60, Appendix A; Government Institutes Inc.: Rockville, MD, 1994.
22. *U.S. EPA Test Method 5-Determination of Particulate Emissions from Stationary Sources*; 40 CFR Part 60, Appendix A; Government Institutes Inc.: Rockville, MD, 1994.
23. Galbreath, K.C.; Zygarlicke, C.J.; Huggins, F.E.; Huffman, G.P.; Wong, J.L. Chemical Speciation of Nickel in Residual Oil Ash; *Energy Fuels* **1998**, *12*, 818-822.
24. Galbreath, K.C.; Zygarlicke, C.J.; Toman, D.L.; Huggins, F.E.; Huffman, G.P. Nickel and Chromium Speciation of Residual Oil Combustion Ash; *Combust. Sci. Technol.* **1998**, *134*, 243-262.
25. Huggins, F.E.; Huffman, G.P.; Robinson, J.D. Speciation of Elements in NIST Particulate Matter SRMs 1648 and 1650; *J. Hazard. Mater.* **2000**, *74*, 1-23.
26. Scotto, M.A.; Peterson, T.W.; Wendt, J.O.L. Hazardous Waste Incineration: The In Situ Capture of Lead by Sorbents in a Laboratory Down-Flow Combustor; *Proceedings of the Combustion Institute*; **1992**, *24*, 1109-1118.
27. Linak, W.P.; Srivastava, R.K.; Wendt, J.O.L. Metal Aerosol Formation in a Laboratory Swirl Flame Incinerator; *Combust. Sci. Technol.* **1994**, *101*(1-6), 7-27.
28. Hillamo, R.E.; Kauppinen, E.I. On the Performance of the Berner Low Pressure Impactor; *Aerosol Sci. Technol.* **1993**, *14*, 33-47.
29. Steele, W.J.; Williamson, A.D.; McCain, J.D. *Construction and Operation of a 10 cfm Sampling System with a 10:1 Dilution Ratio for Measuring Condensable Emissions*; EPA/600-8-88-069 (NTIS PB88-198551); U.S. Environmental Protection Agency; Air and Energy Engineering Research Laboratory: Research Triangle Park, NC, 1988.
30. U.S. EPA Test Method 3050B. In *Test Methods for Evaluating Solid Waste*; EPA-SW-846; U.S. Environmental Protection Agency: Washington, DC, December 1996; Vol 1A. CD-ROM Version 3, Revision 2, <http://www.epa.gov/epaoswer/hazwaste/test/3xxx.htm>.
31. Hardesty, D.R.; Pohl, J.H. *The Combustion of Pulverized Coals-An Assessment of Research Needs*; National Bureau of Standards Special Publication No. 561; National Bureau of Standards: Washington, DC, 1979; pp 1407-1415.
32. Walsh, P.M.; Rovesti, W.C.; Fangmeier, B.A.; Markoja, R.L.; Brown, J.P.; Hopkins, K.C.; Lange, H.B.; Freeman, R.F.; Olen, K.R.; Washington, K.T.; Partick, S.T.; Campbell, G.L.; Harper, D.S.; Teetz, R.D.; Bennett, T.E.; Moore, S.P. Size Distribution of Metals in Particulate Matter Formed During Combustion of Residual Fuel Oil. In *Proceedings of the Electric Power Research Institute 1993 Fuel Oil Utilization Workshop*; EPRI TR-103990, Section 3; Electric Power Research Institute: Palo Alto, CA, 1994; pp 132-149.
33. *Compilation of Air Pollutant Emission Factors*; Vol. 2: Stationary Point and Area Sources, 5th ed.; AP-42; U.S. Environmental Protection Agency; Office of Air Quality Planning and Standards: Research Triangle Park, NC, November 1996.
34. Goldstein H.L.; Siegmund, C.W. Influence of Heavy Fuel Oil Composition and Boiler Combustion Conditions on Particulate Emissions; *Environ. Sci. Technol.* **1976**, *10*(12), 1109-1114.
35. Goldstein H.L.; Siegmund, C.W. Particle Emissions from Residual Fuel Fired Boilers: Influence of Combustion Modifications; *J. Eng. Power* **1977**, *371*-377.
36. McElroy, M.W.; Carr, R.C.; Ensor, D.S.; Markowski, G.R. Size Distribution of Fine Particles from Coal Combustion; *Science* **1982**, *215*(4528), 13-19.
37. Flagan, R.C.; Friedlander, S.K. Particle Formation in Pulverized Coal Combustion-A Review. In *Recent Developments in Aerosol Science*; Shaw, D.T., Ed.; John Wiley & Sons: New York, 1978; pp 25-57.
38. Smith, R.D.; Campbell, J.A.; Nielson, K.K. Characterization and Formation of Submicron Particles in Coal-Fired Plants; *Atmos. Environ.* **1979**, *13*, 607-617.
39. Helble, J.J.; Sarofim, A.F. Influence of Char Fragmentation on Ash Particle Size Distributions; *Combust. Flame* **1989**, *76*, 183-196.
40. Baxter, L.L. Char Fragmentation and Fly Ash Formation During Pulverized-Coal Combustion; *Combust. Flame* **1992**, *90*, 174-184.
41. Seames, W.S.; Wendt, J.O.L. Partitioning of Arsenic, Selenium, and Cadmium during the Combustion of Pittsburgh and Illinois #6 Coals in a Self-Sustained Combustor; *Fuel Process. Technol.*, in press.
42. Gallagher, N.B.; Peterson, T.W.; Wendt, J.O.L. Sodium Partitioning in a Pulverized Coal Combustion Environment; *Proceedings of the Combustion Institute*, **1996**, *26*, 3197-3204.
43. Linak, W.P.; Srivastava, R.K.; Wendt, J.O.L. Sorbent Capture of Nickel, Lead, and Cadmium in a Laboratory, Swirl Flame Incinerator; *Combust. Flame* **1995**, *100*, 241-250.
44. Davis, S.B.; Wendt, J.O.L. Mechanism and Kinetics of Lead Capture by Kaolinite in a Downflow Combustor; *Proceedings of the Combustion Institute*, in press.
45. Kauppinen, E.I.; Pakkanen, T.A. Coal Combustion Aerosols: A Field Study; *Environ. Sci. Technol.* **1990**, *12*, 1811-1818.
46. Miller, C.A.; Linak, W.P. The Influence of Carbon Burnout on Submicron Particle Formation from Emulsified Fuel Oil Combustion; *Fuel*, submitted for publication, 2000.
47. Ghio, A.J.; Stonehurner, J.; Pritchard, R.J.; Piantadosi, C.A.; Quigley, D.R.; Dreher, K.L.; Costa, D.L. Humic-Like Substances in Air Pollution Particles Correlate with Concentrations of Transition Metals and Oxidant Generation; *Inhalation Toxicol.* **1996**, *8*, 479-494.
48. Smith, K.R.; Veranth, J.M.; Lighty, J.S.; Aust, A.E. Mobilization of Iron from Coal Fly Ash Was Dependent Upon the Particle Size and the Source of Coal; *Chem. Res. Toxicol.* **1998**, *11*, 1494-1500.

About the Authors

Dr. William P. Linak and Dr. C. Andrew Miller are principal investigators and senior project engineers with the Air Pollution Technology Branch of the EPA's National Risk Management Research Laboratory. Dr. Jost O.L. Wendt is professor and head of the Department of Chemical and Environmental Engineering at the University of Arizona. Correspondence should be sent to W.P. Linak at the U.S. Environmental Protection Agency, Air Pollution Technology Branch (MD-65), Research Triangle Park, NC 27711, or to linak.bill@epa.gov.

EX 4

Combustion Aerosols: Factors Governing Their Size and Composition and Implications to Human Health

JoAnn Slama Lighty, John M. Veranth, and Adel F. Sarofim

Department of Chemical and Fuels Engineering, University of Utah, Salt Lake City

ABSTRACT

Particulate matter (PM) emissions from stationary combustion sources burning coal, fuel oil, biomass, and waste, and PM from internal combustion (IC) engines burning gasoline and diesel, are a significant source of primary particles smaller than $2.5\ \mu\text{m}$ ($\text{PM}_{2.5}$) in urban areas. Combustion-generated particles are generally smaller than geologically produced dust and have unique chemical composition and morphology. The fundamental processes affecting formation of combustion PM and the emission characteristics of important applications are reviewed. Particles containing transition metals, ultrafine particles, and soot are emphasized because these types of particles have been studied extensively, and their emissions are controlled by the fuel composition and the oxidant-temperature-mixing history from the flame to the stack. There is a need for better integration of the combustion, air pollution control, atmospheric chemistry, and inhalation health research communities. Epidemiology has demonstrated that susceptible individuals are being harmed by ambient PM. Particle surface area, number of ultrafine particles, bioavailable transition metals, polycyclic aromatic hydrocarbons (PAH), and other particle-bound organic compounds are suspected to be more important than particle mass in determining the effects of air pollution. Time- and size-resolved PM measurements are needed for testing mechanistic toxicological hypotheses, for characterizing the relationship between combustion operating conditions and transient emissions, and for source apportionment studies to develop air quality plans. Citations are provided to more specialized reviews, and the concluding comments make suggestions for further research.

INTRODUCTION

Combustion of coal, biomass, and petroleum-based fuels generates particulate matter (PM) ranging from millimeter-sized cinders and soot aggregates to ultrafine nucleation-mode primary particles only a few nanometers in diameter. The largest particles are removed in the combustion zone as bottom ash or wall deposits, or are collected in the

post-combustion gas cleaning devices. The smaller particles travel with the combustion exhaust gas and contribute to ambient air pollution on both the urban and regional scale. Epidemiologic studies reported a correlation between adverse health effects and increases in ambient particulate concentration, even when the mass concentration was below the then-current air quality standards. This correlation motivated a call for stricter air quality regulations even though a toxicological mechanism linking small increases in ambient PM and biological responses is still unavailable. Particles smaller than $2.5\ \mu\text{m}$ ($\text{PM}_{2.5}$) consist of the tail of the coarse-mode particle size distribution generated by mechanical processes and finer particles that are formed from gas-phase precursors by nucleation, condensation, and surface reaction on other particles, followed by particle growth from coagulation and other transformations in the atmosphere.

This review focuses on the submicron inorganic ash and soot produced by practical combustion systems because the processes by which these particles are produced have been extensively studied over the three decades since the passage of the U.S. Clean Air Act. Metal-enriched ash, soot, and ultrafine particles remain a concern for combustion researchers because these particles have been the focus of mechanistic toxicological hypotheses. Fundamental relationships are presented to show how the primary combustion particle size, morphology, and composition are determined by combustion conditions and the post-flame cool down. The implications of these fundamental relationships are illustrated by descriptions of the results of particle characterization studies from specific combustion applications. The relationships between the ability to measure particle characteristics, both at sources and in the atmosphere, the development of health effects hypotheses, and the development of regulations will be discussed. Examples illustrate recent progress and suggest areas for further work.

The epidemiology and toxicology of ambient PM is an active area of research. Recently, efforts in finding the causes of adverse health effects of particles have intensified.

Accumulating evidence suggests that mass concentration is not the most appropriate measure of potential health effects,¹ and that health studies need to consider other characteristics, such as particle number, particle morphology, and detailed chemical speciation.²⁻⁴ The active toxicological hypotheses have been summarized into the following groups.⁵ Some of these, such as mass, are listed based on the epidemiologic studies; others because there are known causal relations with health. There is no hierarchy to the listing.

- (1) *PM Mass Concentration*. The initial epidemiologic studies correlated effects with mass as measured by ambient monitoring procedures. The mass concentration of individual chemical species in PM represents the maximum possible dose.
- (2) *PM Particle Size/Surface Area*. Stronger associations are seen with fine particle mass, and the body interacts with the surface of an insoluble particle, not with the volume.
- (3) *Ultrafine PM*. Particles smaller than 0.1 μm dominate the total number of particles in urban aerosols. Ultrafine particles are deposited deep in the lung by diffusion and can enter the body through the layer of cells lining the alveoli (air sacks) of the lung.
- (4) *Metals*. Transition metals including Fe, V, Cu, and Ni act as catalysts in the formation of reactive oxygen species (ROS) and are associated with the activation of many biochemical processes.
- (5) *Acids*. Inhalation studies have shown toxic responses that are associated with the amount of H^+ delivered to respiratory surfaces.
- (6) *Organic Compounds*. Volatile and semi-volatile organic chemicals associated with particles can act as irritants and allergens. Many aromatic compounds are suspected mutagens or carcinogens and may have acute effects as well.
- (7) *Biogenic Particles*. Pollen, spores, and proteins are known allergens. Ambient PM also includes viable bacteria and viruses, biologically generated toxins, and natural organic aerosols. Most pollen is larger than 10 μm , spores are typically 2–10 μm , bacteria are 0.5–20 μm , and viruses are submicron particles.
- (8) *Salt and Secondary Aerosols*. Soluble salts formed by ocean spray and by gas-to-particle conversion are thought to be relatively benign. However, since secondary aerosols form a large part of the aerosol mass, the resulting particle mass is indirectly implicated by epidemiologic studies.
- (9) *Peroxides*. Ambient peroxides associated with particles may be transported into the lung and may cause oxidant injury.

(10) *Soot*. Carbon black, a surrogate for elemental carbon (EC) in soot, causes tissue irritation and the release of toxic chemical intermediates from scavenger cells in laboratory studies. Soot particles also act as carriers for the organic compounds mentioned in hypothesis 6.

(11) *Cofactors*. The combination of two or more pollutants may cause greater or different effects than the individual pollutants acting separately.

Many of these particle classes or characteristics directly or indirectly involve combustion emissions. This review will emphasize particles containing transition metals, ultrafine particles, and soot because the formation of these types of particles during combustion can be explained by the oxidant-temperature-mixing history of the combustion and gas cleaning processes.

Figure 1 illustrates the main topics covered in this review. An overview of the fundamentals of particle formation in combustion, using coal combustion as a well-studied example, is followed by a discussion of the differences between the PM exiting the combustor and the emissions to the atmosphere. The PM emission characteristics from practical combustion applications, including chemical composition and size distribution, will be reviewed to identify sources of available data. The relationship between specific characteristics of combustion-generated particles and recent work in PM epidemiology, toxicology, and cell biology will be summarized to show the interaction between combustion engineering and the life sciences in addressing questions of public importance. Next, the current U.S. regulations regarding ambient PM will be discussed since the regulatory timetable is driving the need for parallel advances in both health- and engineering-related research. The particles emitted to the atmosphere differ from the particles created in combustion because of size-selective removal and other transformations in any air pollution control devices (APCDs), and examples will be given of studies that have integrated between the combustion and atmospheric emissions research communities. Finally, the need for advances in the ability to conduct time-, size-, and chemically-resolved investigations of fine particles both at combustion sources and in the ambient air will be discussed to illustrate how health studies, air pollution regulations, and control technology all depend on advances in what can be measured.

This paper will focus on the $\text{PM}_{2.5}$, PM_{10} , and ultrafine particles that are emitted as solids from mobile and stationary combustion sources. While combustion emissions of nitrogen and sulfur oxides are of importance from the standpoint of secondary particle formation (nitrates and sulfates), these gas-phase emissions and the subsequent atmospheric transformations will not be discussed. Post-combustion gas cleaning, atmospheric chemistry, and airway

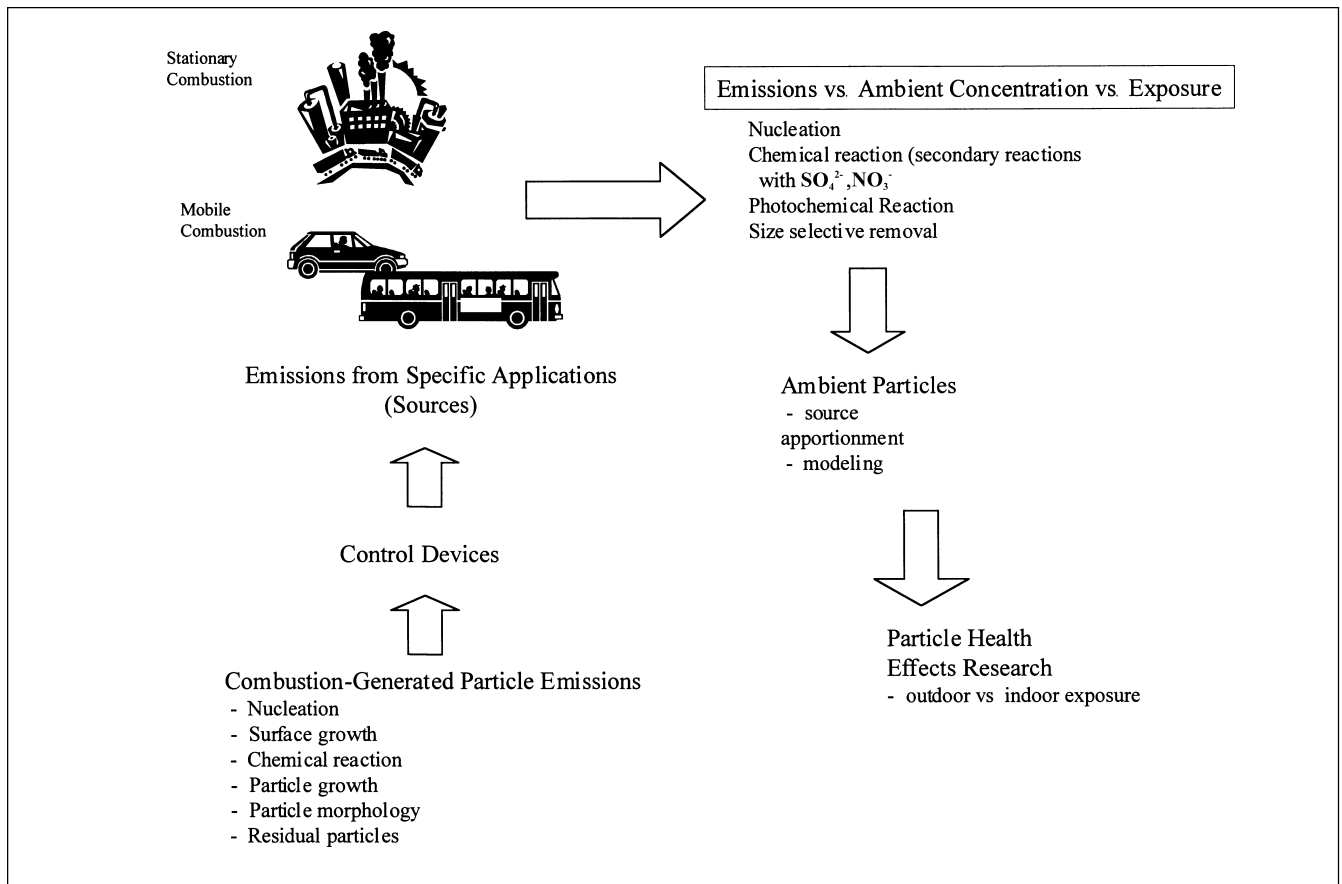


Figure 1. Roadmap to the particle formation and health effects topics discussed in this review.

deposition will also not be discussed in depth even though these processes all modify the characteristics of the aerosol as it travels between the combustion source and the site where the particles interact with the human body.

The following definitions are used in this paper: PM_{10} , $\text{PM}_{2.5}$, and PM_1 refer generically to particles with an aerodynamic diameter smaller than 10, 2.5, and 1 μm , respectively, and not specifically to the ambient particle mass as measured by federal reference test methods. Ultrafine particles refer to particles smaller than 0.1 μm , but it should be noted that the older literature occasionally used a larger size as the definition for ultrafine PM. Nanoparticles will refer to particles smaller than 0.01 μm (10 nm). Primary particles, as used in this paper, will be restricted to the roughly spherical structures of inorganic or carbonaceous condensation aerosols that make up aggregate particles. The term primary particles is also used in atmospheric PM research to refer to particles that are collected on filters at the source in contrast to secondary particles formed in the atmosphere from gas-phase precursors. Atmospheric chemistry references^{6,7} cover secondary particle formation in detail. The term nuclei will be reserved for the nanometer-sized particles initially formed from gas-phase precursors. Accumulation mode will refer

to the 0.1- to 1- μm particles that have long lifetimes in suspension because both diffusion and inertial removal mechanisms are slowest in this size range. The term nucleation mode, as used in the literature, often refers to transient concentrations of submicron particles, which are nuclei that have undergone significant additional growth by condensation and surface reaction. Depending on the context, these particles will be referred to either as a transient mode, to emphasize their rapid transformation, or as a condensation mode, to emphasize that they are derived from vapor-phase material and not from the solid or liquid residue of the fuel.

FUNDAMENTALS OF COMBUSTION-GENERATED PM

The combustion sources of ambient particles include stationary boilers and furnaces, stationary and mobile internal combustion (IC) engines, fugitive emissions from industrial processing, domestic fires, open burning, and accidental fires. The primary particles consist of inorganic or organic species, or a combination of the two. Combustion aerosols are multimodal. The finest particles are produced by gas-to-particle conversions and form the nuclei, or nanoparticles. These grow by coagulation and surface growth into the "accumulation" mode. The larger

supermicron particles are produced from the inorganic material that remains in the solid or liquid phase with the fuel and is referred to as residual ash PM. The emissions depend on the composition of the fuels, the combustion conditions, and the effectiveness of any gas cleaning devices that are used. The emissions of each class of combustor are sufficiently different to merit separate coverage in this review. However, the principles governing their formation are sufficiently alike to warrant collective treatment in this introductory section.

The extensive literature on particle formation and emission, based on both laboratory and field studies, is summarized to show how operating and process conditions affect the size distribution and composition of combustion aerosols. The formation of fly ash from pulverized coal-fired and oil-fired boilers, toxic metal emissions from incinerators, and soot emissions from both stationary combustion and IC engines have been studied extensively and can serve as illustrative examples of the more general processes taking place in all flames. Other important combustion sources of particulate air pollution, such as domestic heating and open burning, are not well characterized compared with large boilers and furnaces or mass-produced engines.

Simplified quantitative relationships give mechanistic insights into the formation of the combustion aerosol under typical conditions. For sufficiently high initial particle number, the evolving size distribution of the submicron aerosol becomes independent of the number of particles nucleated, and the aerosol characteristics can be estimated from algebraic equations. The particle size distribution is determined by the volume fraction of the aerosol that is produced by initial nucleation and by subsequent coagulation and surface growth. Mass transfer limited surface growth can be predicted from the concentration of the condensing species. In multicomponent systems, the growth from condensation and surface reaction can be distinguished by the variation of chemical composition with particle size. The final particle morphology is determined by the ratio of time between collisions and the time for coalescence of the contacting particles.

Particle Inception

There are four classes of particles that form from gas or vapor precursors in combustion systems:

- inorganic particles produced at high temperatures,
- H_2SO_4 produced at exhaust temperatures,
- soot produced at high temperatures, and
- condensable organic particles produced at exhaust temperatures.

Three of these, inorganic ash particles, H_2SO_4 droplets, and condensable organics, involve homogeneous or heterogeneous nucleation. The total amount of condensation for

these three categories is well defined, being approximately equal to the amount of initially vaporized material that is in excess of equilibrium at the ambient temperature. For soot, both the nucleation step and the amount of soot are determined by detailed kinetics rather than by thermodynamic equilibrium.

Particle Inception by Nucleation

The nucleation step involves the transformation of a vapor or liquid to clusters of the vapor "monomer" by a series of reversible steps. The clusters will persist and grow when the free energy change accompanying the phase transformation is negative. The fundamentals of nucleation are covered by Seinfeld and Pandis.⁶ They discuss the dynamics of cluster formation and evaporation and the formation of critical size nuclei using both classical theory and more rigorous approaches. The critical size is the boundary between incipient particles that are stable and can continue to grow and unstable clusters that redisperse into the gas phase.

In combustion systems, the nuclei are expected to consist of clusters of relatively few atoms and to be of a size of tenths of nanometers. Due to the Kelvin effect,⁸ the saturation vapor pressure increases as the particle size decreases, and extremely high supersaturation ratios are needed to make an organic liquid particle smaller than 10 nm stable. These high supersaturations can occur for EC and for refractory metal oxides. It is likely that much of the reported nucleation of condensable acid or organic aerosols in combustion systems actually involves the growth of inorganic ash or soot nuclei that are smaller than the detection limit of the available instruments, resulting in a sudden increase in measured particle number. The Kelvin effect assumes a continuum model and predicts that saturation pressure goes to infinity as the particle radius goes to zero. However, below a certain number of molecules, certain bulk properties, such as surface tension, are no longer applicable.

The classical theory, which assigns bulk properties to clusters, often predicts a critical nucleation size less than the size of a molecule.^{9,10} The classical theory is of value in showing the tendency to nucleate, but not in providing the size of the nuclei. More rigorous approaches are available, such as using density function theory to calculate the free energy of clusters.^{11,12} The nucleation steps in combustion will be complicated by the strong temperature and concentration profiles in a flame and surrounding individual burning particles. The calculations of the nucleation rate are further complicated by the mixtures of condensable compounds present in combustion products, since the favored nuclei will be multicomponent¹³ and the presence of other particles can lead to heterogeneous nucleation.⁶ Fortunately, as pointed out by Flagan

and Friedlander,¹⁴ since the time for the nucleation and growth of particles is small relative to the total residence time in a combustor, the details of the early nucleation steps will, in most cases, have little impact on the final number and size of the inorganic aerosols.

Nucleation versus Surface Growth

The competition between nucleation of new particles and surface growth is an issue whenever combustion products with condensable vapors are cooled in the presence of other aerosols. As the combustion products are cooled, the supersaturated vapors can either condense on the surfaces of existing particles or can form new nuclei. This problem was addressed for pulverized coal combustion by McNallan et al.,¹⁵ who modeled the supersaturation versus time of gases cooling at various rates. They allowed for condensation on the surfaces of existing particles and particle formation according to classical nucleation theory. The criterion for nucleation was the development of the supersaturation partial pressure necessary to yield a nucleation rate of 1 particle/cm³/sec. Assuming a pre-existing aerosol concentration of 1 g/m³ of 8 μm particles, which approximates the residual fly ash encountered in pulverized coal combustion, and assuming an initial condition of silica vapors at equilibrium with pure silica at a temperature of 2400 K, they predicted that nucleation of silica vapors will occur at temperature of 2320 K for a cooling rate of 1000 K/sec, or at 2240 K for a cooling rate of 600 K/sec. Nucleation was not predicted to occur at 200 K/sec. They also examined the condensation of Na₂SO₄ and lead vapor and concluded that nucleation would not occur for these compounds in the presence of high-surface-area submicron particles. Cooling rates in the burner region of boilers are above 600 K/sec, so this simple analysis indicates that refractory oxides, such as SiO₂, will condense in the flame zone to produce a high surface area aerosol, which will prevent the subsequent nucleation of trace elements in the colder exhaust gases.

Experiments with pulverized coal in laboratory reactors show that nucleation occurs early in the flame zone for both soot and inorganic particles.¹⁶⁻²⁰ This is supported by simple treatments of nucleation and growth of particles in a boundary layer.²¹⁻²³ More detailed treatment of nucleation in the boundary layer of a growing particle is presented by Peshty et al.,²⁴ who show that the correct treatment should allow for heat release due to condensation, which tends to suppress the nucleation rate locally.

Temperatures decrease through the convection passes of a steam-generation boiler and on into the stack plume, and a point may be reached where H₂SO₄ is supersaturated. Again, there is the potential to form new particles by nucleation versus deposition on existing particles. This

is a concern because H₂SO₄ deposited as a layer on coal fly ash has been shown to accentuate respiratory impairment.^{25,26} H₂SO₄ condensation is an issue with both high-sulfur and low-sulfur coals because the deposition of H₂SO₄ on particles by SO₃ injection is used to control the resistivity of fly ash in electrostatic precipitators (ESPs).

Another situation where nucleation versus surface growth is important is H₂SO₄ condensation on soot or metal oxide nuclei and the formation of ultrafine particles in the exhaust of diesel engines. The condensation of the organics in diesel exhaust also has a major impact on the size distribution of PM emissions.²⁷ The effect of particle transformations during cool-down and dilution on reported size distributions will be discussed in the measurements section.

Particle (Soot) Inception by Chemical Reaction

Soot, unlike the inorganic oxide particles and condensable organic PM, is produced by a sequence of chemical reactions, some of which are essentially irreversible. The chemical reactions result in clusters of increasing molecular weight that grow into the measurable size range where the structures are considered particles. The smallest soot particles that have been observed by electron microscopy are in the range of 1–2 nm.^{28,29} A soot particle with a diameter of 1.5 nm and a specific gravity of ~1.8 contains ~160 carbon atoms. For soot, particle inception is defined as the particles first capable of measurement, in contrast to the nucleation process where there is a critical particle size at which nucleation occurs for a particular supersaturation.

The vast literature on soot formation and oxidation has been summarized in various reviews and specialized conferences on soot.³⁰⁻³⁵ Despite the large amount of literature on soot, the models of soot formation are still evolving. The three chemical kinetic components of a soot model are particle inception, surface growth, and surface oxidation. Coupled to the chemistry controlling the conversion of molecular precursors into solid soot are the physical models of particle coagulation and coalescence, which determine the soot structure.

Soot forms under fuel-rich conditions in which hydrocarbon fragments have a greater chance of colliding with other hydrocarbon fragments and growing, rather than being oxidized to CO, H₂, CO₂, and H₂O. At equilibrium, soot exists when C/O exceeds 1.0. Soot, however, is observed in flames of premixed hydrocarbons in air at C/O values of between 0.5 and 0.9.³² In diffusion flames, soot forms even in the presence of excess air, since oxygen-deficient conditions will always be found on the fuel side of the flame front.

The reactions leading to soot are shown schematically in Figure 2, which is based on Bockhorn³⁰ and others. One

of the critical steps in soot formation is the formation of the first aromatic ring, usually benzene. It is for this reason that fuels having a high aromatic hydrocarbon content form soot easily. This has been described in terms of a threshold sooting index for various classes of organic compounds.³⁶ Molecular weight growth then proceeds with the formation of polycyclic aromatic hydrocarbons (PAH), which are considered to be precursors to soot. The formation mechanisms proceed either through a sequence of hydrogen abstractions and acetylene addition or by the polymerization of the aromatic moieties that are produced.^{37,38} Both mechanisms occur in parallel. Positive ions in the flame have been proposed as the initial nuclei sites for soot particle formation.^{37,39}

Particle Growth by Collisions

Once particles are formed by either nucleation or chemical reactions, they will grow by a combination of coagulation and surface deposition. The consequences of coagulation will be treated in this section. For the following analysis, it is assumed that all the aerosol mass originates as n_0 particles of diameter d_0 at a time of zero and that the particles coalesce on each collision. The evolution of the particle diameter with time is readily obtained by applying the continuous coagulation equation⁶

$$\frac{dn(v,t)}{dt} = \frac{1}{2} \int_0^v K n(v-q,t) n(q,t) dq - n(v,t) \int_0^\infty K n(q,t) dq \quad (1)$$

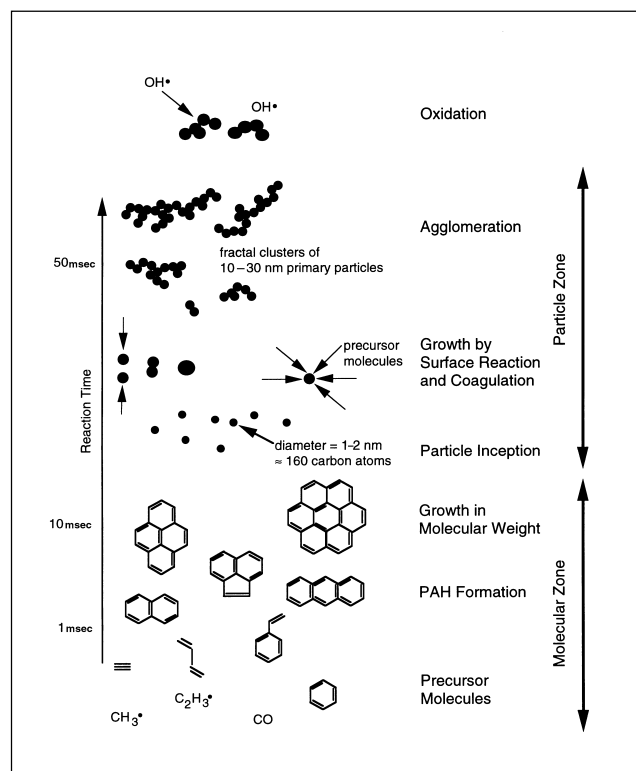


Figure 2. Kinetically limited chemical reactions and physical processes involved in soot formation. Based on Bockhorn.³⁰

where $n(v,t)$ is the number of particles of volume v at time t , and K is the collision coefficient, which varies with particle size. Equation 1 is a simplification of the general dynamic equation⁴⁰ for the limiting case of no particle sources and no transport into the control volume. The first term in eq 1 corresponds to the production of particles of volume v by collisions of all combinations of smaller particles, $(v - q)$ and q . The second term is the loss of particles out of the size range by collisions with all other particles. This form of the aerosol dynamic equation assumes that the initial particle volume is vanishingly small compared to the system volume ($f_v \approx 0$). Expressions for K are available for the continuum, transition, and free molecular regimes, depending upon whether the particle size is much larger than, comparable to, or smaller than the mean free path of the ambient gas.^{40,41}

MAEROS is a widely used numerical code for simulating multicomponent aerosol coagulation. MAEROS solves eq 1 by approximating the polydisperse aerosol with a series of constant size sections.⁴² Sectional methods do not accurately model the behavior of the particle nuclei or molecular clusters. Discrete-sectional methods treat molecular clusters as discrete particles, then switch to a sectional approximation for larger particles.⁴³ Discrete-sectional codes are the most accurate method for numerically solving the aerosol dynamic equation over the entire size spectrum, but these methods are susceptible to problems with numerical diffusion, and care should be exercised in their use.⁴⁴ Analytical approximations for solving eq 1 for polydisperse coagulation have been developed by making simplifying approximations, such as by assuming a lognormal size distribution.^{45,46} Other methods for calculating multicomponent aerosol dynamics have also been developed.⁴⁷⁻⁵⁰

For monodisperse aerosols, $n(v - q)$ is 0, and $n(v,t) = n(q,t) = n$, so eq 1 simplifies to

$$\frac{dn}{dt} = -Kn^2 \quad (2)$$

The collision rate increases with the square of the particle number concentration and increases non-linearly with decreasing particle size, since K varies with particle size in the transition and free molecular regimes. This equation can be solved to obtain the decay in number concentration as function of time

$$n(v,t) = \frac{n_0}{1 + n_0 K t} \quad (3)$$

The characteristic time scale for coagulation, assuming K is constant (valid in the continuum regime), is⁵¹

$$t_c = \frac{2}{Kn_0} \quad (4)$$

For $n_0 K t \gg 1$, the number of particles becomes independent of n_0 , so the details of the initial nucleation rate are not needed to calculate the final aerosol distribution.¹⁴ For a boiler with a residence time of 6 sec to the precipitator, the asymptotic relations will be valid for $n_0 > 10^9$ particles/cm³. U.S. coals average an ash content of 10%. Typically, on the order of 1% of the ash vaporizes to produce the submicron fume. This yields values of n_0 on the order of 10^{14} particles/cm³ for 1-nm particles and 10^{11} particles/cm³ for 10-nm particles. Emission of 0.1% of the fuel as soot will give about the same values of n_0 . The coagulation coefficient, K , varies with particle size and with gas temperature, so eq 3 is approximate. However, K varies by less than an order of magnitude over the 10-nm to 1- μ m size range, and the initial nuclei number is orders of magnitude higher than that needed to make $n_0 K t > 1$. The limiting formulae will be a reasonable model for the submicron condensation aerosols formed by most stationary combustion systems.

In this limit, if the volume of aerosol formed per unit volume of space is f_v , then the particle diameter $d(t)$ is given by⁴⁰

$$d(t) = \left(\frac{6 f_v K t}{\pi} \right)^{1/3} \quad (5)$$

where K is a constant, given by $8kT/3\eta$, for particles in the continuum regime; k is the Boltzmann constant, and η is the gas viscosity.

For the free molecular or kinetic regime, K is a known function of the particle diameter and velocity. The equation for the rate of change in number density, for this case and a fixed f_v , is given by³³

$$\frac{dn}{dt} = -\frac{6}{5} k_i f_v^{1/6} n^{11/6} \quad (6)$$

where

$$k_i = \frac{5}{12} \left(\frac{3}{4\pi} \right)^{1/6} \left(\frac{6kT}{\rho} \right)^{1/2} G\alpha \quad (7)$$

and ρ is particle density; G is the enhancement factor to allow for the van der Waals acceleration factor that is a function of the Hamaker constant,^{8,52} and it has a value of about 2; and α is a factor to allow for the particle size distribution, and it has a value of 5.66 for monodisperse particles. The exponent of n of 11/6 in eq 6 versus the exponent of 2 in eq 2 is a consequence of allowing for the dependence of collision rate with particle size and the constraint that f_v is constant.

Friedlander and co-workers showed that, if allowance is made for the polydisperse particles, a self-preserving size distribution is approached.^{40,53} For this case, the particles have a narrow size distribution with a geometric standard deviation of 1.37 for the diameter, and

the coefficient α has a value of 6.55, not very different from the value of 5.66 for a monodisperse aerosol. Solution of eq 6 for a fixed volume fraction of aerosols f_v then yields the following relations for particle number and particle size:

$$n(t) = (k_i f_v^{1/6} t)^{6/5} \quad (8)$$

$$d(t) = \left(\frac{\pi}{6} \right)^{-1/3} (k_i f_v t)^{2/5} \quad (9)$$

The evolution of particles following these approximate equations has been demonstrated in small-scale studies of aerosols formed from combustion systems for fly ash from coal^{22,54,55} and soot particles^{30,56,57} and waste combustors.^{58,59}

As shown by eqs 8 and 9, the number and size of particles can be determined for $n_0 K t \gg 1$ if the amount of material in the form of the aerosol is known. When f_v is measured from the total amount of submicron ash collected, good agreement is observed between theory and experiment, both for the particle size distribution of the submicron ash⁵⁵ and the dependence of the mean particle diameter on f_v .²²

The value of f_v for the mineral matter is determined by the vaporization kinetics, and is a function of temperature and environment to which the minerals are exposed. The mass of the submicron aerosol is usually dominated by the refractory and alkali metal oxides.^{54,60,61} At typical combustion temperatures, the burning rate of a particle is limited by gas-phase diffusion, and the particle is surrounded by a CO-rich reducing atmosphere. The vaporization of the refractory metal oxides is augmented by the reduction of the oxides by CO to form suboxides such as SiO and Al₂O and elemental metals such as Fe, Ca, and Mg. The suboxides and metals will diffuse through the particle boundary layer into the bulk gas where they are oxidized and condense to produce the submicron aerosols. The vaporization rate is strongly temperature-dependent^{55,62-64} so that the amount of submicron aerosol will vary with combustion conditions. The vaporization of elements is complicated by their interaction with the minerals in the coal. Sodium, for example, will have its vaporization suppressed either because it may be originally present in sodium aluminosilicates or because it is captured by the alumina silicates after release.⁶⁵⁻⁶⁷

Particle Growth by Condensation and Surface Reaction

Vaporized elements distribute on the surfaces of existing submicron and residual ash particles by condensation and chemical reaction. The rate of mass addition to a spherical particle for mass-transfer limited deposition over the entire range of particle size is given by the Fuchs-Sutugin interpolation equation:^{6,41}

$$\frac{dm}{dt} = 2\pi c_{\infty} D d_p \frac{1 + Kn}{1 + 1.71Kn + 1.33Kn^2} MW \quad (10)$$

where c_{∞} is the concentration of the condensing species, MW its molecular weight, D its diffusivity, and Kn the Knudsen number, defined as the ratio of the mean free path in the gas to the particle diameter d_p .

For the case in which the rate of deposition is controlled by chemical reaction, the mass flux to the surface is independent of mass transfer and is given by

$$\frac{dm}{dt} = \pi d^2 MW k_s C \quad (11)$$

where MW is the molecular weight of the depositing species, C is the concentration in the gas, and k_s is the rate of surface reaction. The literature also covers the cases of combined mass transfer and surface kinetics and the additional complication of pore diffusion in porous surfaces.^{33,68,69}

Because of the higher surface area per unit mass, smaller particles tend to be enriched in the compounds that condense or deposit on the surface. The trace elements in coal and waste tend to deposit without significantly changing the particle size distribution. For this case, the mass concentration of the depositing species can be readily calculated by integrating the mass deposition of the depositing species along an ash particle trajectory and dividing the mass deposited by the mass of the ash particle, that is,

$$\text{Mass Conc}(D) = \frac{\int_0^t \frac{dm}{dt} dt}{\frac{\pi d_p^3 \rho}{6}} \quad (12)$$

Applying eqs 10–12 to the trace elements shows that concentration of trace elements on the surface of the ash can be described as a power function of size, with the concentration increasing as the particle size decreases. The mass concentration dependence upon particle size is therefore proportional to $1/d^n$, where the exponent n for the limiting cases is given in Table 1.

An added case is that of a porous particle with chemical kinetics controlling. For this case, the amount of reaction is proportional to volume, and the concentration of the trace reacting species will be independent of particle size. The dependence will be different for the submicron and supermicron particles since these straddle the gas mean free path in size. The gas mean free path varies from $\sim 0.2 \mu\text{m}$ at ambient conditions to $\sim 1 \mu\text{m}$ at combustion conditions, so that ultrafine particles will generally have $Kn \gg 1$ and supermicron particles $Kn \ll 1$. Given that the Kn is the mean free path in the gas (a constant) divided by the particle diameter, eq 10 shows that dm/dt is proportional to d for $Kn \ll 1$ and to d^2 for $Kn \gg 1$.

Table 1. Exponent n in size-dependent mass concentration of trace species: concentration $\propto (1/d^n)$

Controlling Mechanism	Particle Size	Exponent n
External Mass Transfer	Ultrafine ($Kn \gg 1$)	1
External Mass Transfer	Supermicron ($Kn \ll 1$)	2
External Surface Kinetics	All Sizes	1
Internal Surface Kinetics	All Sizes	0

The early studies on the size-dependent concentration of elements in fly ash^{70–72} all were performed for supermicron particles and showed the $1/d^2$ size dependence expected for mass transfer-controlled condensation. Some studies^{21,73} have shown the difference in the dependence on particle size of the trace volatile element concentration between the submicron and supermicron fractions. Other studies have shown an enrichment of the smaller particle sizes in the trace volatile elements.^{21,54,60,61,66,69–72,74–84}

The reasons for attention to the size dependence of trace element concentration are that (1) this provides a diagnostic for the mechanism of surface deposition; (2) the enrichment of submicron particles in certain elements affects the total capture efficiency of that element in the APCDs; and (3) elemental concentrations affect the chemical speciation, which can be important for health effects.

The exponent n that best fits the variation of elemental concentration with size can be used to determine the mechanism of deposition, for example, whether it is condensation or surface reaction. Haynes et al.⁶⁹ deduced from the size dependence of particle composition that the deposition of As and Sb was controlled by chemical reaction. More extensive studies of the size dependence of the deposition have been carried out^{85–87} showing that As, Se, and Sb react with the fly ash to an extent that depends on ash composition, thus leading to a coal-dependent partitioning of the elements between the submicron and supermicron ash.

Elements that deposit by surface reaction or surface condensation are expected to be enriched in the surface layers. Studies using surface spectroscopic techniques have shown that the surface layers of both the supermicron⁸⁸ and submicron²¹ ash particles are enriched in the trace elements. By ion milling of the particles, one can show the stratification that results from the sequential deposition of elements. The implications of this surface stratification to particle toxicology will be discussed later in this review.

To model the partitioning of trace elements in combustion, one needs the particle size distribution of the submicron and supermicron ash and the amount of each of

the trace elements vaporized. Models of the vaporization of trace elements based on equilibrium assumptions⁸⁹⁻⁹¹ have been developed for the vaporization and subsequent condensation or chemical surface reaction of trace elements.

The models are based on the assumption of equilibrium between the trace species and the vapor and the residual ash in the combustor. Subsequent condensation and reaction of the trace species is also taken into account. In the model by Sandelin and Backman, two reactors in series are considered to represent the radiant section of a boiler and the ESP, respectively.⁹⁰ The partitioning of trace elements in the radiant chamber is calculated for a given fuel composition and fuel/air ratio from equilibrium for an assumed distribution of bottom and fly ash and the temperature of the radiant chamber. The distribution of the elements from the ESP is obtained from the temperature in the precipitator and the ash collection efficiency.

Simulations carried out for a boiler for As, Cd, Hg, Ni, Pb, Se, V, and Zn were found to be in reasonable agreement with experimental observations on an operating power plant. In the paper by Yousif et al., the metal partitioning was calculated by a post processor using input obtained from a computational fluid dynamic simulation of a boiler.⁹¹ The major mass of the ash is distributed between the residual fly ash and submicron ash as inlet conditions. The trace species are assumed to be released at a rate proportional to the char burning rate. The concentration distribution of the trace species is then calculated, allowing for condensation on surfaces and nucleation. The vapor species were assumed to be in equilibrium. Simulations were carried out for Pb and Cd, and their distribution between the residual and submicron ash was found to be in good agreement with experiments on a pilot scale combustor fired with coal and sewage sludge. Nucleation was not found to occur, as the supersaturation did not reach the critical level.

Most studies of trace metals from coal combustion (including some by the co-authors) have reported elemental concentration or enrichment factors since this is what is directly measured by the chemical analysis. Enrichment factor is defined as the concentration of an element in a particular size fraction (e.g., the submicron ash) divided by the average concentration for that element in the total ash. The measured concentration is controlled by the mass balance, and an element may be reported as being depleted in the submicrometer ash solely because of dilution by another element. For example, alkali metals dominate the submicrometer ash from low rank coal, while carbon dominates the particulate emissions from oil and biomass combustion. The raw concentration of transition metals in the total ash from oil combustion is largely an artifact of the combustion efficiency, not a result of the

metal vaporization. The relative amounts of elements may be relevant for some health-related studies since the mineral form and valence state of the trace element is often sufficiently described by the equilibrium composition in the bulk ash matrix. For other types of health studies, the absolute amount emitted is of concern. While elemental concentration data is useful, including sufficient data in a publication to calculate a mass balance greatly enhances the value of the particle composition data for reuse in both aerosol formation mechanism and toxicology studies.

Particle Morphology

Soot and submicron ash particles often consist of aggregates of 10–30 nm primary particles. It is important to understand what determines the structure of these particles, since the aggregate size determines the aerodynamic behavior of the particles while the primary particle size determines the surface area.

The coagulation theory described above assumes that particles coalesce on collision. This assumption is valid as long as the coalescence time is short compared with the time between particle collisions. For inorganic particles, coalescence times can be calculated assuming surface tension-driven viscous flow using the theory of Frenkel

$$t_c = \frac{\eta r}{\gamma} \quad (13)$$

where η is the viscosity, and γ the surface tension. Alternatively, the coalescence time can be determined by solid-state sintering^{92,93}

$$t_c = \left(\frac{\Delta L}{L_0} \right)^{5/2} \frac{\sqrt{2} k T d_p^3}{160 D^* \gamma a^3} \quad (14)$$

where $\Delta L/L_0$ is the fractional shrinkage in diameter of two spheres, D^* is the self-diffusion coefficient for the mobile species, and a^3 is the atomic volume of a diffusing vacancy. As long as the characteristic coalescence time is much smaller than the time between collisions, the particles will coalesce and maintain their sphericity. The coalescence time increases because of the increase in particle diameter and the decrease in temperature (leading to an increase in η or a decrease in D^*). After a time, which depends on the combustion conditions, the colliding particles will begin to form aggregates. This transition has been studied for coal combustion aerosols and for the flame synthesis of particles.^{19,94-96}

The aggregates that are produced have a fractal dimension, D_f , which provides the scaling parameter relating the number of particles n_a in an aggregate to the ratio of the radius of gyration r_g and the primary particle size r_0 :⁹⁵

$$n_a \propto (r_g / r_0)^{D_f} \quad (15)$$

where D_f has values of 3 for a solid sphere and of 1 for a string of particles. For soot and submicron ash particles, the value of D_f is about 1.7.^{95,97,98} The theory for the coagulation of aerosols has been extended to aggregates, and a two-dimensional solution was obtained allowing for coagulation and sintering.^{99,100} Application of this theory shows the aggregates still assume a self-preserving size distribution but with a wider size distribution than that for spherical particles.

For soot particles, there are several hypotheses for the formation of aggregates.^{37,39,101} One of these is that the soot precursor particles are liquid polymers³⁸ and will coalesce after collision. In parallel, the liquid polymers will dehydrogenate and their viscosity will increase, leading to a transition from coalescence to aggregation similar to that described above for inorganic aerosols. A second hypothesis³⁷ is that the soot particles form as a solid, then collide and aggregate. Surface growth occurs in parallel with growth by collisions. If the surface growth is sufficiently rapid, the particles in the growing aggregate will be immersed in the deposited carbon and the resulting structure will appear as a spherical particle. Numerical simulations support this hypothesis when realistic values of surface growth and coagulation are used.³⁷ As the particle size increases, and as the species contributing to surface deposition are depleted, the rate of surface growth due to deposition will decrease. After this point, the soot particles will develop as aggregates with a fractal structure.

The final particle morphology at the exit of the high-temperature zone is the result of multiple processes. The characteristic times for these processes can be readily predicted, and examination of particle morphology gives a good indication of which processes are dominant for the given situation. This type of analysis was applied to the behavior of sorbents for toxic metal control.¹⁰²

Residual Ash Formation

Submicrometer particles dominate the number count of particles emitted by combustion sources and very often dominate the surface area as well, but the mass of PM emissions is usually dominated by the organic or inorganic residue of material that remained in a solid or liquid phase throughout combustion. These particles are referred to as residual ash. The residual ash formation process differs from the formation of the submicrometer particles by molecular weight growth processes for soot and by vaporization and condensation for inorganic ash, as described above. The total amount of noncombustible minerals in the residual ash is determined by the mass balance, and the total amount of carbonaceous material in the residual ash is determined by the combustion efficiency.

Most fossil fuels contain inorganic components. For U.S. coals, this inorganic content constitutes ~10% on average of the mass. For petroleum, the maximum ash mass ranges from 0.05% for a light No. 4 oil to 0.15% for a No. 5 fuel oil; a typical value No. 6 or residual oil ash content is 0.8%.¹⁰³ A representative ash content for wood is 2.5%, but it varies widely.

Figure 3 illustrates the major processes affecting the formation of submicron and supermicron ash during the combustion of coal, biomass, and oil.^{69,73} The mass of particle emissions measured at the combustion chamber exit is determined by a number of complicating factors. The first is that, depending upon the type of combustor, only a fraction of the total ash content in the fuel is carried over with the combustion gases as fly ash. The so-called bottom ash is deposited in the ash hopper on the floor of a suspension-fired furnace or is dropped off the end of the grate in a stoker-fired furnace. The ash entering the particulate control equipment downstream from coal-fired boilers varies from 10% of the total fuel ash content for cyclone or wet-bottom furnaces to 85% for dry-bottom pulverized coal-fired furnaces. The fly ash particle size distribution is multimodal. The factors that control the residual ash size distribution will be discussed below for the case of pulverized coal-fired systems, partly because pulverized coal has been most extensively studied, and partly because these boilers account for a large portion of the primary energy production worldwide.

The noncombustible matter in pulverized coal includes mineral grains of clays, pyrites, and quartz that vary in size from less than a micron to the largest sizes that can pass through the pulverizers, which is over 300 μm . Part of the inorganic matter is included in the coal matrix as discrete crystals, some is incorporated in the organic matrix as organo-metallic complexes or as ion-exchanged metals bound to the organic acids, and some of the minerals are present as extraneous particles. These forms of inorganic matter are shown schematically in Figure 4.¹⁰⁴ Detailed characterizations of the mineral content of coals have been conducted by computer-controlled scanning electron microscopy (CCSEM) by a number of research groups.¹⁰⁵⁻¹¹¹ An example of the mineral size distributions as determined by CCSEM is provided in Figure 5, which shows the size distribution of mineral inclusions in raw Kentucky No. 11 coal. The kaolinite and illite inclusions are found in the smaller particle sizes while calcite and pyrites are in the larger particle sizes. Quartz and mixed silicates are distributed over all size ranges.

Given the mineral distribution within the pulverized coal, one can calculate the ash particle size distribution using a material balance. Assume a coal particle of density ρ_c and diameter d_c , and a mass fraction f_a yields n ash particles of density ρ_a and diameter d_a . A mass balance then yields the

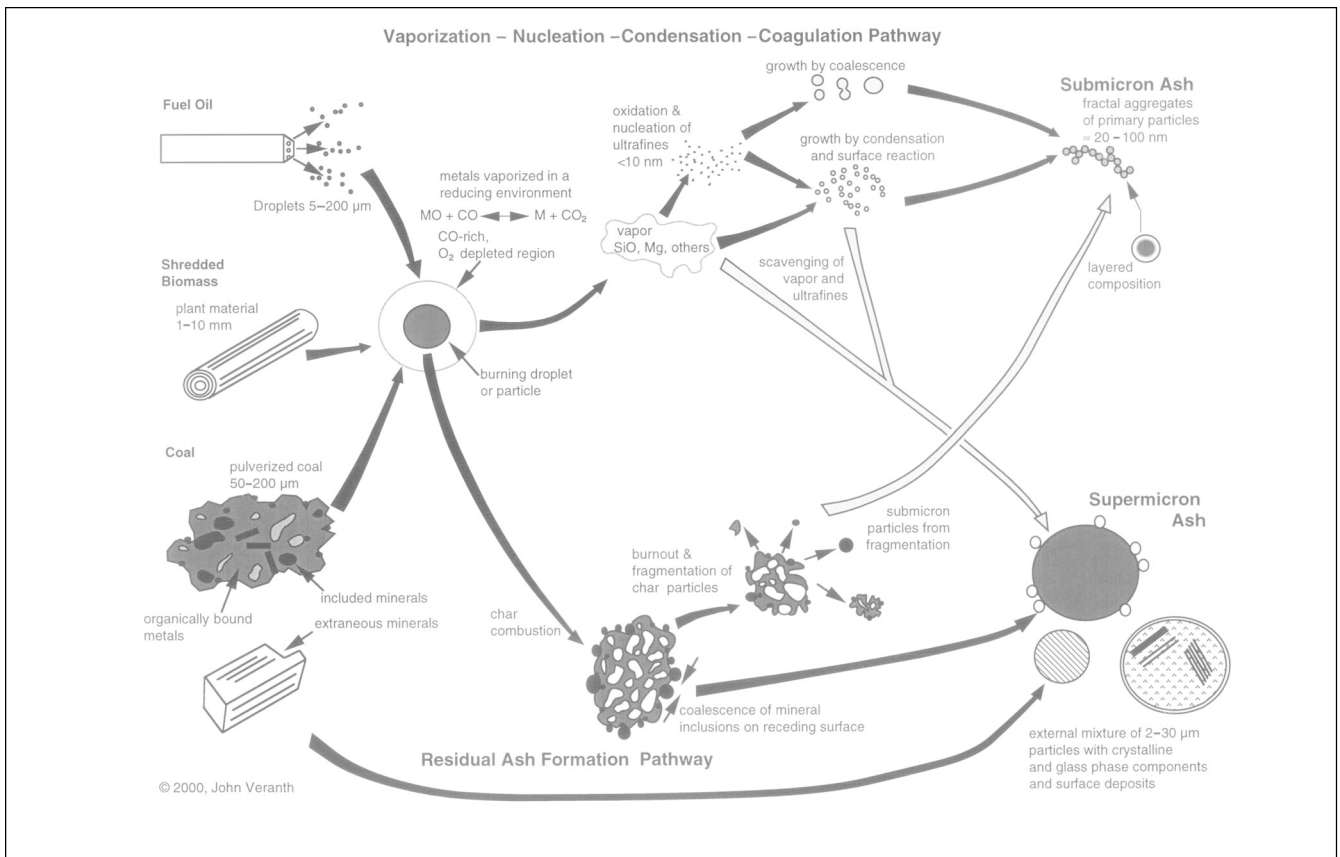


Figure 3. Formation of inorganic submicron and supermicron particles during combustion of solid and liquid fuels. Submicron particles are formed by the vaporization–nucleation–coagulation pathway. Supermicron particles are formed by the residual ash pathway. Based on earlier versions.^{69,73}

following expression for the diameter of the ash particle:

$$d_a = d_c \left(\frac{f_a \rho_c}{n \rho_a} \right)^{\frac{1}{3}} \quad (16)$$

To apply this simplified relationship, assume that the coal specific gravity is constant and equal to 1.3, that the ash specific gravity is constant and has a value typical of glass

of ~2.5, and that each coal particle yields one ash particle, that is, that $n = 1$. For these assumptions, a typical U.S. coal with 10% ash ($f_a = 0.1$) yields a ratio of the ash particle diameter to the coal particle diameter, d_a/d_c of 0.37. A pulverized coal with a mean coal particle diameter of 50 μm would yield a mean ash diameter of ~19 μm

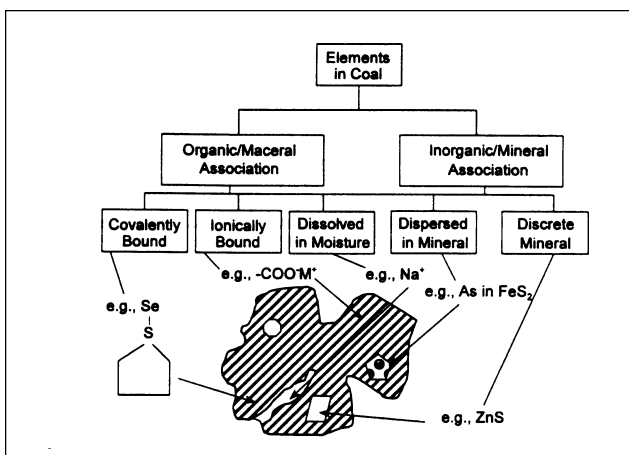


Figure 4. Classification scheme for describing the modes of elemental occurrence in coal. Reproduced by permission of Elsevier Science.¹⁰⁴

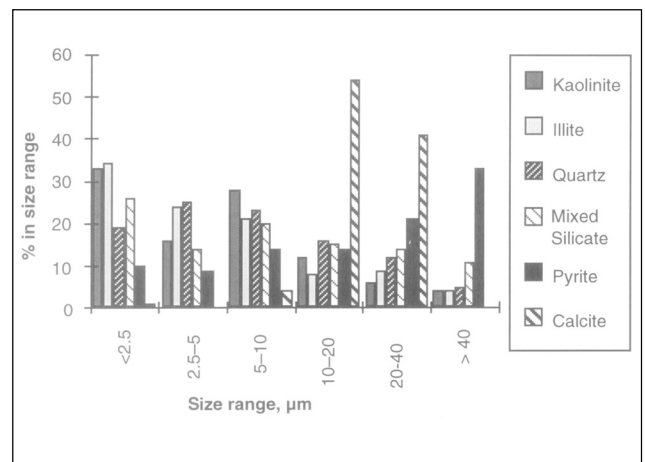


Figure 5. Size distribution of minerals in Kentucky coal. Quartz, kaolinite, and illite are concentrated in the smaller size fractions, while pyrite and calcite are concentrated in the larger sizes. Based on data in ref 111.

under these assumptions. This is a reasonable default value, but the actual transformation mechanisms are more complicated. One needs to account for the different ash content of each coal particle, which will result in variations in both f_a and r_c . The fragmentation of coal char during combustion and the incomplete coalescence of mineral droplets on the shrinking surface both yield values of n other than unity. Also, the ash particle density ρ_a varies due to changes in composition of individual ash particles and to the presence of gas bubbles within the ash.¹¹²⁻¹¹⁴

The mineral inclusions are not distributed evenly between different coal particles. Some particles are nearly inclusion-free and some of the particles are pure minerals (the extraneous ash). The actual distribution of the minerals between the different coal particles is provided by CCSEM.^{109,115} If such information is not available, an approximate distribution can be obtained by assuming that the minerals are randomly distributed between coal particles.¹¹⁶⁻¹¹⁹ The ash particles will have a particle-to-particle variation in composition that will reflect the variation in the mineral content of the individual coal particles from which they are produced. This is illustrated in Figures 6 and 7, which show the Al, Si, and Fe distributions both in the parent coal minerals and in the resulting fly ash, respectively.

The number of ash particles, n , produced by a coal particle will depend upon the competition between coalescence of molten mineral inclusions and fragmentation of the char particle during combustion. The ash produced by the mineral inclusions in coal will adhere to the char surface as it burns and will coalesce with other ash particles as the char surface recedes.¹²⁰ The fragmentation of chars has been shown to depend upon the macroporosity of the chars¹¹⁴ and therefore upon the swelling behavior of coals, dependent upon coal-specific pyrolysis behavior.

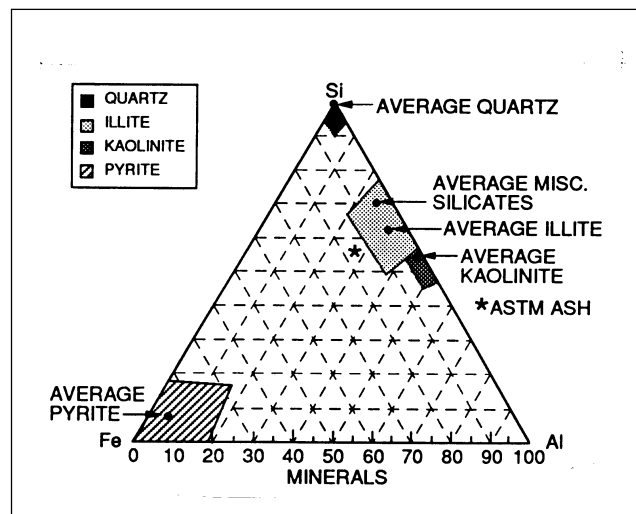


Figure 6. Si-Al-Fe ternary diagram showing typical composition ranges from minerals in coal. Reproduced by permission of Engineering Foundation.¹¹¹

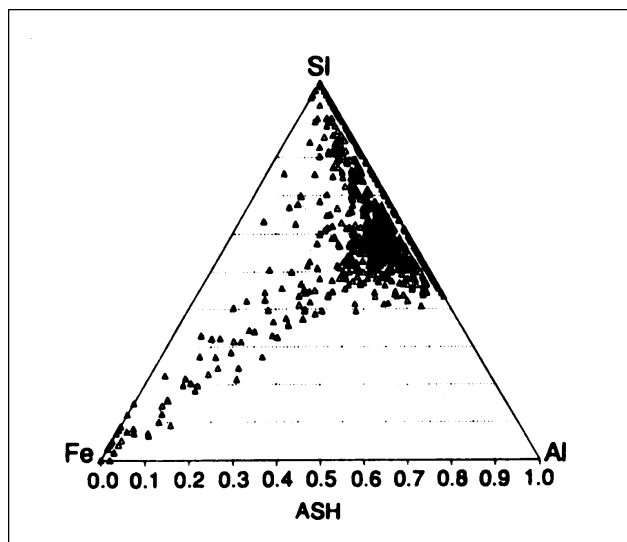


Figure 7. Measured elemental compositions in individual coal fly ash particles. Reproduced by permission of Engineering Foundation.¹¹¹

While complex models have been developed to predict fragmentation behavior,^{113,121-124} validation of these models has been limited, and complicating factors such as adhesive forces have been neglected in past analyses.¹²⁵ The models provide useful qualitative information but cannot predict quantitative trends with confidence. The fragmentation scales with the ratio of the volume fraction of ash in the char to the void fraction, Λ .¹²² For high values of Λ , fragmentation is negligible, and one ash particle is produced per coal particle. For low values of Λ , extensive fragmentation occurs, and each mineral inclusion produces a separate ash particle. These trends are well illustrated by the results of Wu et al., who showed that as pressure increases during pulverized coal combustion, the macroporosity increases and the ash produced becomes finer.¹²⁶

The particle-to-particle variation in particle density is an added complication. Figure 7 shows that a typical ash sample is a mixture of particle compositions. A number of the ash particles have high iron content and may be expected to have densities more than twice that of the aluminosilicate-rich particles. In addition, a large number of the particles will form cenospheres (hollow spheres) or plerospheres (hollow sphere surrounding a number of spherical ash particles).^{83,112,127,128} The mechanism for the cenosphere is the formation of gas within the ash particle in a temperature window where the viscosity is low enough to favor the bubble growth but not so low as to have the gas escape and the bubble collapse. One mechanism for cenosphere formation identified by Raask¹²⁸ is the reaction within the ash of iron oxide with carbon to form CO. The cenospheres can grow to sizes up to 300 μm . Up to 5% of the fly ash has been observed to form cenospheres having a specific gravity less than 1.0.^{112,128} If a 50- μm particle with

a specific gravity of 2.5 formed a cenosphere with an outer diameter of 100 μm , the wall thickness would be $\sim 2 \mu\text{m}$ and the specific gravity of the particle would be 0.625. The wall thickness decreases with the square of the diameter of the cenosphere and therefore will be submicrometer for the largest cenospheres ($>300\text{-}\mu\text{m}$ diameter). Indeed, it has been postulated⁸³ that one source of the submicrometer particles is provided by the fragments of cenosphere shells.

It can be seen that the multimodal distribution of combustion particles is governed by a number of factors. The submicrometer fraction is generated by the vaporization and condensation of particles and, to a lesser extent, the fragmentation of cenospheres. The supermicrometer particle size distribution is governed by the size distribution of the coal, the mineral matter distribution within each size fraction, the fragmentation of the char during combustion, and the formation of cenospheres. Although the processes governing the size distribution of fly ash are well understood qualitatively, they are sometimes difficult to quantify, most particularly the char fragmentation during combustion. The simple models of one ash particle per mineral inclusion and one ash particle per coal particle provide limiting solutions for the impact of fragmentation. A comparison of experimental data with these limiting solutions is shown in Figure 8 for one case. Because of the importance of fly ash as an additive for concrete manufacture, there are extensive compilations of fly ash size distribution and composition.^{129,130}

Special Considerations for Large and Small Particles

Combustion particle diameters range from nanometers to millimeters, a size range which represents a mass range

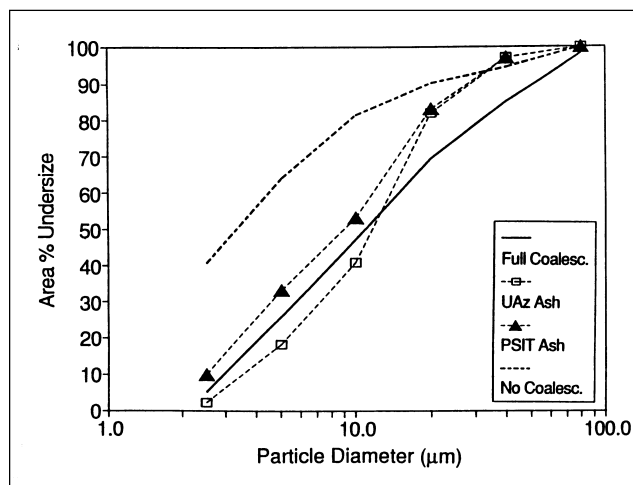


Figure 8. Ash particle size distributions (PSDs), model (solid and heavy dashed line) vs. experiment (symbols) for Upper Freeport coal. Reproduced by permission of Engineering Foundation.¹¹¹

of a factor of 10^{18} . Special considerations are needed for both size extremes. The behavior of the largest particles is dominated by gravity settling, and they are usually considered as bottom ash rather than as aerosols, but this is an arbitrary distinction from a particle formation standpoint. Most reported measurements of combustion particles from coal, biomass, and even from oil are truncated at the upper end by the cutoff of the sampling apparatus. While these macroscopic particles are of no concern for inhalation toxicology, they are important for closing mass balances in both laboratory and full-scale measurements.

The fume formed by nucleation and condensation of vaporized ash, ash, and organic materials is typically a combination of true nuclei, a transient mode of nuclei that have undergone coagulation and surface growth, and accumulation-mode particles, depending on the relationship between the characteristic time for coagulation and the age of the aerosol when it arrives at the sizing instrument. Combustion particle number size distributions often show a truncated curve with the number of particles in each size range still increasing as the small size limit of the instrument is reached. This suggests a pool of particles exists below the 5–10 nm cutoff¹³¹ of most current particle-size instruments.

Recently, the existence of high concentrations of 1–2 nm combustion particles has been reported.^{132,133} These particles cannot be detected by most instruments used for studying submicron aerosols, but can be detected by light scattering and absorption in the near UV. They have a longer life span than would be expected from the coagulation rates discussed above. In the conventional coagulation models, the assumption is made that the sticking coefficient is unity; that is, every collision results in coalescence or aggregation. This is a reasonable assumption for accumulation mode particles; however, nuclei particles on the order of 1–2 nm may have lower sticking coefficients, as was shown by Narsimhan and Ruckenstein in a theoretical study of equal-sized neutral particles that considered the competing effects of van der Waals attraction and Born repulsion.¹³⁴

Acid Aerosols

H_2SO_4 may be considered as either a gas-phase or particle emission depending on the sampling method. Some portion of the total sulfur in the fuel is converted to SO_3 and forms H_2SO_4 in the presence of water in the hot combustion products. The dew point of H_2SO_4 in the undiluted combustion products from fossil fuels is much higher than ambient temperature, and the acid may nucleate and condense to form aerosol particles as the gas is diluted and cooled, either in the unconfined stack plume or in a dilution sampler. Filter-based particle mass measurement methods in which the undiluted gas is

passed through a heated sample train can result in the acid remaining in the gas phase. On-line particle number measurements typically require diluting the stack gas to bring the concentration within the range of the instrument, and this results in the acid being measured as PM.

The amount of acid aerosol formed depends on the partitioning of sulfur between SO_2 and SO_3 and on the temperature and humidity of the dilutant gas. The formation of SO_3 is kinetically limited and can be enhanced by catalytic reactions with metals in coal combustion ash¹³⁵ or in catalytic NO_x reduction equipment. Typical acid dew points for coal combustion are 380–395 K.¹³⁶ For aircraft engines at cruise altitude, the SO_3 measurements are much higher than expected based on hydroxyl and atomic oxygen reaction rates, suggesting another, possibly heterogeneous, pathway.¹³⁷ The influence of dilution conditions on aerosol formation are discussed in the measurements section.

Particle Shrinkage by Evaporation and Oxidation

Unlike inorganic oxide particles, which are stable under post-combustion conditions, both condensable aerosol and soot mass can decrease after particles are formed. The organic aerosol, H_2SO_4 aerosol, and hydrated species can evaporate at rates that are well described by local phase equilibrium and diffusion mass transfer rate equations. Soot is destroyed in the flame by oxidation, and soot emissions are much lower than the initial soot volume fraction that occurs in the fuel-rich zones. The rate of soot oxidation can be estimated from the semiempirical kinetic formula proposed by Nagle and Strickland-Constable.¹³⁸ However, this correlation overstates soot oxidation at temperatures below 1800 K³⁴ and understates the oxidation rate in low-oxygen conditions where OH radicals are important.³³ The fractal aggregate structure typical of soot particles further complicates soot oxidation estimates because simple spherically symmetric mass diffusion equations are a poor approximation.

CONTROL DEVICES

The particles emitted from the stack will have a size and composition distribution very different from that in the combustion system because of the size-dependent collection efficiency of any APCD equipment. Historically, the combustion and atmospheric emission research communities have been uncoupled. Combustion researchers generally concentrate on the particulate formation in the flame zone of laboratory and pilot-scale equipment, since this allows close control of experimental conditions. Most field emission studies focus on measurements in the stack, since stack PM is of regulatory concern. Measurements of uncontrolled emissions at the exit of an industrial-scale

combustion chamber are difficult and expensive, so data are seldom collected. The particle emission mass measured downstream of modern, high-efficiency particle-removal equipment largely reflects variations in gas-cleaning efficiency, not changes in combustion conditions. However, some details of the primary combustion particles, such as particle morphology and elemental concentration within an aerodynamic size range, are preserved from the combustion chamber to the stack. A few researchers have studied the particles upstream and downstream of the APCD. For example, Itkonen and Jantunen present graphs of elemental size distribution upstream and downstream of the ESP from a plant that co-fired peat and oil.¹³⁹ These studies provide an important link between particle formation in combustion and human health impacts.

Gas-cleaning equipment for particle removal includes cyclones, fabric filters, ESPs, and scrubbers on stationary furnaces. Internal combustion engines are equipped with catalytic converters, and particle traps are coming into commercial use on diesels. Particle removal requires some combination of inertial separation, which becomes more efficient with increasing particle size, and diffusion to a solid or liquid collection surface, which becomes more efficient with decreasing particle size. The result is that the removal efficiency of particles from air is least efficient in an intermediate size range from 0.1 to 1 μm . This minimum PM removal efficiency is observed in post-combustion cleanup equipment at the source, in the atmosphere, and in the respiratory system. The fundamental physics of these particle removal processes are covered in aerosol texts,⁵¹ and the related equipment design and performance equations are covered in air pollution control handbooks.^{140–142} The stack emissions of specific combustion particle types depends on both concentration of particles in each size range at the combustion chamber exit and on the size-dependent collection efficiency in the gas-cleaning equipment. Understanding the particle size and composition at the source allows developing computational models that can predict practical information such as the penetration of each trace element through an ESP installed on a coal-fired power plant.¹⁴³

The collection efficiencies of three types of particle collectors are shown in Figure 9.¹⁴⁴ The minimum efficiency for all three devices is in the range between the regimes of deposition by inertial and diffusional processes. For a given technology, the actual efficiencies will, of course, vary widely with changes in design and operational parameters. A measure of the wide variation in the penetration of particles through operating ESPs at power plants is provided by Helble¹⁴³ and summarized in Figure 10. Again, the peak penetration occurs in the 0.1- to 1- μm size range, where the particle size is comparable to the mean free path of the gas. The collection efficiency of the

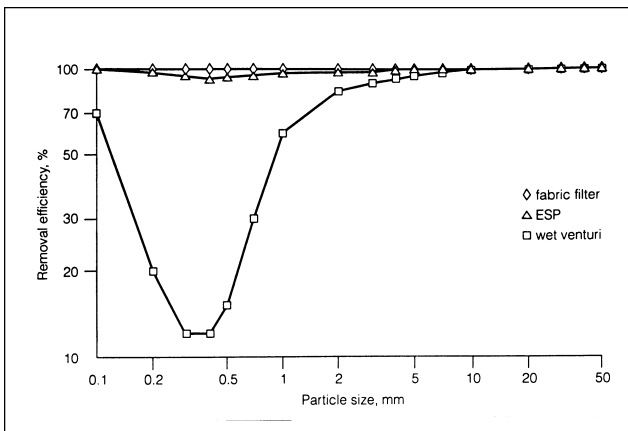


Figure 9. Removal efficiency of three common particle removal technologies used on large stationary combustion systems. Reproduced by permission of IEA.¹⁴⁴

smallest particles by an ESP is reduced because a portion of the incoming ultrafine particles do not receive a charge (partial charging).¹⁴⁵⁻¹⁴⁷ However, in the ultrafine size range, diffusion and particle growth by condensation of water vapor become important removal mechanisms.

Since the collection efficiency of a particle control device is size-dependent, the varying partitioning of elements between the submicron particles, residual fly ash, and vapor will lead to a wide range of elemental collection

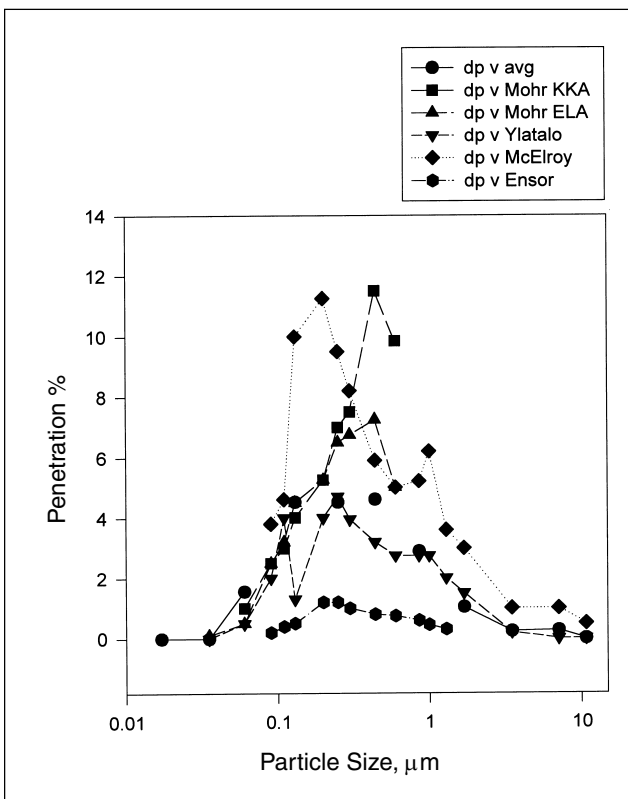


Figure 10. Summary of studies reporting penetration of coal fly ash through an ESP. Reproduced by permission of Elsevier Science.¹⁴³

efficiencies that will differ from the overall PM collection. Kauppinen and Pakkanen reported the emissions of 17 elements by particle size based on measurements in the stack of a coal-fired power plant equipped with an ESP.¹⁴⁸ Three elements are shown in Figure 11. Aluminum is found in the supermicron particles, while sulfur is found in particles smaller than 0.1 μm . Cadmium shows a bimodal distribution.

Extensive data have been obtained by EPRI and the U.S. Department of Energy (DOE) on the collection efficiencies of coal-fired utility boilers for the elements regulated under the Air Toxics provision of the Clean Air Act

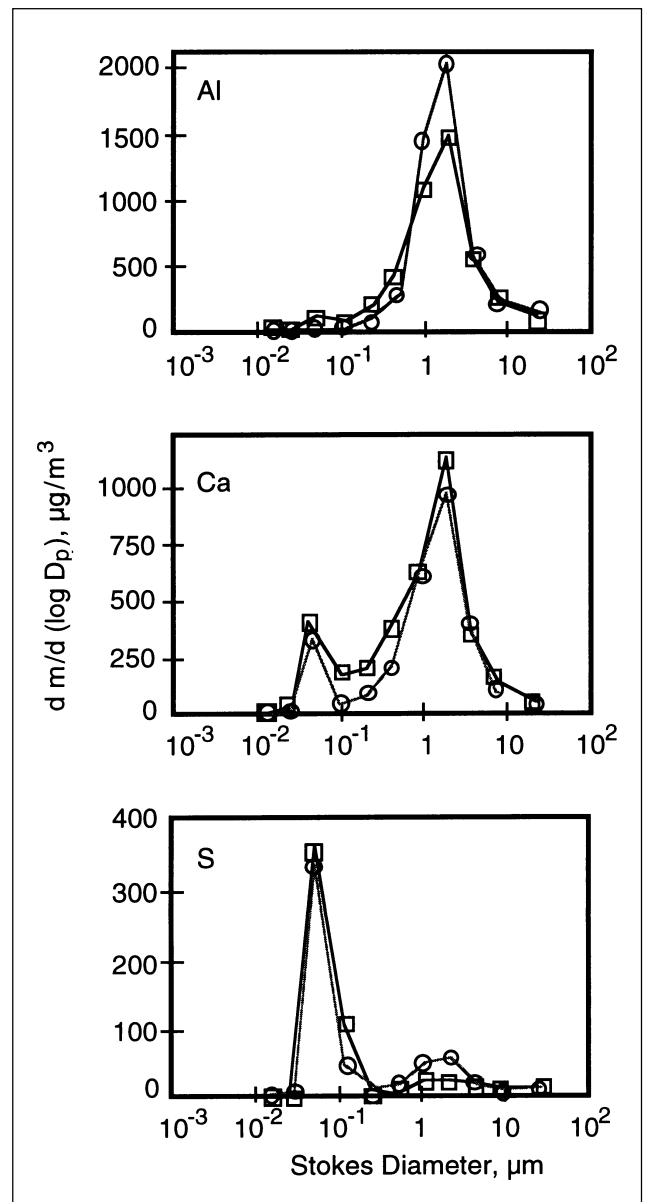


Figure 11. Distribution of selected elements by particle size as measured in the stack of a power plant equipped with an ESP. Some elements, such as Al, are concentrated in the large particles, while others, such as S, are concentrated in the submicron particles. Some elements show a bimodal size distribution. Replotted from more complete data presented by Kauppinen and Pakkanen.¹⁴⁸

Amendments.^{149–151} These data will be used to illustrate the relationship between combustion emissions and stack emissions. The data on the collection efficiencies of particles and elements in ESPs compiled by Helble¹⁴³ is summarized in Table 2. The collection efficiency for some elements approaches the overall particle collection efficiency. Elements enriched in the fine particles have a slightly lower collection efficiency. Metals with high vapor pressure, Hg and Se, have a much lower collection efficiency across the ESP than the total particle removal. A wet scrubber for SO₂ removal also selectively removes species adsorbed on particles and can cause chemical reactions on the particles by humidification at moderate temperature and entrainment of chemicals from the sorbent solution.¹⁵² Additional aqueous-phase and photochemical reactions can take place in the stack plume and atmosphere.

Correlations between the emissions of elements from a boiler with the mass of elements fed with the coal¹⁵⁰ do not provide any insights on the effect of combustion conditions on the emissions. It is desirable to develop models to determine how the emissions are influenced by changes in combustion operating and design parameters. Laboratory studies have provided the mechanism for vaporization and condensation processes that govern the size and composition of the ash that can be used to develop ash transformation models. To be able to determine the effect of changing combustion modifications or changing APCD performance, one needs to combine a size-dependent model of emissions with a size-dependent model of APCD performance. Such a model has been developed by Helble in his retrospective analysis of the EPRI and DOE field studies of air toxics emissions.¹⁴³ For the fundamental combustion particle studies to be useful to the regulatory and health communities, more attention needs to be paid to the role of the downstream heat transfer

sections, the APCD, and the initial plume condensation in modifying composition and size distribution of the emissions from the combustor. Until suitable integrated computational models of the downstream processes are available, the best measures of the contribution to human exposure from various combustion sources will be empirical data from stack or exhaust measurements.

A summary of the emissions from these four different combustion applications follows. It should be noted that there is wide variability in both the source PM and in the downstream particle removal efficiency depending on fuel type and combustor size. Coal-fired boilers are equipped with high-efficiency APCD and emit particles enriched in the 0.1–1 μm range, where the particle removal efficiency is at a minimum. Oil-fired boilers often do not have any APCD because of the low ash and sulfur content of the fuel. As a consequence, large particles, such as coked fuel residue, may be emitted in addition to the submicron condensation aerosols. Small combustors, such as fireplaces and open burning, do not have any particle control devices.

SPECIFIC COMBUSTION APPLICATIONS

This section discusses the particle emissions entering the atmosphere from various practical combustion applications, both with and without post-combustion particle removal and gas cleaning. Typical data on PM mass emissions, size distribution, and composition are provided for convenient reference. The citations can serve as a starting point for a literature search, but a comprehensive review of the literature for each of these individual applications is not attempted. The extensive compilation of combustion emission factors prepared by the EPA¹⁵³ emphasizes PM₁₀ mass and provides little data on particle number distribution or on chemical composition of the PM.

Residential and Commercial Boilers and Furnaces

Distillate fuels, generally kerosene and No. 2 fuel oil, are widely used for domestic and process heat in areas where natural gas is unavailable. Direct population exposure to oil combustion emissions occurs because the fuel is burned in populated areas, and the furnaces do not have post-combustion particulate controls. The PM is mainly sulfate aerosol from fuel sulfur and soot plus organic aerosol from incomplete combustion. The ash content of distillate fuel is small, but not zero, so the emissions also contain inorganic components. In a study of homes with and without kerosene space heaters, the kerosene heaters were estimated to add ~40 μg/m³ of total PM_{2.5} and 15 μg/m³ of SO₄²⁻ to the indoor air.¹⁵⁴ Hildemann reported that the emission factor for particles smaller than 0.7 μm from an industrial-scale boiler fired with No. 2 fuel oil was 8 μg/kJ

Table 2. Field data on trace element capture efficiencies in ESP.

Element	ESP Capture Efficiency	Metal Capture/ Particle Capture
Vapor-Phase Metals		
Hg	28.9%	0.29
Se	49.1%	0.49
Fine-Particle Enriched		
As	96.1%	0.969
Pb	96.8%	0.976
Not Enriched in Fine PM		
Co	98.2%	0.992
Mn	98.5%	0.993

Note: Elemental capture in the ESP depends on the size-dependent partitioning of the metal to particles. Data from Helble.¹⁴³

of fuel.¹⁵⁵ These boiler emissions contained a mode near 50 nm and a larger mode near 0.5 μm . The fine particles consisted of about 32% sulfates, 29% EC, 6% organics, 6% NH_4^+ , and 3% other ionic and oxidized trace species (mainly SiO_2 , Al_2O_3 , Fe_2O_3 and Na^+).¹⁵⁶ The balance of the mass was in unidentified substances and may have included water in the form of hydrolyzed compounds. Detailed composition of the organic carbon (OC) portion of oil-boiler PM was also reported.¹⁵⁷

Residual Oil Fly Ash

Residual fuel oil is a highly viscous product that has a much higher ash content than distillate fuels, since the metals in the crude oil, as well as contamination from refinery catalysts and equipment, are concentrated in this fraction. Residual fuel oil is burned in some power plants, for example, in the eastern United States. Similar heavy fuel oil grades, Bunker C and marine diesel, are burned on ships, and these emissions are suspected to have a significant air quality impact on coastal cities. Metal mobilization from residual oil fly ash has been extensively studied^{158–160} because of the high content of V and Ni, which is different than other combustion PM.

The emissions from residual oil are multimodal, with a mode centered at 70–80 nm, but with most of the mass in a residual ash mode composed of cenospheric carbon-rich particles extending beyond 100 μm in diameter. Carbonaceous material can be greater than 75% of the mass emissions from small residual oil-fired boilers.¹⁶¹ The formation of carbonaceous PM during residual oil combustion is related to the asphaltene content of the fuel.^{162,163} When the residual oil is burned more efficiently under conditions typical of a utility boiler, the carbon content is lower and the PM is almost entirely in the ultrafine (condensation) mode.¹⁶⁴ The transition metals in residual oil combustion ash are in the form of sulfates rather than sulfides or oxides.^{165–167}

Coal-Fired Steam Generation Boilers

The stack emissions from coal-fired utility boilers are affected by the particle generation during combustion and by particle transformations and size-selective removal during cool-down and gas cleaning. Power plant coal combustion including pollutant formation,^{168,169} ash formation and deposition,¹¹⁵ submicron particle formation,^{14,66,170} and metal transformation⁷³ have been reviewed. The inorganic particle stack emissions consist of a supermicron mode containing spheres of mineral ash and a submicron mode formed by mineral vaporization and condensation, as discussed above. The carbonaceous emissions consist of supermicron char particles remaining from incomplete combustion of the parent coal. Submicron carbon-rich particles, suggestive of soot, are also present in the exhaust

from both laboratory- and full-scale coal combustors.^{171–174} Figure 12 shows the cumulative mass emissions versus size for a sample of power plants including both pulverized coal and cyclone burners.^{118,175,176} The multimodal size distribution of the emitted PM is indicated by the changes in slope of the cumulative mass curve. Full-scale data show that an ultrafine particle mode can be detected for both circulating and bubbling fluidized bed coal combustion, but the ultrafine concentration is several orders of magnitude smaller than the ultrafine PM concentration produced by pulverized coal combustion.^{177,178}

Many of the field studies of coal-fired power plants were aimed at obtaining the information needed for regulatory purposes, so the measurements have focused on the total mass of the emissions. Selected field studies have determined the fractions of the trace elements entering a boiler that enter the flue gases and pass out of the unit through the stack.^{63,78,88,148,152,179,180} Additional efforts have focused on the effectiveness of APCDs in removing these potentially toxic substances.^{63,78,179,180} These studies provide the following information:

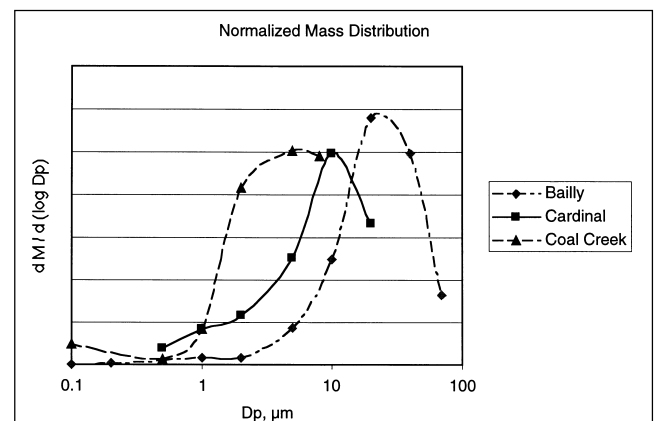


Figure 12. Normalized differential particle mass distributions measured in the stack for a sample of coal-fired power plants using different burner and gas-cleaning technologies. Data compiled from DOE field studies in 1993–1994.^{118,175,176} The stack particle mass emission rates vary between replicate runs by about a factor of 2 due to sensitivity to plant operating conditions.

Plant	Description	Stack Emissions
Bailly	345 MW, Cyclone Burner Dry scrubber, ESP	60 kg/hr
Cardinal	Illinois high-sulfur bituminous 615 MW, well-mounted cell burner ESP, no sulfur removal	100 kg/hr
Coal Creek	Pittsburgh No. 8 bituminous 550 MW, tangential-fired Wet scrubber, ESP North Dakota lignite	260 kg/hr

- The inorganic ash size distribution is multimodal. The submicrometer particles consist of aggregates of primary particles that have grown to 10–50 nm. The larger particles consist of spherical particles, including cenospheres and plerospheres.^{120,127,181}
- Particles entering the APCD are essentially bimodal in terms of mass, with on the order of 1% of the ash consisting of submicrometer particles and the larger residual ash falling into the 1–20 μm range.^{54,63,180,182}
- Particles in the 0.1–0.3 μm range have the highest penetration through APCD compared with both larger and smaller particles,^{63,78,179,180} so the 0.1–1 μm particles form a larger fraction of the mass distribution leaving the APCD than they do in the uncontrolled combustion emissions.⁶³
- The submicrometer ash is enriched in volatile elements relative to the larger particles.^{148,152} The concentration of the trace elements within the submicrometer and supramicrometer ash fraction increases with decreasing particle size.^{73,88}
- The surfaces of the ash particles are also enriched in volatile elements relative to their core.⁸⁸
- The major influence on the fraction of ash that is vaporized is the temperature.

Because NO_x is also temperature-dependent, a correlation between high NO_x emissions and high amounts of submicron particles has been reported^{55,64,76} for boilers in which the thermal (Zeldovich) kinetics dominate the NO_x emissions. For modern, post-New Source Performance Standards boilers, the NO_x emission is dominated by fuel nitrogen. The correlation between NO_x and submicron particle formation is not as well established for these conditions, since conversion of fuel nitrogen to NO_x is controlled by staging the air, and NO_x formation does not necessarily correlate with temperature.^{183–185}

Metals may partition into three major emission streams: the stack, the bottom ash, and the fly ash collected during gas cleaning. An example of this type of

data, summarized in Table 3, shows the points in the power plant process where As, Cr, Hg, and Se are removed and the fraction of that element in the raw coal that is emitted from the stack.¹⁸⁶ The toxic metals in the PM emissions are the result of fuel composition, combustion conditions, and downstream cleanup. Coal washing can greatly reduce the input of toxic metals to the boiler. A small fraction of the volatile metals is removed with the bottom ash, some metals are adsorbed on particles and removed in the ESP, and flue gas desulfurization systems can remove metal ultrafines and vapors. Metal emissions from coal-fired steam generation boilers are not currently regulated in the United States. Table 4 lists typical physical characteristics and chemical composition of coal fly ash.^{129,130,187–189} Coal fly ash typically contains less than 5% unburned carbon, but problems with char burnout can result in much higher carbon values.^{125,190–192}

Elemental balances on power plants show that ~1–4% of most metals in the fuel are emitted in the stack PM.^{143,148,152,178,193} The major exceptions are Se and Hg, which escape as vapors. Rapid quenching from high temperature results in the formation of glass-phase species of indeterminate composition rather than the crystalline minerals with similar elemental composition. Optical microscopy on fly ash from ESPs shows that 11–48% of the fly ash has crystallized at the cooling rate normally encountered in boilers. Iron in an alumino-silicate glass is a characteristic phase found in coal fly ash formed under both oxidizing and reducing conditions.^{194–196} The presence of large concentrations of alkali and alkali earth elements, typical of western U.S. coals, enhances glass formation and decreases crystallization.¹²⁹

Large-Scale Biomass Combustion

Concerns regarding trade balance, global warming, and disposal of agricultural residue have led to an increased interest in biomass as a renewable energy source. The unique characteristic of biomass PM is the high alkali content, especially K,^{197,198} compared to fossil fuel combustion ash. Studies have been conducted of industrial-scale biomass combustion, especially in fluidized bed boilers.^{199,200}

The ash formation processes during suspension firing of wood sawdust and sanderdust have been shown to be similar to the mechanism for pulverized coal combustion,²⁰¹ as indicated in Figure 3. The supermicron particles are predominantly Ca, but also contain Fe, Al, Mn, and Si. The alkali minerals form a submicron condensation aerosol that is ~30% of the total ash mass, which is much higher than the fraction of submicron ash from coal combustion.

Cofiring of crop residues with coal in existing power plants has been proposed as an

Table 3. Elemental partitioning in a coal-fired power plant.

	Coal Washing	Boiler Bottom Ash	ESP or Fabric Filter	Flue Gas Desulfurization	Emitted from Stack
As	65–75	0–2	85–99	0–20	0–5
Cr	30–75	3–20	85–99	0–20	0–2
Hg	30–40	0	0–60	10–90	5–95
Se	25–50	0–5	10–80	0–50	20–80

Note: Data obtained during the DOE PISCES program shows the percent of the element in the raw coal that is removed at various points in the process. Based on original DOE report and other reports.¹⁸⁶

Table 4. Typical coal fly ash properties.

	Typical Value	Range	Notes
Specific Gravity (single particle)	2.2	1.8–2.6	<1 for cenospheres
Specific Gravity (bulk ash)		1.1–1.5	includes voids between particles
Elemental Composition			
	Typical %	Range %	Expressed as Oxides
Al ₂ O ₃	25	13–36	
SiO ₂	45	22–61	
Fe ₂ O ₃	20	4–20	
CaO	2.6	1–22	
MgO	1.3	1–5	
TiO ₂	1.2	1–3	
Na ₂ O	0	0–8	
K ₂ O	2.1	0.3–4	
SO ₃	2	0–25	
Trace Metals		ppm levels	
Phase Distribution			
	Typical %	Range %	
Unburned Carbon	3	0 to >10	
Amorphous Glass		50–90	
Crystalline Minerals		11–48	
Major Minerals			
		Range %	
Mullite		2–20	Al ₆ Si ₂ O ₁₃
Quartz			SiO ₂
Iron Spinel			(Mg,Fe)(Fe,Al) ₂ O ₄
Hematite			Fe ₂ O ₃
Anhydrite			CaSO ₄

Notes: Typical fly ash composition is for Pittsburgh No. 8 high volatile bituminous coal fly ash; ranges compiled from various sources.^{129,187,188}

economical way to reduce PM emissions from open burning in the fields and to replace fossil fuel.²⁰² Laboratory studies of inorganic species behavior during cofiring have been conducted.²⁰³ A field study of cofiring coal and straw reported a number concentration of 5×10^7 particles/cm³.²⁰⁴ This high number concentration may be due to the use of an injector diluter installed directly in the flue.

Domestic Combustion

A significant amount of combustion takes place indoors, for example, tobacco smoking, natural gas appliances, oil-fired furnaces, fireplaces, and wood stoves. Domestic combustion is especially important when considering population exposure to combustion particles on a global basis. Smoke from small-scale domestic combustion of biomass, locally produced coal, and other opportunity fuels results in a direct exposure to sensitive individuals, such as the elderly and children, since the fires are located in or near homes. Fresh and aged wood smoke may be especially important for health effects because the small par-

ticle size results in enhanced deposition in the lower respiratory tract.²⁰⁵ Cooking and heating with biomass represents a large portion of the total combustion in developing economies. For example, household biomass combustion in Pakistan is estimated to represent 37% of the total primary energy consumption of the country.²⁰⁶

Poorly ventilated cooking fires can create indoor particle levels that are far above the U.S. ambient PM standard of 150 µg/m³. A geometric mean kitchen PM₁₀ concentration of 1830 µg/m³ was reported in a study of Bolivian highland villages.²⁰⁷ The kitchen PM_{2.5} concentration in homes using biomass for cooking averaged 555 µg/m³ with a maximum of 1493 µg/m³ ($n = 7$ homes) in rural Mexico.²⁰⁸ Recreational biomass fires are a surprisingly large source of combustion emissions in developed countries, and fireplace restrictions have been imposed in many cities and mountain resort communities to avoid violations of the current PM₁₀ standard. For example, combustion of wood in residential fireplaces has been estimated to contribute 14% of the annual average OC emissions to the Los Angeles urban atmosphere.²⁰⁹

Particle emissions from biomass vary with both the combustion conditions and the fuel type. One study of PM emissions from residential wood fires distinguished between hot, rapid combustion and slower, low-temperature, air-starved combustion.²¹⁰

Hot burning produced a monomodal particle distribution with 30–40% of the particles between 0.3 and 0.6 µm. The particles were predominantly EC and OC, but contained percent levels of K, Cl, and S with 0.01–1% levels of Al, Si, P, Zn, Pb, and Fe. For cool burning, the particles were largely OC, and almost 50% of the carbon was associated with particles between 0.6 and 1.2 µm.

Combustion efficiency, wood moisture, and dilution gas temperature affect the particle size distribution, indicating that the actual winter fireplace PM may have a higher fraction of fine particles than are measured under laboratory conditions.²¹¹ Hildemann provided detailed particle size distribution graphs of fireplace emissions and calculated an emission factor of 10 g PM/kg wood burned based on electrical aerosol analyzer size measurements, and reported 16 g/kg based on filter weight.¹⁵⁵ Rogge reported fine particle emissions from fireplaces ranging from 6.2 g/kg for oak to 13.0 ± 4.0 g/kg for softwood,²⁰⁹ and suggested that unique organic species, such as tricyclic resin acids, can serve as markers of wood smoke in the

atmosphere. The amounts of various PAH compounds resulting from domestic combustion of biomass fuels have been reported.^{209,212,213}

Regional differences in domestic combustion may provide the opportunity to conduct long-term exposure health studies that integrate epidemiologic methods with detailed characterization of the PM. For example, domestic combustion of coal has been associated with the high incidence of lung cancer in Xuan Wei, China.²¹⁴ Chemical characterization of indoor air in homes using smoky and smokeless coals showed 1–2 orders of magnitude differences in the concentration of PAH. The PAH and polar extracts from the particles in homes using smoky coal were highly mutagenic.^{215–217}

Wildfire and Agricultural Burning

Open fires from wildland and agricultural burning are a significant source of atmospheric PM on a global scale. Concerns include acute health effects to people near the fires, climate effects,²¹⁸ and regional visibility.²¹⁹ PM from large fires can be transported over continental distances. High PM₁₀ in the eastern United States during the summer of 1998 was caused by smoke from fires in Mexico,²²⁰ as shown by satellite photos. EPA policy²²¹ does not consider exceedances of National Ambient Air Quality Standards (NAAQS) from natural events such as seismic and volcanic activity, wildland fires, and high wind to constitute a violation for the legal purpose of designating non-attainment areas. However, high particle concentrations are a health and environmental concern whether the source is classified as natural or anthropogenic. Fire is important for recycling nutrients and for preventing the spread of invasive species in many ecosystems. Balancing the ecological role of fire with the goal of minimizing particulate levels in populated areas is a concern for land management in the western United States and in other areas with grassland ecosystems.

Emissions from wildland and agricultural fires are poorly characterized because of the variability in combustion conditions, for example, upwind versus downwind propagation, fuel loading per area, and fuel moisture. Hot fires produce more NO_x, but less CO, unburned hydrocarbons, and soot than smoldering fires. Quantitative data on particle size, number concentration, and chemical composition that would be useful for epidemiology correlations and for mechanistic toxicology studies are limited by the difficulty of field measurements and the uncertainty of how to scale from laboratory experiments to real open fires. Inventory estimates of PM emissions from open fires are based on empirical factors for PM per weight of fuel burned multiplied by an ecosystem-based estimate of fuel loading

per area. Typical emissions factors are: 4 g of total suspended PM/kg of biomass burned for piled logging slash with no soil debris; 16 g/kg for smoldering combustion of conifers in temperate forests;¹⁵³ and 20 g/kg for tropical forest fires.²²² Emissions of PAH have been measured in a wind tunnel for simulated open burning of cereal grasses and tree prunings.^{223,224} Weakly spreading fires were observed to produce higher levels of the heavier PAH with more of the PAH partitioned to the particulate phase. PAH emissions were more strongly influenced by the burning conditions than by the type of fuel.

Oil Pool Fires

Management of large oil spills presents another case of balancing ecosystem health and ambient air quality standards for PM. Igniting an offshore oil spill can reduce the impact on aquatic and shoreline species, but also creates a large plume of particulate air pollution. An understanding of the characteristics of the PM emissions, as well as an understanding of the atmospheric dispersion and clearance, are needed to assess when to burn. Limited data on pool fire emissions are available from laboratory and mesoscale measurements.²²⁵ The PM mass emissions range from 5% of fuel burned (50 g/kg) for laboratory fires to 15% of the fuel for a 17.2 m pool fire, showing that the smoke yield increases with increasing fire size. The particle size distribution from one mesoscale measurement was 50% of the mass in particles less than 0.7 μm and 90% in those less than 20 μm.²²⁶ This is much larger than typical soot emissions, suggesting that the high particle loading in pool fire plumes allows large aggregates to form. The size of the primary particles that form the smoke aggregates increases with increasing fire diameter.^{98,227} The primary particle size trends and morphology determined by thermophoretic sampling²²⁸ for TEM examination are consistent with formation of soot on the fuel-rich side of the flame and agglomeration upon local flame interface extinction. Oil pool fire smoke is greater than 90% EC, and the PAH emissions from oil pool fires on water have been measured.²²⁹

Incineration Emissions

Much research has been done on metal transformations during hazardous waste incineration due to the controversial nature of the projects, and due to regulations that require quantifying metal emissions of incinerators during the permit application process prior to facility construction. Although incineration is a small source of PM emissions on a global scale, the unusual compositions of the waste feeds provide valuable insights into the thermochemistry of trace metals. For incinerators, the ash vaporization is affected by both temperature and Cl concentration, since the chlorides of many metals have a high

vapor pressure.^{59,230} The formation of submicron particles and the formation of a bimodal particle size distribution in incinerators is very similar to the process that has been observed for coal. Unusual waste streams may result in incineration fly ash containing high levels of volatile metals, but in many cases the bulk of the particle mass from incinerator combustion is the refractory oxides.

An extensive review has been conducted by Linak and Wendt,⁵⁹ and Lighty and Veranth²³¹ have also discussed the issue. The partitioning of a metal in a hazardous waste incinerator depends not only on the temperature⁵⁹ and the gas environment, but also on the constituents within the solid matrix.²³² The metals either react with the solid matrix to form solid materials that might be nonleachable, or they may vaporize and undergo nucleation and particle growth similar to the processes previously discussed for submicron inorganic ash from coal. Vaporization also depends upon the type of metal. Normally, Cd²³³ is found to be more volatile than Cr; however, the results depend on the solid matrix. The high levels of Cl present in incineration gas-phase emissions compared with fossil-fuel combustion affect the formation of fine PM.^{230,234,235} The metal chlorides are generally more volatile than the metal oxides, so Cl causes higher vaporization, which leads to increased formation of submicron particles enriched in trace elements. Differences have been observed between the effect on particle size of inorganic versus organic Cl, that is, NaCl and PVC in the feed,²³⁶ suggesting the importance of intermediate species in the reaction pathway.

If a listed toxic metal remains with the solid, the ash must meet land-disposal regulations, which require a leachability test. Research has shown that Pb may interact with the aluminosilicates in solid materials.^{59,237,238} Others have studied the injection of sorbents for metals control, which captures the volatile metals in a sorbent-derived particle.^{102,232,239,240} In some cases, a non-leachable solid was formed.

Laboratory-scale elemental composition and particle size data have been reported for conditions applicable to commercial incinerators.²⁴¹ Metal speciation data is more difficult to find since the metals are normally present only in trace amounts, which are difficult to detect by many speciation methods. However, Linak et al. demonstrated that the toxic form of chromium, Cr VI, was only a few percent of the total chrome emitted from a laboratory scale system,²⁴² except in the presence of Cl. When large amounts of Cl were present, the percent emitted was between 5 and 8%, still low. Thermodynamic calculations also show that input waste composition has a greater effect on Cr VI formation than does operating temperature.²⁴³

Data on full-scale incinerators are collected at the stack to demonstrate compliance with emissions limits. Due to the high particle removal efficiency, the emissions from

incinerators are controlled by gas cleaning equipment performance. Combustion conditions impact emissions indirectly through changes in the particle size distribution, which influences air pollution control equipment performance. A study to characterize the performance of various incinerator gas cleaning systems showed that the PM mass concentration, corrected to 7% oxygen, measured at the secondary combustion chamber exit was 5 ± 0.6 mg/m³, while the concentration downstream of a baghouse and ionizing wet scrubber combination was 0.013 ± 0.009 mg/m³.²⁴⁴ The control efficiency for individual elements ranged from 95 to 99.995% removal between the gas cleaning inlet and the stack. The differences in removal efficiency between elements are expected to reflect differences in the partitioning of each element to different particle size fractions, and to the liquid and gas phases. Kauppinen and Pakkanen presented graphs showing the elemental distribution in the emissions from a hospital incinerator,²⁴⁵ which shows that Pb and Cd are enriched in the submicron particles. The authors are unaware of similar published data on the detailed size distribution of combustion exhaust or stack PM from commercial hazardous waste incineration.

Internal Combustion Engines

IC engines represent 20–40% of the fossil energy combustion in developed countries, and contribute emissions that are concentrated in urban areas. Particulate emissions from engines have been extensively studied due to concerns over the smoke emitted by diesel engines, lead emissions prior to the phase-out of leaded gasoline, and health effects of ultrafine particles. The general process of particle formation as discussed in the fundamentals section is fully applicable to IC engines. However, understanding particle formation in the cylinder of a high-speed engine involves both the chemical kinetics which have been determined from experiments in idealized laboratory flames and the transient temperature and volume changes, fuel/air mixing, and heat transfer unique to in-cylinder conditions.

A large body of specialized literature on IC engines exists. Details of engine design,^{246,247} combustion in the cylinder,^{248–252} in-cylinder measurements,²⁵³ the use of fuel formulation and additives for soot control,²⁵⁴ PM from catalytic converters,²⁵⁵ and the development of particle traps for diesel engines²⁵⁶ are outside the scope of this paper, and the reader is referred to the cited reviews and collected papers.

The filterable particles from IC engines, including both soot and inorganic PM, are either individual submicron particles or are loosely bound aggregates formed from ultrafine primary particles, as discussed in the fundamentals section. Soot and organic PM result from incomplete combustion. The inorganic particles are derived from fuel

and lubricant additives, fuel contamination, engine wear, and ambient PM that passed through the air filter. Caution is needed when looking for data on the fraction of ambient PM attributed to IC engines, because non-combustion particles from resuspended road dust and from the wear of tires and brakes are listed under "mobile sources" in some emissions inventories.

Soot formation in IC engines has been studied due to regulation of the black smoke that can be emitted by diesel engines under heavy load, and due to the importance of soot on radiant heat transfer and flame structure. The topic of soot from internal combustion is covered in detail in books by Heywood²⁵⁷ and Sher.²⁵⁸ Empirical data show that diesel smoke emissions increase with load, but can be reduced by improved fuel-air mixing and by better control of fuel injection. Work by John Dec and colleagues²⁵⁹ using laser sheet visualization has shown that, under typical diesel conditions, the initial premix phase of diesel combustion occurs in a fuel-rich vapor-fuel/air mixture (equivalence ratio of ~4) in the leading portion of the fuel jet, just downstream of the maximum liquid-fuel penetration. This vapor-fuel/air mixture is fairly uniform with a sharp well-defined boundary at the jet periphery.

The measurements show that as autoignition occurs, the fuel breaks down over the whole premixed, fuel-rich region almost simultaneously (i.e., within ~70 μsec), followed very quickly (less than 70 μsec) by PAH formation throughout this region. Then, ~140 μsec later, initial soot formation occurs with very small particles forming throughout large sections of this leading portion of the jet. Within an additional 70 μsec , the entire region is filled with small soot particles whose volume fraction is increasing rapidly. The actual emission from the cylinder to the exhaust manifold is the result of competition between soot formation and soot oxidation. Soot oxidation is reduced when the combustion process is prematurely quenched. This occurs when excessive injection of fuel results in the burning mixture contacting the cylinder walls.

Table 5 summarizes exhaust measurements of particle size and number concentration data from selected studies of diesel and gasoline engines.^{27,260-266} The exhaust tailpipe data show that IC engines are a source of particles smaller than 100 nm at initial concentrations greater than $10^6/\text{cm}^3$, which is consistent with measurements of ambient particle size distributions at various distances from urban highways.^{267,268}

The sizes of diesel particulate emission can be approximated by a bimodal lognormal distribution.²⁶² The nanoparticles in the ultrafine transient mode of diesel engines represent only 0.1–1.5% of particle volume (mass) but 35–97% of the particle number.²⁶² Most of the PM mass is in a mode with a diameter between 0.01 and 0.1 μm . From the available studies, the relative importance

of surface growth and coalescence in determining the particle size in this larger mode is unclear. Typical exhaust PM mass concentrations from well-maintained modern diesel engines are 15–30 mg/m^3 .²⁶² With older engines, the PM mass is higher, the number of ultrafines is much lower, and a condensation or accumulation mode dominates the number distribution.²⁶⁹ The high particle number of $1 \times 10^9/\text{cm}^3$ reported for a 1991 Cummins engine by Bagley et al.²⁶⁰ has led to the speculation that the reduced particle mass emissions in the newer diesels has resulted in increased particle number. The hypothesis is that there are insufficient soot particles to provide surface for the condensation of the heavier organic or acid molecules, which therefore become supersaturated in the vapor phase and nucleate as the exhaust cools in the sampling train.²⁷

Gasoline engines have much lower PM mass emissions than diesel engines. Tailpipe particle emission mass is as low as 0.1 mg/mi , and the baseline number concentration is 10^5 – 10^6 particles/ cm^3 ,^{264,266} which is consistent with the reported accumulation mode particle size. Graskow et al.²⁶⁴ reported that the particle number from gasoline engines is highly unstable and that they observed intermittent spikes in particle number up to 2 orders of magnitude above the baseline. The formation of deposits in gasoline engines, which can contribute to particulate emission spikes, has been reviewed by Kalghatgi.²⁷⁰ Fuel parameters have a strong effect on the fuel/air ratio at which the maximum gasoline engine particulate emissions occur.²⁷¹

A single instrument cannot measure the entire range of inhalable particles from less than 10 nm to over 10 μm that are potentially emitted by an IC engine. By using both a scanning mobility particle sizer (SMPS) and an aerodynamic particle sizer, the full particle size distribution from an engine can be reported in segments. For a diesel engine, Morawska et al. reported 10^4 – $10^5/\text{cm}^3$ in the accumulation mode centered on 0.1 μm and ~1 particle/ cm^3 in the range from 1 to 10 μm .²⁶³ One particle at 5- μm diameter weighs the same as 1.2×10^5 particles at 0.1- μm diameter. The uncertainty introduced by interconverting particle mass concentration and particle number concentration data for the purpose of testing health effects hypotheses related to vehicle emissions is apparent.

Mass and surface area of submicron particles are inferred from number and diameter measurements assuming a spherical shape and an appropriate density. Comparisons of filter samples and the total emission mass calculated from integrating particle size and number data agree semiquantitatively,²⁶⁵ generally within a factor of 2. This difference may not be significant compared with the wide range of PM emissions from real vehicles depending on age, operating conditions, and maintenance history.

Table 5. Selected measurements of particle emissions from internal combustion engines.

DIESEL			
Engine & Condition	Number Mean	Results	Reference
1991 Cummins—various modes with and without catalyst	Nuclei 11–17 nm Accumulation 55–73 nm	>10E9 particles/cm ³ . High number count in smallest size bin measured. Size distribution graphs and lognormal fit.	260
Newer catalyst-equipped, LNG-fueled, and older leaded-fuel vehicles	Count Median Diameter 39–60 nm	Exhaust number concentration, 1.5E4 for catalyst, 8.4E4 for LNG, 7.9E5 for leaded.	261
1995 direct injection—various modes	Nuclei 5–9 nm Accumulation 29–40 nm	1–7E7 particles/cm ³ . High number count in smallest size bin measured. Size distribution graphs and lognormal fit. Mass 15–30 mg/m ³ .	262
Various in-service engines 1983–1996	Accumulation 30–160 nm Also data on 0.3–30 μm size range.	0.7–3.9E7 particles/cm ³ in SMPS range. Particle number increased with increasing power.	263
Review paper	Nuclei 5–50 nm Accumulation 0.1–0.3 μm.	1E7–1E8 particles/cm ³ . Graphs of particle number and size vs fuel/air ratio for various engines.	27
GASOLINE			
Engine & Condition	Number Mean	Results	Gasoline
1993 4-cylinder	Nuclei <10 nm Accumulation 70 nm	Emissions highly unstable. Baseline 1E5/cm ³ with spikes to 1E7/cm ³ .	264
Review paper	40–70 nm	1E5–1E6 particles/cm ³ . Varies with fuel/air ratio.	27
Various automobiles 1994–1997	30–70 nm	Did comparisons of total particle number and filter collected mass over test cycle.	265
Various automobiles 1995–1998	25–107 nm	Compared various results from test cycles. Mass 0.1–9.6 mg/mi.	266

A program of dynamometer tests on 23 in-service spark ignition vehicles ranging from 1976 to 1990 model years showed particulate emissions ranging from 7.2 to 1342 mg/mi,²⁷² and the OC ranged from 35 to 95% of the total carbon.

Various investigators have reported the chemical composition of IC engine PM as a function of particle size and operating conditions. The PM is a mixture of EC, organic compounds, metal oxides, and sulfates. The exhaust from a typical heavy-duty diesel is 31–41% EC or soot, 25–40% unburned oil, 7% unburned fuel, up to 14% SO₄²⁻ and H₂O, depending on fuel sulfur content, and 13% ash and other inorganic, and there is usually some mass listed under unknown origin.^{27,273}

Data on partitioning between soot and the soluble organic fraction²⁷⁴ and between EC and OC by thermal/optical reflectance from IC engine emissions are available.²⁷²

Detailed organic composition of emissions from in-service gasoline and diesel engines by GC/MS analysis of extracts have also been reported.^{272,275,276} As will be discussed in the measurements section, the H₂SO₄ and heavy organic products of incomplete combustion may form particles in the atmosphere that are not included in the PM as measured by standard procedures. In the United States, particulate emissions are regulated by the mass collected on a filter at 325 K (125 °F) followed by equilibration at 295 K and 45% relative humidity before weighing.²⁷⁷ Figure 13 shows the complex nature of the condensable organic aerosol collected from diesel engines using a dilution sampler.²⁷⁶ Only a small fraction of particle-bound material is resolved into known compounds, and even the resolved fraction contains multiple chemical compounds within each category. Dilution samplers^{155,278} can quantify the mass and composition of the condensable

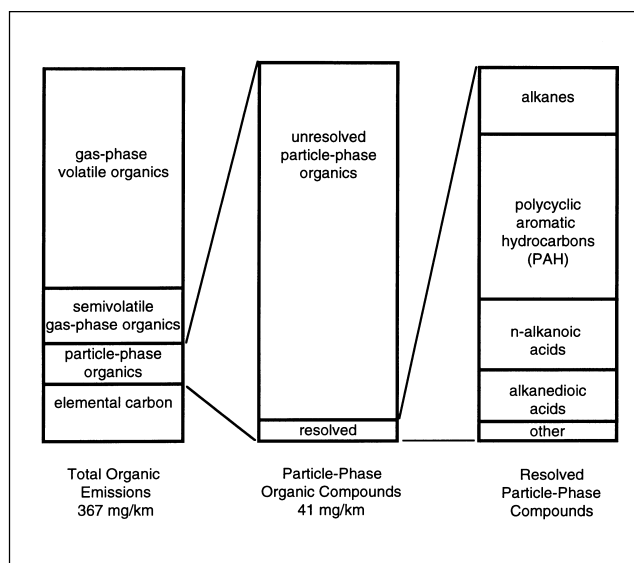


Figure 13. Organic analysis of the exhaust emissions from medium-duty diesel trucks. Only a small fraction of the particle-phase organics were resolved into identified compounds. Replotted from data by ref 276.

PM, but may distort the size distribution. The effects of dilution on PM size distribution will be discussed in the measurements section.

Vehicles need to be considered as a potential source of particle-bound transition metals in health-related studies. Table 6 provides illustrative data showing the metals content of diesel and gasoline emissions, and shows that IC engine emissions have significant metal content. Metals are reported in mg/mi for the average of two in-service diesel trucks sampled in 1996 in California²⁷⁶ and for the average of four 1995 model-year Ford automobiles.²⁷⁹ The variation in the data is large, and only the elements where Schauer et al.²⁷⁶ reported a mean greater than twice the standard deviation are listed. The total mass emissions from the gasoline contain 9–31% metallic elements

Table 6. Metals emissions from internal combustion engines.

	Diesel Trucks	Automobiles
Total Mass	845 ± 22	7 ± 4
EC	260 ± 9	NR
OC	166 ± 6	NR
Si	5.3 ± 0.2	0.12 ± 0.12
Fe	0.42 ± 0.02	0.11 ± 0.09
Zn	0.59 ± 0.03	0.009 ± 0.005
S	1.86 ± 0.07	0.7 ± 0.9
SO ₄ ²⁻	8.5 ± 0.5	NR
NH ₄ ⁺	6.2 ± 0.3	NR

Notes: Emissions in mg/mi were calculated by the authors from data reported by Schauer et al.²⁷⁶ and Ball.²⁷⁹ NR = not reported.

by weight. PM emissions of 27 elements from in-use high-emitting vehicles were reported by Cadle et al.²⁸⁰

Leaded gasoline has been phased out in the United States and in many developed countries, but it is still used. The particulate emissions from automobiles burning fuel with 0.4 g Pb/liter are about 25% Pb,²⁸¹ and the mass mean particle size is 1–2 μm,²⁴⁸ which is much larger than the PM from spark ignition engines running on unleaded fuel. The Pb emissions are on the order of 60 mg/mi. The measured Pb concentration also reflects dilution by the higher EC and OC content of emissions from gasoline engines that are not equipped with modern pollution control technology. Use of methylcyclopentadienyl manganese tricarbonyl (MMT) as an octane-boosting additive results in the emission of amorphous manganese sulfate and phosphate particles with a size ranging from 0.2 to 10 μm.²⁸²

Modern IC engines produce PM in both the ultrafine mode and in a larger accumulation mode, with nearly all the mass being in particles smaller than 1 μm. Emissions of PM, unburned hydrocarbons, NO_x, and CO all have declined as stricter regulations on new vehicle models have forced improvements in combustion technology and in post-combustion gas cleanup. The limits of current technology are being reached, and air-quality models are predicting an increase in total emissions from vehicles in the next decade as increases in vehicle-miles driven begin to outweigh the reductions in emissions that have been achieved by retiring older vehicles. Health concerns regarding particle number, ultrafines, and transition metals will lead to a need for more detailed characterization of IC engine emissions, especially under in-service conditions.

Aircraft Turbines

The aircraft PM emissions literature includes studies addressing both ground-level emissions near airports^{283,284} and cruise altitude studies emphasizing stratospheric chemistry and global climate effects.^{285–288} Visible smoke emissions from aircraft engines were first regulated by the 1970 Clean Air Act. The engine manufacturers retrofitted jet aircraft with smokeless combustors by 1978,²⁸⁹ and there is little published research on soot emissions from gas turbines from the late 1970s until the mid-1990s. Ground-level PM measurements show that most of the particle mass is soot and semivolatile products of incomplete combustion. Cruise altitude particle number is dominated by H₂SO₄ aerosol. Table 7 compares the mass, size, and number concentration for ground-level testing of engines representing 1970s²⁹⁰ and 1990s²⁸⁵ design technology. Conversion to smokeless combustion chamber designs has reduced particle mass and number concentration. However, aircraft engines still can be a locally significant source of submicron particles.

Table 7. Ground-level emissions from aircraft turbine engines.

	Stockham, 1979		Petzold, 1998 ^a	
Engine Type	TF-30, JT8D, JT9D		Rolls Royce	
Particulate Mass	Idle	1.85–4.41g/kgfuel	Total carbon	
	Cruise	0.29–2.09	0.27–0.74 g/kg fuel	
	Takeoff	2.8–7.06		
Particle Size	Idle	0.043 μm	Primary	0.045 μm
	Cruise	0.69	Coagulation	0.18
	Takeoff	0.60	Coarse	0.56
Particle Number Concentration	Idle	$9.3 \times 10^7/\text{cm}^3$	Primary	$8 \times 10^5/\text{cm}^3$
	Cruise	2.27×10^7	Coagulation	$2.5 \times 10^4/\text{cm}^3$
	Takeoff	1.9×10^7	Coarse	$1.5 \times 10^3/\text{cm}^3$

^aParticle number reported by Petzold was measured 200 m behind the engine and was not corrected for dilution.

EMISSIONS, AMBIENT CONCENTRATION, AND INHALATION EXPOSURE

The legal authority of air quality agencies extends only to the component of exposure that is attributable to ambient air,²⁹¹ and indoor air quality is controlled indirectly through public health advice, building codes, and product design regulations. Most of the average person's day is spent indoors or in vehicles, and sensitive individuals, infants, the sick, and the elderly spend even more time indoors than healthy working adults. Indoor particle concentrations can be very different from the outdoor ambient particle concentration that is measured by central monitoring stations. The indoor PM concentration and size distribution depend on the rate of outside air exchange, personal activity patterns, and indoor particle sources. In general, the concentration of coarse particles is lower indoors than outside, but activities such as sweeping, or even walking on a dusty carpet, can resuspend large quantities of coarse PM.

Institutional buildings have central air-handling systems that include filtration. A comparison of air samples in patient areas of three hospitals showed little correlation between indoor air PM_{10} and ambient PM_{10} at local air monitoring stations.²⁹² A better correlation is observed between indoor and outdoor fine-particle concentration. Accumulation mode ambient PM can penetrate into buildings because these particles are not efficiently removed by gravitational and inertial mechanisms. However, activities such as cooking and tobacco smoking are indoor PM sources that can increase fine-particle concentrations far above ambient levels. Personal exposure to particles depends on physical activity (ventilation rate) and on the amount of time spent in various environments indoors, in vehicles, and outdoors.

Health effects research must look at the actual human exposure, and many of the indoor sources involve combustion-generated particles. When discussing the health effects of combustion particles, one must consider that, with the exceptions of domestic combustion and tobacco smoking, people do not directly inhale combustion emissions. Persons inhale particles that have undergone post-combustion and atmospheric transformation. Different particle sizes are removed from the atmosphere at different rates, and the particles may become coated with condensable species. The cells deep in the lung are not exposed to the same particle mixture that is

measured by an ambient filter, due to size-selective removal in the airway. Some gas-phase chemicals that would ordinarily be removed by diffusion to the airway wall may penetrate deep into the lung when adsorbed on an inert particle, the "Trojan Horse" hypothesis.

Ambient PM Characteristics

As originally reported by Whitby and Sverdrup,²⁹³ and since confirmed by many studies, atmospheric particles have a multimodal size distribution, as shown in Figure 14.^{6,293–296} These modes include the coarse mode, which is usually mechanically generated; the accumulation mode of 0.1–1 μm particles; and a mode of fine particles resulting from nucleation and surface growth. The latter two modes are the consequence of nucleation, condensation, and coagulation to produce particles from gas-phase precursors. The true accumulation mode is the result of particles growing into the range where further growth is slow, because of decreased collision frequency, and where removal is slow, because inertial deposition and gravity settling are inefficient. The size and shape of the ultrafine particle mode in the urban atmosphere represents a dynamic balance between the generation of new particles (nuclei) by nearby sources and growth into the accumulation mode by coagulation and surface deposition.

The process of forming new particles by nucleation and the subsequent growth by coagulation and condensation are similar both in combustion systems and in the atmosphere. Nanoparticles are created from vaporized compounds by gas-to-particle conversion due to chemical reaction or cooling. These reactions may take place in the combustor, during initial dilution of the plume, or over a period of hours in the atmosphere. Nanoparticles are rapidly removed from the atmosphere by coagulation

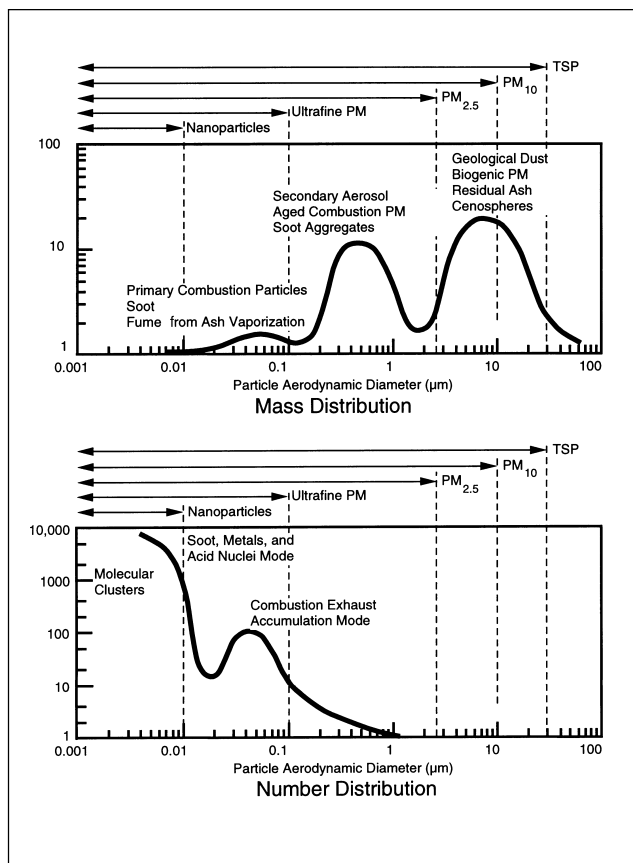


Figure 14. Typical PM mass and number distributions showing the multimodal nature of the ambient aerosol. Adapted from data by refs 6 and 293–295.

with each other and with larger particles. In addition, species condensing from the gas phase are deposited on ultrafine particles since they represent a large fraction of the available surface area. These condensing species include organic compounds, SO_4^{2-} , and NO_3^- formed by reactions in the atmosphere from precursors that are emitted as gases from combustion systems. Eventually, the ultrafine nuclei-mode mass is transferred into the accumulation mode consisting of particles between 0.1- and 1- μm diameter. Accurately measuring the ultrafine size distribution, in both the ambient air and combustion source emissions, is difficult because particle number is not conserved, ultrafine particles undergo rapid transformations, and there are few calibration standards available. Seinfeld and Pandis provide a detailed treatment of ambient aerosol characteristics.⁶

Gravimetric measurements of particle mass generally show only the coarse and accumulation modes unless the data are plotted on a logarithmic scale. Likewise, optical and electrical mobility measurements of particle number usually show only the nucleation and accumulation modes. Natural PM includes wind-transported geological material, biogenic PM (pollen, spores, and secondary PM from VOCs), and sea salt. Naturally released sulfur and

nitrogen compounds produce additional PM, but the anthropogenic emissions of sulfur and nitrogen compounds dominate secondary particle formation in industrialized areas. Comparison of oceanic, polar, and remote desert aerosols²⁹⁷ to urban aerosols²⁹³ shows that the natural nucleation and accumulation modes are small compared to the anthropogenic contribution to fine PM. Reported concentrations of ultrafines in ambient air vary from 100 to 1000/cm³ in rural and oceanic environments, 10⁴/cm³ time-averaged in urban areas,²⁹⁸ and ~10⁶/cm³ near an urban freeway.⁶ Janecke²⁹⁷ provides quantitative descriptions of typical ambient aerosols as the sum of three log-normal distributions, which are useful for modeling input.

Source Apportionment and Modeling

Figure 15 shows that 80–90% of the PM mass emitted from combustion sources is below 1- μm diameter, while less than 10% of the mass of dust from geological material is PM_{2.5}.²⁹⁴ However, the evidence for the relative contribution of various PM_{2.5} sources is contradictory, and some source apportionment studies²⁹⁹ suggest that ambient PM_{2.5} is dominated by sources other than combustion particles. For example, Figure 16 shows ~62% of emissions coming from geological material and only 38% coming from combustion sources.^{300,301} Emissions inventories are based on multiplying census-type data by emission

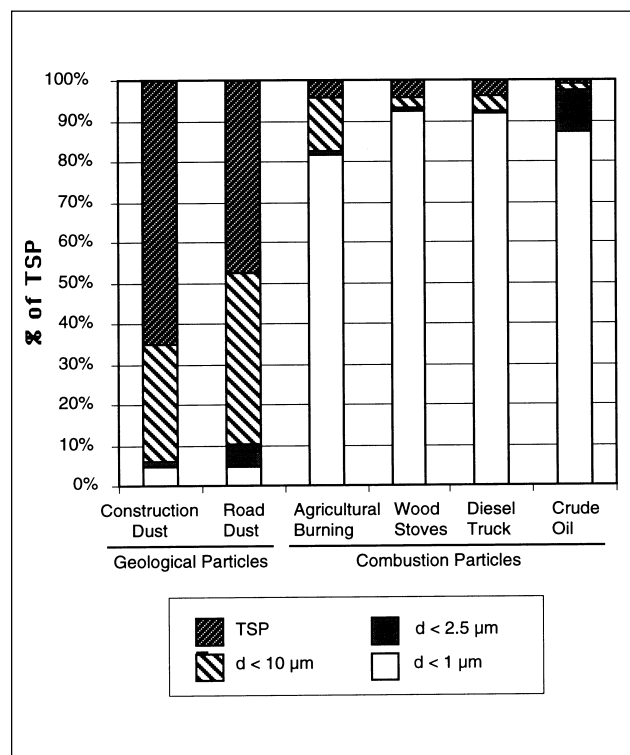


Figure 15. Typical size distribution for the emissions from geological dust sources and from combustion sources. PM₁ dominates the mass of combustion emissions, while most geological dust is larger than PM₁₀. Replotted from data in Watson and Chow.²⁹⁴

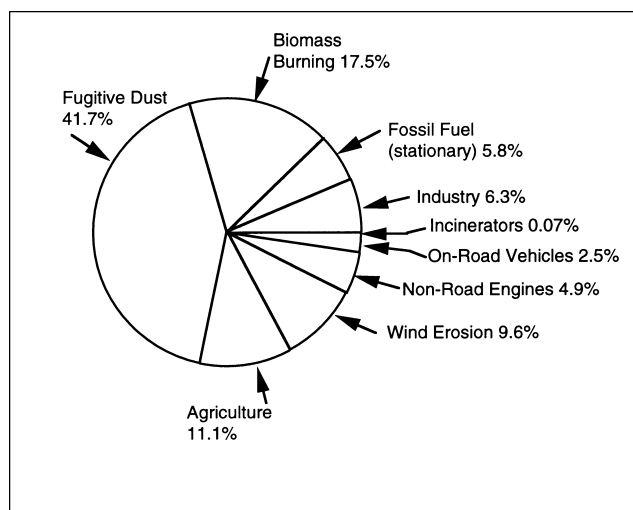


Figure 16. Inventory of the 1997 U.S. nationwide $PM_{2.5}$ emissions.³⁰⁰ Total mass was estimated as 10 Tg/yr. Major differences exist between inventory data and source apportionments based on the composition of particles collected at receptor sites. Source: U.S. Environmental Protection Agency.

factors, which are often based on only a few measurements. Both researchers and air quality agencies suspect that the fugitive dust component is overstated by these methods.²⁹⁴ If the fugitive dust is overstated, then some other contribution, such as combustion, is understated, as many urban areas are in violation of the PM standards. Suspected sources of the differences between emissions inventory and receptor-based methods of calculating source contributions include comparing national averages which are dominated by rural areas with monitoring stations which are concentrated in urban areas; not fully accounting for redeposition of wind-blown PM near the source area; and not including the effect of "super-emitter" sources such as improperly maintained and operated combustion sources in the inventory emission factors.

As EPA compiles information from speciated PM monitoring sites, it will be interesting to learn more about the chemical characteristics of ambient PM and how this can relate to specific sources, including combustion. International variation in the relative contribution of combustion and geological processes to ambient PM are expected because of local climate, geography, and technology preferences. For example, in urban areas in Taiwan, $PM_{2.5}$ was found to be as high as 80–90% of PM_{10} ,³⁰² and combustion was found to be a major source of both the coarse and fine PM.³⁰³ Likewise, particles larger than $2.5 \mu m$, or even larger than $0.5 \mu m$, are rare in the central European urban environment.³⁰⁴

The combination of particle size and chemical composition data provides insights into the sources. For example, the $PM_{2.5}$ in the eastern United States has a much

larger SO_4^{2-} component and a much smaller NO_3^- component than does the $PM_{2.5}$ from California.³⁰⁵ This result is likely due to the effects of coal-fired power plants in the east and of agriculture and mobile sources in the west. Source apportionment based on matching chemical composition of particles collected from known sources with the mixture collected at receptor sites is an active area of research.^{294,306–308} Reconciling source inventories with the particles actually collected at receptor sites has important public policy implications.

A mechanistic air quality model has been developed that allows computing the contribution of individual emission source types to the size and chemical-composition aerosol distributions.³⁰⁹ The model predicts that the submicron fraction of the PM does not contain appreciable amounts of secondary particles. Specifically, little SO_4^{2-} and no NO_3^- was predicted in the particles less than $0.1 \mu m$. For particles between 0.1 and $1 \mu m$, SO_4^{2-} concentration was slightly higher with a larger increase in NO_3^- concentration. Data from filters confirmed the modeling results,³¹⁰ although the sulfur concentration in the particles less than $0.1 \mu m$ was higher on the filters than predicted. The model explains the measured 0.2 - to $0.3\text{-}\mu m$ particles as transformed emissions from diesel engines and other combustion, and explains the observed 0.7 - to $0.8\text{-}\mu m$ particles as fine background aerosol that has been transformed by fog and gas-to-particle conversion in the urban air.³¹⁰ The model predictions are only as accurate as the source data and the atmospheric transformation chemistry models.

The observed particle size distribution in urban environments is the result of a dynamic balance between generation of ultrafine particles by combustion sources and the transfer of these particles to the accumulation mode by coagulation and by surface growth from secondary aerosol gas to particle conversion. While computational modeling may provide insights into the relationships between sources and human exposure, models are limited by the source data, and there is a need for more detailed characterization of combustion sources.

PARTICLE HEALTH EFFECT RESEARCH

Particles have long been implicated in the deterioration of visibility and the environment and as the cause of adverse health effects. As early as 1661, John Evelyn wrote,³¹¹ "It is this horrid smoake, which obscures our churches and makes our palaces look old, which fouls our clothes and corrupts the waters so that the very rain and refreshing dews which fall in the several seasons precipitate this impure vapour, which with its black and tenacious quality, spots and contaminates whatever is exposed to it." Evelyn goes on to say, "London fires, there results a great quantity of volatile Salts, which being sharp and dissipated

by the Smoake doth infect the Aer, and so incorporate with it, that though the very Bodies of those corrosive particles escape our perception, yet we soon find their effects, by the destruction of all things they do but touch; with their fuliginous qualities." Evelyn not only implicated combustion, but also inferred that the cause was from small particles.

This section discusses the ongoing research into the health effects of particulate air pollution, with an emphasis on the toxicological hypotheses that relate to specific types of combustion-generated particles. Table 8 summarizes

combustion particle characteristics that are suspected to be important for health effects and the results of selected epidemiology and toxicology studies that have addressed these physical and chemical characteristics.^{6,8,25,213,305,308,312-348} Recent reviews discuss the toxicologic and epidemiologic evidence for health risks from gasoline and diesel engine emissions;^{324,349} the toxicology of ultrafine anthropogenic atmospheric aerosols;³⁴⁵ and the relationship of particle air pollution to asthma.³⁵⁰ The proceedings of recent conferences are sources of more detailed coverage of current health-related research.^{351,352}

Table 8. Combustion particle characteristics investigated in toxicology studies.

Characteristic	Relation to Combustion	Epidemiology Studies	Toxicology Studies
Mass	Filterable combustion aerosols are a minor component of urban aerosol, which is dominated by organic, secondary, and geological PM. ³⁰⁵	Health outcomes have been associated with ambient PM mass. ³⁴⁰	Exposure of young, healthy adults to concentrated ambient particle does not cause acute effects. ^{323,336}
Particle Size	Combustion is the major source of submicron and ultrafine PM. (This review.)	Coarse particles are not associated with mortality, ^{338,341} but health outcomes are associated with fine PM. ³¹⁸	Iron mobilization from coal fly ash in cell culture increases with decreasing particle size. ³⁴³ Mutagenic activity is associated with fine PM. ³³³
Ultrafine and Nanoparticles	Inorganic ultrafines are formed by mineral vaporization during combustion followed by nucleation and condensation. (This review.)	Respiratory effects associated with ultrafine PM number. ^{335,345}	Differences between fine and ultrafine particles of the same material. ^{319,331,332,346}
Transition Metals	Submicron particles from combustion are enriched in transition metals. Fe is more bioavailable from coal fly ash than from geological dust with similar size and total Fe. ³⁴⁸	Associations of health outcomes and transition metals were found in some studies, ^{327,334} but not in others. ³²⁵	Transition metals catalyze formation of reactive oxygen species. ^{326,342} Metals from ambient PM ^{314,322} and coal fly ash ³⁴⁴ induce synthesis of proinflammatory cytokines in cells and lung inflammation in rats. ³¹⁷
EC (Soot)	Combustion produces 10- to 50-nm diameter carbon-rich primary particles. (This review.) Diesel exhaust is the major source of urban soot. ³⁰⁸	Weak association between diesel exhaust and cancer risk ³²⁴ but uncertain dose-response relationship. ³⁴⁷	Carbon black and whole diesel exhaust produced similar lung lesions in rats. ³³⁰ Ultrafine carbon causes lung inflammation. ³²⁹
OC	Incomplete combustion produces a wide range of organic species. ^{213,312}	Exposure studies ³²⁴ to whole diesel exhaust include the soluble organic fraction.	PAH compounds include known and suspected carcinogens and mutagens. ^{324,328}
Secondary SO ₄ ²⁻ and NO ₃ ⁻	Most of the urban ambient PM _{2.5} is secondary aerosol formed from combustion-generated SO ₂ and NO _x . ^{6,8}	SO ₄ ²⁻ and NO ₃ ⁻ are implicated by studies that correlated risk with PM mass. ³¹⁸	NO ₃ ⁻ not toxic at 1 mg/m ³ agricultural worker exposure. ³¹³ High levels of SO ₄ ²⁻ associated with increased airway resistance. ³¹⁵
Acidity	Cl and S in fuels produce HCl and SO ₂ in the combustion products.	Some evidence for a correlation of health outcomes with H ⁺ . ³⁴⁰	Various responses reported to laboratory inhalation of acid aerosols. ³²¹
Synergistic Effects	Combustion emissions contain EC, OC, metal-rich particles, CO, and acid gases.	Epidemiologic studies are confounded by the complex mixture of pollutants in ambient air. ^{337,339}	Exposure to pairs of pollutants can produce greater effect than either one alone: ultrafine PM and O ₃ , ³²⁰ coal fly ash and H ₂ SO ₄ , ²⁵ benzo[a]pyrene and carbon black. ³¹⁶

Epidemiology

Epidemiology, the medical science that investigates the quantitative factors controlling the frequency and distribution of disease, provided the initial evidence that the PM_{10} ambient air standard did not meet the legal criteria in the Clean Air Act to “protect the public health” while “allowing an adequate margin of safety.”³⁵³ The current emphasis on the health effects of particulate air pollution was set in motion by the seminal studies of Pope, Schwartz, and Dockery. Pope compared hospital records for years when a steel mill in Utah was operating and closed and showed that elevated PM_{10} concentration was associated with increased hospital admissions for pneumonia, pleurisy, bronchitis, and asthma.³⁵⁴ Schwartz and Dockery showed that variation in total suspended PM correlated with the number of deaths per day in Steubenville, OH, over an 11-year period.³⁴⁰ Dockery et al. showed that fine-particulate air pollution, or a factor correlated with fine PM, contributed to excess mortality in six U.S. cities.³¹⁸

The methods used in recent air pollution epidemiology studies have been reviewed,^{355,356} and these methods are based on general correlation models described in advanced statistics texts.³⁵⁷ Several studies have involved reexamining previous results by an independent group of investigators to verify the conclusions by alternative statistical methods.^{358,359} The statistical association of fine PM and various health end points appears to be robust, that is, independent of the specific correlation model used. Pope reviewed epidemiology studies of particulate air pollution from 1953–1996 and listed approximate ranges of estimated effects.^{337,355} For a $10\text{-}\mu\text{g}/\text{m}^3$ increase in PM_{10} , the effects were a 1.5–4.0% increase in respiratory mortality, a 0.5–2.0% increase in cardiovascular mortality, a 0.5–4.0% increase in respiratory hospital admissions, and a 1.0–4.0% increase in grade-school absences. Detecting such a small increase requires an extremely sensitive statistical method. Since the average death rate in the United States is about 20 deaths/day/million persons, a 1% increase in mortality represents 1–2 excess deaths above the daily average in a metropolitan area containing 5 million people.

Epidemiology methods have limitations. These studies can only correlate data that have been consistently measured over a sufficient geographical area or period of time to show detectable variation. For example, to test for the effect of geological particles, studies have had to use indirect measures of wind-blown dust such as the dates of dust storms³⁴¹ or the atmospheric clearing index.³³⁸ Epidemiologists have not correlated health effects with either ultrafine ambient particles or with the ambient concentration of biologically available transition metals because these suspect particle characteristics have not been routinely measured. Although epidemiology can show a

correlation, it cannot prove causality. Two well-correlated factors may both be individually correlated with a third unknown factor that is the actual cause. There have been frequent suggestions that the observed health effects that have been correlated with particles are actually due to another pollutant that correlates with PM. Stagnant air conditions in urban areas can lead to the simultaneous buildup of multiple pollutants including PM, O_3 , SO_2 , CO, soot, and numerous gas-phase and particle-bound organic species, so this is a reasonable hypothesis. As will be discussed in the measurements section of this review, a need exists for the development of robust, precise, economical methods for measuring the various particle characteristics that are possible factors for health studies.

Epidemiology studies in Spokane, WA,³⁴¹ and in Utah³³⁸ suggest that coarse, wind-blown particles are not the cause of the observed health effects. This implies that some other component of the urban PM, such as fine particles from combustion, is related to the observed effects. An important distinction must be made between chronic and acute health effects. Some health effects, such as chronic bronchitis, emphysema, pneumoconiosis, fibrosis, and lung cancer, are associated with many years of exposure to the combustion emissions or other inhalable toxic agents. The acute effects of particle inhalation include hospital admissions associated with asthma, bronchitis, pleurisy, pneumonia, and cardiovascular disease. Time-series epidemiology studies show that these effects typically lag the changes in PM level by 1–5 days.³⁵⁵ During the 1952 London Fog event, a temperature inversion trapped the air pollution, allowing the buildup of combustion emissions to lethal concentrations over a period of four days in December. The increase in deaths was almost 4-fold during the episode, and the effects started within a day of the onset of the pollution increase.

The mass concentration increments addressed by ambient air epidemiology studies are orders of magnitude below the inhalable particle concentrations for PM in occupational settings. Average concentrations of diesel PM ranging up to $1400\ \mu\text{g}/\text{m}^3$ have been reported in studies of underground mines.³⁶⁰ Typical allowable 8-hr concentrations for general “nuisance dusts” in occupational settings range from 2000 to $10,000\ \mu\text{g}/\text{m}^3$, and these measurements are usually stated in mg.³⁶¹ Few papers have proposed toxicological mechanisms that are based on particle mass alone at ambient concentrations. Particle mass, which has been the focus of most ambient PM epidemiology, is likely to be a surrogate for the real agent. However, Harrison and Yin,³⁶² in a review of PM health effects, discussed the uniformity of epidemiologic correlations between PM concentration and health end points observed in different regions of the world with different proportions of SO_4^{2-} , NO_3^- , crustal material, and other

major PM components. They concluded that the available data provides little support for the idea that any single major or trace component of PM is responsible for adverse effects, but acknowledged that there is evidence that particle size rather than mass may be the appropriate measure to correlate with health effects.

Respiration and Particle Inhalation

The respiratory system will be briefly discussed to provide a background for the discussion of human population, whole animal, and cell culture studies of combustion particles. Concise descriptions of the human respiratory system, written in the context of air pollution engineering, include those by Carel³⁶³ and Degobert.²⁴⁸ Guyton and Hall's textbook is recommended for a comprehensive introduction to cardiopulmonary physiology,³⁶⁴ while Netter's collection of illustrations is recommended for visualizing respiratory anatomy.³⁶⁵

The observed statistical associations of ambient PM mass concentration with morbidity and mortality lead to the mechanistic question: How can a small increase in the mass of inhaled particles deposited cause sickness or premature death? A person inhales from 6 to over 12 m³/day of ambient air, depending on age and physical activity. This air contains a wide variety of natural particles from geological and biological sources as well as anthropogenic pollutants. The deposition of supermicron particles by inertial impaction and of submicron particles by diffusion depends on the gas velocity and residence time in various sections of the airway and lung. A widely used model of size-dependent deposition in the nasopharyngeal, tracheo-bronchial, and pulmonary regions of the respiratory system³⁶⁶ is reproduced in many references, for example, Wilson and Spengler.³⁶⁷ Most of the PM₁₀ mass is deposited in the nose and throat, while ~60% of inhaled PM_{0.1} is deposited in the lung. Actual size-dependent particle deposition depends on age, health, and especially on nasal versus oral breathing.³⁶⁸

Assuming typical values for respiratory volume and alveolar deposition efficiency, a calculation shows that a 10- $\mu\text{g}/\text{m}^3$ increment in ambient PM_{2.5} results in an increment of 0.02–0.05 mg of particles deposited in the lung per day. This has led to the opinion that either some component of ambient PM is highly toxic or that some individuals are highly susceptible. Alternatively, particle number may be considered. Assuming typical values for ventilation rate, lung surface area, and epithelial cell size, a calculation indicates that a typical urban, near-highway concentration of 10⁵ particles/cm³ results in an alveolar deposition rate of ~1 particle per cell per day. Figure 17 shows the relative size of the microscale structures in the alveolar region of the lung compared to a range of ambient particles.^{364,365,369} The accompanying graphs in

Figure 17 show a typical urban aerosol mass distribution and the calculated number of particles deposited per alveolus per day as a function of size. The calculated deposition assumes an ambient concentration of 100 $\mu\text{g}/\text{m}^3$ of PM₁₀, with 40% of the mass being smaller than 2.5 μm , and 2% being smaller than 0.1 μm . The deposition is calculated using the size-dependent deposition fraction³⁶⁶ and assumes uniform deposition to all alveoli. This analysis shows that fewer than 1 in 1000 alveoli has a coarse particle deposited per day, but that a typical alveolus may be exposed to several hundred ultrafine particles per day.

The body has defenses to rapidly remove inhaled particles. A mucus layer, moved upward by cilia on the cells lining the airways, transports particles from the respiratory system to the throat, where they can be coughed up or swallowed. The terminal airways and alveoli lack ciliated cells. Mobile macrophage cells take up particles by phagocytosis and remove the particles from the alveoli by active transport into the ciliated airways. Particles are also removed from the lung by dissolution and by transport into the lymphatic drainage system. A fraction of the inhaled particles is retained for a long time in the respiratory system, either in the airways or in the interstitial spaces. The process of clearing particles from the lungs can induce secondary physiological responses including coughing and inflammation. The mammalian respiratory system is likely to have evolved clearance mechanisms that are appropriate for the natural background particle number concentrations. A plausible hypothesis is that the large numbers of ultrafine particles in the urban aerosol may simply overload the ability to clear particles from the lungs. Alternatively, some specific types of inhaled particles may interact with the body's nervous and biochemical signaling pathways, resulting in an amplified response.

Identification of specific particle types in the ambient mixture that are biologically active for specific health effects is an active area of research.^{2,3} The effects of inhaled particles may increase with decreasing particle size due to several factors: finer particles are deposited in the lung rather than in the upper airway; finer particles have greater surface area per unit mass, which enhances solubility; and finer particles can enter cells more readily and can be transported from the lung to other organs. The living cell interacts with the surface of a particle, so surface chemistry, not the volume average composition, is likely to be most relevant for biological effects of low-solubility particles.

Controlled Exposure to Concentrated Ambient Particles

Inhalation exposure studies complement the results of epidemiology studies. The effect of particulate air pollution

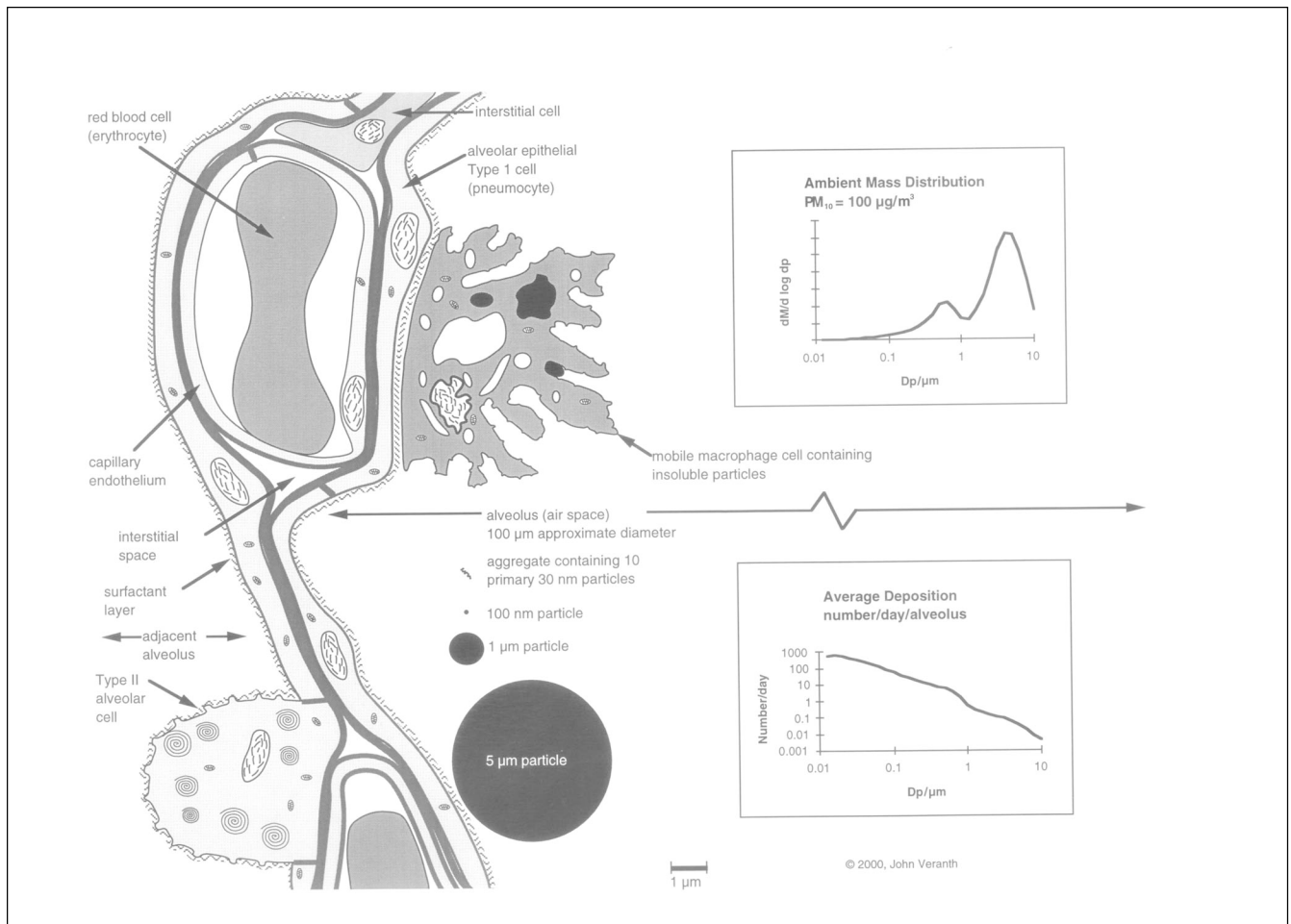


Figure 17. Scale drawing comparing ambient particles to structures in the aveoli of the human lung. The graphs show a typical ambient PM mass distribution and the expected number of particles of each size deposited per alveolus per day. Submicron particles are suspected to be important for health effects because of the large number deposited in the lung and because these particles can move into the interstitial space and blood stream. Compiled from information in refs 364, 365, 369.

can be amplified by conducting controlled inhalation exposure studies with concentrated ambient PM. This has been facilitated by the development of virtual impactor particle concentrators³⁷⁰⁻³⁷² and centrifugal particle concentrators³⁷³ that keep the aerosol suspended while separating the gas from the particles. These particle concentrators can be staged to supply an inhalation chamber with air containing a 10-fold or higher concentration of ambient PM. Studies of this type are being conducted with both human volunteers³²³ and with laboratory animals.^{374,375} An early conclusion is that healthy adults show no adverse impacts from short duration exposure to concentrated ambient particles.^{323,326}

Laboratory Studies with Surrogate Particles

A disadvantage of both epidemiologic studies and studies using concentrated ambient PM is that the subject is exposed to a complex mixture containing contributions from many sources, most of which are unknown or poorly characterized. An alternative is to conduct

studies with laboratory-generated surrogate particles from well-characterized sources. This approach is most appropriate for conducting mechanistic hypothesis-based toxicological experiments, since the investigator can specify the particle characteristics used for the test and control condition pairs. An example of this type of study involved supplying fresh laboratory-generated coal fly ash particles to animal inhalation chambers as part of a study of the combined effects of H_2SO_4 and coal fly ash.^{25,376} Inhalation studies involving ultrafine and nanoparticle PM also require having a laboratory particle generator connected to the inhalation chamber due to the rapid transformation of the particles by coagulation.³⁷⁷ Surrogate particle inhalation studies require close cooperation between the life sciences and aerosol team members as well as physical proximity of the animal care and combustion facilities. Due to the cost and complexity of conducting animal inhalation studies at combustion facilities, alternative experimental methods are common.

Inhalation of resuspended particles allows the particle generation and collection to be separated from the exposure studies. There is little difficulty in resuspending 2.5- to 10- μm aerosol particles, and resuspension is also suitable for testing hypotheses related to particle chemical composition if particles with size-independent composition are available. Surface forces make the dispersion of submicron particles difficult, so resuspension has serious disadvantages if the hypothesis involves testing size-dependent effects. Improved methods for particle resuspension have been developed.³⁷⁸⁻³⁸⁰

Alternatively, particles may be instilled into the lung as a suspension in saline solution. Despite the artifacts introduced by this invasive procedure, instillation studies have been used to investigate combustion particle effects.^{317,329,331,381} Cell culture studies involve mammalian cells or bacteria growing in an appropriate medium. Normally, the cells grow as a layer on the bottom of the culture dish or flask. The cells can be systematically exposed to various types of combustion particles or particle extracts to test specific biochemical hypotheses.^{314,382} The biochemistry of single cells, especially cell lines derived from tumors, can differ from the responses that occur in the normal whole animal. Also, cell culture studies do not include any effects related to the interaction of the respiratory tract and nervous system with the particles.

In vitro experiments performed with purified chemicals under cell-free conditions can isolate specific mechanism steps such as the rate of mass transfer of a potentially toxic component from a combustion particle. But even experiments that simulate physiologically relevant conditions simulate only a fraction of the biochemistry that takes place in a living organism.

Laboratory experiments with surrogate particles can be conducted in vitro, using cell-free models of selected biochemical steps; in cell culture, using established cell lines; and in animal models of the human respiratory system. Specific mechanistic hypotheses can be tested by using well-characterized particles from known sources. These types of studies provide an important link between fundamental biochemistry and human population studies. The next section will discuss some of the hypotheses that are topics of current PM research.

Cardiopulmonary Effects of Particles

An active hypothesis is that the observed cardiac symptoms associated with particle inhalation may be mediated by the nervous system. Certain nervous system-activated changes in heart rate, blood pressure, blood viscosity, and heart-rate variability are associated with an increased likelihood of sudden cardiac death.³⁸³ A study of 90 elderly subjects showed that changes in blood oxygen saturation were not associated with exposure to

particle air pollution, but increased pulse rate was associated with exposure to particle air pollution on the previous 1–5 days.³⁸⁴ A decline in heart-rate variability is a quantitative indication of impairment of the autonomic function, that is, a decline in the ability of the cardiorespiratory system to respond to changes. A decrease in heart-rate variability has been observed for persons exposed to increased ambient PM_{10} in Utah³⁸⁵ and to increased $\text{PM}_{2.5}$ in the Boston area.³⁸⁶ Cardiac monitoring may provide a sensitive indication of acute response that will be useful in identifying the relative importance of different components of ambient aerosol. Exposure of dogs with induced coronary occlusion to concentrated ambient particles affected one of the major electrocardiogram signs of myocardial ischemia,³⁷⁵ and other cardiac and respiratory parameters were also affected. This suggests a plausible mechanism by which persons with existing heart disease may become more susceptible to serious cardiac effects when they are exposed to some component of ambient PM.

Biochemical Signaling

The nervous system and other biological signaling pathways can result in enormous amplification of a stimulus. Persons with hay fever or asthma are familiar with the massive response that can occur within minutes of exposure to an allergen. Cytokines are intracellular signaling molecules that mediate many protective physiological functions such as increasing the blood circulation and recruiting leukocytes (white blood cells) at the site of an infection. Cytokines can also induce potentially harmful responses such as prolonged tissue inflammation and development of fibrosis in response to irritants.^{387,388} Lung inflammation has been associated with exposure to elevated ambient PM,^{389,390} and a number of studies are focusing on the relationship of inhalable particles to the biochemical events leading to lung inflammation.^{158,317,326,344,391-394} Combustion particles may contain specific chemical species that are able to activate biological signaling pathways, and a number of these hypotheses involve transition metals.

Transition Metals and Biochemical Processes

Particles provide a vehicle for metals to enter the body in inappropriate amounts. Much of the literature on the toxicity of solid-phase metal compounds is based on ingestion rather than on inhalation.³⁹⁵ Ingestion dose-response relationships may be relevant for the effects of larger particles that are deposited in the upper airways but are rapidly cleared from the respiratory system to the throat, where they are swallowed. However, submicron particles are deposited deep in the lung, and ultrafine particles are able to pass from the lung directly into the body.³³¹ There is increasing evidence that the same element has very

different behavior when inhaled than when ingested. Mn, a necessary trace mineral in the diet and a controversial octane-boosting additive in gasoline,³⁹⁶ provides an example. Dietary Mn is homeostatically regulated by the liver, and ~3% of ingested Mn is absorbed.³⁹⁷ Inhalation bypasses the digestive system, and up to 40% of inhaled Mn is absorbed.³⁹⁸

The dose of a particle-bound element that is available to the body depends on the entry route, the particle size and morphology, and the mineral species in the particle. When conducting laboratory experiments on metal bioavailability, it is necessary to distinguish between in vitro, extracellular, and intracellular behavior, since the solubility of transition metals from a given combustion ash mineral species depends on the pH and the presence of chelators. Many chelators are present in cells, and some, such as citrate, are present at millimolar concentrations.

Transition metals on inhaled particles may act as biochemical catalysts that can induce other biochemical responses. Transition metals, such as V, Cu, Fe, and Pt, can catalyze the generation of ROS³⁹⁹ that have been associated with both direct molecular damage and with the induction of biochemical synthesis pathways. Coal fly ash and residual oil fly ash have been studied as examples of combustion particles enriched in transition metals. Residual oil fly ash has been shown to induce inflammatory cytokines in human bronchial epithelial cells³¹⁴ and both lung inflammation³²⁶ and cardiac arrhythmia¹⁵⁸ in inhalation studies with rats. Coal fly ash has been shown to be a source of bioavailable iron³⁴³ and can also induce inflammatory cytokines in human lung epithelial cells.³⁴⁴ Generation of ROS and induction of cytokines in human bronchial cells has also been reported in studies of diesel exhaust particles.⁴⁰⁰ The amount of bioavailable transition metals contained in particles has been associated with acute lung inflammation from both combustion and ambient particles.³¹⁷ Studies have considered the water-soluble transition metals,¹⁵⁹ metals associated with organic material,³⁹² and metals that can be mobilized by an intracellular chelator at physiological conditions.³⁴²

A study of ROS generation in polymorphonuclear leukocytes (a white blood cell type frequently found in the airways of persons exposed to particles) using oil fly ash, coal fly ash, carbon black, natural dust, and ambient particles reported that the ROS correlated with the fraction of Si, Fe, Mn, Ti, and Co that was not removed by distilled-water washing.⁴⁰¹ In studies with coal fly ash and geological dusts,⁴⁰² the amount of bioavailable Fe under physiologically relevant in vitro conditions did not correlate with the total Fe in the particles, as shown in Figure 18.^{342,343,403,404} Cultured human lung epithelial cells (Type A549) were exposed to PM₁-enriched coal fly ash

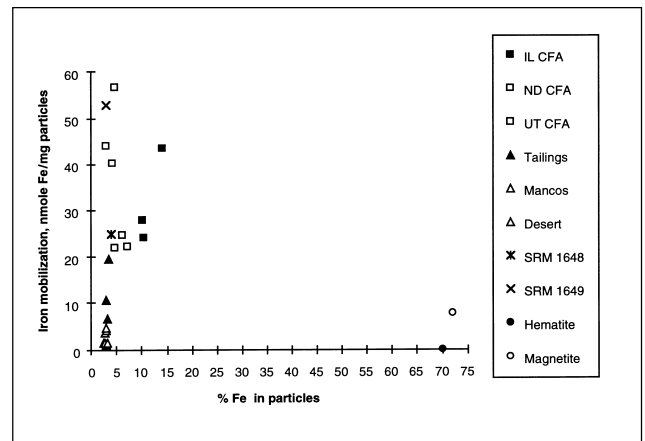


Figure 18. Iron mobilized by the chelator citrate and physiological pH from three types of coal fly ash, two types of dust from unpaved desert roads, mine tailings, urban particles, and pure iron oxides. The mobilized iron does not correlate with the total iron in the particles. Data sources: urban particles,³⁴² CFA,³⁴³ geological dusts,⁴⁰³ iron oxides.⁴⁰⁴

both as-collected and after pretreatment with the chelator desferrioxamine B. The chelator removed the ability of the coal fly ash to induce the synthesis of the proinflammatory cytokine IL-8.³⁴⁴ Mössbauer spectroscopy of the coal fly ash before and after the desferrioxamine B treatment showed that Fe in an aluminosilicate glass phase was preferentially removed.³⁴⁸ Fe in aluminosilicate glass occurs in combustion ash that is produced by rapid quenching from high temperature, but is not commonly found in dusts with similar elemental composition that have been produced by geological weathering.

Traditional mass transfer and heterogeneous chemical reaction theory⁴⁰⁵ was applied to analysis of the measured rate of Fe mobilization from various sizes of coal fly ash by the chelator citrate. The rate of Fe mobilization was consistent with solid-phase-limited diffusion mass transfer, but the final values were consistent with size-dependent differences in initial composition.⁴⁰² Such size-dependent composition differences are expected from the mechanism of coal fly ash formation described in the fundamentals section above. These results show the importance of particle size and chemical speciation in the activation of specific biochemical pathways and suggest mechanistic reasons for differences in the response of the body to combustion and geological particles.

Soot and Biochemical Processes

Soot is the major type of combustion-derived ultrafine PM, and associated organic and inorganic compounds cause soot to have mutagenic, carcinogenic, and irritant properties. A study of size-fractionated urban PM showed that the mutagenic activity increased with decreasing particle size,³³³ which is consistent with expectations for organic compounds

condensed on submicron combustion particles. The indeterminate chemical composition of the EC and OC mixture emitted from combustion, ranging from fuel-like hydrocarbons to primary particles formed from graphite-like fused aromatic rings, greatly complicates biochemical studies. Carbon black is often used as a surrogate for the EC component of real combustion soot.^{329,330} Various solvent extracts of soot, or isolated compounds such as specific PAH species, have been used as surrogates in toxicological studies of the OC fraction of combustion soot. Many PAHs are suspected carcinogens and mutagens,⁴⁰⁶ and there has been considerable controversy regarding the role of nitroaromatic compounds because of the differing results in bacteria and mammalian cells.⁴⁰⁷ Quantified compounds account for only a fraction of the observed mutagenicity of real soot mixtures.

Chlorinated polycyclic aromatic compounds, especially polychlorinated dibenzo-p-dioxins, and furans are also associated with combustion emissions. These compounds are fat-soluble, accumulate up the food chain, and have been suspected to disrupt or mimic the action of developmental hormones.⁴⁰⁸ The most-studied effects involve chronic exposure, but the possibility of acute effects from these compounds cannot be ruled out. The chlorinated dioxin and furan compounds are a special concern for municipal and medical waste incineration.²³¹ Emissions of chlorinated dioxin and furan compounds do not appear to be a problem when burning fuels that contain more sulfur than chlorine, such as coal.

Ultrafines

Ultrafine particles and nanoparticles have been proposed by some health researchers³⁷⁷ as the biologically important ambient particle. Ultrafine particles are deposited by diffusion deep in the lung and have been found by Oberdörster et al.³³¹ to be retained in the lungs. Ultrafine particles can also pass through the cells lining the lung and enter the interstitial space. Table 9 summarizes studies with micron-sized and ultrafine particles of the same compound.^{319,329,331,409-411} The data show that ultrafine particles often have a greater biological effect than an equal mass of larger particles of the same substance.

For slightly soluble particles, the high surface area of ultrafine and nanoparticles can result in a faster release of toxic compound than would result from larger particles of the same composition. The concentration of a toxic substance reached in cells or in body fluids is the dynamic result of the relative rates of release from the particle and of clearance of the toxic material from the body.

Synergistic Effects

The combination of multiple toxic substances often has a much greater effect than the sum of the effects of the

individual substances. Historically, emissions of combustion particle and sulfur oxides have been closely linked. Separating the effects of these pollutants was difficult since both were produced from burning coal. Coal was used extensively in urban areas for both industrial steam engines and domestic heating in Europe and North America prior to the 1950s, when natural-gas pipelines, automobiles, and regulations for large industrial sources changed the emission pattern. European regulations treated these pollutants as a combination and set a limit on SO₂ that varied with the smoke concentration (roughly a measure of EC).^{362,412} The assumption underlying this approach was that acid gases adsorbed on the surface of particles could be transported into the lung, whereas vapor-phase acid would diffuse to the wall of the upper respiratory tract. Amdur and coworkers conducted extensive studies of the health effects of H₂SO₄ aerosols, both as a pure component and in combination with coal fly ash.^{25,26,413}

Amdur^{25,26} reported that a 10-fold increase in dose with acid aerosol alone was required to match the effect on lung-diffusing capacity caused by inhalation of H₂SO₄ condensed on PM. A concentration of 310 mg/m³ of H₂SO₄ mist corresponded to the same change in diffusion capacity as occurred when the H₂SO₄ was surface-layered on a coal fly ash particle at a concentration of 30 mg/m³. In addition, the type of particle was also important. Amdur found that with lignite, which has higher Ca and Na than does bituminous coal, the H₂SO₄ reacted with the alkali to form sulfates. With bituminous coal, which has Al, Si, and Fe-rich ash, H₂SO₄ persisted on the particles. Synergistic effects between other combustion-generated pollutants occurring on the same particle have been studied. For example, the combination of benzo[a]pyrene adsorbed on carbon black caused release of tumor necrosis factor- α and caused programmed cell death of lung macrophages, but neither carbon black nor benzo[a]pyrene had this effect alone.³¹⁶ Other synergistic effects involve particles plus a gas-phase pollutant, such as O₃.³²⁰

Importance of Chemically Speciated PM Sampling

Equal mass doses of sea salt, desert dust, and diesel exhaust are unlikely to have the same effect on the body. The startup of a large number of air monitoring sites that will routinely report individual chemical categories of PM (EC, OC, SO₄²⁻, NO₃⁻, other inorganic) and the funding of EPA particulate research centers and Supersites will provide input data for epidemiology studies. Improved characterization of combustion and other PM sources will provide data needed to relate the chemical speciation at receptor sites to the major sources. Controlled toxicology studies using exposure to well-characterized components

Table 9. Studies of ultrafine vs. larger particles of the same substance.

Material	Dose/Method	References	Results
Titanium dioxide 20-nm and 200-nm	Rat, instillation	331	Increased pulmonary toxicity of ultrafines related to surface area and the ability to enter interstitial spaces. Alveolar macrophage involvement.
Titanium dioxide 20-nm and 250-nm	Rat, inhalation, 22 mg/m ³ , 6 hr/day for 6 months	410	Greater inflammatory response at equal dose with 20-nm particles.
Titanium dioxide 21-nm and 120-nm	Rat explants in vitro	411	Ultrafine particles were able to induce procollagen expression, which is related to development of airway fibrosis.
Carbon black 14-nm and 260-nm	Rat, instillation	329	Ultrafine carbon black had greater ability to produce lung inflammation at low dose.
Carbon black 14-nm and 260-nm	Rat, inhalation 1 mg/m ³ , 7 hr one-time	319	No effect with 260-nm particles. Ultrafine produced proinflammatory response, oxidative stress, increased procoagulant blood factor.
Magnesium dioxide UF, 28% < 0.1 μm F, 98% < 2.5 μm	Human, inhalation	409	No significant differences in bronchoalveolar lavage cell concentration or cytokine concentration. Suggested that particle composition, not size alone, is significant.

of ambient aerosol will be needed to develop a mechanistic understanding of how particles affect the body.

AIR QUALITY REGULATIONS

The preceding discussion of the respiratory system and air pollution health effects sets the framework for discussing air quality regulations. These regulations have the primary purpose of protecting human health and the secondary purpose of reducing other environmental impacts of pollution. Environmental laws must be unambiguous for the regulated sources, the enforcement agencies, and the affected public. A prerequisite to developing a rule is that a means must exist to measure the component(s) to be regulated so that compliance monitoring can take place. This monitoring must be cost-effective and reproducible. As a result, the existing regulations focus on regulating ambient concentrations of pollutants for which reasonable cost, robust, and precise measurement methods are available.

Three sections of the U.S. Clean Air Act apply directly to PM. The most important of these are the NAAQS, which include PM₁₀ and the newly implemented PM_{2.5} regulations. The EPA³⁰¹ has indicated that the PM₁₀ trend is improving, with a decrease of 26% in average ambient concentrations from 1988 to 1997. In 1987, the original NAAQS for total suspended PM was replaced by a PM₁₀ standard set at 150 μg/m³ 24-hr average and 50 μg/m³ annual average. The legal requirement to periodically review the standards, combined with growing epidemiologic evidence and a citizen lawsuit, lead to further

rulemaking. In 1997, the EPA revised its existing PM standards by adding the PM_{2.5} standard.⁴¹⁴ The annual standard is set at 15 μg/m³, with a new 24-hr standard set at 65 μg/m³. The PM₁₀ annual standard was retained, but the statistical method of determining compliance with the 24-hr average was modified. The scientific evidence considered by the EPA in setting the standard was compiled into a criteria document.³⁰⁵

It should be noted that the standard was recently (May 14, 1999) challenged, and a panel of the U.S. Court of Appeals for the District of Columbia remanded the new standards for PM_{2.5} and O₃. In a summary of the decision, the EPA points out that the court did not question the health evidence for the standard; rather, the decision required more explanation of the process used to set the standard. Congress has required the National Research Council to form a committee to guide the PM research and monitoring agenda. This committee is charged to write four reports between 1998 and 2002, when EPA is to complete a 5-year scientific review of the standards, leading to possible revision. Two of the four reports have been completed.^{415,416} The current regulation is based on PM_{2.5} measured by the Federal Reference Method. This mass is dominated by secondary SO₄²⁻ and NO₃⁻ aerosol and by EC and OC. Submicron inorganic ash and ultrafines from combustion are a small part of the PM_{2.5} mass in many locations. However, the mass measurements do not directly relate to the previously discussed mechanistic toxicological hypotheses. Other characteristics, such as the morphology and chemistry of ultrafine particles, may be more important than

simple mass. The EPA is attempting to address this fact by its ambitious Supersite program. These Supersites intend to support the on-going health studies by obtaining chemical- and time-resolved data using a range of research methods. However, one must realize that cost-effective, robust, and simple monitoring methods must be available before any change in the present standards can be realistically promulgated and implemented.

The second regulation can be found in the regional haze rule.⁴¹⁷ Decreased visibility occurs due to the scattering and absorption of light by particles. This is of particular concern in the 156 National Parks and Wilderness Areas that are designated as mandatory Class I air quality areas in the United States. Since fine particles are transported over hundreds of miles, all 50 states will have to participate in planning, analysis, and, in some cases, emission control programs. Since submicron particles scatter light efficiently, combustion-generated PM has a large impact on visibility, even when the primary combustion PM represents a small part of the total PM_{2.5} mass. The EC, which results in light absorption rather than light scattering, is particularly important for visibility. In addition, secondary PM, not covered by this review, is important. Regulations to control acid rain precursors and photochemical smog precursors also reduce the ambient particle concentration, since SO₂ and NO_x are also the precursors of secondary SO₄²⁻ and NO₃⁻ particles. Visibility rules may prove to be more stringent than health standards in controlling the emission of submicron particles from combustion sources.

Finally, the Clean Air Act Amendments of 1990 require the EPA to address 188 hazardous air pollutants (HAPs). Included in this list are As, Be, Cd, Co, Cr, Hg, Ni, Mn, Pb, Sb, and Se, which are contained in fuels. The accumulation of toxic metals, such as Se and Hg, and the accumulation of persistent organic compounds, such as chlorinated dioxins and furans, in ecosystems is a concern that affects standards for combustion particle emissions. Current regulations focus on sources emitting greater than 25 tons/year, and electric utility steam-generating boilers are temporally exempt from the regulations. Due to amplification in the food chain, and to public concern for wildlife and endangered species, these indirect effects of particles may also result in more stringent regulation of sources. Complying with the ecological goals of the HAP regulations will require an understanding of the relationship between combustion conditions and the emissions of these trace elements.

Adverse health effects originally identified by epidemiology studies motivated the public perceptions and legal actions that have resulted in new regulations for ambient PM. Current air quality standards are based on the mass of particles smaller than a specified size; however, toxicological studies may eventually identify

specific categories of ambient PM that need stricter control to protect public health. Advances in understanding the formation and transformation of combustion aerosols and advanced monitoring techniques must take place to meet the challenge of setting and complying with regulatory standards.

TIME- AND SIZE-RESOLVED PARTICLE MEASUREMENTS

The ability to test various health-related hypotheses is closely linked to which PM characteristics can be measured at combustion sources and in the ambient air. The particle measurement issues that are especially relevant for testing current health effects hypotheses regarding metals, ultrafines, and soot from combustion sources include

- *Measurement Artifacts.* This includes all the particle transformations that can be different between a sampling train and the ambient air. Due to the effects of temperature-dilution history on the partitioning of chemical species between the gas phase and the particles, the PM that is measured in the laboratory may have a different size-dependent composition than the PM to which the population is exposed. Also, transformation of the particle size distribution due to coagulation, surface condensation, chemical reactions, and size-selective removal may occur as a result of the sampling methodology.
- *Instrument Limitations.* Methods are needed to measure particle-to-particle variation, which provides information that is lost in the bulk average properties of the PM collected by filter sampling. Rapid response instruments are needed to quantify short duration transients in particulate air pollution that may have significant health effects. Many methods for measuring aerosols that were developed for supermicron particles need to be modified or extended for ultrafine PM.

Measurement Artifacts

The historic regulation of the total PM mass smaller than a given size has produced precise mass measurement techniques. Since the largest particles dominate the mass, there has been an emphasis on isokinetic sampling. There has also been concern about equilibrating the samples to constant humidity before weighing, even though the mass of particle-bound water is unlikely to have biological importance. The techniques that yield precise mass measurements may, however, introduce serious artifacts if the goal is to obtain data on submicron particle composition and size distribution. For example, allowing air of variable temperature, pollutant concentration, and humidity to pass over the accumulating filter deposit for 1–6 days can strip

the more volatile species from the collected particles before the sample is weighed. This has led to the development of samplers that can quantify the volatile PM.^{418,419} While there is uncertainty regarding the significance of the mass of volatiles adsorbed on particles, this serves as an example of the importance of using appropriate particle measurement methods when testing a given toxicological hypothesis.

Condensable PM, that is, material that condenses into a liquid or solid within a few seconds of leaving the stack, can be comparable in mass to the filterable PM₁₀ measured in the stack of a power plant.⁴²⁰ Currently, U.S. regulations do not require measuring condensable PM when stack-testing stationary sources. This is another example of how measurement protocols developed for regulatory compliance do not collect the data that is most needed for health and environmental studies.

Dilution tunnels were developed for measuring condensable particulate, including both SO₄²⁻ aerosol and organic compounds from vehicle exhaust and stationary sources of VOCs.^{278,421} The dilution tunnel process involves mixing the hot combustion emissions with filtered air, allowing a short residence time, then extracting a particulate sample for either on-line analysis or for collection on a filter. Dilution tunnels were developed to measure mass and chemical composition of PM. The possibility that a laboratory dilution tunnel could create a different particle size distribution than the size distribution that occurs during natural dilution was pointed out by Kittelson and Dolan 20 years ago.⁴²² Since then, many papers have discussed the artifacts that can occur in dilution tunnels.^{265,423-428}

The formation of particles during dilution depends on the opposing effects on condensation of the decreasing saturation pressure of the volatile species due to cooling and the decreasing partial pressure of the volatile species due to mixing. The saturation reaches a peak in the dilution range of 5:1 to 50:1, depending on the boiling point of the volatile species and the initial temperatures of the exhaust and dilution gases. Particles will be formed by nucleation if the mixture stays in this dilution range for sufficient time for significant mass transfer to take place. Typical dilution tunnels operate in the range of 3:1 to 20:1 and have residence times on the order of seconds, so critical supersaturation may be exceeded long enough for formation of nuclei particles followed by rapid growth from condensation. The formation of H₂SO₄/H₂O particles is an example in which dilution conditions influence the measured particle number both in dilution tunnels⁴²⁹ and in the atmosphere.⁴³⁰

Unlike mass, particle number is not conserved, and the effect of dilution conditions makes it difficult to compare the particle number size distributions measured by different investigators. This is especially important when

using combustion source measurements for investigating the health effects of ultrafines and nanoparticles. Changes in particle number of up to 2 orders of magnitude have been reported when conditions were varied over the typical range used in laboratory dilution systems.⁴²⁹ Initial combustion exhaust conditions, dilution history, dilution gas temperature and relative humidity, and the residence time interact to affect nucleation and surface growth. Careful interpretation of conditions used for experiments is required. For example, diesel exhaust studies have reported that high dilution ratio both increases⁴²⁶ and decreases⁴²⁹ formation of particles below 50 nm.

Research studies of the particulate emissions from IC engines fall into two groups: studies of the transient mixing and chemical reactions inside the cylinder, and studies of the tailpipe emissions to the atmosphere. Between these points is the exhaust system in which the undiluted exhaust cools and ages, but is not diluted. The gas residence time in the engine cylinder is 10–30 msec, depending on engine speed. The time from the cylinder to the atmosphere for a typical heavy-duty truck engine exhaust system is 100–300 msec, about 10 times greater. The extractive particle sampling systems used by various investigators can add another 0.25–1 sec or more to the age of the aerosol before dilution begins. The dilution of tailpipe exhaust under highway conditions starts at the tailpipe and is about 1000:1 after 1 sec.⁴²³ The coagulation of equal size particles is proportional to n^2 , so most particle growth by coagulation takes place prior to the onset of exhaust dilution. Under urban conditions, once combustion exhaust is diluted more than ~100:1, the collisions between accumulation mode particles from the ambient air and ultrafines from the combustion source become significant compared with the coagulation between ultrafine particles originating from a single source.

The ultrafine particle size distribution formed from hot diesel exhaust in a laboratory dilution tunnel operating with filtered air may be very different from the size distribution formed under roadway dilution conditions with ambient air. Ambient air contains accumulation mode particles that, due to the increased collision rate between particles of different size, increase the rate at which the nuclei and condensation mode ultrafines are depleted. A novel approach to studying dilution effects involves the simultaneous use on a moving truck of both a dilution tunnel extracting from the tailpipe and an in-plume sampler with the inlet mounted on the rear of the trailer.⁴³¹ For these experiments, the dilution system measurement showed a smaller accumulation mode mean size than did the in-plume measurement.⁴³²

Nanoparticles are difficult to measure because they are rapidly transformed by coagulation, surface growth, and transport to the walls of the equipment. Internal

combustion engine particle number measurements may contain artifacts from the sampling lines due to both desorption of condensed material and reentrainment of deposits. A dynamometer study comparing tailpipe and dilution tunnel measurements of gasoline vehicle exhaust particle concentration found that a heated and insulated transfer line resulted in a very intense nanoparticle mode when the drive cycle involved operation at high vehicle speed.⁴³³ This ultrafine mode was not detected under identical operating conditions with an unheated transfer line. This artifact was attributed to the hot exhaust increasing the transfer line temperature above 180–250 °C, resulting in desorption/pyrolysis of organic material in the line.

There is a need for improved technology for making laboratory measurements of combustion PM that can be related to the real behavior of particles in the combustor exhaust, the initial plume, and the atmosphere. Computer simulations of the fundamental mechanisms of aerosol formation and transformation can be used to interpret and compare particle size distribution data collected under various dilution configurations. Rapid dilution is essential if the ultrafines generated in combustion are to be measured. Likewise, ultrafines are most likely to survive from the combustion source to inhalation exposure when there is rapid dilution with relatively clean ambient air.

The commonly used instruments have limitations that may introduce artifacts into measurements of ultrafine particles. Many published graphs of combustion particle number distributions show the highest concentration in the smallest size range measured by an SMPS. This makes the integrated total particle number suspect since there may be extremely high concentrations of undetected nuclei particles present. Some authors explicitly acknowledge this measurement truncation problem by stating the results as the total number within the range of the SMPS. Another approach, for example, that used by Khalek et al.,²⁶² is to fit a lognormal distribution to the data with an algorithm that allows for truncated measurements. Truncation of the measured size distribution is an important issue both when using experimental data as the input to a coagulation model calculation and when testing toxicological hypotheses related to ultrafine particle number.

Characterization of particle number and chemical composition from combustion and other PM sources is important for both source apportionment studies of the submicron ambient aerosol and for designing controlled tests of particular toxicological hypotheses regarding ultrafines, metals, and synergistic effects between particle components. The size distribution measured from dilution tunnel sampling shows artificially high numbers of particles. However, there is also the possibility

that a substantial portion of the nuclei is below the detection limit of the instruments used.

Instrumentation Needs

To understand what particle characteristics affect human health, we must develop ways to make inexpensive, robust measurements of particle size distribution, morphology, and chemical speciation. The important variables have not yet been identified, but the current inhalation toxicology research direction suggests that a better understanding of health effects will require more time-resolved, size-segregated, chemically speciated data from both combustion sources and ambient monitors. Testing of epidemiologic hypotheses requires wide-scale, long-term measurement of PM characteristics. The characteristics selected for measurement should be economical to quantify under field conditions and should be well correlated with the factors that are suspected to be biologically significant.

Filter samples provide only time-averaged aerosol properties, but individual particle composition contains information that is important for both source apportionment and toxicology studies. The urban aerosol contains contributions from nearby and regional sources, both natural and anthropogenic, that have aged in the atmosphere from minutes to days. A typical ambient particle that is inhaled consists of coagulated primary combustion particles or geological particles, coated with some mixture of condensable organic species, secondary SO_4^{2-} and NO_3^- , and H_2O at equilibrium with local humidity. The particle-to-particle variation reflects different sources and transformation histories. The different particle types within the ambient mixture are likely to have different effects when inhaled. The information on particle-to-particle variation is preserved by single particle techniques, such as electron microscopy and aerosol mass spectrometry. However, it is necessary to efficiently measure a statistically large population of particles to obtain meaningful ensemble averages of the ambient PM as a function of time and place.

The wide variation in the physical and chemical characteristics of combustion PM emissions as operating conditions change creates a need for near-real-time measurements that can capture both the transient emissions and the variation between individual sources in a category. For IC engines, toxicological hypotheses motivate a desire to characterize the soot, the soluble organic compounds including individual PAH, the ultrafine particle number, and the metal speciation with various fuels at various speeds and loads. Likewise, measurements of a few boilers, gas turbines, or fireplaces cannot be expected to fully describe the emissions from all similar sources. One of the most challenging combustion PM problems is

to characterize highly variable sources such as open burning and domestic biomass combustion. Compliance monitoring methods such as filter sampling of an automobile over the FTP drive cycle, or a 2- to 4-hr steady-state stack test of a boiler, cannot measure the transients. Collecting statistical data on a representative sample of in-service sources is slow and very expensive using compliance methods. This section will discuss some of the research instruments that may offer improved capability to make time- and size-resolved measurements of $PM_{2.5}$ and ultrafine PM.

Desirable instrument characteristics for testing epidemiologic hypotheses include low cost per data point to allow collection of sufficient data to perform statistical analysis, rapid response to allow tracking of transients, reliability and ruggedness to allow use under field conditions, and reproducibility to allow comparisons between investigators. Desirable characteristics for source apportionment and toxicology studies are the ability to provide information on detailed morphology and chemical composition that is relevant to the origin of the particle and its behavior inside the body.

Chemical analysis techniques for source apportionment rely on variation in the concentration of specific compounds that provide individual "markers" or "fingerprints" (i.e., characteristic patterns) for identification of sources. The pioneering studies used elemental composition: Pb for gasoline engines, V for oil-burning power plants, Se for coal-fired boilers, and Al for geological materials.³⁰⁶ This allowed identification of only a few categories, and changes in technology, such as the phase-out of leaded gasoline, have eliminated some of the markers. Compared with less than 50 elements that are potential markers of combustion particles, organic compounds provide tens of thousands of potential markers, allowing detailed identification of combustion sources.^{156,298,434,435} A "memory" of the original fuel is preserved in the detailed composition of the products of incomplete combustion. A limitation of these organic markers is the time needed to collect and analyze a sample by conventional solvent-extraction and gas chromatography. An alternative technique, currently being tested in research programs, is thermal desorption gas chromatography (TD-GC),⁴³⁶ which involves controlled heating of a lightly loaded particulate filter. This method has been shown to provide composition data with 2-hr time resolution that are nearly identical to collocated 24-hr samples that were analyzed by conventional solvent-extraction, GC/MS methods. Prototypes indicate that TD-GC has the potential to be fully automated in a field-transportable unit.

Another option for rapid organic analysis is the photoelectric aerosol sensor (PAS),^{437,438} which provides a real-time indication of changes in the amount of particle-bound PAH. This instrument is compact and has

a sensitivity of about 1 ng PAH/m³.⁴³⁹ The value of rapid time-resolved PAH measurement is illustrated by a study in which a PAS was installed near the runway of an Air Force base. The spikes in the signal could be correlated with flight logs showing the activity of specific aircraft, as indicated in Figure 19.⁴⁴⁰ The PAS signal is a weighted sum from many chemical species. Some research has been completed to quantify the relationship between the PAS instrument reading and conventional measurements of individual PAH by traditional methods for a range of sources. The ability to make rapid semi-quantitative measurements of PAH is extremely valuable for characterization of the variation in the emissions from large populations of similar sources, and to study the effect of combustion transients on the time-averaged emissions. Ongoing research includes developing methods to use the PAS to monitor for high PM-emitting equipment in an operational fleet through edge-of-roadway or edge-of-runway real-time measurements.

Soot is a functional definition and actual combustion particulate emissions are a complex mixture of organic compounds ranging from unburned fuel to graphite-like polycyclic structures, making an arbitrary division into composition categories necessary. These divisions are based on behavior in an analytical procedure. The measured split between OC and EC is based on the light-adsorbing properties of a filter punch as a function of temperature, first under a helium atmosphere and then under an oxygen/helium atmosphere.⁴⁴¹ Changes in the procedure, for example, the NIOSH and IMPROVE methods, give different results.⁴⁴² The fuel- and lubricant-derived hydrocarbons are alternatively distinguished from the graphite-like carbon structures in soot by measuring the soluble organic fraction using dichloromethane or a similar solvent.⁴⁴³ Further separation of the soluble organic compounds usually involves extraction with aqueous and organic solvents, acidic and basic solvents, and polar and non-polar solvents until various classes such as paraffins, aromatics, and oxygenates are isolated for analysis by gas chromatography.^{275,276,444,445}

EC, or soot, is an important class of particulate air pollution, and the ability to economically make near-real-time measurements of EC is valuable for characterizing transient emissions from combustion sources. The photoacoustic analyzer detects light-absorbing particles (black carbon) by the transient heating resulting from a pulsating laser beam passing through the sample chamber.^{446,447} A preliminary study of IC engine exhaust showed that the photoacoustic instrument response and the EC analyzed on filter samples by thermal/optical reflectance⁴⁴¹ correlated as shown in Figure 20.⁴⁴⁸ This technique provides a rapid signal, making time-resolved measurements of events, such as sudden acceleration of

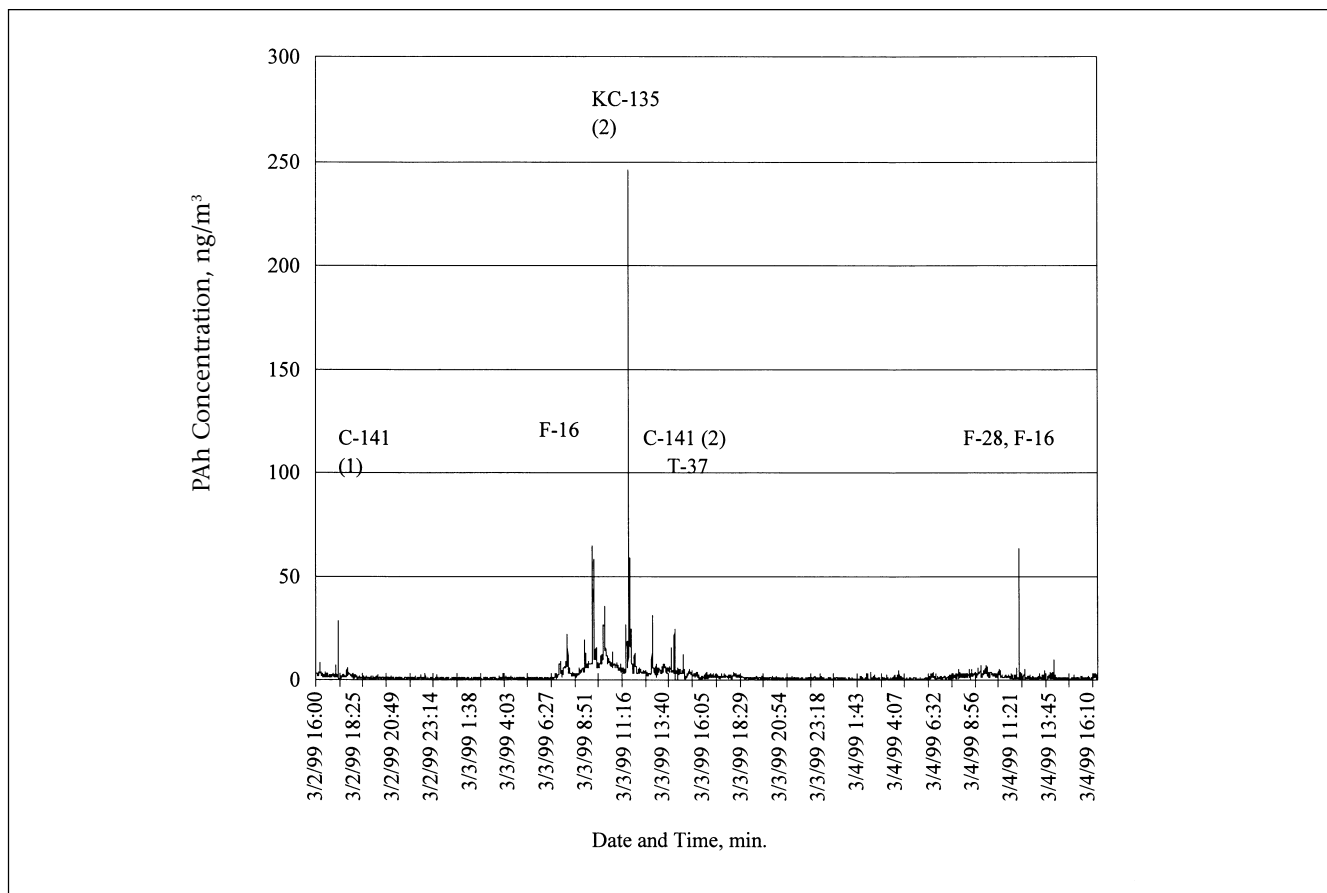


Figure 19. Time-trend data obtained by a PAS sampling at an Air Force base. The spikes in PAH concentration can be correlated with aircraft operations and with local ground traffic. Courtesy of G. Palmer.⁴⁴⁰

the engine, feasible. The instrument also has a wide dynamic range, making it suitable both for studies of transient emissions from combustion sources and for monitoring spikes in ambient concentration. The lower limit of detection for EC is 40 ng/m³.⁴⁴⁷ When developing alternative methods for measuring the health and visibility impacts of soot and of particle-bound organics, there is a need to compare these methods to existing EC and OC data. However, EC, as currently reported, is a method-dependent definition, so the relationship between methods is only an empirical correlation, not a fundamental relationship.

Electron microscopy, coupled with energy dispersive X-ray analysis, can provide size, shape, and elemental composition information on individual particles. Automated electron microscopy, also called CCSEM, allows the characterization of several hundred particles per hour and provides a powerful technique for characterizing both source and receptor samples for source apportionment studies.^{449,450}

Concern over acid rain has motivated studies that have looked for coal particles in lake sediments as a tracer for rain-out from power-plant plumes. The methods used to identify coal fly ash in sediments can also be extended

to plume tracking for health studies. An early example of using CCSEM in a health-related combustion particle study involved collecting particles from the plume of a coal-fired power plant using a helicopter. Kim et al.⁴⁵¹ showed that the plume particles could be distinguished from background PM by the characteristic morphology and composition of coal fly ash. Characteristics of combustion ash include large carbonaceous spheroidal particles⁴⁵² and glassy aluminosilicate spheres.^{453,454} Advanced techniques for single particle analysis by microscopy have been reviewed.^{455,456} A limitation to the study of submicron particles is that the spatial resolution of many techniques, such as energy-dispersive X-ray analysis, is comparable to the size of the particles.

The aerosol time-of-flight mass spectrometer (ATOFMS) is the most sensitive technique currently available for on-line measurement of the size and chemical composition, both organic and inorganic, of individual aerosol particles. The size and chemical composition of hundreds of particles per minute can be obtained. Fundamentals of the ATOFMS technique and recent advances in aerosol mass spectrometry are discussed in a review,⁴⁵⁷ which lists the contributions of 17 research groups. Figure 21 illustrates the capabilities of an ATOFMS research

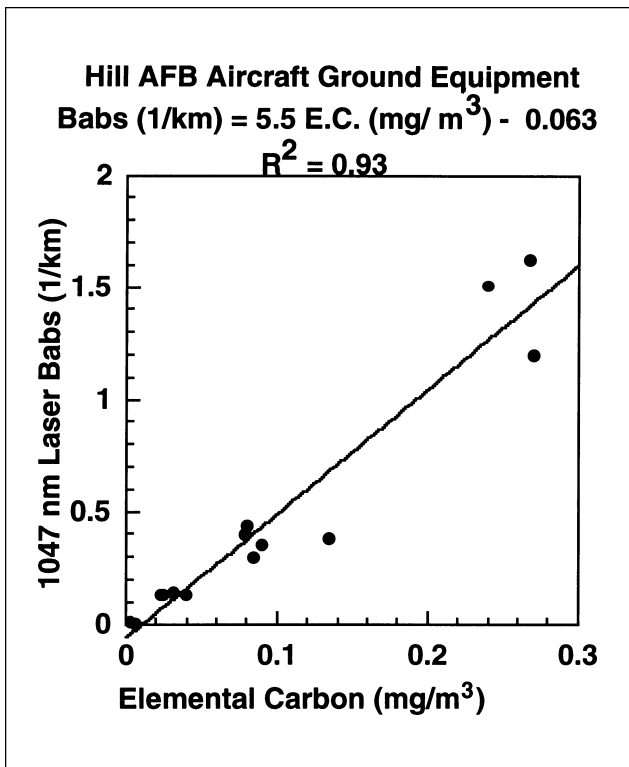


Figure 20. Comparison of near-real-time light absorption measured by the photoacoustic analyzer (PA) and EC measured by thermal-optical reflectance (TOR) of filter samples.⁴⁴⁸ The two techniques show good correlation for a range of IC engine sources. Courtesy of P. Arnott.

instrument similar to a design that is now commercially available. Studies have compared the composition of source PM and of ambient PM by cascade impactor time-averaged samples and by time trend data from the ATOFMS.⁴⁵⁸ Real-time characterization of aerosol time-of-flight mass spectroscopy has also been used in studies of diesel exhaust to study PAH composition under various operating conditions.⁴⁵⁹

Figure 21 illustrates four single particle mass spectra sampled using an on-line single particle mass spectrometer developed at the University of California, Riverside.^{457,460} These four single particles are representative of (a) diesel- and (b) gasoline-powered vehicular OC-containing particulate emissions, (c) coal combustion, and (d) ambient dust. Figures 21a-c show single particles collected during controlled source characterization studies utilizing a dilution sampler.^{276,278} These illustrate how single particle source characterization studies allow for the identification and differentiation of PM sources. Figures 21a-1 and 21a-2 are the cation and anion spectra, respectively, of an OC-containing particulate emitted from a 1994 Ford E350 diesel truck. The cation spectrum contains many low mass organic fragments, as well as nitrogen-containing species. Peaks of interest from the cation spectrum include m/z 12 (C^+), m/z 18 (NH_4^+), m/z 27 ($C_2H_3^+$), m/z 43 ($C_3H_7^+$, $C_2H_3O^+$, $CHNO^+$) m/z 86, and m/z 101. The

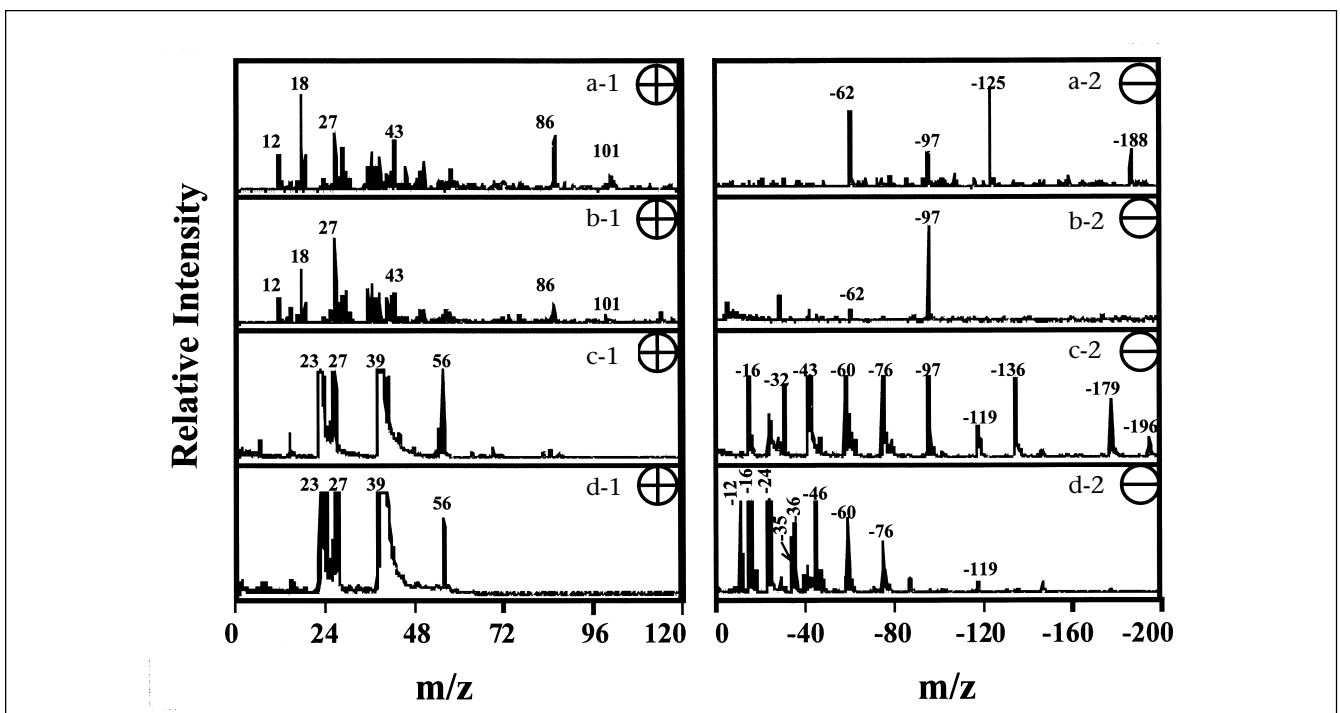


Figure 21. Mass spectra from four different single aerosol particles. a-1 through d-1 are single particle cation spectra and a-2 through d-2 are their associated anion spectra. a-1 and a-2 are from a single particle emitted from a diesel-powered 1994 Ford E350 truck. b-1 and b-2 represent a single particle emitted from a gasoline-powered 1993 Honda Civic. c-1 and c-2 represent a single particle emitted from the combustion of Illinois coal. d-1 and d-2 represent an ambient Riverside, CA, dust particle collected on Oct. 7, 1999. Each of these single particles is representative of its specific source or type. Courtesy of K. Prather and D. Suess.

anion spectrum contains fewer signals, and these are dominated by sulfur- and nitrogen-containing species including m/z -62 (NO_3^-), m/z -97 (HSO_4^-), m/z -125 (HN_2O_6^-) and m/z -188 ($\text{H}_2\text{N}_3\text{O}_9^-$).

Figures 21b-1 and 21b-2 are representative OC-containing single particles emitted from a gasoline-powered 1993 Honda Civic. The cation spectrum, Figure 21b-1, contains very similar low-mass organic fragments to those observed from the diesel-powered vehicle, 21a-1. Therefore, differentiating OC-containing single particles from gasoline- and diesel-powered vehicles solely by their positive spectra is not possible. However, with additional information from the anion spectra, these OC-containing single particles can be differentiated. Figure 21b-2 does not contain signals at m/z -125 or m/z -188. As shown in Figure 21a-2, signals at these m/z values are associated with diesel-powered OC vehicular emissions.

Figures 21c-1 and 21c-2 are representative Illinois coal combustion. The cation spectrum contains signals at m/z 23 (Na^+), m/z 27 (Al^+), m/z 39 (K^+) and m/z 56 (Fe^+). In contrast to Figures 21a and b, the complexity of this inorganic particle type lies in the anion spectrum. Chemical species present in Figure 21c-2 include m/z -16 (O_2^-), m/z -32 (S^- , O_2^-), m/z -43 (BO_2^-), m/z -60 (SiO_2^-), m/z -76 (SiO_3^-), m/z -97 (HSO_4^-), m/z -119 (AlSiO_4^-), m/z -136 (Si_2O_5^-), m/z -179 ($\text{AlSi}_2\text{O}_6^-$), and m/z -196 (Si_3O_7^-). Figures 21d-1 and 21d-2 represent an ambient dust particle sampled in Riverside, CA, on October 7, 1999. The cation ambient dust spectrum is indistinguishable from the coal combustion single particle cation spectrum in Figure 21c-1, but the anion spectra allow for differentiation between these single particle types. Signals in Figure 21d-2 differing from Figure 21c-2 include m/z -12 (C^-), m/z -24 (C_2^-), m/z -35 (Cl^-), m/z -36 (C_3^-), and m/z -46 (NO_2^-). Interestingly, the sulfur-containing species are absent from the ambient dust single particle, as well as from higher mass silicate clusters.

As more single particle source characterization studies are performed, the goal of performing source apportionment of ambient aerosols on a single particle basis becomes more feasible. Data such as these illustrate that it should be possible to distinguish vehicle emission particles from different engine types from other combustion processes such as coal. In addition, the differentiation of coal from ambient dust should be possible using the unique combination of ion markers shown here.

The ATOFMS measurements of single particle composition can provide data on the variation in both source and ambient particles that is lost in filter samples. This allows detailed characterization of both combustion sources and ambient particles on a level of detail that will be suitable for testing of specific toxicological hypotheses; however, this technique has limitations. Large particles are

preferentially detected by the ATOFMS, which requires correcting the raw data for the counting efficiency.⁴⁶¹ The current limit of detection is $\sim 0.2 \mu\text{m}$. Work is on-going to extend the capability of this technology to characterize ultrafines and nanoparticles.

Both source-based modeling and ambient studies with real-time instruments have demonstrated that the composition of the ambient aerosol has short-term variation as the wind brings in particles from various mixtures of sources. Presently, the relative importance of time-averaged exposure versus short-term exposure to spikes in the ambient aerosol composition is unknown. Some laboratory studies have shown strong responses from short exposures to high particle concentrations.⁴⁶² Figure 22 shows the time-resolved PM_{10} and $\text{PM}_{2.5}$ measured at an active military base located near an urban area.⁴⁴⁰ These transients are suspected to result from nearby sources. The ATOFMS, PAS, and photoacoustic analyzer and similar near-real time instruments provide the analytical tools needed to begin testing hypotheses related to transient exposure. Advances in both data reduction capability and in instrumentation capability, especially with regard to the submicron and nanoparticle components, are still needed.

CONCLUDING COMMENTS

Providing the scientific basis for improved regulation of the emission of combustion particles requires an interdisciplinary approach with interactions between researchers in combustion, air pollution control, atmospheric transport and transformation, exposure assessment, and health effects, together with the regulatory community. The review has touched briefly on relevant information in these areas, providing references for the reader interested in more detailed coverage. Gaps exist in the scientific understanding of all elements of the problem, but the greatest gaps are at the interfaces between the fields. In addition to the need to fill these gaps, there is a need for a better balance between applying the knowledge that has been gained to answer pressing questions and refining the theory to gain better solutions. Significant progress has been made in understanding the processes governing combustion particle formation:

- Particles emitted from combustors are either generated by condensation or, in the case of soot, molecular weight growth reactions that lead to the formation from the gas phase of submicron aggregates of primary particles. Significant progress has been made in understanding the factors controlling the amount, size, and composition of these submicron particles. Their mass is determined primarily in the early stages of combustion for soot, inorganic ash, and condensable hydrocarbons. H_2SO_4 is controlled by

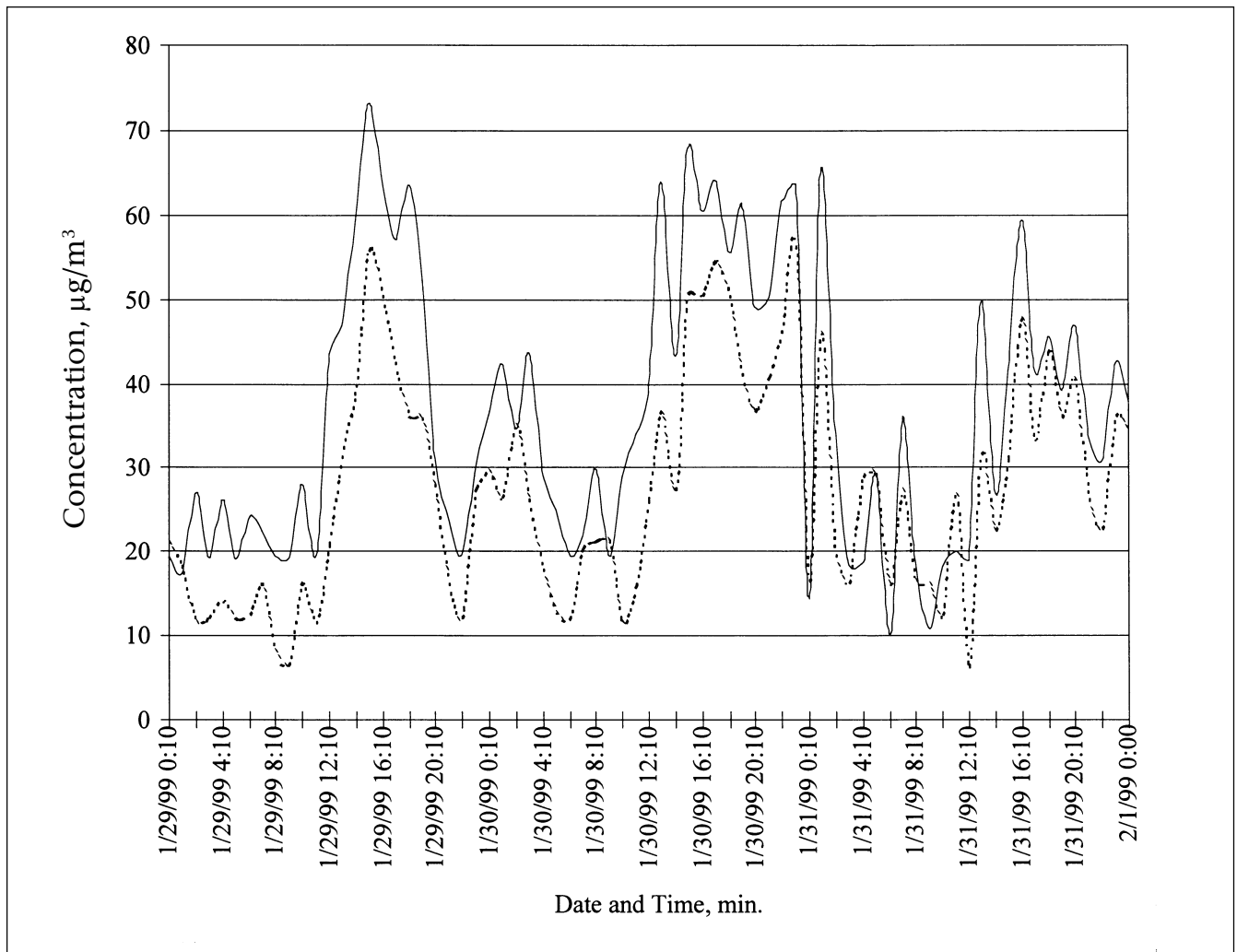


Figure 22. Time trend measurements of PM_{10} (—) and $PM_{2.5}$ (-----) by a beta attenuation meter show short-term spikes in fine particles, presumably from nearby combustion sources. Courtesy of G. Palmer.⁴⁴⁰

the oxidation of SO_2 , primarily catalytically, on tube surfaces, fly ash, and, for certain vehicles, catalytic converters. The number and size distribution of the aggregates is controlled by collision and coagulation processes that are relatively well understood.

- Supramicron combustion-generated particles are produced by the agglomeration of the mineral content in fuels and by the coking of heavy hydrocarbons in fuel oils or coals. The size of these particles is, to an order of magnitude, equal to that of the parent fuel particles for pulverized or atomized fuels. The larger particles will be emitted only in the case of combustion systems not equipped with particulate control equipment. Large particles of carbonaceous material are also important for uncontrolled combustors such as fireplaces and open burning.
- Trace, sometimes toxic, elements are emitted in small enough amounts not to contribute significantly

to the mass of the emitted particles. They are distributed between the sub- and supramicron particles emitted by combustors by condensation and surface reaction, sometimes modified by diffusion through pores. The processes governing the distribution of the trace elements are relatively well known; the size dependence of the concentration depends on the controlling mechanism and can provide a means for determining that mechanism.

The particle formation mechanisms have been used mainly in interpreting laboratory data. Although imperfect, they are at a stage where they can be incorporated in computational fluid dynamics simulations of furnaces and boilers to make predictive calculations of the particle size distribution and composition. In order to predict emissions, one needs to combine the information on the size and composition distribution of the particles emerging from combustors with information on the collection efficiency of the APCDs. The penetration of the APCD by

particles will vary with the design and operation of the APCD. No control devices are installed on many small combustors or combustors operated with clean fuels, so that the emissions are closely approximated by the combustion emissions.

The limited studies of the PM at the inlet and outlet of APCD devices on full-scale combustion systems show that particle penetration is greatest in the 0.1–1.0 μm range, that is, in the transition of dominance of inertial forces to particle diffusion. There is a need to integrate models of the APCD with those of particle formation. At present, the greatest investment in the measurement of particle emissions has been carried out for compliance purposes and provides data on the total (not size-dependent) penetration efficiency of different elements. Without a mechanistic model, it is not possible to determine how these emission parameters change with changes in fuel, combustion conditions, or the operation and maintenance of the APCD. Further, little effort has been directed at extending the knowledge gained from studies of particle formation in engineered combustion chambers to some of the more mundane sources, such as domestic combustion and open burning. These types of sources are of increasing environmental importance as the emissions from boilers, furnaces, and IC engines become better controlled through improved technology.

Empirical emission factors become quickly dated as regulations are tightened, and as technological changes impact fuel composition and combustor design. The trends in emissions for major combustion sources show decreasing total mass emissions from coal-fired and oil-fired boilers and from on-road diesel engines. Modifications of older stationary sources and the retirement of older vehicles have more than offset the increases due to growing population and economic activity. More attention needs to be focused on biomass sources if these are used to significantly supplant fossil fuel combustors. A major question, however, arises as to whether decrease in mass emission per se achieves the desired impacts of safeguarding human health, since in many cases, the decrease in mass is accompanied by an increase in numbers of smaller particles.

Examination of the size and composition of combustion-generated particles shows that, compared with geologically generated ambient PM, they are smaller and have unique chemical composition and morphology that reflect the fuel composition, the combustion conditions, and the particle transformations between the furnace and the stack. The data generated for compliance purposes provide a starting point, but are not adequate to answer many of the health-related hypotheses being proposed. More characterization studies will be needed for particle

sources, including measurements of transient emissions, detailed chemical speciation, and ultrafine particle number. The complex aerosol mixture produced by combustion is further transformed in the atmosphere before human exposure by mechanisms that, though subject to uncertainty, are sufficiently well understood to provide reasonable models of ambient particles from well-characterized emissions.

Epidemiology has demonstrated that susceptible individuals are being harmed by ambient particulate air pollution at levels comparable to the current air quality standards. Based on these findings, new regulations have been proposed for $\text{PM}_{2.5}$, but these have been contested. The proposed regulations based on mass loading are to be subject to review as current research leads to better understanding of the mechanism for the health impact of particles and of which specific size fractions and chemicals are responsible for these effects. Controlled studies with surrogate particles are being conducted to help unravel the various hypotheses proposed for the biological effects associated with the exposure to ambient particles. The problem is confounded by the probability that different particle characteristics are associated with different health end points in different susceptible populations. Particle surface area, number of ultrafine particles, and bioavailable transition metals are likely to be found to be more important than particle mass when correlating health effects with air pollution.

The understanding of the effects of particle air pollution on health has benefited from great advances in biochemistry and molecular biology on one side and from improved particle measurement capabilities on the other. Mechanistic toxicology studies are currently looking at the activation of specific genes and the synthesis of specific proteins in response to exposure to particles. Advances in the ability to collect time- and size-resolved research data on the composition of the ambient air will provide valuable input data for health studies and help identify the particle characteristics that are actually responsible for biological responses.

As the particles of importance to human health are identified, time- and size-resolved data will be needed for source apportionment studies both during the development of plans to improve air quality, and for the development of particle-control engineering technology for stationary and mobile sources. The health effects and apportionment studies can be assisted by the knowledge derived from the more fundamental studies on how fuel and combustion conditions affect size and composition of particulate emissions.

The observed association of increased ambient PM with adverse health effects and the lack of a toxicological mechanism provide the dilemma of balancing the added

Table 10. Nomenclature.

APCD	Air pollution control device
ATOFMS	Aerosol time-of-flight mass spectrometer
D_p	Aerodynamic or physical diameter of a particle
EC/OC	Elemental carbon and organic carbon, respectively, as measured by thermal/optical reflectance or a similar method
ESP	Electrostatic precipitator
EPA	United States Environmental Protection Agency
f_v	Volume fraction of a species (metal oxide or soot) per volume of gas
GC	Gas chromatograph
NAAQS	National Ambient Air Quality Standards
PAH	Polycyclic aromatic hydrocarbons
PM	Airborne particulate matter
SMPS	Scanning mobility particle sizer

cost to society of implementing imperfect regulations against the health costs of delaying action. The role of epidemiology during the 1854 cholera outbreak in London is instructive.⁴⁶³ Dr. John Snow showed a correlation between cholera deaths and water from the Broad Street pump. Discovery of the germ theory of disease by Louis Pasteur was still 11 years in the future, and isolation of the cholera bacteria was 32 years in the future.⁴⁶⁴ However, closing the well, based solely on associations and in the absence of a biological mechanism, stopped the epidemic and saved lives. Implementing a stricter fine particle standard can be seen as an analogous to “removing the pump handle.” However, closing the offending well had a small cost, since other sources of water were nearby. Major reductions in the emissions of primary particles, especially ultrafines, from stationary and mobile combustion sources will require both advances in engineering practice and major investments of capital.

The cost of the implementation of the regulations can, however, be reduced by contributions provided by advances in the fields of aerosol and combustion science, combined with advances in biochemistry and toxicology. A causal relationship between ambient particles from different sources and specific health end points is needed to provide a sound scientific basis for regulations. These scientific contributions will eventually allow better prioritization of air pollution control resources. The tradeoffs between social costs and health risks are value judgments that need to be resolved through the political process, but that process can be assisted by the clarification of the scientific issues.

ACKNOWLEDGMENTS

The review draws on the results generated in part through projects supported by the Strategic Environmental

Research and Development Program and by the U.S. Department of Energy through a subcontract from Physical Sciences, Inc.

The authors also acknowledge Pat Arnott, Brian Griffin, Glen Palmer, Dave Suess, Kimberly Prather, John Watson, and Ann Aust, who provided unpublished data and figures; William Linak, Terttaliisa Lind, Frank Huggins, Peter Reilly, and Bruce Harris, who furnished preprints of work in progress; and Richard Kanner, George Mulholland, Kent Pinkerton, Judith Chow, Martha Veranth, and the anonymous reviewers, who all provided valuable comments on the manuscript. We are grateful to Tom Brown for providing the data on the DOE field studies on the emission of air toxics from coal-fired power plants.

REFERENCES

1. Mauderly, J.L. Summary of the Third Colloquium on Particulate Air Pollution and Human Health, Durham, North Carolina, June 6-8, 1999. In *Third Colloquium on Particulate Air Pollution and Human Health, Durham, North Carolina*; Air Pollution Health Effects Laboratory: University of California, Irvine, 1999; pp 3-9-3-14.
2. Glovsky, M.M.; Miguel, A.G.; Cass, G.R. Particulate Air Pollution: Possible Relevance in Asthma; *Allergy Asthma Proc.* 1997, 18(3), 163-166.
3. Mauderly, J.L. Toxicological Approaches to Complex Mixtures; *Environ. Health Perspect.* 1993, 101(Suppl. 4), 155-165.
4. Albritton, D.; Greenbaum, D.S. Atmospheric Observations: Helping Build the Scientific Basis for Decisions Related to Airborne Particulate Matter. In *PM Measurements Research Workshop*; Health Effects Institute: Chapel Hill, NC, 1998; pp 9-12.
5. Mauderly, J.; Neas, L.; Schlesinger, R. PM Monitoring Needs Related to Health Effects. In *Atmospheric Observations: Helping Build the Scientific Basis for Decisions Related to Airborne Particulate Matter*; PM Measurements Research Workshop; Health Effects Institute: Chapel Hill NC, 1998; pp 9-14.
6. Seinfeld, J.H.; Pandis, S.N. *Atmospheric Chemistry and Physics—From Air Pollution to Climate Change*; Wiley: New York, 1998.
7. Finlayson-Pitts, B.J.; Pitts, J.N.J. *Chemistry of the Upper and Lower Atmosphere: Theory, Experiments, and Applications*; Academic Press: San Diego, CA, 2000.
8. Flagan, R.C.; Seinfeld, J.H. *Fundamentals of Air Pollution Engineering*; Prentice Hall: Englewood Cliffs, NJ, 1988.
9. Ulrich, G.D. Theory of Particle Formation and Growth in Oxide Synthesis Flames; *Combust. Sci. Technol.* 1971, 4, 47-57.
10. George, A.P.; Murley, R.D.; Place, E.R. The Formation of TiO₂ Aerosol from the Combustion Supported Reaction of TiCl₄ and O₂; *Faraday Symp. Chem. Soc.* 1973, 7, 63-71.
11. Oxtoby, D.W. Nucleation. In *Fundamentals of Inorganic Fluids*; Henderson, D., Ed.; Marcel Dekker: New York, 1992; pp 407-442.
12. Oxtoby, D.W. Homogeneous Nucleation: Theory and Experiment; *J. Phys.: Condens. Matter* 1992, 4, 7627-7650.
13. Mirabel, P.; Katz, J.L. Binary Homogeneous Nucleation as a Mechanism for the Formation of Aerosols; *J. Chem. Phys.* 1974, 60, 1138-1144.
14. Flagan, R.C.; Friedlander, S.K. Particle Formation in Pulverized Coal Combustion—A Review. In *Recent Developments in Aerosol Science*; Symposium on Aerosol Science and Technology, Atlantic City, NJ, August 1976; Shaw, D.T., Ed.; Wiley: New York, 1976; pp 25-59.
15. McNallan, M.J.; Yurek, G.J.; Elliott, J.F. The Formation of Inorganic Particulates by Homogeneous Nucleation in Gases Produced by the Combustion of Coal; *Combust. Flame* 1981, 42, 45-60.
16. McLean, W.J.; Hardesty, D.R.; Pohl, J.H. Direct Observations of Devolatilizing Pulverized Coal Particles in a Combustion Environment. In *18th Symposium (International) on Combustion*; The Combustion Institute: Pittsburgh, PA, 1981; pp 1239-1248.
17. Seeker, W.R.; Samuelsen, G.S.; Heap, M.P.; Trolinger, J.D. The Thermal Decomposition of Pulverized Coal Particles. In *18th Symposium (International) on Combustion*; The Combustion Institute: Pittsburgh, PA, 1981; pp 1213-1226.
18. Timothy, L.D.; Froelich, D.; Sarofim, A.F.; Béer, J.M. Soot Formation and Burnout During the Combustion of Dispersed Pulverized Coal Particles. In *21st Symposium (International) on Combustion*; The Combustion Institute: Pittsburgh, PA, 1986; pp 1141-1148.
19. Helble, J.; Neville, M.; Sarofim, A.F. Aggregate Formation from Vaporized Ash during Pulverized Coal Combustion. In *21st Symposium (International) on Combustion*; The Combustion Institute: Pittsburgh, PA, 1986; pp 411-417.

20. Helble, J.J.; Sarofim, A.F. Factors Determining the Primary Particle Size of Flame-Generated Inorganic Aerosols; *J. Colloid Interface Sci.* **1989**, *128*(2), 348-362.
21. Neville, M.; Sarofim, A.F. The Stratified Composition of Inorganic Submicron Particles Produced during Coal Combustion. In *19th Symposium (International) on Combustion*; The Combustion Institute: Pittsburgh, PA, 1982; pp 1441-1449.
22. Neville, M.; Quann, R.J.; Haynes, B.S.; Sarofim, A.F. Vaporization and Condensation of Mineral Matter during Pulverized Coal Combustion. In *18th Symposium (International) on Combustion*; The Combustion Institute: Pittsburgh, PA, 1981; pp 1267-1274.
23. Senior, C.L.; Flagan, R.C. Ash Vaporization and Condensation during Combustion of a Suspended Coal Particle; *Aerosol Sci. Technol.* **1982**, *1*, 371-383.
24. Peshty, A.J.; Flagan, R.C.; Seinfeld, J.H. The Effect of a Growing Aerosol on the Rate of Homogeneous Nucleation of a Vapor; *J. Colloid Interface Sci.* **1981**, *82*(2), 465-479.
25. Amdur, M.O.; Sarofim, A.F.; Neville, M.; Quann, R.J.; McCarthy, J.F.; Elliot, J.F.; Lam, H.F.; Rogers, A.E.; Conner, M.W. Coal Combustion Aerosols and SO₂: An Interdisciplinary Approach; *Environ. Sci. Technol.* **1986**, *20*(2), 138-145.
26. Amdur, M. Animal Toxicology. In *Particles In Our Air: Concentrations and Health Effects*; Wilson, R., Spengler, J., Eds.; Harvard University Press: Cambridge, MA, 1996; pp 85-122.
27. Kittelson, D.B. Engines and Nanoparticles: A Review; *J. Aerosol Sci.* **1998**, *29*(5/6), 575-588.
28. Dobbins, R.A.; Subramaniasivam, H. Soot Precursor Particles in Flames. In *Soot Formation in Combustion*; Bockhorn, H., Ed.; Springer Series in Chemical Physics; Springer-Verlag: Berlin, 1994; pp 290-301.
29. Howard, J.B.; Wersborg, B.L.; Williams, G.C. Coagulation of Carbon Particles in Premixed Flames; *Faraday Symp. Chem. Soc.* **1973**, *7*, 109-119.
30. Bockhorn, H. *Soot Formation in Combustion, Mechanisms and Models*; Springer Series in Chemical Physics; Springer-Verlag: Berlin, 1994; Vol. 59.
31. Palmer, H.B.; Cullis, C.F. *Chem. Phys. Carbon* **1965**, *1*, 265-325.
32. Haynes, B.S.; Wagner, H.G. Sooting Structure in a Laminar Diffusion Flame; *Ber. Bunsen-Ges. Phys. Chem.* **1980**, *84*(5), 499-506.
33. Haynes, B.S. Soot and Hydrocarbons in Combustion. In *Fossil Fuel Combustion*; Sarofim, A.F., Bartok, W., Eds.; Wiley Interscience: New York, 1991; pp 261-326.
34. Kennedy, I.M. Models of Soot Formation and Oxidation; *Prog. Energy Combust. Sci.* **1997**, *23*, 95-132.
35. Gulder, O.L. Soot Particulate Formation in Combustion; *Trans. Can. Soc. Mech. Eng.* **1999**, *23*, 225-240.
36. Olsen, D.B.; Pickens, J.C. *Combust. Flame* **1984**, *57*, 199-208.
37. Appel, J.; Bockhorn, H.; Frenklach, M. Kinetic Modeling of Soot Formation with Detailed Chemistry and Physics: Laminar Premixed Flames of C₂ Hydrocarbons; *Combust. Flame* **2000**, *121*, 122-136.
38. Violi, A.; D'Anna, A. Modeling of Aromatics Formation in Rich Premixed Flames. In *21st Event of the Italian Section of the Combustion Institute*; The Combustion Institute: Naples, Italy, 1998; pp 249-260.
39. Howard, J.B. On the Mechanism of Carbon Formation in Flames. In *12th Symposium (International) on Combustion*; The Combustion Institute: Pittsburgh, PA, 1969; pp 877-887.
40. Friedlander, S.K. *Smoke, Dust, and Haze, Fundamentals of Aerosol Behavior*; John Wiley & Sons: New York, 1976.
41. *The Mechanics of Aerosols*; Fuchs, N.A., Ed.; Translated from the Russian by R. E. Daisley and M. Fuchs, Translation edited by C. N. Davies; Macmillan: New York, 1964.
42. Gelbard, F.; Steinfield, J. Simulation of Multicomponent Aerosol Dynamics; *J. Colloid Interface Sci.* **1978**, *78*(2), 485-501.
43. Wu, J.J.; Flagan, R.C. A Discrete-Sectional Solution to the Aerosol Dynamic Equation; *J. Colloid Interface Sci.* **1988**, *123*(2), 339-352.
44. Wu, C.-Y.; Biswas, P. Study of Numerical Diffusion in a Discrete-Sectional Model and Its Application to Aerosol Dynamics Simulation; *Aerosol Sci. Technol.* **1998**, *29*, 359-378.
45. Park, S.H.; Lee, K.W.; Otto, E.; Fissan, H. The Log-Normal Size Distribution Theory of Brownian Aerosol Coagulation for the Entire Particle Size Range: Part I—Analytical Solution Using the Harmonic Mean Coagulation Kernel; *J. Aerosol Sci.* **1999**, *30*(1), 3-16.
46. Otto, E.; Fissan, H.; Park, S.H.; Lee, K.W. The Log-Normal Size Distribution Theory of Brownian Aerosol Coagulation for the Entire Particle Size Range: Part II—Analytical Solution Using Dahneke's Coagulation Kernel; *J. Aerosol Sci.* **1999**, *30*(1), 17-34.
47. Landgrebe, J.D.; Pratsinis, S.E. Discrete-Sectional Model for Particulate Production by Gas-Phase Chemical Reaction and Aerosol Coagulation in the Free-Molecular Regime; *J. Colloid Interface Sci.* **1990**, *139*(1), 63-86.
48. Mick, H.J.; Hospital, A.; Roth, P. Computer Simulation of Soot Particle Coagulation in Low Pressure Flames; *J. Aerosol Sci.* **1991**, *22*(7), 831-841.
49. Jokiniemi, J.K.; Lazaridis, M.; Lehtinen, K.E.J.; Kauppinen, E.I. Numerical Simulation of Vapour-Aerosol Dynamics in Combustion Processes; *J. Aerosol Sci.* **1994**, *25*(3), 429-446.
50. Pilinis, C.; Capaldo, K.P.; Nenes, A.; Pandis, S.N. MADM—A New Multicomponent Aerosol Dynamics Model; *Aerosol Sci. Technol.* **2000**, *32*(5), 482-502.
51. Hinds, W.C. *Aerosol Technology: Properties, Behavior, and Measurement of Airborne Particles*; John Wiley & Sons: New York, 1982.
52. Marlow, W.H. Derivation of Aerosol Collision Rates for Singular Attractive Contact Potentials; *J. Chem. Phys.* **1980**, *73*, 6284-6287.
53. Lai, F.S.; Friedlander, S.K.; Pich, J.; Hindy, G.M. *J. Colloid Interface Sci.* **1972**, *39*, 395-405.
54. Desrosiers, R.E.; Riehl, J.W.; Ulrich, G.D.; Chiu, A.S. Submicron Fly-Ash Formation in Coal-Fired Boilers. In *17th Symposium (International) on Combustion*; The Combustion Institute: Pittsburgh, PA, 1978; pp 1395-1403.
55. Taylor, D.D.; Flagan, R.C. The Influence of Combustor Operation on Fine Particles from Coal Combustion; *Aerosol Sci. Technol.* **1982**, *1*, 103-117.
56. *Soot in Combustion Systems and Its Toxic Properties*; Lahaye, J., Prado, G., Eds.; NATO Conference Series, VI Materials Science v. 7; Plenum Press: New York, 1983.
57. Harris, S.J.; Weiner, A.M. *Combust. Sci. Technol.* **1984**, *38*, 75-87.
58. Sethi, V.; Biswas, P. Modeling of Particle Formation and Dynamics in a Flame Incinerator; *J. Air & Waste Manage. Assoc.* **1990**, *40*(1), 42-46.
59. Linak, W.P.; Wendt, J.O.L. Toxic Metal Emissions from Incineration: Mechanisms and Control; *Prog. Energy Combust. Sci.* **1993**, *19*, 145-185.
60. Flagan, R.C.; Taylor, D.D. Laboratory Studies of Submicron Particles from Coal Combustion. In *18th Symposium (International) on Combustion*; The Combustion Institute: Pittsburgh, PA, 1981; pp 1227-1237.
61. Quann, R.J.; Sarofim, A.F. Vaporization of Refractory Oxides during Pulverized Coal Combustion. In *19th Symposium (International) on Combustion*; The Combustion Institute: Pittsburgh, PA, 1982; pp 1429-1440.
62. Mims, C.A.; Neville, M.; Quann, R.J.; House, K.; Sarofim, A.F. Laboratory Studies of Mineral Matter Vaporization during Coal Combustion. In *Emission Control from Stationary Power Sources: Technical, Economic, and Environmental Assessments*; Engle, A.J., Slater, S.M., Gentry, J.W., Eds.; American Institute of Chemical Engineers: New York, 1980; pp 188-194.
63. McElroy, M.W.; Carr, R.C.; Ensor, D.S.; Markowski, G.R. Size Distribution of Fine Particles from Coal Combustion; *Science* **1982**, *215*, 13-19.
64. McElroy, M.W.; Carr, R.C. Relationship between NO_x and Fine Particle Emissions. In *Joint Symposium on Stationary Combustion NO_x Control*; Electric Power Research Institute: Palo Alto, CA, 1981; pp 311-329.
65. Lindner, E.R.; Wall, T.F. Sodium-Ash Reactions during the Combustion of Pulverized Coal. In *23rd Symposium (International) on Combustion*; The Combustion Institute: Pittsburgh, PA, 1991; pp 1313-1321.
66. Damle, A.S.; Ensor, D.S.; Ranade, M.B. Coal Combustion Aerosol Formation Mechanisms: A Review; *Aerosol Sci. Technol.* **1982**, *1*, 119-133.
67. Neville, M.; Sarofim, A.F. The Fate of Sodium during Pulverized Coal Combustion; *Fuel* **1985**, *64*, 384-490.
68. Seames, W.S.; Wendt, J.O.L. Partitioning of Arsenic, Selenium, and Cadmium during the Combustion of Pittsburgh and Illinois #6 Coals in a Self-Sustained Combustor; *Fuel Process. Technol.* **2000**, *63*, 179-196.
69. Haynes, B.S.; Neville, M.; Quann, R.J.; Sarofim, A.F. Factors Governing the Surface Enrichment of Fly Ash in Volatile Trace Species; *J. Colloid Interface Sci.* **1982**, *87*(1), 266-278.
70. Davison, R.L.; Natusch, D.F.S.; Wallace, J.R.; Evans, C.A.J. Trace Elements in Fly Ash Dependence of Concentration on Particle Size; *Environ. Sci. Technol.* **1974**, *8*(13), 1107-1113.
71. Ondov, J.M.; Ragini, R.C.; Biermann, A.H. Elemental Particle-Size Emissions from Coal-Fired Power Plants: Use of an Inertial Cascade Impactor; *Atmos. Environ.* **1978**, *12*, 1175-1185.
72. Biermann, A.H.; Ondov, J.M. Application of Surface-Deposition Models to Size-Fractionated Coal Fly Ash; *Atmos. Environ.* **1980**, *14*, 289-295.
73. Linak, W.P.; Wendt, J.O.L. Trace Metal Transformation Mechanisms during Coal Combustion; *Fuel Process. Technol.* **1994**, *39*(1), 173-198.
74. Ondov, J.M.; Ragini, R.C.; Biermann, A.H. Elemental Emissions from a Coal-Fired Power Plant. Comparison of a Venturi Wet Scrubber System with a Cold-Side Electrostatic Precipitator; *Environ. Sci. Technol.* **1979**, *13*(5), 598-607.
75. Coles, D.G.; Ragini, R.C.; Ondov, J.M. Behaviour of Radionuclides in Western Coal-Fired Power Plants; *Environ. Sci. Technol.* **1978**, *12*(4), 442-446.
76. Gladney, E.S.; Small, J.A.; Gordon, G.E.; Zoller, W.H. Composition and Size Distribution of In-Stack Particulate Material at a Coal-Fired Power Plant; *Atmos. Environ.* **1976**, *10*, 1071-1077.
77. Kaakinen, J.W.; Jorden, R.M.; Lawasani, M.H.; West, R.E. Trace Element Behavior in a Coal-Fired Power Plant; *Environ. Sci. Technol.* **1975**, *9*(9), 862-869.

78. Shendrikar, A.D.; Ensor, D.S.; Cowen, S.J.; Woffinden, G.J.; McElroy, M.W. Size-Dependent Penetration of Trace Elements through a Utility Baghouse; *Atmos. Environ.* **1983**, *17*(8), 1411-1421.
79. Klein, D.H.; Andren, A.W.; Carter, J.A.; Emery, J.F.; Feldman, C.; Fulkerson, W.; Lyon, W.S.; Ogle, J.C.; Talmi, Y.; van Hook, R.I.; Bolton, N. Pathways of Thirty-Seven Trace Elements through Coal-Fired Power Plant; *Environ. Sci. Technol.* **1975**, *9*(10), 973-979.
80. Linak, W.P.; Peterson, T.W. Mechanisms Governing the Composition and Size Distribution of Ash Aerosol in a Laboratory Pulverized Coal Combustor. In *21st Symposium (International) on Combustion*; The Combustion Institute: Pittsburgh, PA, 1986; pp 399-410.
81. Markowski, G.R.; Ensor, D.S.; Hooper, R.G.; Carr, R.C. A Submicron Aerosol Mode in Flue Gas from a Pulverized Coal Utility Boiler; *Environ. Sci. Technol.* **1980**, *14*(11), 1400-1402.
82. Neville, M.; McCarthy, J.F.; Sarofim, A.F. Size Fractionation of Submicrometer Coal Combustion Aerosol for Chemical Analysis; *Atmos. Environ.* **1983**, *17*(12), 2599-2604.
83. Smith, R.D.; Campbell, J.A.; Nielson, K.K. Characterization and Formation of Submicron Particles in a Coal-Fired Plant; *Atmos. Environ.* **1979**, *13*, 607.
84. Smith, R.D.; Campbell, J.A.; Nielson, K.K. Volatility of Fly Ash and Coal; *Fuel* **1980**, *59*, 661-665.
85. Senior, C.L.; Bool, L.E.I.; Morency, J.R. Laboratory Study of Trace Element Vaporization from Combustion of Pulverized Coal; *Fuel Process. Technol.* **2000**, *63*, 109-124.
86. Helble, J.J. Trace Element Behavior during Coal Combustion: Results of a Laboratory Study; *Fuel Process. Technol.* **1994**, *39*(1), 159-172.
87. Senior, C.L.; Bool, L.E.I.; Srinivasachar, S.; Pease, B.R.; Porle, K. Pilot Scale Study of Trace Element Vaporization and Condensation during Combustion of a Pulverized Sub-Bituminous Coal; *Fuel Process. Technol.* **2000**, *63*, 149-165.
88. Linton, R.W.; Loh, A.; Natusch, D.F.S. Surface Predominance of Trace Elements in Airborne Particles; *Science* **1976**, *191*, 852-854.
89. Frandsen, F.; Dam-Johansen, K.; Rasmussen, P. Trace Elements from Combustion and Gasification of Coal—An Equilibrium Approach; *Prog. Energy Combust. Sci.* **1994**, *20*(2), 115-138.
90. Sandelin, K.; Backman, R. A Simple Two-Reactor Method for Predicting Distribution of Trace Elements in Combustion Systems; *Environ. Sci. Technol.* **2000**, *33*(24), 4508-4513.
91. Yousif, S.; Lockwood, F.C.; Abbas, T. Modeling of Toxic Metal Emissions from Solid Fuel Combustors. In *27th Symposium (International) on Combustion*; The Combustion Institute: Pittsburgh, PA, 1998; pp 1647-1654.
92. Mocellin, A.; Kingery, W.D. Microstructural Changes during Heat Treatment of Sintered Al₂O₃; *J. Amer. Ceram. Soc.* **1973**, *56*(6), 309-314.
93. Kingery, W.D.; Bowen, H.K.; Uhlmann, D.R. *Introduction to Ceramics*; Wiley: New York, 1976.
94. Ulrich, G.D.; Subramanian, N.S. Particle Growth in Flames-3. Coalescence as a Rate-Controlling Process; *Combust. Sci. Technol.* **1984**, *17* (3-4), 119-126.
95. Pratsinis, S.E. Flame Aerosol Synthesis of Ceramic Powders; *Prog. Energy Combust. Sci.* **1998**, *24*, 197-219.
96. Woolridge, M.S. Gas-Phase Combustion Synthesis of Particles; *Prog. Energy Combust. Sci.* **1998**, *24*(1), 63-87.
97. Muñoz, R.H.; Charalampopoulos, T.T. Evolution of Compositional and Structural Properties of Soot in Premixed Flames. In *27th Symposium (International) on Combustion*; The Combustion Institute: Pittsburgh, PA, 1998; pp 1471-1479.
98. Mulholland, G.W.; Liggett, W.; Koseki, H. Effect of Pool Diameter on the Properties of Smoke Produced by Crude Oil Fires. In *26th Symposium (International) on Combustion*; The Combustion Institute: Pittsburgh, PA, 1996; pp 1445-1452.
99. Koch, W.; Friedlander, S.K. Effect of Particle Coalescence on the Surface Area of a Coagulating Aerosol; *J. Colloid Interface Sci.* **1990**, *140*, 419-427.
100. Xiong, Y.; Pratsinis, S.E. Gas Phase Production of Particles in Reactive Turbulent Flows; *J. Aerosol Sci.* **1991**, *22*(5), 637-655.
101. Reilly, P.T.A.; Whitten, W.B.; Ramsey, J.M. Evidence for the Emergence of Whole Mature Soot Aggregates from Single PAH-Containing Droplets. In *2000 Technical Meeting of the Central State Section of the Combustion Institute*; The Combustion Institute: Pittsburgh, PA, 2000.
102. Biswas, P.; Wu, C.Y. Control of Toxic Metal Emissions from Combustors Using Sorbents: A Review; *J. Air & Waste Manage. Assoc.* **1998**, *48*(2), 113-127.
103. Goldstein, H.L.; Siegmund, C.W. Influence of Heavy Oil Composition and Boiler Combustion Conditions on Particulate Emission; *Environ. Sci. Technol.* **1976**, *10*(12), 1109-1114.
104. Senior, C.L.; Zeng, T.; Che, J.; Ames, M.R.; Sarofim, A.F.; Olmez, I.; Huggins, F.E.; Shah, N.; Huffman, G.P.; Kolker, A.; Mroczkowski, S.; Palmer, C.; Finkelman, R. Distribution of Trace Elements in Selected Pulverized Coals as a Function of Particle Size and Density; *Fuel Process. Technol.* **2000**, *63*(2-3), 215-241.
105. Huggins, F.E.; Huffman, G.P.; Lee, R.J. Scanning Electron Microscope-Based Automated Image Analysis (SEM-AIA) and Mossbauer Spectroscopy: Quantitative Characterization of Coal Minerals. In *Coal and Coal Products: Analytical Characterization Techniques*; Fuller, E.L., Ed.; American Chemical Society: 1982; pp 239-258.
106. Straszheim, W.E.; Markuzewski, R. Characterization of Mineral Matter in Coal for Prediction of Ash Composition and Particle Size. In *Engineering Foundation Conference on Inorganic Transformations and Ash Deposition During Combustion*; ASME: 1992; pp 165-177.
107. Steadman, E.N.; Erikson, T.A.; Folkedahl, B.C.; Brekke, D.W. Coal and Ash Characterization: Digital Image Analysis Application. In *Engineering Foundation Conference on Inorganic Transformations and Ash Deposition during Combustions*; ASME: 1991; pp 147-164.
108. Yang, N.Y.C.; Baxter, L.L. Instrument and Sample Preparation Considerations for CCSEM Analysis. In *Engineering Foundation Conference on Inorganic Ash Transformations and Ash Deposition during Combustion*; ASME: 1991; pp 191-201.
109. Yu, H.; Marchek, J.E.; Adair, N.L.; Harb, J.N. Characterization of Minerals and Coal/Mineral Associations in Pulverized Coal. In *Engineering Foundation Conference on the Impact of Ash Deposition on Coal Fired Plants*; Taylor and Francis: 1993; pp 361-372.
110. Wigley, F.; Williamson, J.; Gibb, W.H. The Distribution of Mineral Matter in Pulverized Coal Particles in Relation to Burnout Behaviour; *Fuel* **1997**, *76*, 1283-1288.
111. Wilemski, G.; Srinivasachar, S.; Sarofim, A.F. Modeling of Mineral Matter Redistribution and Ash Formation in Pulverized Coal Combustion. In *Engineering Foundation Conference on Inorganic Ash Transformations and Ash Deposition during Combustion*; ASME: 1991; pp 545-564.
112. Sarofim, A.F.; Howard, J.B.; Padia, A.S. The Physical Transformation of Mineral Matter in Pulverized Coal under Simulated Combustion Conditions; *Combust. Sci. Technol.* **1977**, *16*, 187-204.
113. Kang, S.-G.; Helble, J.J.; Sarofim, A.F.; Béer, J.M. Time-Resolved Evolution of Fly Ash during Pulverized Coal Combustion. In *22nd Symposium (International) on Combustion*; The Combustion Institute: Pittsburgh, PA, 1988; pp 231-238.
114. Baxter, L.L. *Coal Char Fragmentation during Pulverized Coal Combustion*; SAND95-8250 UC-1409; Sandia National Laboratories: 1995.
115. Benson, S.A.; Jones, M.L.; Harb, J.N. Ash Formation and Deposition. In *Fundamentals of Coal Combustion for Clean and Efficient Use*; Smoot, L.D., Ed.; Elsevier: New York, 1993; pp 299-373.
116. Barta, L.E.; Toqan, M.A.; Béer, J.M.; Sarofim, A.F. Prediction of Fly Ash Size and Chemical Composition Distributions: The Random Coalescence Model. In *24th Symposium (International) on Combustion*; The Combustion Institute: Pittsburgh, PA, 1992; pp 1135-1144.
117. Barta, L.E.; Vámos, G.; Toqan, M.A.; Béer, J.M.; Sarofim, A.F. A Statistical Investigation on Particle-to-Particle Variation of Flyash Using SEM-AIA-EDAX Technique; *Mater. Res. Soc. Symp. Proc.* **1990**, *178*, 67-81.
118. *A Study of Toxic Emissions from a Coal-Fired Power Plant Utilizing an ESP/Wet FGD System*; Batelle Columbus; DOE/PC/93251-T2; DE94017941; U.S. Department of Energy; Pittsburgh Energy Technology Center: 1994; Vol. 1.
119. Charon, O.; Sarofim, A.F.; Béer, J.M. Distribution of Mineral Matter in Pulverized Coal; *Prog. Energy Combust. Sci.* **1990**, *16*, 319-326.
120. Raask, E.; Wilkins, D.M. Volatilization of Silica in Gasification and Combustion Processes; *J. Inst. Fuel* **1965**, *38*, 255-262.
121. Kerstein, A.R.; Edwards, B.F. Percolation Model for Simulation of Char Oxidation and Fragmentation Time-Histories; *Chem. Eng. Sci.* **1987**, *42*(7), 1629-1634.
122. Kang, S.-G. Fundamental Studies of Mineral Matter Transformation during Pulverized Coal Combustion: Residual Ash Formation. Ph.D. Thesis, Massachusetts Institute of Technology, Cambridge, MA, 1991.
123. Kerstein, A.R.; Niksa, S. Fragmentation during Carbon Conversion: Predictions and Measurements. In *20th Symposium (International) on Combustion*; The Combustion Institute: Pittsburgh, PA, 1984; pp 941-949.
124. Seggiani, M.; Bardi, A.; Vitolo, S. Prediction of Fly-Ash Size Distribution: A Correlation between Char Transition Radius and Coal Properties; *Fuel* **2000**, *79*, 999-1002.
125. Hurt, R.H.; Davis, K.A. Near-Extinction and Final Burnout in Coal Combustion. In *25th Symposium (International) on Combustion*; The Combustion Institute: Pittsburgh, PA, 1994; pp 561-568.
126. Wu, H.; Bryant, G.; Benfell, K.; Wall, T. Experimental Study on the Effect of System Pressure on Char Structure of an Australian Bituminous Coal; *Energy Fuels* **2000**, *14*(2), 282-290.
127. Fischer, G.L.; Chang, D.P.Y.; Brummer, M. Fly Ash Collected from Electrostatic Precipitators: Micro-Crystalline Structures and the Mystery of Spheres; *Science* **1976**, *192*, 553.
128. Raask, E. *Mineral Impurities in Coal Combustion: Behavior, Problems, and Remedial Measures*; Hemisphere Publishing: New York, 1985.
129. Sloss, L.L.; Smith, I.M.; Adams, D.M.B. Pulverized Coal Ash—Requirements for Utilization; *IEA Coal Research* **1996**, IEACR/88.

130. McCarthy, G.J.; Solem, J.K.; Manz, O.; Hassett, D.J. Use of a Database of Chemical, Mineralogical, and Physical Properties of North American Fly Ash to Study the Nature of Fly Ash and Its Use as a Mineral Admixture in Concrete; *Miner. Res. Soc. Symp. Proc.* **1990**, *178*, 2-31.
131. Hering, S.V. *Air Sampling Instruments*; American Conference of Governmental Industrial Hygienists: Cincinnati, OH, 1995.
132. D'Alessio, A.; D'Anna, A.; Gambi, G.; Minutolo, P.; Sgro, L.A.; Violi, A. Combustion-Generated Nanoparticles; *Chim. Ind.* **1999**, *81*, 1001-1006.
133. D'Alessio, A.; D'Anna, A.; Minutolo, P.; Sgro, L.A. Nanoparticles in Combustion Systems: Their Formation and Impact on Climate Change and Health Effects. In *Chemical Engineering, Greetings to Prof. Mario Dente on the Occasion of his 65th Birthday*; AIDIC, Eds.; Milano, Italy, 1999; pp 99-110.
134. Narsimhan, G.; Ruckenstein, E. The Brownian Coagulation of Aerosols over the Entire Range of Knudsen Numbers: Connection between the Sticking Probability and the Interaction Forces; *J. Colloid Interface Sci.* **1985**, *104*(2), 344-369.
135. Graham, K.A. Submicron Ash Formation and Interaction with Sulfur Oxides During Pulverized Coal Combustion. Ph.D. Thesis, Chemical Engineering, Massachusetts Institute of Technology, Cambridge, MA, 1991.
136. Linak, W.P. The Effect of Coal Type, Residence Time, and Combustion Configuration on the Submicron Aerosol Composition and Size Distribution from Pulverized Coal Combustion. Ph.D. Thesis, University of Arizona, Tucson, AZ, 1985.
137. Miake-Lye, R.C.; Anderson, B.E.; Cofer, W.R.; Wallio, H.A.; Nowicki, G.D.; Ballenthin, J.O.; Hunton, D.E.; Knighton, W.B.; Miller, T.M.; Seelye, J.V.; Viggiano, A.A. SO_x Oxidation and Volatile Aerosol in Aircraft Exhaust Plumes Depend on Fuel Sulfur Content; *Geophys. Res. Lett.* **1998**, *25*(10), 1677-1680.
138. Park, C.; Appleton, J.P. Shock-Tube Measurements of Soot Oxidation Rates; *Combust. Flame* **1973**, *20*, 369-379.
139. Itkonen, A.O.; Jantunen, M.J. Emissions and Particle-Size Distribution of Some Metallic Elements of Two Peat/Oil-Fired Boilers; *Environ. Sci. Technol.* **1986**, *20*(4), 335.
140. *Industrial Air Pollution Control Systems*; Heumann, W.L., Ed.; McGraw-Hill: New York, 1997.
141. *Handbook of Air Pollution Technology*; Calvert, S., Englund, H.M., Eds.; Wiley: New York, 1986.
142. *Air Pollution*, 3rd Ed.; Stern, A.C., Ed.; Academic Press: New York, 1976.
143. Helble, J.J. A Model for the Air Emissions of Trace Metallic Elements from Coal Combustors Equipped with Electrostatic Precipitators; *Fuel Process. Technol.* **2000**, *63*, 125-147.
144. Soud, H.N. Developments in Particulate Control for Coal Combustion; *IEA Coal Research 1995*, IEACR/78.
145. Zhuang, Y.; Kim, Y.J.; Lee, T.G.; Biswas, P. Experimental and Theoretical Studies of Ultra-Fine Behavior in Electrostatic Precipitators; *J. Electrostat.* **2000**, *48*(3), 245-260.
146. Yoo, K.H.; Lee, J.S.; Oh, M.D. Charging and Collection of Submicron Particles in Two-Stage Parallel-Plate Electrostatic Precipitators; *Aerosol Sci. Technol.* **1997**, *27*, 308-323.
147. Watanabe, T.; Tochikubo, E.; Koizumi, Y.; Tsuchida, T.; Hautanen, J.; Kauppinen, E.I. Submicron Particle Agglomeration by an Electrostatic Agglomerator; *J. Electrostat.* **1995**, *34*, 367-383.
148. Kauppinen, E.I.; Pakkanen, T.A. Coal Combustion Aerosols: A Field Study; *Environ. Sci. Technol.* **1990**, *24*, 1811-1818.
149. Miller, S.J.; Ness, S.R.; Weber, G.F.; Erickson, T.A.; Hassett, D.J.; Hawthorne, S.B.; Katrinak, K.A.; Louie, P.K. *A Comprehensive Assessment of Toxic Emissions from Coal-Fired Power Plants: Phase I Results from the U.S. Department of Energy Study*; U.S. DOE Pittsburgh Energy Technology Center Contract DE-FC21-93MC30097; Energy & Environmental Research Center; University of North Dakota: 1996.
150. Chow, W.; Miller, M.J.; Torrens, I.M. Pathways of Trace Elements in Power Plants: Interim Research Results and Implications; *Fuel Process. Technol.* **1994**, *39*(1), 5-20.
151. Moore, T. Hazardous Air Pollutants: Measuring in Micrograms; *EPRI J.* **1994**, *19*(1), 7-15.
152. Meij, R. Trace Element Behaviour in Coal-Fired Power Plants; *Fuel Process. Technol.* **1994**, *39*(1), 199-217.
153. *Compilation of Air Emission Factors*; AP-42; EP 4.9:42/985; U.S. Environmental Protection Agency: 1982.
154. Leaderer, B.P.; Naeher, L.; Jankun, T.; Balenger, K.; Holford, T.R.; Toth, C.; Sullivan, J.; Wolfson, J.M.; Koutrakis, P. Indoor, Outdoor and Regional Summer and Winter Concentrations of PM₁₀, PM_{2.5}, SO₄²⁻, H⁺, NO₃⁻ and NH₃ and Nitrous Acid in Homes with and without Kerosene Space Heaters; *Environ. Health Perspect.* **1999**, *107*(3), 223-231.
155. Hildemann, L.M.; Markowski, G.R.; Jones, M.C.; Cass, G.R. Submicron Aerosol Mass Distributions of Emissions from Boilers, Fireplaces, Automobiles, Diesel Trucks, and Meat-Cooking Operations; *Aerosol Sci. Technol.* **1991**, *14*, 138-152.
156. Hildemann, L.M.; Markowski, G.R.; Cass, G.R. Chemical Composition of Emissions from Urban Sources of Fine Organic Aerosol; *Environ. Sci. Technol.* **1991**, *25*(4), 744-759.
157. Rogge, W.F.; Hildemann, L.M.; Mazurek, M.A.; Cass, G.R.; Simoneit, B.R.T. Sources of Fine Organic Aerosol. 8. Boilers Burning No. 2 Distillate Fuel Oil; *Environ. Sci. Technol.* **1997**, *31*(10), 2731-2737.
158. Watkinson, W.P.; Campen, M.J.; Costa, D.L. Cardiac Arrhythmia Induction after Exposure to Residual Oil Fly Ash Particles in a Rodent Model of Pulmonary Hypertension; *Toxicol. Sci.* **1998**, *41*, 209-216.
159. Dreher, K.L.; Jaskot, R.H.; Lehmann, J.R.; Richards, J.H.; McGee, J.K. Soluble Transition Metals Mediate Residual Oil Fly Ash-Induced Acute Lung Injury; *J. Toxicol. Environ. Health* **1997**, *50*, 285-305.
160. Samet, J.M.; Reed, W.; Ghio, A.J.; Devlin, R.B.; Carter, J.D.; Dailey, L.A.; Bromberg, P.A.; Madden, M.C. Induction of Prostaglandin H Synthase 2 in Human Airway Epithelial Cells Exposed to Residual Oil Fly Ash; *Toxicol. Appl. Pharmacol.* **1996**, *141*, 159-168.
161. Miller, C.A.; Linak, W.P.; King, C.; Wendt, J.O.L. Fine Particle Emissions from Heavy Fuel Oil Combustion in a Firetube Package Boiler; *Combust. Sci. Technol.* **1998**, *134*, 477-502.
162. Villasenor, R.; Garcia, F. Experimental Study of the Effects of Asphaltenes on Heavy Fuel Oil Droplet Combustion; *Fuel* **1999**, *78*, 933-944.
163. Urban, D.L.; Huey, S.P.; Dryer, F.L. Evaluation of the Coke Formation Potential of Residual Fuel Oils. In *24th Symposium (International) on Combustion*; The Combustion Institute: Pittsburgh, PA, 1992; pp 1357-1364.
164. Linak, W.P.; Miller, C.A.; Wendt, J.O.L. Comparison of the Particle Size Distributions and Elemental Partitioning from the Combustion of Pulverized Coal and Residual Fuel Oil; *J. Air & Waste Manage. Assoc.* **2000**, *50*, 1532-1543.
165. Galbreath, K.C.; Zygarlicke, C.J.; Huggins, F.E.; Huffman, G.P.; Wong, J.L. Chemical Speciation of Nickel in Residual Oil Fly Ash; *Energy Fuels* **1998**, *12*, 818-822.
166. Galbreath, K.C.; Zygarlicke, C.J.; D, L.T.; Huggins, F.E.; Huffman, G.P. Nickel and Chromium Speciation of Residual Oil Combustion Ash; *Combust. Sci. Technol.* **1998**, *134*, 243-262.
167. Huffman, G.P.; Huggins, F.E.; Shah, N.; Huggins, R.; Linak, W.P.; Miller, C.A.; Pumire, R.J.; Meuzelaar, H.L.C.; Seehra, M.S.; Manivannan, A. Characterization of Fine Particulate Matter Produced by Combustion of Residual Fuel Oil; *J. Air & Waste Manage. Assoc.* **2000**, *50*, 1106-1114.
168. Smoot, L.D.; Smith, P.J. *Coal Combustion and Gasification*; Plenum Press: New York, 1985.
169. Smoot, L.D. *Fundamentals of Coal Combustion for Clean and Efficient Use*; Elsevier: New York, 1993.
170. Flagan, R.C. Submicron Particles From Coal Combustion. In *17th Symposium (International) on Combustion*; The Combustion Institute: Pittsburgh, PA, 1978; pp 97-104.
171. Fletcher, T.H.; Ma, J.; Rigby, J.R.; Brown, A.L.; Webb, B.W. Soot in Coal Combustion Systems; *Prog. Energy Combust. Sci.* **1997**, *23*, 283-301.
172. Sadakata, M.; Yoshino, A.; Sakai, T.; Matsuoka, H. Formation of Submicron Unburnt Carbon and NO_x from Pulverized Coal Combustion System. In *20th Symposium (International) on Combustion*; The Combustion Institute: Pittsburgh, PA, 1984; pp 913-920.
173. Veranth, J.M.; Pershing, D.W.; Sarofim, A.F.; Shield, J.E. Sources of Unburned Carbon in the Fly Ash Produced from Low-NO_x Pulverized Coal Combustion. In *27th Symposium (International) on Combustion*, Boulder, CO; The Combustion Institute: Pittsburgh, PA, 1998; pp 1737-1744.
174. Veranth, J.M.; Fletcher, T.H.; Pershing, D.W.; Sarofim, A.F. Measurement of Soot and Char in Pulverized Coal Fly Ash; *Fuel* **2000**, *79*(9), 1067-1075.
175. *Characterizing Toxic Emissions from a Coal-Fired Power Plant Demonstrating the AFGD ICCT Project and a Plant Utilizing a Dry Scrubber/Baghouse System*; Final Report Bailly Station Units 7 and 8; SRI Report SRI-ENV-94-827-7960; DOE Contract DE-AC22-93PC93254; U.S. Department of Energy, Pittsburgh Energy Technology Center; Southern Research Institute: 1994.
176. *Assessment of Toxic Emissions from a Coal-Fired Power Plant Utilizing an ESP*; DOE Contract DE-AC22-93PC93252; Energy and Environmental Research Corporation; U.S. Department of Energy; Pittsburgh Energy Technology Center: 1994.
177. Lind, T.; Kauppinen, E.I.; Jokiniemi, J.K.; Maenhaut, W. A Field Study on the Trace Metal Behaviour in Atmospheric Fluidized Bed Combustion. In *25th International Symposium on Combustion*; The Combustion Institute: Pittsburgh, PA, 1994; p 201.
178. Lind, T.; Kauppinen, E.I.; Maenhaut, W.; Shah, A.; Huggins, F. Ash Vaporization in Circulating Fluidized Bed Coal Combustion; *Aerosol Sci. Technol.* **1996**, *24*(3), 135-150.
179. Mohr, M.; Ylätaalo, S.; Klippel, N.; Kauppinen, E.I.; Riccius, O.; Burtcher, H. Submicron Fly Ash Penetration through Electrostatic Precipitators at Two Coal Power Plants; *Aerosol Sci. Technol.* **1996**, *24*, 191-204.
180. Ylätaalo, S.I.; Hautanen, J. Electrostatic Precipitator Penetration for Pulverized Coal Combustion; *Aerosol Sci. Technol.* **1998**, *29*, 17-30.
181. Littlejohn, R.F. Mineral Matter and Ash Distribution in "As-Fired" Samples of Pulverized Fuels; *J. Inst. Fuel* **1966**, *39*, 59-67.

182. Ulrich, G.D.; Subramanian, N.S. Particle Growth in Flames III. Coalescence as a Rate-Controlling Process; *Combust. Sci. Technol.* **1977**, *17*, 119-126.
183. Lee, C.M.; Davis, K.A.; Heap, M.P.; Eddings, E.; Sarofim, A. Modeling the Vaporization of Ash Constituents in a Coal-Fired Boiler; *Combust. Inst.*, in press.
184. Linak, W.P.; Peterson, T.W. Effect of Coal Type and Residence Time on the Submicron Aerosol Distribution from Pulverized Coal Combustion; *Aerosol Sci. Technol.* **1984**, *3*, 77-96.
185. Schmidt, E.W.; Gieseke, J.A.; Allen, J.M. Size Distribution of Fine Particulate Emissions from a Coal-Fired Power Plant; *Atmos. Environ.* **1976**, *10*, 1065-1069.
186. Couch, G.R. Power from Coal—Where to Remove Impurities? *IEA Coal Research* **1995**, IEACR/82.
187. Smith, K.L.; Smoot, L.D.; Fletcher, T.H.; Pugmire, R.J. *Structure and Reaction Processes of Coal*; Plenum Press: New York, 1994.
188. Zygarić, C.J.; Jones, M.L.; Steadman, E.N.; Benson, S.A. *Characterization of Mineral Matter in ACERC Coals*; Advanced Combustion Engineering Research Center and Environmental Systems Research Institute; University of North Dakota: 1990.
189. Itonen, A.O.; Jantunen, M.J. The Properties of Fly Ash and Fly Ash Mutagenicity. In *Encyclopedia of Environmental Control Technology, Volume 1: Thermal Treatment of Hazardous Wastes*; Cheremisinoff, P.N., Ed.; Gulf Publishing: Houston, TX, 1989; pp 755-789.
190. Hurt, R.H.; Mitchell, R.E. Unified High-Temperature Char Combustion Kinetics for a Suite of Coals of Various Rank. In *24th Symposium (International) on Combustion*; The Combustion Institute: Pittsburgh, PA, 1992; pp 1243-1250.
191. Hurt, R.H.; Gibbins, J.R. Residual Carbon from Pulverized Coal-Fired Boilers: 1. Size Distribution and Combustion Reactivity; *Fuel* **1995**, *74*(4), 471-479.
192. Freeman, E.; Gao, Y.-M.; Hurt, R.; Suuberg, E. Interactions of Carbon-Containing Fly Ash with Commercial Air-Entraining Admixtures for Concrete; *Fuel* **1997**, *76*(8), 761-765.
193. Ratafia-Brown, J.A. Overview of Trace Element Partitioning in Flames and Furnaces of Utility Coal-Fired Boilers; *Fuel Process. Technol.* **1994**, *39*(1), 137-154.
194. McLennan, A.R.; Bryant, G.W.; Stanmore, B.R.; Wall, T.F. Ash Formation Mechanisms during pf Combustion in Reducing Conditions; *Energy & Fuels* **2000**, *14*, 150-159.
195. Nathan, Y.; Dvorachek, M.; Pelly, I.; Mimram, U. Characterization of Coal Fly Ash from Israel; *Fuel* **1999**, *78*, 205-213.
196. Huffman, G.P.; Huggins, F.E.; Shah, N.; Shah, A. Behavior of Basic Elements during Coal Combustion; *Prog. Energy Combust. Sci.* **1990**, *16*, 243-251.
197. Nielsen, H.P.; Baxter, L.L.; Sclippab, G.; Morey, C.; Frandsen, F.J.; Dam-Johansen, K. Deposition of Potassium Salts on Heat Transfer Surfaces in Straw-Fired Boilers: A Pilot-Scale Study; *Fuel* **2000**, *79*(2), 131-139.
198. Jenkins, B.M.; Baxter, L.L.; Miles, T.R.J.; Miles, T.R. Combustion Properties of Biomass; *Fuel Process. Technol.* **1998**, *54*(1-3), 17-46.
199. Valmari, T.; Lind, T.; Kauppinen, E.I.; Sfiris, G.; Nilsson, K.; Maenhaut, W. Field Study on Ash Behaviour during Circulating Fluidized-Bed Combustion of Biomass. 1. Ash Formation; *Energy Fuels* **1999**, *13*, 379-389.
200. Lind, T.; Valmari, T.; Kauppinen, E.I.; Sfiris, G.; Nilsson, K.; Maenhaut, W. Volatilization of the Heavy Metals during Circulating Fluidized Bed Combustion of Forest Residue; *Environ. Sci. Technol.* **1999**, *33*, 496-502.
201. Chenevert, B.C.; Kramlich, J.C.; Nichols, K.M. Ash Characteristics of High Alkali Sawdust and Sanderdust Biomass Fuels. In *27th Symposium (International) on Combustion*; The Combustion Institute: Pittsburgh, PA, 1998; pp 1719-1725.
202. Robinson, A.L.; Junker, H.; Buckley, S.G.; Sclippa, G.; Baxter, L.L. Interactions between Coal and Biomass when Cofiring. In *27th Symposium (International) on Combustion*; The Combustion Institute: Pittsburgh, PA, 1998; pp 1351-1359.
203. Dayton, D.C.; Belle-Oudry, D.; Nordin, A. Effect of Coal Minerals on Chlorine and Alkali Metals during Biomass/Coal Cofiring; *Energy Fuels* **1999**, *13*(6), 1203-1211.
204. Nielsen, L.B.; Jensen, L.S.; Pedersen, C.; Rokke, M.; Livbjerg, H. Field Measurements of Combustion Aerosols from Co-Firing of Coal and Straw; *J. Aerosol Sci.* **1996**, *27*(Suppl 1), S365-S366.
205. Raunemaa, T.; Yli-Tuomi, T.; Leskinen, A.; Tissari, J.; Alander, T. Wood Combustion Aerosol and Lung Exposure Estimates; *J. Aerosol Sci.* **1999**, *30*(Suppl 1), S735-S736.
206. Amur, G.O.; Bhattacharya, S.C. A Study of Biomass as an Energy Source in Pakistan; *REIC International Energy J.* **1999**, *21*(1), 25-36.
207. Albalak, R.; Keeler, G.J.; Frisanchi, A.R.; Haber, M. Assessment of PM₁₀ Concentrations from Domestic Biomass Fuel Combustion in Two Rural Bolivian Highland Villages; *Environ. Sci. Technol.* **1999**, *33*(15), 2505-2509.
208. Brauer, M.; Bartlett, K.; Regalado-Pineda, J.; Perez-Padilla, R. Assessment of Particulate Concentrations from Domestic Biomass Combustion in Rural Mexico; *Environ. Sci. Technol.* **1996**, *30*(1), 104-109.
209. Rogge, W.F.; Hildemann, L.M.; Cass, G.R.; Simoneit, B.R.T. Sources of Fine Organic Aerosol. 9. Pine, Oak, and Synthetic Log Combustion in Residential Fireplaces; *Environ. Sci. Technol.* **1998**, *32*(1), 13-22.
210. Rau, J.A. Composition and Size Distribution of Residential Wood Smoke Particles; *Aerosol Sci. Technol.* **1989**, *10*, 181-192.
211. Purvis, C.R.; McCrillis, R.C.; Kariher, P.H. Fine Particulate Matter (PM) and Organic Speciation of Fireplace Emissions; *Environ. Sci. Technol.* **2000**, *34*(9), 1653-1658.
212. Kozinski, J.A.; Saade, R. Effect of Biomass Burning on the Formation of Soot Particles and Heavy Hydrocarbons. An Experimental Study; *Fuel* **1998**, *77*(4), 225-237.
213. Oanh, N.T.K.; Reutehgardh, L.B.; Dung, N.T. Emission of Polycyclic Aromatic Hydrocarbons and Particulate Matter from Domestic Combustion of Selected Fuels; *Environ. Sci. Technol.* **1999**, *33*(16), 2703-2709.
214. Mumford, J.L.; Harris, D.B.; Wilson, W.E.; Chapman, R.S.; Cao, S.; Xian, Y.; Li, X.; Chuang, J.C.; Cooke, W.M. Lung Cancer and Indoor Air Pollution in Xuan Wei, China; *Science* **1987**, *235*, 217-220.
215. Chuang, J.C.; Cao, S.R.; Xian, Y.L.; Harris, D.B.; Mumford, J.L. Chemical Characterization of Indoor Air in Homes from Communes in Xuan Wei, China, with High Lung Cancer Mortality Rate; *Atmos. Environ.* **1992**, *26A*(12), 2193-2201.
216. Chuang, J.C.; Wise, S.A.; Cao, S.; Mumford, J.L. Chemical Characterization of Mutagenic Fractions of Particles from Indoor Coal Combustion: A Study of Lung Cancer in Xuan Wei, China; *Environ. Sci. Technol.* **1992**, *26*, 999-1004.
217. Mumford, J.L.; Helmes, C.T.; Lee, X.; Seidenberg, J.; Nesnow, S. Mouse Skin Tumorigenicity Studies of Indoor Coal and Wood Combustion Emissions from Homes for Residents in Xuan Wei, China with High Lung Cancer Mortality; *Carcinogenesis* **1990**, *11*(3), 397-404.
218. Christopher, S.A.; Wang, M.; Berendes, T.A.; Welch, R.M.; Yang, S.-K. 1985 Biomass Burning Season in South America: Satellite Remote Sensing of Fires, Smoke, and Regional Radiative Energy Budgets; *J. Appl. Meteorology* **1998**, *37*(7), 661-678.
219. *Recommendations for Improving Western Vistas*; Grand Canyon Visibility Transport Commission: 1996.
220. Husar, R.B.; Schichtel, B.A.; Falke, C.R.; Wilson, W.E. Dust and Smoke Events over the USA in 1998. In *Proceedings of PM2000—Particulate Matter and Health*, Charleston, SC, 2000; Air and Waste Management Association: Pittsburgh, PA, 2000; Session 10AS, p 22-23.
221. *Areas Affected by PM10 Natural Events*. Memorandum issued by M.D. Nichols, Assistant Administrator for Air and Radiation to Regional Directors; U.S. Environmental Protection Agency, 1996.
222. Ward, D.E. Factors Influencing the Emissions of Gases and Particulate Matter from Biomass Burning. In *Fire in the Tropical Biota: Ecosystem Processes and Global Challenges*; Goldammer, J.G., Ed.; Ecological Studies; Springer Verlag: Berlin, 1990; pp 418-436.
223. Jenkins, B.M.; Jones, A.D.; Turn, S.Q.; Williams, R.B. Emission Factors for Polycyclic Aromatic Hydrocarbons from Biomass Burning; *Environ. Sci. Technol.* **1996**, *30*, 2462-2469.
224. Jenkins, B.M.; Jones, A.D.; Turn, S.Q.; Williams, R.B. Particle Concentrations, Gas-Particle Partitioning, and Species Correlations for Polycyclic Aromatic Hydrocarbons (PAH) Emitted during Biomass Burning; *Atmos. Environ.* **1996**, *30*(22), 3825-3835.
225. Walton, W.D.; Evans, D.D.; McGrattan, K.B.; Baum, H.R.; Twilley, W.H.; Madrzykowski, D.; Putorti, A.D.; Rehm, R.G.; Koseki, H.; Tennyson, E.J. In Situ Burning of Oil Spills: Mesoscale Experiments and Analysis. In *16th Arctic and Marine Oil Spill Program Technical Seminar*; Ministry of Supply and Services: Calgary, Alberta, Canada, 1993; pp 679-734.
226. Evans, D.; Walton, W.; Baum, H.; Mulholland, G.; Lawson, J.; Koseki, H. Smoke Emission from Burning Crude Oil. In *14th Arctic and Marine Oil Spill Technical Seminar*; Ministry of Supply and Services: Vancouver, British Columbia, Canada, 1991; pp 421-449.
227. Williams, J.M.; Gritz, L.A. In Situ Sampling and Transmission Electron Microscope Analysis of Soot in the Flame Zone of Large Pool Fires. In *27th Symposium (International) on Combustion*; The Combustion Institute: Pittsburgh, PA, 1998; pp 2707-2714.
228. Dobbins, R.A.; Megaridis, C.M. Morphology of Flame-Generated Soot as Determined by Thermophoretic Sampling; *Langmuir* **1987**, *3*, 254-259.
229. Benner, B.A.J.; Bryner, N.P.; Wise, S.A.; Mulholland, G.W.; Lao, R.C.; Fingas, M.F. Polycyclic Aromatic Hydrocarbon Emissions from the Combustion of Crude Oil on Water; *Environ. Sci. Technol.* **1990**, *24*, 1418-1427.
230. Barton, R.G.; Clark, W.D.; Seeker, W.R. Fate of Metals in Waste Combustion Systems; *Combust. Sci. Technol.* **1990**, *74*, 327-342.
231. Lighty, J.S.; Veranth, J.M. The Role of Research in Practical Incineration Systems—A Look at the Past and the Future. In *27th Symposium (International) on Combustion, Boulder, CO*; The Combustion Institute: Pittsburgh, PA, 1998; pp 1255-1273.
232. Durlak, S.K.; Biswas, P.; Shi, J. Equilibrium Analysis of the Effect of Temperature, Moisture and Sodium Content on Heavy Metal Emissions from Municipal Solid Waste Incinerators; *J. Hazard. Mater.* **1997**, *56*, 1-20.

233. Holbert, C.; Lighty, J.S. Trace Metals Behavior during Thermal Treatment of Sludge Wastes; *J. Waste Manage.* **1999**, *18*, 423-431.
234. Smith, J.D.; Vandell, R.; Hixon, E.M. Application of Computational Fluid Mechanics to Modeling the Incineration of Chlorinated Hydrocarbon Wastes in Thermal Oxidizers; *Combust. Sci. Technol.* **1994**, *101*, 397-423.
235. Lee, C.C. A Model Analysis of Metal Partitioning in a Hazardous Waste Incineration System; *J. Air Pollut. Control Assoc.* **1988**, *38*(7), 941-945.
236. Wey, M.-Y.; Hwang, J.-H.; Chen, J.-C. Mass and Elemental Size Distribution of Chromium, Lead, and Cadmium under Various Incineration Conditions; *J. Chem. Eng. Jpn.* **1998**, *31*(4), 506-517.
237. Eddings, E.G.; Lighty, J.S.; Kozinski, J.A. Determination of Metal Behavior during the Incineration of a Contaminated Montmorillonite Clay; *Environ. Sci. Technol.* **1994**, *28*, 1791-1800.
238. Rink, K.K.; Kozinski, J.A.; Lighty, J.S. Biosludge Incineration in FBCs: Behavior of Ash Particles; *Combust. Flame* **1995**, *100*, 121-130.
239. Biswas, P.; Zachariah, M.R. In Situ Immobilization of Lead Species in Combustion Environments by Injection of Gas Phase Silical Sorbent Precursors; *Environ. Sci. Technol.* **1997**, *31*(9), 2455-2463.
240. Wendt, J.O.L. Mechanisms Governing the Partitioning of Semi-Volatile Alkali and Toxic Metals during Waste and Waste Fuel Combustion. In *1st International Symposium on Incineration and Flue Gas Treatment Technologies*; Sheffield University, United Kingdom: 1997.
241. Linak, W.P.; Srivastava, R.K.; Wendt, J.O.L. Metal Aerosol Formation in a Laboratory Swirl Flame Incinerator. In *3rd International Congress on Toxic Combustion Byproducts*; Cambridge, MA: 1993.
242. Linak, W.P.; Ryan, J.V.; Wendt, J.O.L. Formation and Destruction of Hexavalent Chromium in a Laboratory Swirl Flame Incinerator; *Combust. Sci. Technol.* **1996**, *116-117*(1-6), 479-498.
243. Chen, J.-C.; Wey, M.-Y. Simulation of Hexavalent Chromium Formation under Various Incineration Conditions; *Chemosphere* **1998**, *36*(7), 1553-1564.
244. *Draft Test Report: A Performance Test on a Spray Dryer, Fabric Filter, Wet Scrubber System*; Radian Corporation; Report prepared for Shiva Garg; Office of Solid Waste; U.S. Environmental Protection Agency: 1989.
245. Kauppinen, E.I.; Pakkanen, T.A. Mass and Trace Element Size Distributions of Aerosols Emitted by a Hospital Refuse Incinerator; *Atmos. Environ.* **1990**, *24A*, 423-429.
246. Heywood, J.B. Future Engine Technology. Lessons from the 1980s for the 1990s; *J. Eng. Gas Turbines & Power, Transactions of the ASME* **1991**, *113*(3), 319-330.
247. Khair, M.K. Progress in Diesel Engine Emissions Control; *J. Eng. Gas Turbines & Power, Transactions of the ASME* **1992**, *114*(3), 568-577.
248. Degobert, P. *Automobiles and Pollution*; Society of Automotive Engineers: Warrendale, PA, 1995.
249. *Diesel Engines: Combustion and Emissions*; Society of Automotive Engineers: Warrendale, PA, 1999; Vol. SP-1484.
250. *Diesel Combustion, Emissions, and Exhaust Aftertreatment*; E193010685312; Society of Automotive Engineers: Warrendale, PA, 1992.
251. Johnson, J.H.; Baines, T.M.; Clerc, J.C. *Diesel Particulate Emissions: Measurement Techniques, Fuel Effects and Control Technology*; Society of Automotive Engineers: Warrendale, PA, 1992; Vol. PT-42.
252. *Processes of Diesel Engine Combustion SP-1444*; Society of Automotive Engineers: Warrendale, PA, 1999.
253. Zhao, H.; Ladommatos, N. Optical Diagnostics for Soot and Temperature Measurements in Diesel Engines; *Prog. Energy Combust. Sci.* **1998**, *24*(3), 221-255.
254. van Beekhoven, L.C. *Effects of Fuel Properties on Diesel Engine Emissions. A Review of Information Available to the EEC-MVEG Group*; SAE Technical Paper Series; Society of Automotive Engineers: Warrendale, PA, 1991.
255. Koltsakis, G.C.; Stametelos, A.M. Catalytic Automotive Exhaust Aftertreatment; *Prog. Energy Combust. Sci.* **1997**, *23*(1), 1-39.
256. Neeft, J.P.A.; Makkee, M.; Moulijn, J.A. Diesel Particulate Emission Control; *Fuel Process. Technol.* **1996**, *47*(1), 1-69.
257. Heywood, J.B. *Internal Combustion Engine Fundamentals*; McGraw Hill: New York, 1988.
258. *Handbook of Air Pollution from Internal Combustion Engines Pollutant Formation and Control*; Sher, E., Ed.; Academic Press: Boston, MA, 1998.
259. Flynn, P.F.; Durrett, R.; Hunter, G.; zur Loye, A.; Akinyemi, O.C.; Dec, J.; Westbrook, C. *Diesel Combustion: An Integrated View Combining Laser Diagnostics, Chemical Kinetics, and Empirical Validation*; 1999-01-0509; Society of Automotive Engineers: Warrendale, PA, 1999.
260. Bagley, S.T.; Baumgard, K.J.; Gratz, L.D.; Johnson, J.H.; Leddy, D.G. *Characterization of Fuel and Aftertreatment Device Effects on Diesel Emissions*; Research Report 76; Health Effects Institute: Cambridge, MA, 1996.
261. Ristovski, Z.D.; Morawska, L.; Bofinger, N.D.; Hitchins, J. Submicrometer and Supermicrometer Particulate Emission from Spark Ignition Vehicles; *Environ. Sci. Technol.* **1998**, *32*(24), 3845-3852.
262. Abdul-Khalek, I.S.; Kittelson, D.B.; Graskow, B.R.; Wei, Q.; Brear, F. *Diesel Exhaust Particle Size: Measurement Issues and Trends*; 980525; Society of Automotive Engineers: Warrendale, PA, 1998.
263. Morawska, L.; Bofinger, N.D.; Kocis, L.; Nwankwoala, A. Submicrometer and Supermicrometer Particles from Diesel Vehicle Emissions; *Environ. Sci. Technol.* **1998**, *32*(14), 2033-2042.
264. Graskow, B.R.; Kittelson, D.B.; Abdul-Khalek, I.S.; Ahmadi, M.R.; Morris, J.E. *Characterization of Exhaust Particulate Emissions from a Spark Ignition Engine*; 980528; Society of Automotive Engineers: Warrendale, PA, 1998.
265. Maricq, M.M.; Podsiadlik, D.H.; Chase, R.E. Examination of the Size-Resolved and Transient Nature of Motor Vehicle Particle Emissions; *Environ. Sci. Technol.* **1999**, *33*(10), 1618-1626.
266. Maricq, M.M.; Podsiadlik, D.H.; Chase, R.E. Gasoline Vehicle Particle Size Distributions: Comparison of Steady State, FTP, and US06 Measurements; *Environ. Sci. Technol.* **1999**, *33*(12), 2007-2015.
267. Harrison, R.M.; Jones, M.; Collins, G. Measurements of the Physical Properties of Particles in the Urban Atmosphere; *Atmos. Environ.* **1999**, *33*, 309-321.
268. Hitchins, J.; Morawska, L.; Wolff, R.; Gilbert, D. Concentrations of Submicrometre Particles from Vehicle Emissions near a Major Road; *Atmos. Environ.* **1999**, *34*, 51-59.
269. Kittelson, D.B.; Dolan, D.F.; Oliver, R.B.; Aufderheide, E. Diesel Exhaust Particle Size Distributions—Fuel and Additive Effects. In *The Measurement and Control of Diesel Particulate Emissions*; Progress in Technology Series No. 17; Society of Automotive Engineers: Warrendale, PA, 1979; pp 233-244.
270. Kalghatgi, G.T. *Deposits in Gasoline Engines—A Literature Review*; SAE Paper 902108; Society of Automotive Engineers: Warrendale, PA, 1990.
271. Kayes, D.; Hochgreb, S. Mechanisms of Particulate Matter Formation in Spark-Ignition Engines. 2. Effect of Fuel, Oil, and Catalyst Parameters; *Environ. Sci. Technol.* **1999**, *33*, 3968-3977.
272. Sagebiel, J.C.; Zielinska, B.; Walsh, P.A.; Chow, J.C.; Cadle, S.H.; Mulawa, P.A.; Knapp, K.T.; Zweidinger, R.B.; Snow, R. PM10 Exhaust Samples Collected during IM-240 Dynamometer Tests of In-Service Vehicles in Nevada; *Environ. Sci. Technol.* **1997**, *31*(1), 75-83.
273. Hawley, J.G.; Brace, C.J.; Wallace, F.J.; Horrocks, R.W. Combustion-Related Emissions in CI Engines. In *Handbook of Air Pollution from Internal Combustion Engines*; Sher, E., Ed.; Academic Press: Boston, MA, 1998; pp 280-357.
274. Tanaka, S.; Shimizu, T. A Study of Composition and Size Distribution of Particulate Matter from DI Diesel Engine SAE 1999-01-3487. In *Diesel Engines: Combustion and Emissions*; Society of Automotive Engineers: Warrendale, PA, 1999.
275. Rogge, W.F.; Hildemann, L.M.; Mazurek, M.A.; Cass, G.R. Sources of Fine Organic Aerosol 2. Noncatalyst and Catalyst-Equipped Automobiles and Heavy-Duty Diesel Trucks; *Environ. Sci. Technol.* **1993**, *27*(4), 636-651.
276. Schauer, J.J.; Kleenam, M.J.; Cass, G.R.; Simoneit, B.R.T. Measurement of Emission from Air Pollution Sources. 2. C1 through C30 Organic Compounds from Medium Duty Diesel Trucks; *Environ. Sci. Technol.* **1999**, *33*(10), 1578-1587.
277. *Emission Regulations for New Otto-Cycle and Diesel-Cycle Heavy-Duty Engines; Gaseous and Particulate Exhaust Test Procedures*; 40CFR86 Subpart N; Office of the Federal Registrar; U.S. Government Printing Office: 1998.
278. Hildemann, L.M.; Cass, G.R.; Markowski, G.R. A Dilution Stack Sampler for Collection of Organic Aerosol Emissions: Design, Characterization, and Field Tests; *Aerosol Sci. Technol.* **1989**, *10*, 193-204.
279. Ball, J.C. *Emission Rates and Elemental Composition of Particles Collected from 1995 Ford Vehicles Using the Urban Dynamometer Driving Schedule, The Highway Fuel Economy Test, and the US06 Driving Cycle*; SAE 972914; Society of Automotive Engineers: Warrendale, PA, 1997.
280. Cadle, S.H.; Mulawa, P.A.; Ball, J.; Donase, C.; Weibel, A.; Sagebiel, J.C.; Knapp, K.T.; Snow, R. Particulate Emission Rates from In-Use High-Emitting Vehicles Recruited in Orange County, California; *Environ. Sci. Technol.* **1997**, *31*(12), 3405-3412.
281. Williams, D.J. Particulate Emissions from "In-Use" Motor Vehicles. 1. Spark Ignition Engines; *Atmos. Environ.* **1989**, *23*, 2639-2645.
282. Zayed, J.; Hong, B.; L'Espérance, G. Characterization of Manganese-Containing Particles Collected from the Exhaust Emissions of Automobiles Running with MMT Additive; *Environ. Sci. Technol.* **1999**, *33*(19), 3341-3346.
283. Rote, D.M. *Impact of Aircraft Emissions on Air Quality in the Vicinity of Airports, Volume III: Air Quality and Emission Modeling Needs*; FAA Report FAA-EE-84-13; USAF Report ESL-TR-84-35; U.S. Department of Transportation Federal Aviation Administration: 1984.
284. Douglas, E. *Effectiveness of Fuel Additives in Reducing Visible Emissions from J79-GE-15A Gas Turbine Engines*; ASEO Report No. 3-96; Aircraft Environmental Support Office; Naval Aviation Depot: 1996.
285. Petzold, A.; Schröder, F.P. Jet Engine Exhaust Aerosol Characterization; *Aerosol Sci. Technol.* **1998**, *28*, 62-76.
286. Anderson, B.E.; Cofer, W.R.; Bagwell, D.R.; Barrick, J.W.; Hudgins, C.H.; Burke, K.E. Airborne Observations of Aircraft Aerosol Emissions I: Total Nonvolatile Particle Emission Indices; *Geophys. Res. Lett.* **1998**, *25*(10), 1689-1692.
287. Hagen, D.; Whitefield, P.; Paladino, J.; Trueblood, M.; Lilienfeld, H. Particle Sizing and Emission Indices for a Jet Engine Exhaust Sampled at Cruise Altitude; *Geophys. Res. Lett.* **1998**, *25*(10), 1681-1684.

288. Hagen, D.E.; Trueblood, M.B.; Whitefield, P.D. A Field Sampling of Jet Exhaust Aerosols; *Part. Sci. Technol.* **1992**, *10*, 53-63.
289. Jones, R.E. Gas Turbine Emissions—Problems, Progress, and Future; *Prog. Energy Combust. Sci.* **1978**, *4*, 73-112.
290. Stockham, J.D.; Luebecke, E.H.; Fenton, D.L.; Johnson, R.H.; Campbell, P.P. *Turbine Engine Particulate Emission Characterization*; FAA-RD-79-15; Federal Aviation Administration: 1979.
291. Wilson, W.E.; Mage, D.T.; Grant, L.D. Estimating Separately Personal Exposure to Ambient and Non-Ambient Particulate Matter for Epidemiology and Risk Assessment: Why and How, *J. Air & Waste Manage. Assoc.* **2000**, *50*, 1167-1183.
292. Lillquist, D.R.; Lee, J.S.; Ramsey, J.R.; Boucher, K.M.; Walton, Z.L.; Lyon, J.L. A Comparison of Indoor/Outdoor PM₁₀ Concentrations Measured at Three Hospitals and a Centrally Located Monitor in Utah; *Appl. Occup. Environ. Hyg.* **1998**, *13*(6), 409-415.
293. Whitby, K.T.; Sverdrup, G.M. California Aerosols: Their Physical and Chemical Characteristics. In *The Character and Origins of Atmospheric Aerosols: A Digest of Results from the California Aerosol Characterization Experiment (ACHEX)*; Hidy, G.M., et al., Eds.; Advances in Environmental Science and Technology; Wiley: New York, 1980; pp 477-517.
294. Watson, J.G.; Chow, J.C. *Reconciling Urban Fugitive Dust Emissions Inventory and Ambient Source Concentration Estimates: Summary of Current Knowledge and Needed Research*; DRI Document No. 6110.4D2; Desert Research Institute: 1999.
295. Harrison, R.M.; Brimblecombe, P.; Derwent, R.G.; Dollard, G.J.; Eggleston, S.; Hamilton, R.S.; Hickman, A.J.; Holman, C.; Laxen, D.P.H.; Moorcroft, S. *Airborne Particulate Matter in the United Kingdom*; Third Report of the Quality of Urban Air Review Group; Department of the Environment; University of Birmingham, United Kingdom: 1996.
296. Ahuja, K.O.; Paskind, J.J.; Houck, J.E.; Chow, J.C. Design of a Study for the Chemical and Size Characterization of Particulate Matter Emissions from Selected Sources in California. In *Transactions, Receptor Models in Air Resources Management*; Watson, J.G., Ed.; Air & Waste Management Association: Pittsburgh, PA, 1989; pp 145-158.
297. Jaenicke, R. Tropospheric Aerosols. In *Aerosol-Cloud-Climate Interactions*; Hobbs, P.V., Ed.; Academic Press: San Diego, CA, 1993; pp 1-31.
298. Hughes, L.C.; Cass, G.R.; Gone, J.; Ames, M.; Olmez, I. Physical and Chemical Characterization of Atmospheric Ultrafine Particulates in the Los Angeles Area; *Environ. Sci. Technol.* **1998**, *32*(9), 1153-1161.
299. Penchin, P.M. National PM Study: OPPE Particulate Programs Evaluation System, 1994. In *Particles in Our Air*; Wilson, R., Spengler, J., Eds.; Harvard University Press: 1996.
300. *National Air Quality and Emissions Trends Report, 1997*; EPA 454/R-98-016; U.S. Environmental Protection Agency; Office of Air Quality Planning and Standards: 1998.
301. *Latest Findings on National Air Quality: 1997 Status and Trends*; EPA 454/F-98-009; U.S. Environmental Protection Agency; Office of Air Quality Planning and Standards: 1998.
302. Chen, M.L.; Mao, I.F.; Lin, I.K. The PM_{2.5} and PM₁₀ Particles in Urban Areas of Taiwan; *Sci. Total Environ.* **1999**, *226*(2-3), 227-235.
303. Chen, W.-C.; Wang, C.-S.; Wei, C.-C. Assessment of Source Contributions to Ambient Aerosols in Taiwan; *J. Air & Waste Manage. Assoc.* **1997**, *47*(4), 501-509.
304. Tuch, T.; Brand, P.; Wichmann, H.E.; Heyder, J. Variation of Particle Number and Mass Concentration in Various Size Ranges of Ambient Aerosol in Eastern Germany; *Atmos. Environ.* **1997**, *31*(24), 4193-4197.
305. *Air Quality Criteria for Particulate Matter*; EPA/600/P-95-001 aF thru cF; U.S. Environmental Protection Agency: 1996.
306. *Receptor Modeling for Air Quality Management*; Hopke, P.K., Ed.; Data Handling in Science and Technology; Elsevier: New York, 1991.
307. Watson, J.G.; Robinson, N.F.; Fujita, E.M.; Chow, J.C.; Pace, T.G.; Lewis, C.; Coulter, T. *CMB8—Applications and Validation Protocol for PM_{2.5} and VOCs*; DRI Document No. 1980.2D1; Desert Research Institute: 1998.
308. Cass, G.R.; Gray, H.A. *Regional Emissions and Atmospheric Concentrations of Diesel Engine Particulate Matter: Los Angeles as a Case Study in Diesel Exhaust: A Critical Analysis of Emissions, Exposure, and Health Effects*; Health Effects Institute: 1995.
309. Kleeman, M.J.; Eldering, A.; Cass, G.R. Modeling the Airborne Particulate Complex as a Source-Oriented External Mixture; *J. Geophys. Res.* **1997**, *102*(D17), 21,355-21,372.
310. Kleeman, M.J.; Cass, G.R. Source Contributions to the Size and Composition Distribution of the Urban Particulate Air Pollution; *Atmos. Environ.* **1998**, *32*(16), 2803-2816.
311. Evelyn, J. Fumigorum or the Inconvenience of the Aer and Smoake of London Dissipated: Together with Some Remedies Homly Proposed, 1661. Cited in *Advances in Environmental Science*; Pitts, Metcalf, Eds.; Wiley-Interscience: New York, 1969.
312. Bonfanti, L.; De Michele, G.; Riccardi, J.; Lopes-Doriga, E. Influence of Coal Type and Operating Conditions on the Formation of Incomplete Combustion Products. Pilot Plant Experiments; *Combust. Sci. Technol.* **1994**, *10*, 505-525.
313. Busch, R.H.; Buschbom, R.L.; Cannon, W.C.; Lauhala, K.E.; Miller, F.J.; Graham, J.A.; Smith, L.G. Effects of Ammonium Nitrate Aerosol Exposure on Lung Structure of Normal and Elastase-Impaired Rats and Guinea Pigs; *Environ. Res.* **1986**, *39*(2), 237-252.
314. Carter, J.D.; Ghio, A.J.; Samet, J.M.; Devlin, R.B. Cytokine Production by Human Airway Epithelial Cells after Exposure to an Air Pollution Particle Is Metal-Dependent; *Toxicol. Appl. Pharmacol.* **1997**, *146*(2), 180-188.
315. Chen, L.C.; Lam, H.F.; Ainsworth, D.; Guty, J.; Amdur, M.O. Functional Changes in the Lungs of Guinea Pigs Exposed to Sodium Sulfite Aerosols; *Toxicol. Appl. Pharmacol.* **1987**, *89*, 1.
316. Chin, B.Y.; Choi, M.E.; Burdick, M.D.; Strieter, R.M.; Risby, T.H.; Choi, A.M. Induction of Apoptosis by Particulate Matter: Role of TNF-Alpha and MAPK; *Am. J. Physiol.* **1998**, *275*(5 Pt 1), L942-949.
317. Costa, D.L.; Dreher, K.L. Bioavailable Transition Metals in Particulate Matter Mediate Cardiopulmonary Injury in Healthy and Compromised Animal Models; *Environ. Health Perspect.* **1997**, *105*(Suppl 5), 1053-1060.
318. Dockery, D.W.; Pope, A.C.; Xiping, X.; Spengler, J.D.; Ware, J.H.; Fay, M.E.; Ferris, B.G.; Speizer, F.E. An Association between Air Pollution and Mortality in Six U.S. Cities; *New Engl. J. Med.* **1993**, *329*(24), 1753-1759.
319. Donaldson, K. Local Inflammatory and Systemic Effects Following Short-Term Inhalation Exposure to Fine and Ultrafine Carbon Black in Rats. In *The Health Effects of Fine Particles: Key Questions and the 2003 Review, Brussels, Belgium*; Health Effects Institute: Cambridge, MA, 1999; pp II-171.
320. Elder, A.C.P.; Gelein, R.; Finkelstein, J.N.; Cox, C.; Oberdörster, G. Endotoxin Priming Affects the Lung Response to Ultrafine Particles and Ozone in Young and Old Rats; *Inhal. Toxicol.* **2000**, *12*(Suppl 1), 85-98.
321. *An Acid Aerosols Issue Paper: Health Effects and Aerometrics*; EPA-600/8-88-005F, NTIS PB91-125864; U.S. Environmental Protection Agency: 1989.
322. Frampton, M.W.; Ghio, A.J.; Samet, J.M.; Carson, J.L.; Carter, J.D.; Devlin, R.B. Effects of Aqueous Extracts of PM₁₀ Filters from the Utah Valley on Human Airway Epithelial Cells; *Lung Cell. Mol. Physiol.* **1999**, *21*, L960-L967.
323. Gong, H.; Sioutas, C.; Linn, W.S.; Clark, K.W.; Terrell, S.L.; Terrell, L.L.; Anderson, K.R.; Kim, S.; Chang, M.-C. Controlled Human Exposures to Concentrated Ambient Fine Particles in Metropolitan Los Angeles: Methodology and Preliminary Health-Effect Findings; *Inhal. Toxicol.* **2000**, *12*(Suppl 1), 107-119.
324. *Diesel Exhaust: A Critical Analysis of Emissions, Exposure, and Health Effects*; Health Effects Institute: Cambridge, MA, 1995.
325. Hoek, G.; Schwartz, J.D.; Groot, B.; Eilers, P. Effects of Ambient Particulate Matter and Ozone on Daily Mortality in Rotterdam, The Netherlands; *Arch. Environ. Health* **1997**, *52*(6), 455-463.
326. Kadiiska, M.B.; Mason, R.P.; Dreher, K.L.; Costa, D.L.; Ghio, A.J. In Vivo Evidence of Free Radical Formation in the Rat Lung after Exposure to an Emission Source Air Pollution Particle; *Chem. Res. Toxicol.* **1997**, *10*(10), 1104-1108.
327. Kennedy, T.; Ghio, A.J.; Reed, W.; Samet, J.; Zagorski, J.; Quay, J.; Carter, J.; Dailey, L.; Hoidal, J.R.; Devlin, R.B. Copper-Dependent Inflammation and Nuclear Factor-kB Activation by Particulate Air Pollution; *Am. J. Respir. Cell Mol. Biol.* **1998**, *19*, 1-14.
328. Lewtas, J. Genotoxicity of Complex Mixtures: Strategies for the Identification and Comparative Assessment of Airborne Mutagens and Carcinogens from Combustion Sources; *Fundam. Appl. Toxicol.* **1988**, *10*, 571-589.
329. Li, X.Y.; Brown, D.; Smith, S.; MacNee, W.; Donaldson, K. Short-Term Inflammatory Responses following Intratracheal Instillation of Fine and Ultrafine Carbon Black in Rats; *Inhal. Toxicol.* **1999**, *11*(8), 709-731.
330. Nikula, K.J.; Snipes, M.B.; Barr, E.B.; Griffith, W.C.; Henderson, R.F.; Mauderly, J.L. Comparative Pulmonary Toxicities and Carcinogenicities of Chronically Inhaled Diesel Exhaust and Carbon Black in F344 Rats; *Fundam. Appl. Toxicol.* **1995**, *25*(1), 80-94.
331. Oberdörster, G.; Ferin, J.; Gelein, R.; Soderholm, S.C.; Finkelstein, J. Role of the Alveolar Macrophage in Lung Injury; Studies with Ultrafine Particles; *Environ. Health Perspect.* **1992**, *97*, 193-199.
332. Oberdörster, G.; Ferin, J.; Lehnert, B.E. Correlation between Particle Size, In Vivo Particle Persistence, and Lung Injury; *Environ. Health Perspect.* **1994**, *102*(Suppl 5), 173-179.
333. Pagano, P.; Zaiacomo, T.D.; Scarcella, E.; Bruni, S.; Calamosca, M. Mutagenic Activity of Total and Particle-Sized Fractions of Urban Particulate Matter; *Environ. Sci. Technol.* **1996**, *30*(12), 3512-3516.
334. Patterson, E.; Eatough, D.J. Indoor/Outdoor Relationships for Ambient PM_{2.5} and Associated Pollutants: Epidemiological Implications in Lindon, Utah; *J. Air & Waste Manage. Assoc.* **2000**, *50*(1), 103-110.
335. Peters, A.; Wichmann, H.E.; Tuch, T.; Heinrich, J.; Heyder, J. Respiratory Effects Are Associated with the Number of Ultrafine Particles; *Am. J. Respir. Crit. Care Med.* **1997**, *155*(4), 1376-1383.

336. Petrovic, S.; Urch, B.; Brook, J.; Datema, J.; Purdham, J.; Liu, L.; Lukic, Z.; Zimmerman, B.; Tofler, G.; Downar, E.; Cory, P.; Tarlo, S.; Broder, I.; Dales, R.; Silverman, F. Cardiorespiratory Effects of Concentrated Ambient PM_{2.5}: A Pilot Study Using Controlled Human Exposures; *Inhalation Toxicol.* **2000**, *12*(Suppl 1), 173-188.
337. Pope, C.A. Epidemiology Investigations of the Health Effects of Particulate Air Pollution: Strengths and Limitations; *Appl. Occup. Environ. Hyg.* **1998**, *13*(6), 356-363.
338. Pope, A.C.; Hill, R.W.; Villegas, G.M. Particulate Air Pollution and Daily Mortality on Utah's Wasatch Front; *Environ. Health Perspect.* **1999**, *107*(7), 567-573.
339. Samet, J.M.; Zerer, S.L.; Kelsall, J.E.; Xu, J. Particulate Air Pollution and Mortality: The Particle Epidemiology Evaluation Project; *Appl. Occup. Environ. Health* **1998**, *13*(6), 364-369.
340. Schwartz, J.; Dockery, D.W. Particulate Air Pollution and Daily Mortality in Steubenville, Ohio; *Am. J. Epidemiol.* **1992**, *135*(1), 12-19.
341. Schwartz, J.; Norris, G.; Larson, T.; Sheppard, L.; Claiborne, C.; Koenig, J. Episodes of High Coarse Particle Concentrations Are Not Associated with Increased Mortality; *Environ. Health Perspect.* **1999**, *107*(5), 339-342.
342. Smith, K.R.; Aust, A.E. Mobilization of Iron from Urban Particulates Leads to Generation of Reactive Oxygen Species In Vitro and Induction of Ferritin Synthesis in Human Lung Epithelial Cells; *Chem. Res. Toxicol.* **1997**, *10*(7), 828-834.
343. Smith, K.R.; Veranth, J.M.; Lighty, J.S.; Aust, A.E. Mobilization of Iron from Coal Fly Ash Was Dependent upon Particle Size and Source of Coal; *Chem. Res. Toxicol.* **1998**, *11*(12), 1494-1500.
344. Smith, K.R.; Veranth, J.M.; Hu, A.A.; Lighty, J.S.; Aust, A.E. Interleukin-8 Levels in Human Lung Epithelial Cells Are Increased in Response to Coal Fly Ash and Vary with Bioavailability of Iron, as a Function of Particle Size and Source of Coal; *Chem. Res. Toxicol.* **2000**, *13*, 118-125.
345. Spurny, K.R. On the Physics, Chemistry and Toxicology of Ultrafine Anthropogenic, Atmospheric Aerosols (UAAA): New Advances; *Toxicol. Lett.* **1998**, *96-97*, 253-261.
346. Takenaka, S.; Dornhöfer-Takenaka, H.; Muhle, H. Alveolar Distribution of Fly Ash and of Titanium Dioxide after Long-Term Inhalation by Wistar Rats; *J. Aerosol Sci.* **1986**, *17*, 361-364.
347. Valberg, P.A.; Watson, A.Y. Lack of Concordance between Reported Lung-Cancer Risk Levels and Occupation-Specific Diesel Exhaust Exposures; *Inhalation Toxicol.* **2000**, *12*(Suppl 10), 199-208.
348. Veranth, J.M.; Smith, K.R.; Rohrbough, J.G.; Huggins, F.; Hu, A.A.; Lighty, J.S.; Aust, A.E. Mossbauer Spectroscopy Indicates that Iron in an Aluminosilicate Glass Phase Is the Source of the Bioavailable Iron from Coal Fly Ash; *Chem. Res. Toxicol.* **2000**, *13*, 161-164.
349. Mauderly, J.L. Toxicological and Epidemiological Evidence for Health Risks from Inhaled Engine Emissions; *Environ. Health Perspect.* **1994**, *102*(Suppl 4), 165-171.
350. Goldsmith, C.A.; Kobzik, L. Particulate Air Pollution and Asthma: A Review of Epidemiological and Biological Studies; *Rev. Environ. Health* **1999**, *14*(3), 121-134.
351. Phalen, R.; Bell, Y.M. *Proceedings of the 3rd Colloquium on Particulate Air Pollution and Health*; Air Pollution Health Effects Laboratory; University of California: Irvine, CA, 1999.
352. *PM2000: Particulate Matter and Health—The Scientific Basis for Regulatory Decision-Making*, Charleston, SC; *Extended Abstract Book*; Air & Waste Management Association: Pittsburgh, PA, 2000.
353. USC, Clean Air Act, Section 109 (b)(1), 42 USC 7401. Public Law 101-549, 1990.
354. Pope, A.C. Respiratory Disease Associated with Community Air Pollution and a Steel Mill, Utah Valley; *Am. J. Pub. Health* **1989**, *89*(5), 623-628.
355. Dockery, D.W.; Pope, C.A.I. Outdoor Air 1: Particulates. In *Topics in Environmental Epidemiology*; Steenland, K., Savitz, D.A., Eds.; Oxford University Press: New York, 1997; pp 119-166.
356. Samet, J.M.; Jaakkola, J.J.K. The Epidemiologic Approach to Investigating Outdoor Air Pollution. In *Air Pollution and Health*; Holgate, S.T., et al., Eds.; Academic Press: San Diego, CA, 1999; pp 406-460.
357. McCullagh, P.; Nelder, J.A. *Generalized Linear Models*; Chapman and Hall: London, 1989.
358. Samet, J.; Zeger, S.; Xu, J. Particulate Air Pollution and Mortality: The Particle Epidemiology Evaluation Project; *Appl. Occup. Environ. Hyg.* **1998**, *13*(6), 364-369.
359. *Particulate Air Pollution and Daily Mortality: Analysis of the Effects of Weather and Multiple Air Pollutants*; The Phase I.B Report of the Particle Epidemiology Evaluation Project; Health Effects Institute: Cambridge, MA, 1997.
360. Watts, W.F.J. Assessment of Occupational Exposure to Diesel Emissions. In *Diesel Exhaust: A Critical Analysis of Emissions, Exposure, and Health Effects*; Group, D.W., Ed.; Health Effects Institute: Cambridge, MA, 1995; pp 107-123.
361. *TLVs Threshold Limit Values for Chemical Substances and Physical Agents and Biological Exposure Indices*; American Conference of Governmental Industrial Hygienists: Cincinnati, OH, 2000.
362. Harrison, R.M.; Yin, J. Particulate Matter in the Atmosphere: Which Particle Properties Are Important for Its Effects on Health? *Sci. Total Environ.* **2000**, *249*, 85-101.
363. Carel, R.S. Health Aspects of Air Pollution. In *Handbook of Air Pollution from Internal Combustion Engines*; Sher, E., Ed.; Academic Press: Boston, MA, 1998; pp 42-64.
364. Guyton, A.C.; Hall, J.E. *Textbook of Medical Physiology*; Saunders: Philadelphia, PA, 1996.
365. Netter, F.H. *Respiratory System: A Compilation of Paintings Depicting Anatomy and Embryology, Physiology, Pathology, Pathophysiology, and Clinical Features and Treatment of Diseases*; Divertie, M.B., Ed.; CIBA Pharmaceutical Products: Summit, NJ, 1980.
366. International Commission on Radiological Protection Task Force on Lung Dynamics; *Health Physics* **1966**, *12*, 173-207.
367. Wilson, R.; Spengler, J. *Particles in Our Air: Concentrations and Health Effects*; Harvard University Press: Cambridge, MA, 1996.
368. Lennon, S.; Zhang, Z.; Lessmann, R.; Webster, S. Experiments on Particle Deposition in the Human Upper Respiratory System; *Aerosol Sci. Technol.* **1998**, *28*(5), 464-474.
369. Matthews, L.R. *Cardiopulmonary Anatomy and Physiology*; Lippincott: Philadelphia, PA, 1996.
370. Sioutas, C.; Koutrakis, P.; Burton, R.M. A High-Volume Small Cutpoint Virtual Impactor for Separation of Atmospheric Particulate from Gaseous Pollutants; *Part. Sci. Technol.* **1994**, *12*, 207-221.
371. Sioutas, C.; Koutrakis, P.; Burton, R.M. A Technique to Expose Animals to Concentrated Fine Ambient Aerosols; *Environ. Health Perspect.* **1995**, *103*(2), 172-177.
372. Sioutas, C.; Koutrakis, P. Inertial Separation of Ultrafine Particles Using a Condensational Growth/Virtual Impaction System; *Aerosol Sci. Technol.* **1996**, *25*, 424-436.
373. Gordon, T.; Gerber, H.; Fang, C.P.; Chen, L.C. A Centrifugal Particle Concentrator for Use in Inhalation Toxicology; *Inhalation Toxicol.* **1999**, *11*(1), 71-87.
374. Clarke, R.W.; Catalano, P.; Coull, B.; Koutrakis, P.; Murthy, G.G.K.; Rice, T.; Godleski, J.J. Age-Related Responses in Rats to Concentrated Urban Air Particles (CAPs); *Inhalation Toxicol.* **2000**, *12*(Suppl 10), 73-84.
375. Godleski, J.; Verrier, R.L.; Koutrakis, P.; Catalano, P. *Mechanisms of Morbidity and Mortality from Exposure to Ambient Air Particles*; Research Report 91; Health Effects Institute: Cambridge, MA, 2000.
376. Amdur, M.O.; Chen, L.C. Furnace-Generated Acid Aerosols: Speciation and Pulmonary Effects; *Environ. Health Perspect.* **1989**, *79*, 147-150.
377. Oberdörster, G.; Gelein, R.M.; Ferin, J.; Weiss, B. Association of Particulate Air Pollution and Acute Mortality: Involvement of Ultrafine Particles? *Inhalation Toxicol.* **1995**, *7*, 111-124.
378. Fonda, M.; Petach, M.; Rogers, C.F.; Huntington, J.; Stratton, D.; Nishioka, K.; Tipo, M. Resuspension of Particles by Aerodynamic Deagglomeration; *Aerosol Sci. Technol.* **1999**, *30*(6), 509-529.
379. Chow, J.C.; Watson, J.G.; Houck, J.E.; Pritchett, L.C.; Rogers, C.F.; Frazier, C.A.; Egami, R.T.; Ball, B.M. A Laboratory Resuspension Chamber to Measure Fugitive Dust Size Distributions and Chemical Compositions; *Atmos. Environ.* **1994**, *28*(21), 3463-3481.
380. Kousaka, Y.; Horiuchi, T.; Endo, Y.; Aotani, S. Generation of Aerosol Particles by Boiling Suspensions; *Aerosol Sci. Technol.* **1994**, *21*, 236-240.
381. Terashima, T.; Wiggs, B.; English, D.; Hogg, J.C.; van Eeden, S.F. Phagocytosis of Small Carbon Particles (PM₁₀) by Alveolar Macrophages Stimulates the Release of Polymorphonuclear Leukocytes from Bone Marrow; *Am. J. Respir. Crit. Care Med.* **1997**, *155*(4), 1441-1447.
382. Liu, W.K.; Wong, C.C. Cytotoxicity of Fly-Ash in Alveolar Macrophages from Hypothyroid Rats; *Toxicol. In Vitro* **1989**, *3*(2), 95-102.
383. Kennedy, H.L. Beta Blockade, Ventricular Arrhythmias, and Sudden Cardiac Death; *Am. J. Cardiol.* **1997**, *80*(9B), 29J-34J.
384. Dockery, D.W.; Pope, C.A.; Kanner, R.E.; Villegas, G.M.; Schwartz, J. *Daily Changes in Oxygen Saturation and Pulse Rate Associated with Particulate Air Pollution and Barometric Pressure*; Research Report 83; Health Effects Institute: Cambridge, MA, 1999; p 1-19.
385. Pope, C.A.; Verrier, R.L.; Lovett, E.G.; Larson, A.C.; Raizenne, M.E.; Kanner, R.E.; Schwartz, J.; Villegas, G.M.; Gold, D.R.; Dockery, D.W. Heart Rate Variability Associated with Particulate Air Pollution; *Am. Heart J.* **1999**, *138*(5 Pt 1), 890-899.
386. Gold, D.R.; Litonjua, A.; Schwartz, J.; Lovett, E.; Larson, A.; Nearing, B.; Allen, G.; Verrier, M.; Cherry, R.; Verrier, R. Ambient Pollution and Heart Variability; *Circulation* **2000**, *101*(11), 1267-1273.
387. Nelson, S.; Martin, T.R. *Cytokines in Pulmonary Disease: Infection and Inflammation*; *Lung Biology in Health and Disease*; Marcel Dekker: New York, 2000; Vol. 141.
388. Thèze, J. *The Cytokine Network and Immune Functions*; Oxford University Press: New York, 1999.
389. Seaton, A.; MacNee, W.; Donaldson, K.; Godden, D. Particulate Air Pollution and Acute Health Effects; *Lancet* **1995**, *345*(8943), 176-178.

390. Souza, M.B.; Saldiva, P.H.; Pope, C.A.; Capelozzi, V.L. Respiratory Changes Due to Long-Term Exposure to Urban Levels of Air Pollution: A Histopathologic Study in Humans; *Chest* **1998**, *113*(5), 1161-1162.
391. Prichard, R.J.; Ghio, A.J.; Lehmann, J.R.; Witsett, D.W.; Tepper, J.S.; Park, P.; Gilmour, M.I.; Dreher, K.L.; Costa, D.L. Oxidant Generation and Lung Injury after Particulate Air Pollutant Exposure Increase with the Concentrations of Associated Metals; *Inhal. Toxicol.* **1996**, *8*(5), 457-477.
392. Ghio, A.J.; Stonehuerner, J.; Prichard, R.J.; Pintadosi, C.A.; Quigley, D.R.; Dreher, K.L.; Costa, D.L. Humic-Like Substances in Air Pollution Particulates Correlate with Concentrations of Transition Metals and Oxidant Generation; *Inhal. Toxicol.* **1996**, *8*, 479-494.
393. Driscoll, K.E. TNF-alpha and MIP-2: Role in Particle-Induced Inflammation and Regulation by Oxidative Stress; *Toxicol. Lett.* **2000**, *112-113*, 177-183.
394. Ghio, A.J.; Kennedy, T.P.; Whorton, A.R.; Crumbliss, A.L.; Hatch, G.E.; Hoidal, J.R. Role of Surface Complexed Iron in Oxidant Generation and Lung Inflammation Induced by Silicates; *Am. J. Physiol.* **1992**, *263*, L511-L518.
395. Lewis, R.J.J. *Sax's Dangerous Properties of Industrial Materials*; Van Nostrand Reinhold: New York, 1992; Vol. v1-v3.
396. Wallace, L.; Slonecker, T. Ambient Air Concentrations of Fine (PM_{2.5}) Manganese in U.S. National Parks and in California and Canadian Cities: The Possible Impact of Adding MMT to Unleaded Gasoline; *J. Air & Waste Manage. Assoc.* **1997**, *47*, 642-653.
397. Mena, I. Trace Minerals. In *Disorders of Mineral Metabolism*; Bronner, F., Coburn, J.W., Eds.; Academic Press: New York, 1981; Vol. 1.
398. Mena, I.; Horiuchi, K.; Burke, K.; Cotzias, G.C. Chronic Manganese Poisoning: Individual Susceptibility and the Absorption of Iron; *Neurology* **1969**, *19*, 1000-1006.
399. Halliwell, B.; Gutteridge, J.M.C. *Free Radicals in Biology and Medicine*; Oxford University Press: Oxford, United Kingdom, 1999.
400. Vogt, G.; Elstner, E.F. Diesel Soot Particles Catalyze the Production of Oxyradicals; *Toxicol. Lett.* **1989**, *47*, 17-23.
401. Prahalad, A.K.; Soukup, J.M.; Inmon, J.; Willis, R.; Ghio, A.J.; Becker, S.; Gallagher, J.E. Ambient Air Particles: Effects on Cellular Oxidant Radical Generation in Relation to Particulate Elemental Chemistry; *Toxicol. Appl. Pharmacol.* **1999**, *158*(2), 81-91.
402. Veranth, J.M.; Smith, K.R.; Hu, A.A.; Lighty, J.S.; Aust, A.E. Mobilization of Iron from Coal Fly Ash Was Dependent upon the Particle Size and the Source of Coal: Analysis of Rates and Mechanisms; *Chem. Res. Toxicol.* **2000**, *13*, 382-389.
403. Veranth, J.M.; Smith, K.R.; Aust, A.E.; Dansie, S.L.; Griffith, J.B.; Hu, A.A.; Huggins, M.L.; Lighty, J.S. Coal Fly Ash and Mineral Dust for Toxicology and Particle Characterization Studies: Equipment and Methods for PM_{2.5}- and PM₁-Enriched Samples; *Aerosol Sci. Technol.* **2000**, *32*(2), 127-141.
404. Fang, R.; Aust, A.E. Ferritin Induction in Human Lung Epithelial Cells as an Indicator of Intracellular Iron Mobilization from Particulates, submitted for publication.
405. Levenspiel, O. *Chemical Reaction Engineering*; Wiley: New York, 1972.
406. Shirmamé-Moré, L. Genotoxicity of Diesel Emissions Part I: Mutagenicity and Other Genetic Effects. In *Diesel Exhaust: A Critical Analysis of Emissions, Exposure, and Health Effects*; Group, D.W., Ed.; Health Effects Institute: Cambridge, MA, 1995; pp 221-242.
407. Rosenkranz, H.S. Genotoxicity of Diesel Emissions Part II: The Possible Role of Dinitropyrenes in Lung Cancer. In *Diesel Exhaust: A Critical Analysis of Emissions, Exposure, and Health Effects*; Group, D.W., Ed.; Health Effects Institute: Cambridge, MA, 1995; pp 221-242.
408. Peterson, R.E.; Theobald, H.M.; Kimmel, G.L. Developmental and Reproductive Toxicity of Dioxins and Related Compounds: Cross-Species Comparisons; *Crit. Rev. Toxicol.* **1993**, *23*(3), 285-335.
409. Kuschner, W.G.; Wong, H.; D'Alessandro, A.; Quinlan, P.; Blanc, P.D. Human Pulmonary Responses to Experimental Inhalation of High Concentration Fine and Ultrafine Magnesium Oxide Particles; *Environ. Health Perspect.* **1997**, *105*(11), 1234-1237.
410. Baggs, R.B.; Ferin, J.; Oberdörster, G. Regression of Pulmonary Lesions Produced by Inhaled Titanium Dioxide in Rats; *Vet. Pathol.* **1997**, *34*(6), 592-597.
411. Churg, A.; Gilks, B.; Dai, J. Induction of Fibrogenic Mediators by Fine and Ultrafine Titanium Dioxide in Rat Tracheal Explants; *Am. J. Physiol.* **1999**, *277*, L975-L982.
412. Council Directive of 15 July 1980 on Air Quality Limit Values for Sulphur Dioxide and Suspended Particulates; O.J. L229/30; Council of the European Communities: 1980.
413. Amdur, M.O. Sulfuric Acid: The Animals Tried to Tell Us. In the 1989 Herbert E. Stokinger Lecture; *Appl. Ind. Hyg.* **1989**, *4*(8), 189-197.
414. EPA National Ambient Air Quality Standards for Ozone and Particulate. *Fed. Regist.* **1996**, *61*(114), 29719-29725.
415. *Research Priorities for Airborne Particulate Matter: I. Immediate Priorities and a Long-Range Research Portfolio*; National Research Council; National Academy Press: Washington, DC, 1998.
416. *Research Priorities for Airborne Particulate Matter: II. Evaluating Research Progress and Updating the Portfolio*; National Research Council; National Academy Press: Washington, DC, 1999.
417. EPA Final Regional Haze Regulations for Protection of Visibility in National Parks and Wilderness Areas. *Fed. Regist.* **1999**, *64*(126), 35713-35774.
418. Tang, H.; Lewis, E.A.; Eatough, D.J.; Burton, R.M.; Farber, R.J. Determination of the Particle Size Distribution and Chemical Composition of Semi-Volatile Organic Compounds in Atmospheric Fine Particles with a Diffusion Denuder Sampling System; *Atmos. Environ.* **1994**, *28*(5), 939-947.
419. Cui, W.; Eatough, D.J.; Eatough, N.L. Fine Particulate Organic Matter in the Los Angeles Basin-I: Assessment of the High-Volume Brigham Young University Organic Sampling System BIG BOSS; *J. Air & Waste Manage. Assoc.* **1998**, *48*(11), 1024-1037.
420. Corio, L.A.; Sherwell, J. In-Stack Condensable Particulate Matter Measurements and Issues; *J. Air & Waste Manage. Assoc.* **2000**, *50*, 207-218.
421. Lipkea, W.H.; Johnson, J.H.; Vuk, C.T. The Physical and Chemical Character of Diesel Particulate Emissions—Measurement Techniques and Fundamental Considerations. In *The Measurement and Control of Diesel Particulate Emissions*; Progress in Technology, Number 17; Society of Automotive Engineers: Warrendale, PA, 1979; pp 1-58.
422. Kittelson, D.B.; Dolan, D.F. Diesel Exhaust Aerosols. In *Generation of Aerosols and Facilities for Exposure Experiments*; Willeke, K., Ed.; Ann Arbor Science: Ann Arbor, MI, 1980; pp 337-359.
423. Kittelson, D.B.; Watts, F.W., Jr.; Arnold, M. *Review of Diesel Particulate Matter Sampling Methods: Supplemental Report #2, Aerosol Dynamics, Laboratory, and On-Road Studies*; University of Minnesota, Department of Mechanical Engineering: 1998.
424. Kittelson, D.B.; Arnold, M.; Watts, W.F. *Review of Diesel Particulate Matter Sampling Methods—Final Report*; University of Minnesota; Center for Diesel Research: 1998.
425. Vogt, R.; Scheer, V.; Maricq, M.M. Nanoparticle Artifacts: Comparison of Tailpipe Dilution Tunnel Measurements of Vehicle PM. Presented at International ETH-Workshop on Nanoparticle Measurement, Zurich, Switzerland; ETH Zurich Laboratorium für Festkörperphysik: 1999.
426. Shi, J.P.; Harrison, R.M. Investigation of Ultrafine Particle Formation during Diesel Exhaust Dilution; *Environ. Sci. Technol.* **1999**, *33*(21), 3730-3736.
427. Khalek, I.A. Nanoparticle Growth during Dilution and Cooling of Diesel Exhaust: Experimental Investigation and Theoretical Assessment. Presented at International ETH-Workshop on Nanoparticle Measurement, Zurich, Switzerland; ETH Zurich Laboratorium für Festkörperphysik: 1999.
428. Pagan, J. *Study of Particle Size Distributions Emitted by a Diesel Engine*; 1999-01-1141; Society of Automotive Engineers: Warrendale, PA, 1999.
429. Abdul-Khalek, I.; Kittelson, D.; Breaer, F. *The Influence of Dilution Conditions on Diesel Exhaust Particle Size Distribution Measurements*; 1999-01-1142; Society of Automotive Engineers: Warrendale, PA, 1999.
430. Chen, J.-P. Particle Nucleation by Recondensation in Combustion Exhausts; *Geophys. Res. Lett.* **1999**, *26*(15), 2403-2406.
431. Harris, D.B.; King, F.G.J.; Brown, J.E. Development of On-Road Emission Factors for Heavy-Duty Diesel Vehicles Using a Continuous Sampling System. In *The Emissions Inventory: Programs and Progress*; Publication No. VIP-56; Air and Waste Management Association: Pittsburgh, PA, 2000; pp 290-308.
432. Brown, J.E.; Clayton, M.J.; Harris, D.B. Comparison of Particle Size Distribution of Heavy-Duty Diesel Exhaust Using a Dilution Tailpipe Sampler and an In-Plume Sampler On-Road Operation; *J. Air & Waste Manage. Assoc.* **2000**, *50*, 1407-1416.
433. Maricq, M.M.; Chase, R.E.; Podsiadlik, D.H.; Vogt, R. *Vehicle Exhaust Particle Size Distributions: A Comparison of Tailpipe and Dilution Tunnel Measurements*; 1999-01-1461; Society of Automotive Engineers: Warrendale, PA, 1999.
434. Saxena, P.; Cass, G. Designing Atmospheric Experiments to Enable Estimation of Source-Receptor Relationships for Fine Particles. In *Atmospheric Observations: Helping Build the Scientific Basis for Decisions Related to Airborne Particulate Matter*; PM Measurements Research Workshop, Chapel Hill, North Carolina; Health Effects Institute: Cambridge, MA, 1998.
435. Schauer, J.J.; Rogge, W.F.; Hildemann, L.M.; Mazurek, M.A.; Cass, G.R.; Simoneit, B.R.T. Source Apportionment of Airborne Particulate Matter Using Organic Compounds; *Atmos. Environ.* **1996**, *30*, 3837-3855.
436. Meuzelaar, H.; Arnold, N.; Jarman, W. Paso del Norte Air Research Program, Scoping Study, Interim Report; Southwest Center for Environmental Policy and Research. <http://www.scerp.org/>, accessed 1999.
437. Burtcher, H. Measurement and Characteristics of Combustion Aerosols with Special Consideration of Photoelectric Charging and Charging by Flame Ions; *J. Aerosol Sci.* **1992**, *23*(6), 549-595.
438. Burtcher, H.; Siegmann, H.C. Monitoring PAH-Emissions from Combustion Processes by Photoelectric Charging; *Combust. Sci. Technol.* **1994**, *101*, 327-332.

439. Burtscher, H.; Schmidt-Orr, A.; Siegmann, H.C. Monitoring Particulate Emissions from Combustion by Photoemission; *J. Aerosol Sci.* **1988**, *18*, 125.
440. Palmer, G.R. Ambient Air Monitoring of Fine Particulate Matter at Hill Air Force Base, UT and the Influence of Mobile Sources. M.S. Thesis, University of Utah, Salt Lake City, UT, 1999.
441. Chow, J.C.; Watson, J.G.; Pritchett, L.C.; Pierson, W.R.; Frazier, C.A.; Purcell, R.G. The DRI Thermal/Optical Reflectance Carbon Analysis System: Description, Evaluation and Application in U.S. Air Quality Studies; *Atmos. Environ.* **1993**, *27A(8)*, 1185-1201.
442. Chow, J.C.; Watson, J.G.; Crow, D.; Lowenthal, D.H.; Merrifield, T. Comparison of IMPROVE and NIOSH Carbon Measurements; *Aerosol Sci. Technol.*, in press.
443. Funkenbusch, E.F.; Leddy, D.G.; Johnson, J.H. The Characterization of the Soluble Organic Fraction of Diesel Particulate Matter. In *Measurement and Control of Diesel Particulates*; Society of Automotive Engineers: Warrendale, PA, 1979; pp 123-143.
444. Fraser, M.P.; Cass, G.R.; Bernd, R.T.S. Gas-Phase and Particle Phase Organic Compounds Emitted from Motor Vehicle Traffic in a Los Angeles Roadway Tunnel; *Environ. Sci. Technol.* **1998**, *32(14)*, 2051-2060.
445. Hildemann, L.M.; Mazurek, M.A.; Cass, G.R. Quantitative Characterization of Urban Sources of Organic Aerosol by High-Resolution Gas Chromatography; *Environ. Sci. Technol.* **1991**, *25(7)*, 1311-1325.
446. Arnott, W.P.; Moosmüller, H.; Rogers, C.F.; Jin, T.; Bruch, R. Photoacoustic Spectrometer for Measuring Light Absorption by Aerosol: Instrument Description; *Atmos. Environ.* **1999**, *33*, 2845-2852.
447. Moosmüller, H.; Arnott, W.P.; Rogers, C.F.; Chow, J.C.; Frazier, C.A.; Sherman, L.E.; Dietrich, D.L. Photoacoustic and Filter Measurements Related to Aerosol Light Absorption during the Northern Front Range Air Quality Study (Colorado 1996/1997); *J. Geophys. Res.* **1998**, *103(D21)*, 28,149-28,157.
448. Arnott, W.P.; Rogers, C.F.; Sagebiel, J.; Zielinski, B.; Fujita, E.; Lighty, J.S.; Sarofim, A.F.; Griffin, J.B. Evaluation of Five Instruments for the Real-Time Measurement of Diesel Particulate Emissions. In *10th CRC On-Road Vehicle Emissions Workshop, San Diego, CA*; Coordinating Research Council, Inc.: Atlanta, GA, 2000.
449. Hopke, P.; Casuccio, G.S. Scanning Electron Microscopy. In *Receptor Modeling for Air Quality Management*; Hopke, P.K., Ed.; Elsevier: New York, 1991; pp 149-208.
450. Spurny, K.R. Review of Applications. In *Physical and Chemical Characterization of Individual Airborne Particles*; Spurny, K.R., Ed.; Ellis Horwood Series in Analytical Chemistry; Wiley: New York, 1986.
451. Kim, D.S.; Hopke, P.K.; Casuccio, G.S.; Lee, R.J.; Miller, S.E.; Sverdrup, G.M.; Garber, R.W. Comparison of Particles Taken from the ESP and Plume of a Coal-Fired Power Plant with Background Aerosol Particles; *Atmos. Environ.* **1989**, *23(1)*, 81-84.
452. Watt, J. Automated Characterization of Individual Carbonaceous Fly Ash Particles by Computer-Controlled Scanning Electron Microscopy: Analytical Methods and Critical Review of Alternative Techniques; *Water, Air, Soil Pollut.* **1998**, *106*, 309-327.
453. Webber, J.S.; Dutkiewicz, V.A.; Husien, L. Identification of Submicrometer Coal Fly Ash in a High-Sulfate Episode at Whiteface Mountain, New York; *Atmos. Environ.* **1985**, *19*, 285-292.
454. Eatough, D.J.; Eatough, M.; Lamb, J.D.; Lewis, L.J.; Lewis, E.A.; Eatough, N.L.; Missen, R. Apportionment of Sulfur Oxides at Canyonlands during the Winter of 1990—I. Study Design and Particulate Chemical Composition; *Atmos. Environ.* **1996**, *2*, 269-281.
455. Anderson, J.R.; Buseck, P.R. 5.3 Special Examples of Applications of Minerology and Geochemistry to Environmental Problems. In *Advanced Minerology*; Marfunin, A.S., Ed.; Springer-Verlag: Berlin, 1998; Vol. 3; pp 300-313.
456. Buseck, P.R.; Anderson, J.R. Analysis of Individual Airborne Mineral Particles. In *Advanced Minerology*; Marfunin, A.S., Ed.; Springer-Verlag: Berlin, 1998; Vol. 3; pp 292-299.
457. Suess, D.T.; Prather, K.A. Mass Spectroscopy of Aerosols; *Chem. Rev.* **1999**, *99*, 3007-3095.
458. Hughes, L.S.; Allen, J.O.; Kleeman, M.J.; Johnson, R.J.; Cass, G.R.; Gross, D.S.; Gard, E.E.; Gälli, M.E.; Morrical, B.D.; Ferguson, D.P.; Dienes, T.; Noble, C.A.; Liu, D.-Y.; Silva, P.J.; Prather, K.A. Size and Composition Distribution of Atmospheric Particles in Southern California; *Environ. Sci. Technol.* **1999**, *33(20)*, 3506-3515.
459. Reilly, P.T.; Gieray, R.A.; Whitten, W.B.; Ramsey, J.M. Real-Time Characterization of the Organic Composition and Size of Individual Diesel Engine Smoke Particles; *Environ. Sci. Technol.* **1998**, *32*, 2672-2679.
460. Gard, E.; Mayer, J.E.; Morrical, B.D.; Dienes, T.; Ferguson, D.P.; Prather, K.A. *Anal. Chem.* **1997**, *69*, 4083-4091.
461. Allen, J.O.; Ferguson, D.P.; Gard, E.E.; Hughes, L.S.; Morrical, B.D.; Kleeman, M.J.; Gross, D.S.; Gälli, M.E.; Prather, K.A.; Cass, G.R. Particle Detection Efficiencies of Aerosol Time of Flight Mass Spectrometers under Ambient Sampling Conditions; *Environ. Sci. Technol.* **2000**, *34(1)*, 211-217.
462. Serita, F.; Kyono, H.; Seki, Y. Pulmonary Clearance and Lesions in Rats after a Single Inhalation Dose of Ultrafine Metallic Nickel at Dose Levels Comparable to the Threshold Limit Value; *Ind. Health* **1999**, *37(4)*, 353-363.
463. Snow, J. *On the Mode of Communication of Cholera*. Reprinted in Snow on Cholera: A Reprint of Two Papers, 1965; Hafner Publ. Co.: New York, 1855.
464. Gertsman, B.B. *Epidemiology Kept Simple: An Introduction to Modern and Classical Epidemiology*; Wiley-LISS: New York, 1998.

EX 5

Supplier	Filter	Mass/area (oz./yd.)	Outlet PM2.5 Concentration (gr/dscf)
Hamon Research -Cottrell, Inc.	SunCoke proposed bag (PPS)	18	n/a, guarantee 0.005 PM
BWF America, Inc's	Grade 700 MPS Polyester Felt	18	0.0000086
Donaldson Company, Inc.	Tetratex #6255 Filtration Media	22	0.0000090
Donaldson Company, Inc.	6277 Filtration Media	8	0.0000034
Donaldson Company, Inc.	6282 Filtration Media	10	0.0000020
Southern Filter Media, LLC	PE-16/M-SPES Filter	16	0.0000220
W.L. Gore & Associates, Inc.	L3650 Filter	22	0.0000070
Air Purator Corp.	Huyglas 1405M Filter	22	0.0000065
Albany International Corp.	Primatex Plus I Filter	16	0.000014
BASF Corp.	AX/BA-14/9-SAXP Filter	14	0.00011
GE BHA Group, Inc.	QG061 Filter		0.0000009
GE BHA Group, Inc.	QP131 Filter		0.0000003
BWF America, Inc.	Grade 700 MPS Polyester Felt Filter	18-20	0.0000045
Inspec Fibres	5512BRF Filter	16	0.00016
Menardi-Criswell	50-504 Filter	16	0.0000083
Polymer Group, Inc.	DURAPEX PET Filter	10	0.0000185
Standard Filter Corp.	PE16ZU Filter		0.0000041
Tetratex PTFE Technologies	Tetratex 6212 Filter	16	0.0000023
Tetratex PTFE Technologies	Tetratex 8005	16	0.000022
W.L. Gore & Associates, Inc.	L4347 Filter		0.0000059
W.L. Gore & Associates, Inc.	L4427 Filter		0.0000021

Test Procedure

Conditioning period with 10,000 rapid pulse cleaning cycles

Recovery period with 30 normal filtration cycles

Six-hour performance test period

Inlet particle concentration = 18.4 ± 3.6 g/dscm with average particle size of 1.5 micron diameter
= 8.0 ± 1.6 gr/dscf

**GE acquired and is still selling the BHA Group filters

Description	Status
	never verified
micro-pore-size, high-efficiency, scrim-supported felt, singed cake side	currently verified
woven fiberglass with Tetratex PTFE membrane	currently verified
Polyester Spunbond with Tetratex PTFE membrane	currently verified
Pleatable polyphenylene sulfide (PPS) with Tetratex PTFE membrane	currently verified
singed Micro-Denier polyester felt	currently verified
membrane/fiberglass fabric laminate	currently verified
PTFE film applied to a glass felt	prev. verified
polyethylene terephthalate filtration fabric with fine fibrous surface layer	prev. verified
	prev. verified
woven-glass-base fabric with an expanded, micro porous PTFE membrane	prev. verified
polyester needle felt substrate with an expanded, micro porous PTFE membrane	prev. verified
micro-pore size high efficiency scrim supported felt, singed cake side	prev. verified
100% scrim supported P84 needle felt	prev. verified
singed microdenier polyester felt	prev. verified
100 percent polyester, non-woven fabric, non-scrim supported	prev. verified
stratified microdenier polyester non-woven	prev. verified
polyester needle felt with Tetratex® expanded PTFE membrane	prev. verified
polyester scrim-supported needle felt with a Tetratex® expanded PTFE membrane	prev. verified
GORE-TEX® ePTFE (expanded polytetrafluoroethylene) membrane/polyester felt laminate	prev. verified
GORE-TEX® membrane/polyester felt laminate	prev. verified

	Outlet PM2.5 concentration (gr/dscf)		
	Best	Worst	Average
Currently verified	0.000002	0.000022	0.0000087
All verified (including expired)	0.0000009	0.00016	0.0000207